VŠB – Technical University of Ostrava
Faculty of Electrical Engineering
and Computer Science

Performance Analysis of Full-Duplex Relaying Networks: an Application in 5G

Ph.D. THESIS

2021 **Tam Nguyen Kieu**

VSB TECHNICAL UNIVERSITY OF OSTRAVA

FACULTY OF ELECTRICAL ENGINEERING AND COMPUTER SCIENCE
DEPARTMENT OF TELECOMMUNICATIONS

Performance Analysis of Full-Duplex Relaying Networks: an Application in 5G

Ph.D. Thesis; Ostrava, January 2021

Doctoral Study Programme: P1807 Computer Science, Communication Technology and Applied Mathematics
Doctoral Study Branch: 2601V018 Communication Technology

Ph.D. Student:

Ing. Tam Nguyen Kieu
VŠB - Technical University of Ostrava
Faculty of Electrical Engineering and Computer Science
17. listopadu 2172/15, 708 00 Ostrava, Czech Republic
e-mail: tam.kieu.nguyen.st@vsb.cz

Supervisor:

prof. Ing. Miroslav Vozňák, Ph.D.
VŠB - Technical University of Ostrava
Faculty of Electrical Engineering and Computer Science
17. listopadu 2172/15, 708 00 Ostrava, Czech Republic
e-mail: miroslav.voznak@vsb.cz

2021 **Tam Nguyen Kieu**

Declaration

I declare that I have written the doctoral dissertation independently, under the guidance of my advisor and using exclusively the technical references and other sources of information cited in the dissertation and listed in the comprehensive bibliography at the end of the dissertation.

As the author of the doctoral dissertation I furthermore declare that, with respect to the creation of this doctoral dissertation, I have not infringed any copyright or violated anyone's personal and/or ownership rights.

In this context, I am fully aware of the consequences of breaking Regulation S 11 of the Copyright Act No. 121/2000 Coll. of the Czech Republic, as amended, and of any breach of rights related to intellectual property or introduced within amendments to relevant Acts such as the Intellectual Property Act or the Criminal Code, Act No. 40/2009 Coll., Section 2, Head VI, Part 4.

Viet Nam, January 2021

.....

Author's signature

Acknowledgement

First of all, I would like to sincerely thank my Supervisor, Prof. Ing. Miroslav Vozňák, Ph.D. for expert advice and direction during my study, who provided me the opportunity to be the researcher.

Many thanks to Dr. Do Dinh Thuan, Dr. Nguyen Huu Khanh Nhan and Dr. Tran Thanh Phuong and colleagues at Ton Duc Thang university, in particular, ECC, Europe cooperation center.

Many thanks to my friends from high school and universities for encouraging me to pursue this program.

Many thanks to my comrades, the soldiers who are being or not being, who are Uncle's Ho's soldiers severing at the 579 south-west front in Cambodia, provide me with inspiration and energy to accomplish this dissertation.

Last but not least, I would like to deeply thank my parents, my sisters and brothers and my dear wife and my children for their endless support and love. Without them, I would not have been able to achieve this. Greatly thanks for always being with me.

Viet Nam, January 2021

.....

Author's signature

Abstract

This dissertation deals with the wireless full-duplex relaying networks where the relay node is employed with energy harvesting (EH) capability. First, various communication and harvesting protocols are investigated, including amplify-and-forward (AF) and decode-and-forward (DF) for relaying strategies, and time-switching (TSR) and power-splitting (PSR) for EH. In particular, I provide the derived closed-form expressions describing key performance factors, including outage probability (OP), throughput, Ergodic capacity, and study the impact of configuration parameters such as channel conditions, transmit power, energy harvesting protocol parameters, etc. on the overall system performance.

Secondly, this dissertation aims to study the impact of antenna configurations on the outage probability and throughput, which are two key performance factors of EH-based wireless full-duplex relaying networks. Regarding antenna configurations for EH, two configurations for antennas at the relay node are considered, namely, using single-antenna configuration or two-antenna configuration for collecting the energy from source nodes, while only one antenna is used to forward the information signal to the destination. To further enhance the system performance, multiple-input multiple-output (MIMO) communication scheme is also considered in my dissertation, especially, three diverse techniques, i.e., Zero Forcing at Transmitter (TZF), Zero Forcing at Receiver (RZF), and Maximal Ratio Combining (MRC), which are employed to strengthen the performance of MIMO system.

Finally, this dissertation deals with the performance analyses of the energy harvesting based full-duplex relay networks for various transmission modes including instantaneous, delay-limited and delay-tolerant transmissions. Specifically, the outage probability and the throughput for the proposed system as the functions of all system parameters such as the position of relay nodes, the data transmission rate, the noise at the source and relay as well as the energy conversion factor are derived. Based on the analyses, optimal energy harvesting parameters and best communication strategy for the presented model are proposed. All analytical results are validated by Monte Carlo simulations.

Keywords

Wireless relay networks, energy harvesting, delay-limited transmission, delay tolerant transmission, full-duplex transmission, half-duplex transmission, amplify-and-forward strategy, decode-and-forward strategy.

Abstrakt

Tato dizertační práce se zabývá bezdrátovými plně duplexními relay sítěmi, kde je užíván relay uzel se schopností získávat energii z okolí, dále jako EH (Energy harvesting). Nejprve jsou zkoumány různé komunikační a EH protokoly, včetně amplify-and-forward (AF) a decode-and-forward (DF) pro strategie předávání a time-switching (TSR) a power-splitting (PSR) pro získávání energie. Zejména poskytuji odvozená vyjádření v uzavřené formě popisující klíčové výkonnostní charakteristiky vč. pravděpodobnosti výpadku (OP), propustnosti, ergodické kapacity a studii vlivu konfiguračních parametrů jako jsou podmínky kanálu, vysílací výkon, parametry EH protokolů atd. na výkonnost systému.

Dále si tato disertační práce klade za cíl prozkoumat dopad konfigurací antén na propustnost a pravděpodobnost výpadku přenosu zpráv, což jsou dva klíčové faktory bezdrátových plně duplexních relay sítí založených na EH. Pokud jde o konfiguraci antény pro EH, uvažují se dvě konfigurace antén v uzlu relé, a to použití s jednou anténou nebo konfigurace s dvěma anténami pro získávání energie ze zdrojových uzlů, zatímco k odeslání informace do cíle je používána jedna. Pro další zvýšení výkonu systému je v mé disertační práci uvažováno také komunikační schéma s více vstupy a více výstupy (MIMO), zejména tři různé techniky TZF (Zero Forcing at Transmitte), RZF (Zero Forcing at Receiver) a nakonec MRC (Maximal Ratio Combining), které se používají ke zvýšení výkonu systému MIMO.

Nakonec se tato dizertace zabývá výkonnostními analýzami různých přenosových režimů plně duplexních realy sítí založených na EH, a to pro přenosy okamžité, limitované zpožděním a tolerantní ke zpoždění. Konkrétně je odvozena pravděpodobnost výpadku přenosu zpráv a propustnost pro navržený systém pomocí funkce všech systémových parametrů jako je např. umístění uzlů, přenosová rychlost, šum zdroje a relay uzlu a rovněž také faktor přeměny energie. Na základě analýz jsou navrženy optimální EH parametry a nejlepší komunikační strategie pro předložený model. Všechny analytické výsledky jsou validovány simulacemi metodou Monte Carlo.

Klíčová slova

Bezdrátové relay sítě, získávání energie, přenos limitovaný zpožděním, přenos toleratní ke zpoždění, plně duplexní přenos, poloduplexní přenos, strategie zesil a přepošli, strategie dekóduj a přepošli.

Contents

List of Figures

List of Abbreviations

EH	**E**nergy Harvesting.
FD	**F**ull- duplex.
HD	**H**alf- duplex.
DT	**D**elay- tolerant.
DL	**D**elay- limited.
AF	**A**mpli- and - forward.
DF	**D**ecode- and - forward
TSR	**T**ime switching based relaying
RF	**R**adio frequency
SWIPT	**S**imultaneous wireless information and power transfer
SI	**S**elf-interferences
CSI	**C**hannel state information
PSR	**P**ower splitting based relaying
OP	**O**utage probability
FDRN	**F**ull-duplex relaying network
MIMO	**M**ultiple Input - Multiple Output
CP	**C**yclic prefix
OFDM	**O**rthogonal frequency division multiplexing
OFDMA	**O**rthogonal frequency division multiplexing access
FBMC	**F**ilter bank multi-carrier
GFDM	**G**eneralized frequency division multiplexing
LTE	**L**ong-term evolution
NOMA	**N**on-orthogonal multiple accesses
SCMA	**S**parse code multiple accesses
SIC	**S**elf-interference cancellation
RAN	**R**adio access network
IoT	**I**nternet-of-Things
SU	**S**econdary user
CR	**C**ognitive radio
TZF	**Z**ero Forcing at Transmitter
RZF	**Z**ero Forcing at Receiver
RAT	**R**adio access technologies
MRC	**M**aximal Ratio Combining
D2D	**D**evice-to-device
M2M	**M**achine-to-machine
WPT	**W**ireless power transfer
SPS	**S**olar power satellite
PT	**P**rimary transmitters
RSI	**R**esidual self-interference
TS-TWR	**T**S-based two-way relaying
TS	**T**ime switching
SRB	**S**ecure relay beam
SNDR	**S**ignal to noise-and-distortion ratio

1 Introduction

1.1 Motivation and goals

With the setting of today's world, there are certain ways in which social development will require to vary in the way that mobile and wireless information networks are utilised. Basic electronic services will keep being developed fast and become more dynamic. The mobile and wireless information networks will transmit on-demand information and entertainment with supper high data rate. Therefore, those developments will trigger an explosion of mobile and wireless traffic quantity.

Not long ago, the study method towards 5G has been developed based on the evolution of new wireless conceptions that are designed to respond to the challenging demand of utilization, which the present wireless access networks cannot help. Amazingly, relied on the latest radio conceptions such as massive MIMO, relaying networks, device-to-device communication, the renovation models will permit 5G to achieve the expected intensification in the mobile data quantity, meanwhile widening the range of application areas that mobile communications can help beyond this year. Energy efficient communication means something different from what it did a decade ago.

From a communication network designer's point of view, what do energy harvesting networks bring to us? Communication with energy harvesting nodes that consists of green, self-supplied nodes with extended network lifetime, is a relatively new field with increasing interest.

In this report, I deploy a low-complexity protocol for two-way relaying networks, in which the relay node amplifies or decodes the received signal and then transfers it to the destination. A formulation and examination of the outage probability and the throughput for the proposed full-duplex energy harvesting enabled relaying networks with instantaneous, delay-limited, and delay-tolerant modes, will also be conducted. Besides, I compare the performance of transmission methods and then derive the solution for some optimization problems. Our mathematical and simulation analyses provide the information on how the performance of communications changes with respect to residual SI and energy harvesting efficiency factors.

1.2 The dissertation structure

This dissertation is organized as follows: Section 2 presents the background of the dissertation, Section 3 determines the aims of the proposed research, and Section 4 shows the State-of-the-Art. Section 5 introduces performance

analysis of energy harvesting protocol for full-duplex relay networks. Section 6 is focused on the study of energy harvesting performance in full-duplex relay networks with various antenna configurations at the relay. Section 7 analyses energy harvesting performance for various transmission modes. Last but not least, section 8 contains a conclusion and future work plans. The references and candidate's published research papers are at the end of the thesis.

2 Background

This chapter provides background knowledge for understanding the goals of the dissertation. In particular, Section 2.1 introduces the background information on 5G in the general and energy harvesting in specific.

2.1 5G mobile communications and energy harvesting

5G Technology stands for 5th generation mobile technique. It defines the next main stage of mobile telecommunication standards over the current 4G ones. Users have never witnessed such a high quality technique before. The 5G technology involve all sort of progressive characters making it into the strongest and most requested technique in the near future.

Wireless system designers have been facing the continuously increasing demand for high data rates and mobility required by new wireless applications. Therefore, they have started research on fifth generation wireless systems that are expected to be deployed beyond this year **[1]**. In this section, I will report potential cellular architectures and promising technologies for 5G wireless communication systems, such as massive MIMO, energy-efficient communications, small-cell networks, and mm Wave communications.

2.1.1 Novel radio access technologies (RAT)

GFDM / FBMC / NOMA / SCMA

Today's latest cellular technology, i.e., LTE, relies on orthogonal frequency division multiplexing (OFDM). While its advantages have been proven for years, there are shortcomings that prevent it from satisfying the vast demand of 5G networks. These include spectral leakage, sensitivity to carrier frequency offsets and constrained bandwidth efficiency due to a lot of cyclic prefixes. Therefore, novel concepts for multi-carrier communication are researched, and schemes like filter bank multi-carrier (FBMC) **[2]** and generalized frequency division multiplexing (GFDM) **[3]**, are considered in the research community.

GFDM scheme offers more flexibility by ordering the data in a two-sized time-frequency block structure, introducing flexible pulse shaping for the individual sub-carriers and potentially reducing the amount of CP when comparing to the amount of useful data.

In contrast to OFDM where orthogonality must be ensured for all the carriers, FBMC requires orthogonality for the neighboring sub-channels only. In fact, OFDM exploits a given frequency bandwidth with a number of carriers, while FBMC divides the transmission channel associated with this

given bandwidth into a number of sub-channels. In order to fully exploit the channel bandwidth, the modulation in the sub-channels must adapt to the neighbour orthogonality constraint and offset quadrature amplitude modulation (OQAM) is used to that purpose. The combination of filter banks with OQAM modulation leads to the maximum bit rate, without the need for a guard time or cyclic prefix as in OFDM **[2]**.

Multiple access in 5G mobile networks is an emerging research topic, since it is the key technology for the next generation network to keep pace with the exponential growth of mobile data and multimedia traffic. Non-orthogo -nal multiple accesses (NOMA) has recently received considerable attention as a promising candidate for 5G multiple access **[4]**. Particularly, NOMA uses the power domain for multiple access, where different users are served at different power levels. The users with better channel conditions employ successive interference cancellation (SIC) to remove the messages intended for other users before decoding their own.

Sparse code multiple accesses (SCMA) is a new frequency domain non-orthogonal multiple-access technique which can improve spectral efficiency of wireless radio access. With SCMA, different incoming data streams are directly mapped to code words of different multi-dimensional cookbooks, where each code word represents a spread transmission layer. Multiple SCMA layers share the same time-frequency resources of OFDM **[5]**.

2.1.2 Massive MIMO

Massive makes a clean break with current practice through the use of a very large number of service antennas (e.g., hundreds or thousands) that are operated fully coherently and conformably. Extra antennas can support by focusing the transmission and reception of signal energy into ever-smaller regions of space. This brings huge improvements in throughput and energy efficiency, in particularly when combined with simultaneous scheduling of many user terminals **[6**; **7]**.

2.1.3 Millimeter Wave communication

Millimeter Wave is a promising technology for future cellular systems. Since a limited spectrum is available for commercially cellular systems, much research has focused on increasing spectral efficiency by using OFDM, MIMO, efficient channel coding, and interference coordination. Network density has also been studied to increase area spectral efficiency, including the use of heterogeneous infrastructure (maco-, pico-, femto-cells, relays, distributed antennas) but increased spectral efficiency is not enough to guarantee high per-user data rates. The alternative is a more extended spectrum. Millimeter wave (mm Wave) cellular systems, operating in the 10-300GHz band, appear to be a promising candidate for next-generation cellular systems by which multiple gigabit-per-second data rates can be supported **[8]**.

Enabling mm Wave cellular systems in practice, however, requires properly dealing with the channel impairments and propagation characteristics of the high frequency band. The main propagation-related obstacles in realizing mm Wave cellular are that free-space path loss is much larger in mm Wave due to the higher carrier frequency, scattering is less significant which

reduce the available diversity, and non-line-of-sight paths are weaker making blockage and coverage holes more pronounced. Furthermore, the noise power is larger due to the use of larger bandwidth channels.

2.1.4 Small-cell networks

A key enabling technology to support a high data rate service scenario appears to be a small cell network **[1]**. Theoretically it is known that, when a network is in the interference-limited regime, spectral efficiency per area increases linearly with the number of small cells. From the viewpoint of spatial domain; however, there are huge differences in wireless channel characteristics between small cell networks (e.g., outdoor-to-indoor or indoor-to-indoor) and conventional macro cell networks. First, the elevation angle of the ray propagation becomes highly influential. Second, various channel environments may occur in a small cell network. Hence, not only the density of the network is needed but also the small cell technologies that reflect the above issues are enhancing the network performance and fulfilling 5G target.

2.1.5 Cloud RAN

Leveraging cloud-based computing infrastructure to implement the Radio Access Network (RAN) functionality and possibly virtue base station processing would enable new forms of scheduling and coordinated multi-point transmissions, while leveraging the many advantages of cloud infrastructure, such as shared resources, reliability, and greener and lower cost operation **[9]**. From a network architectures perspective, Cloud RAN enables semi-centralized scheduling and network resource allocation algorithms which can lead to increased network performance in throughput, and reliability.

2.1.6 Device-to-device (D2D) communications

While the conventional cellular architecture consists of connections from base stations to user equipment, 5G systems may well rely upon a two-tier architecture consisting of a macro-cell tier for base station to device communication, and a second device tier for device to device (D2D) communications. Such architectures are a hybrid of conventional cellular and adhoc designs **[10]**.

2.1.7 Energy harvesting

Energy-harvesting technologies are fundamental in enabling the realization of "zero-power" wireless sensors and implementing the Internet-of-Things (IoT) and machine-to-machine (M2M) communication. Their increasing utilization in low-power and power-efficient sensors and electronics could potentially find application in 5G cellular networks **[11]**.

Energy harvesting is a promising solution to maintain the lifetimes of wireless systems. The performance of wireless information systems is tied by the limit battery life of wireless equipment which is the reason why EH method has drawn remarkable attention lastly. Energy collected from the

ambient environment (i.e., wind, heat, solar, etc.) can be utilized to prolong the system lifetime. Replacing these batteries made much costly, hazardous, unhoped and unreal. Therefore, energy harvesting from RF signals has been investigated. Especially, wireless powered communications with the helping of relays, which are equipped with energy harvesting capability, has drawn a lot of attention recently. This will be the focus of this dissertation. We extract the closed-form expression of the instantaneous throughput and then compare them together by applying time switching based relaying (TSR) protocol and Amplify-and-Forward (AF) scheme. An essential result can be found distinctly that the time-switching factor, the position of a relay, the noise coefficient at a relay, the energy conversion efficiency as well as the target rate in TSR act on their throughput in **[12]** and through utilizing the time switching based relaying (TSR) protocol and Decode-and-Forward (DF) model, we extract the approximate clause of the outage probability and after that work out the maximal throughput of delay-limited and delay-tolerant models. A worth outcome can be taken evidently that the noise coefficient, the time-switching factor, the target rate as well as the position of relay in TSR effected the maximal throughput **[13]**.

2.2 Wireless power communications

Radiation wireless power transfer (WPT) is a promising technology to provide cost-effective and real-time power supplies to wireless devices. Although radiation WPT shares many similar characteristics with the extensively studied wireless information transfer or communication, they also differ significantly in terms of design objectives, transmitter/receiver architectures and hardware constraints, etc.

Radiation WPT has a wide range of applications, spanning from low-power wireless charging with devices such as radio frequency identification (RFID) tags, wireless sensors, Internet of Things (IoT) devices, and consumer electronics (smart phones, laptops, household robots, etc.), to high-power applications such as microwave powered aircraft **[14]** as well as solar power satellite (SPS) **[15]**. Encouragingly, several startup companies such as Energous (Wattup) **[16]** and Ossia (Cota) **[17]**.

2.3 Full-duplex and half-duplex relaying network

Traditional relay systems operate in a half-duplex mode, where the source-to relay and the relay-to-destination links are kept orthogonal by either frequency division or time division multiplexing. On the other hand, in the full-duplex mode, the source and relay can share a common time-frequency signal-space, so that the relay can transmit and receive simultaneously over the same frequency band. Theoretically, half-duplex operation causes loss of spectral efficiency since the capacity achieved in the full-duplex mode can be twice as that of the half-duplex mode. However, full-duplex operation is difficult to implement in practice, because of the significant amount of self-interference observed at the receiving antenna as a result of the signal from the transmitting antenna of the same node in **[18]**.

3 State-of-the-Art

The normal energy-constrained communication networks have a limited lifetime for operating, and in order to keep the network operating constantly, the frequently replacement of battery is carried out. However, this is inconvenient, costly and sometimes impossible, so the energy harvesting technique, in which network nodes dredge energy from ambient sources such as sun, wind or wave vibration, has drawn a huge attention, especially when it brings out a cheaper solution to maintain the lifetime of wireless communication networks. Nevertheless, the amount of energy collected from nature is accidental and based upon some uncontrollable coefficients like the weather condition. An effective method that remedies this precious limits is to scavenge energy from artificially radio frequency (RF) electromagnetic radiation as in **[19; 20]**.

As RF signals can bring both information and power, there has been a great explosion of research operations in the domain of simultaneous wireless information and power transfer (SWIPT). In the leading jobs on SWIPT by Varshney **[21]** and Grover **[22]**, the fundamental trade-off between the capacity and energy was investigated. Then in **[23]**, real structures, i.e., time-switching and power-splitting, for SWIPT systems were offered, and the maximal transfer covariant attaining the rate-energy region was extracted.

The impact of incomplete channel state information (CSI) at the transmitter was indicated in **[24]**. Recently, the well-innovating structures of rate-energy area were suggested in **[25; 26]**. Furthermore, the energy effect of OFDMA networks with SWIPT was considered in **[27]**, and the application of SWIPT in multi-user and cellular networks was given in **[28; 29]**. Alongside with the above jobs which mostly concentrate in single-stage scenario, using discontinued relays to make RF EH and information transmission, has also induced great interest. The work in **[30]** studied the symbol error rate of relay selective modes in cooperation systems, where energy-constrained relay nodes with the limit power reservation were based on some outside charging structure to help the information transfer.

In **[31]**, the authors investigated the throughput performance of an AF relay network for both time-switching and power-splitting protocols, and then, the same authors extended the analysis to the proper time-switching protocol in **[32]**. The throughput of the DF throughput relays systems was studied in **[33]**, meanwhile the power distribution strategies for DF relay systems with multiple source-destination pairs were examined in **[34]**.

In addition, the performance of EH based cooperation networks with randomly allocated users was surveyed in **[35- 37]**. It is worth indicating that all these jobs were restricted to the HD relay mode, where the relay node cannot be collect and transfer information simultaneously in the same frequency band.

The HD structure is broadly accepted in normal wireless relay networks, because it can simplify the network design and execution; nevertheless, it suffers from remarkable loss in spectrum efficiency. With the development of antenna techniques and signal processing ability, in an attempt to restore the spectral loss, FD relaying scheme, in which the relay node collects and transfers simultaneously in the same frequency band, has drawn large amount of research interest of the authors in **[38 - 43]**.

Nonetheless, to the best of the authors's knowledge, there has not been any work surveyed to the applied area of FD relaying in RF EH based networks. Motivated by this fact, I concentrate on a source-relay-destination two-stage scenario that the relay is energized through RF energy harvesting, and study the performance of FD transfer in terms of the network throughput in a RF EH based relay network. For FD relaying, I investigate various antenna configurations, i.e., the relay is equipped with two antennas, one for data transfer and one for data receiver, or just one antenna. Moreover, the time-switching protocol and power-splitting protocol are both employed in this part.

Finally, I investigate the throughput of both AF and DF relaying strategies, and characterize the fundamental trade-off between EH duration and information transfer duration. Specially, focusing on how the time-switching factor is maximized, three different information transfer modes are considered, so called, instantaneous transmission, delay-constrained transmission, and delay-tolerant transmission modes. In order to show the efficiency of the FD relay structure, the comparison with the HD relay structure is also presented. The main conclusion of this dissertation is that FD relaying system is an interesting and promising solution to enhance the throughput of RF EH based relay networks.

4 Aims

This part enumerates the concrete goals and an outline plan of each section of the research suggested.

4.1 Aim 1: provide the basic performance analysis for full-duplex relaying networks where the relay is equipped with energy harvesting technology

Relaying networks are the effective way to combat the performance degradation caused by fading, shadowing, and path loss. Full-duplex (FD) relay network has the potential to realize the successful information exchange of two sources and more spectral efficiency than conventional half-duplex (HD) technique. When comparing to the HD mode, the FD mode has higher capacity in practical channel conditions. Alternatively, the FD mode can tolerate high loop interference power while achieving the same capacity as the half-duplex mode. The main disadvantage of FD communication is the self-interference from own node transmission, which is much larger than signal of interest from the distant node. To help the communication node that can transmit and receive signals over the same frequency band, many techniques of suppressing self-interference have been proposed in **[44-46]**.

Energy harvesting (EH) based on ambient radio frequency (RF) has recently become advanced method to prolong the lifetime of the wireless networks. The first goal of my research is to integrate the energy harvesting technology with the full-duplex relaying networks. By applying time switching based relaying (TSR) protocol for both Amplify-and-Forward (AF) and Decode-and-forward (DF) relaying schemes, I derive the closed-form expression of the outage probability and hence compute the optimal throughput. An important result can be seen clearly that the time switching factor in TSR impacts is on the optimal throughput. Finally, numerical results show an efficient relaying strategy in full-duplex cooperative networks.

To have a better view of the proposed method, I also compare the performance of energy harvesting protocols applied for FD relaying networks to the one applied for the HD relaying networks, both by analysis and numerical simulation.

4.2 Aim 2: extend the basic performance analysis to various models of full-duplex relaying networks, in particular, one-antenna versus two-antenna configuration

As mentioned in the previous section, the relay node in the FD relaying networks is normally equipped with two antennas, one for receiving and one for transmitting signals, which creates the self-interference from own transmission of the relay. When the TSR energy harvesting protocol is applied, there are alternative methods to use only one antenna or both antennas to harvest energy.

The second contribution of my dissertation is to provide the thorough analysis of the impact of different configurations of relay antennas to the performance of FD relay networks which employ the energy harvesting technology. In particular, I compare the performance of at least two cases: (1) only one antenna is used to collect energy from the source, while the other is used for information forwarding and (2) both antennas are exploited to collect energy, while only one of them used to transmit the information signal. In both two cases, analytic expressions are derived for outage probability and throughput of the network. Based on these formulas, the impact of various parameters such as time-switching factor, noise coefficient, relay position, energy transfer efficiency is carefully studied. It is illustrated that using both relay antennas for energy harvesting is always profitable, and the throughput gain is most significant when fraction of source energy is small. For further goal, I'm going to investigate other relay and antenna configurations for FD relay networks in the support of energy harvesting.

4.3 Aim 3: extend the performance analysis to various transmission mode, including instantaneous transmission, delay-limited transmission, and delayed tolerant transmission modes

For FD relaying networks, the communication between the source node and the relay as well as the destination can be divided into three communication modes **[47]**: instantaneous transmission, delay-limited transmission, and delayed tolerant transmission. For the purpose of performance analysis, these three communication modes can be distinguished from the others based on the availability of the channel state information (CSI) at the relay (in fact, CSI is assumed to be known at the destination). For the instantaneous transmission mode, the optimal time switching factor is updated for each channel realization, which is computed by a centralized entity having access to the global instantaneous CSI. On the other hand, for the delay-limited transmission and delay-tolerant transmission modes, only the channel statistics are required to compute the optimal time switching factor **[47]**. For delay-limited transmission, the source transmits at a constant rate, which may subject to outage due to the random fading of the wireless channel. In the delay-tolerant (DT) context, the source transfers at any unchanged rate upper bounded by the ergodic capacity.

For the third goal of this dissertation, I continue to extend the performance analysis of energy harvesting in FD relaying networks, by comparing the system performance in three communication modes as mentioned above. Similar to the second goal, here I aim to derive the mathematical closed-form or approximated expression for the throughput of the system at three transmission modes. Based on these formulas, a rigorously comparative analysis on these modes is provided. The analysis results match well with numerical results based on Monte-Carlo simulation.

5 Performance analysis of energy harvesting protocol for full-duplex relay networks

This chapter discusses my process to achieve Aim 1 in Chapter 4. Here, I study different approaches to obtain a low-complexity protocol for wireless full-duplex relaying wireless networks, in which the relay nodes are equipped by EH technology. Specifically, closed-form expressions of outage probability and throughput of the considered system have been derived rigorously for different energy harvesting strategies, different communication schemes as listed below:

- Energy harvesting protocols: two protocols are investigated, including TSR **[TNK07**; **TNK10**; **TNK14**; **TNK18**; **TNK22]** and PSR **[TNK19]**.
- Relaying protocols: AF **[TNK11**; **TNK13-TNK15**; **TNK18**; **TNK19]** and DF **[TNK10**; **TNK12**; **TNK20**; **TNK21]**.
- Different antenna configurations: single-antenna or two-antenna **[TNK08]**.
- Transmission modes: instantaneous **[TNK01**; **TNK09]** , delay-limited, and delay-tolerant **[TNK20]**.
- Different channel conditions: Rayleigh channel **[TNK03]**, Nakagamim channel **[TNK05**; **TNK06]**, hardware impairment **[TNK04**; **TNK11**; **TNK17]**, with the presence of eavesdropper **[TNK05**; **TNK06]**.
- Different communication strategies to enhance the outage performance: NOMA **[TNK03**; **TNK05**; **TNK06**; **TNK17]**, MIMO **[TNK04**; **TNK05**; **TNK06]**, relay selection **[TNK15**; **TNK16]**, cognitive radio networks **TNK16]**, power beacon aided **[TNK17]**.

Our mathematical analysis and numerical simulation show how communication performance changes due to the impact of residual SI and EH parameters. The optimal time-switching factor of EH FD system is also obtained by our analysis **[TNK02]**. To have a better view of the proposed method, I will also make a comparison between the performance of energy harvesting protocol that is applied for FD relaying networks to the one that is applied for HD relaying networks, both by analysis and numerical simulation **[TNK01]**; **[TNK10]**; **[TNK12]**.

5.1 Wireless Information and Power Transfer for Full-Duplex Relaying Networks: Performance Analysis

Applications of renewable energy in the next-generation wireless networks will bring huge benefits for continuing operation in mobile equipment. Among energy sources including solar and wind power, power extracted from radio-frequency (RF) signals in ambient transmitters can be considered as a replacement for traditional wired power grids. Energy harvested from the natural environment is a promising approach to prolong the lifetime of energy-constrained wireless networks such as cellular networks or wireless sensor networks. Simultaneous wireless information and power transfer technology (SWIPT) becomes appealing candidates since it realizes both useful information and energy from RF signals at the same time, and thus potentially offers great convenience to mobile equipment. Varshney first proposed the idea of transmitting information and energy simultaneously in **[25]**. Using a relay to facilitate RF energy harvesting and information transfer that is can extend the transmission range and increased system capacity has also drawn significant attention. In **[31]**, the authors studied the throughput performance of amplify and forward (AF) relaying system for both time-switching and power-splitting protocols.
More importantly, relaying network is an effective way to combat the performance degradation caused by fading, shadowing, and path loss. Full-duplex (FD) relay network has the potential to realize the successful information exchange of two sources and more spectral efficiency the than conventional half-duplex (HD) technique. When comparing to HD mode, the FD mode has a higher capacity in practical channel conditions. Alternatively, the FD mode can tolerate high loop interference power while achieving the same capacity as the half-duplex mode. The main disadvantage of FD communication is the self-interference from the own transmission, which is much larger than the signal of interest at the distant node. To help the communication node transmit and receive signals over the same frequency band, many techniques of suppressing self-interference have been proposed in **[44-46]**. Unfortunately, the self-interference is residual due to the limited technique. The residual interference still decreases system performance. In fact, **[52]** indicates that the full-duplex mode is an attractive choice for fixed relays provided that the loop interference power is maintained at a tolerable level. The authors in **[53]** presented a power allocation strategy to maximize the sum-rate of the FD-two-way relaying system under realistic residual self-interference.
Recently, a few research trends have been conducted in the FD relay system in the context of the SWIPT. In **[48]**, the throughput was analyzed for three relay control schemes, including the maximum relay, optimal relay, and target relay. Analytical expressions for outage probability and ergodic capacity were also presented for this considered relay control scheme. Later in **[47]**, the authors considered two cases depending on the number of antennas used for harvesting and demonstrated that employing both relay antennas for energy harvesting is always beneficial, compared to the HD relaying architecture, results indicate that FD relaying can substantially boost the system throughput. The author in **[54**; **55]** analyzed the performance

of two-way relaying networks under non-ideal hardware where is linearly affected by impairment levels. However, there has not been any work related to optimal throughput having considered the application of one-way FD relaying in RF energy harvesting systems.
Therefore, in this part, we analyze the outage probability of full-duplex relaying with the novel ability of energy harvesting and information transfer. Based on the analytical expressions, the optimal throughput and energy harvesting time are figured out.

5.1.1 System model

Let us consider a wireless dual-hop relay network with AF protocol system illustrated in Fig. (5.1), in which the destination node can receive signals at a long distance thanks to relaying node. The system consists of three nodes, the source node denoted by S and the destination node denoted by D and one relay node R. Each node has two antennas, one of them is responsible for signal transmission and the other is responsible for signal reception. The cooperative relay is assumed to be an energy-constrained device so that it must harvest energy from the source, and use that energy to amplify and forward the source information to the destination node. We assume that the link between two sources is not available due to the deep shadowing effect.

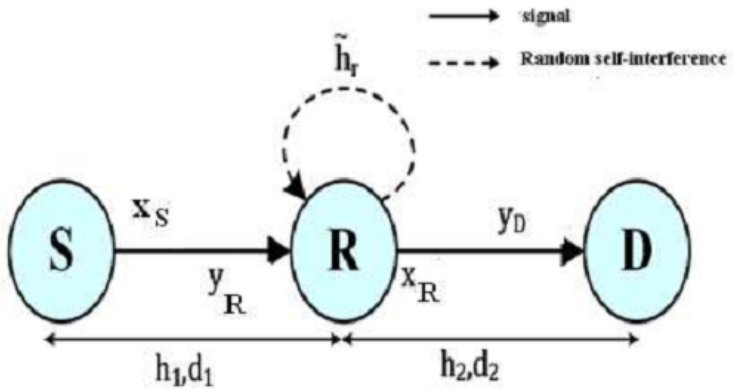

FIGURE 5.1: System model of one way full-duplex.

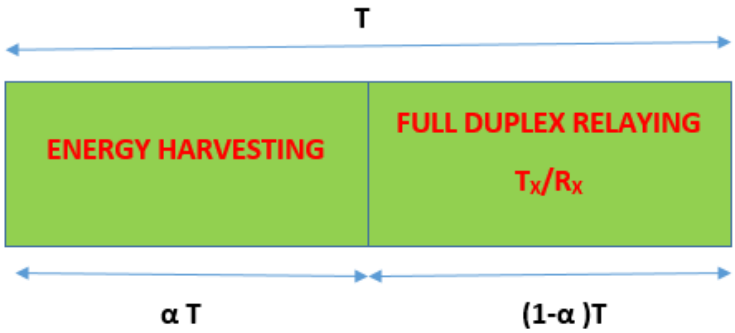

FIGURE 5.2: Illustration of the parameters of TSR protocol.

The interference cancellation mechanism is adopted to mitigate the self-interference. As the self-interference can not be eliminated, a certain amount of self-interference remains. The residual self-interference channel at R is denoted by $\widetilde{h}_R$. Let $d_j, j = 1, 2$ denote the distance between $S - R$ link and $R - D$ link respectively and $h_j, j = 1, 2$ denote the channel coefficients between $S-R$ link and $R-D$ link respectively. The scheme used in this investigation is the Time Switching-based Relaying (TSR) protocol as described in **[31]**. The main parameters of the protocol are expressed in Fig. (5.2).
Based on the TSR protocol proposed in **[31]**, the communication process is divided into two phases. In the first phase, energy is transferred from the source to the relay with a duration of $\alpha T, (0 < \alpha < 1)$ and in the second phase, i.e, the remaining time of length, $(1 - \alpha) T$ the duration of information is transmitted, here α is time switching coefficient and T is the duration of the considered signal block. During the energy harvesting phase, the received signal at the relay is given as:

$$y_R = \sqrt{\frac{P_S}{d_1^m}} h_1 x_S + n_R, \tag{5.1}$$

where P_S is the source transmission power, which is the same for both sources, n_R is the additive white Gaussian noise at R with zero-mean and variance of σ_n^2. Regarding wireless received power, the harvested energy at the relay is given by **[31]**

$$E_h = \eta \alpha T \frac{P_s |h_1|^2}{d_1^m}, \tag{5.2}$$

where m is the path loss exponent, η is the energy conversion efficiency, h_1, h_2 are the channel coefficients between source-relay link and relay destination link, respectively. In the information transfer phase, assume that the source node transmits signal x_S to R and R re-transmits signal x_r to the destination node $x_j,\ j = S, R$ have unit energy and zero–mean, i.e, $E\left[|x_j|^2\right] = 1$ and $E[x_j] = 0$. Therefore, the received signal at the relay under self-interference source is rewritten as:

$$y_R = \sqrt{\frac{P_S}{d_1^m}} x_S h_1 + \widetilde{h}_R x_R + n_R, \tag{5.3}$$

where $\widetilde{h}_R$ is the residual self-interference factor at R. We assume that R receives y_R and in the next time slot, R uses the harvested energy to amplify and forward y_R. Hence, the magnification of the prior received signal, x_R, is:

$$x_R = G\sqrt{P_R} y_R, \tag{5.4}$$

where G is the amplification factor of R. Based on AF relaying scheme at R, according to **[41]**, the amplification factor is given by

$$G^{-1} = \sqrt{\frac{P_S}{d_1^m} |h_1|^2 + P_R \left|\widetilde{h}_R\right|^2 + \sigma_n^2}. \tag{5.5}$$

It is worth noting that harvested power that helps operate the next hop transmission, P_R, is given by

$$P_R = \frac{E_h}{(1 - \alpha) T} = \mu P_S \frac{|h_1|^2}{d_1^m}, \tag{5.6}$$

where μ is defined as $\mu \triangleq \frac{\alpha\eta}{1-\alpha}$.
Next, we obtain the received signal at the destination as

$$y_D = \frac{h_2}{\sqrt{d_2^m}} x_R + n_D, \tag{5.7}$$

where n_d is the Gaussian noise at destination node. By substituting Eq. (5.4), Eq. (5.6) into Eq. (5.7), we can calculate the received signal as

$$y_D(\kappa) = \underbrace{\frac{h_2}{\sqrt{d_2^m}} G\sqrt{P_R}\frac{h_1\sqrt{P_S}}{\sqrt{d_1^m}} x_S}_{signal} + \underbrace{\frac{h_2}{\sqrt{d_2^m}} G\sqrt{P_R}\widetilde{h}_R x_R}_{RSI} + \underbrace{\frac{h_2}{\sqrt{d_2^m}} G\sqrt{P_R} n_R + n_D}_{noise}. \tag{5.8}$$

In the above equations, the instantaneous received SINR from S_j through R is determined as

$$\gamma_{\text{OW}} = \frac{E\left\{|signal|^2\right\}}{E\left\{|noise|^2\right\} + E\left\{|RSI|^2\right\}}. \tag{5.9}$$

By simple replacement, we obtain the new formula as

$$\gamma = \frac{\frac{P_S|h_1|^2 P_R|h_2|^2}{d_1^m d_2^m P_R\left|\widetilde{h}_R\right|^2}}{\frac{\sigma_n^2 P_S|h_1|^2}{P_R\left|\widetilde{h}_R\right|^2 d_1^m} + \frac{P_R|h_2|^2}{d_2^m} + \sigma_n^2}. \tag{5.10}$$

We assume that the channel gains $|h_1|^2, |h_2|^2$ are independent and identically distributed (i.i.d.) exponential random variables.

5.1.2 Outage Probability and Throughput Analysis

In this section, we analyze the outage probability of full-duplex one-way relaying with energy-harvesting and information transfer. Based on analytical expressions, the throughput of this scheme is derived and the optimal value of the time-switching factor for harvesting energy is also achieved.

Outage probability analysis

The outage probability of FD relaying network is calculated as

$$P_{out} = \Pr(\gamma \leq Z), \tag{5.11}$$

where R is the target rate and $Z = 2^R - 1$.
Proposition 1:
The outage probability of the energy harvesting enabled two way full-duplex relay is derived as

$$P\{out\} = \Pr\left\{ \frac{\frac{P_S|h_1|^2 P_R|h_2|^2}{d_1^m d_2^m P_R|\widetilde{h}_r|^2}}{\frac{\sigma_n^2 P_S|h_1|^2}{P_R|\widetilde{h}_R|^2 d_1^m} + \frac{P_R|h_2|^2}{d_2^m} + \sigma_n^2} < Z \right\}$$
$$= 1 - \int_0^{1/\mu Z} 2\sqrt{\frac{d_1^m d_2^m Z\left(\frac{\sigma_n^2}{\mu} + \sigma_n^2 y\right)}{\lambda_s \lambda_d \left(P_S - \mu P_S Z y\right)}} K_1\left(2\sqrt{\frac{d_1^m d_2^m Z\left(\frac{\sigma_n^2}{\mu} + \sigma_n^2 y\right)}{\lambda_s \, lambda_d \left(P_S - \mu P_S Z y\right)}}\right) D, \tag{5.12}$$

where $D = \frac{1}{\lambda_r} e^{-\frac{y}{\lambda_r}} dy$ and $\lambda_s, \lambda_d, \lambda_r$ are the mean value of the exponential random variables $h_1, h_2, \widetilde{h}_R$, respectively and $K_1(x)$ is Bessel function defined as Eq. (8.423.1) in **[49]**.

Proof:

We denote $x = |h_1|^2 |h_2|^2$ and $y = \left|\widetilde{h}_R\right|^2$. Then we have:

$$P_{out} = \begin{cases} \Pr\left\{ x < \frac{d_1^m d_2^m Z\left(\frac{\sigma_n^2}{\mu} + \sigma_n^2 y\right)}{P_S - \mu P_S Z y} \right\}, & y < \frac{1}{\mu Z}. \\ 1, & y > \frac{1}{\mu Z}. \end{cases} \tag{5.13}$$

Interestingly, the cumulative distribution function of x can be calculated by

$$F_x(a) = \Pr(x < a) = 1 - 2\sqrt{a/\lambda_s \lambda_d} K_1\left(2\sqrt{a/\lambda_s \lambda_d}\right), \tag{5.14}$$

and $f_y(b) = (1/\lambda_r) e^{(b/\lambda_r)}$, y can be modeled with the Probability distribution function. Afterwards, the Proposition 1 is achieved after some simple manipulations.

Optimal throughput analysis

In the Proposition 1, when the relay harvests energy from the source information and uses that power to amplify and forward the source information to the destination, the outage probability of the considered system is a function of the energy harvesting time factor α, and varies when α increase from 0 to 1. In the delay-limited transmission protocol, the transmitter is communicating at a fixed transmission rate R bits/sec/Hz and $(1-\alpha)T$ is the effective communication time. Therefore, the throughput of the system is obtained as

$$\tau = (1 - P_{out}) R (1 - \alpha). \tag{5.15}$$

Unfortunately, it is difficult to derive optimal throughput mathematically, but we can obtain the optimal value by numerical methods as presented in the next section.

5.1.3 Numerical results

In this section, we use the derived analytical results to plot the outage probability, optimal throughput, optimal energy harvesting time. We set the source transmission rate $R = 3,\ 4,\ 5\ (bps/Hz)$, and hence, the outage SINR threshold is given by $Z = 2^R - 1$. The energy harvesting efficiency is set

to be $\eta = 1$, the path loss exponent is set to be $m = 3$. For simplicity, we set the distance $d_1 = d_2 = 1$. Also, we set $\lambda_s = \lambda_d = 1; \lambda_r = 0.1$. It can be seen from Fig. (5.3) that the outage probability varies with a different value of time-switching factor α. The outage probability is 1 when $\alpha = 0$, $\alpha = 1$ and this is the worst performance of the system. The outage is minimum approximately at $\alpha = 0.75, R = 3$. As we can observe, the analysis curves match perfectly with simulation curves.
As your observation, Fig. (5.4) examines the impact of energy harvesting time α on the optimal throughput of systems. The throughput is maximized approximately at $\alpha = 0.36$ for $R = 4$, and $\tau \approx 1.45$ is the optimal throughput. The throughput increases as α increases from 0 to optimal value α^*, however, it starts decreasing as α increases over its optimal value. This is because the values of α are smaller than the optimal α^*, there is less time for information transmission. Consequently, less time for forwarding the signal and smaller values of throughput are observed at the destination node due to outage probability increases. On the other hand, for the values of α greater than the optimal α^*, more time is wasted on energy harvesting and less time is available for information transmission. As a result, smaller throughput results are at the destination node due to a smaller value of $(1 - \alpha)$.

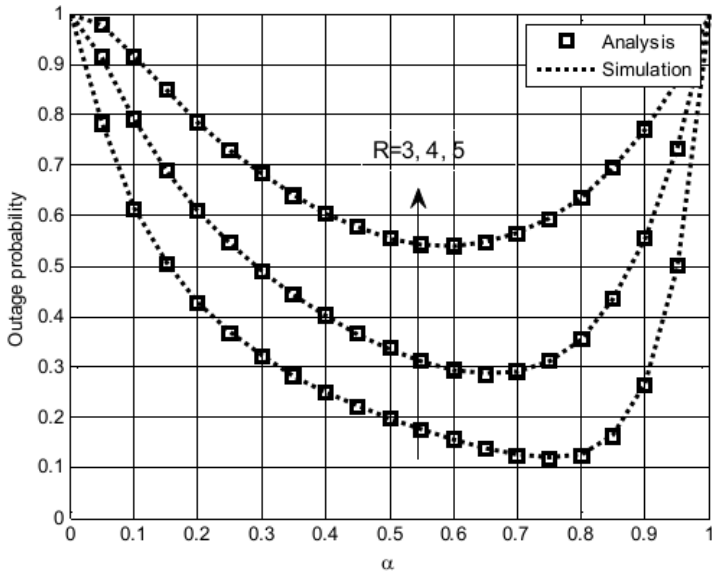

FIGURE 5.3: Outage probability of FD energy-aware relaying network.

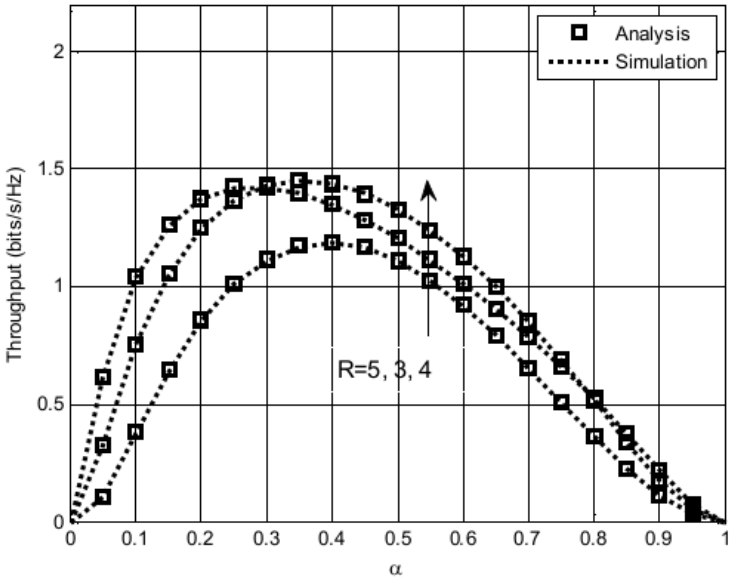

FIGURE 5.4: Optimal throughput of FD relaying.

In this part, we have proposed a full-duplex relaying network with wireless energy harvesting and information transfer protocol, where an energy-constrained relay node harvests energy from the received RF signal and uses that harvested energy to forward the source message to the other sources. To determine the achievable throughput, analytical expressions for the outage probability, and the optimal value of energy harvesting time in TSR protocol can be found by simulation.

5.2 An Optimal Analysis in Wireless Powered Full-duplex Relaying Network

The use of the regenerated energy in the next-generation wireless systems such as 5G cellular networks will bring about the considerable profits for the continuous operation in the wireless devices. Together with the other power resources such as solar and wind energy, the power which is drawn from the radio-frequency (RF) signals in the surrounding transmitters can be counted as the changes for the normal wired energy networks. Such energy harvested from the natural environment is a promising approach to maintain the lifetime of the energy-constrained wireless systems in **[56]**.
The simultaneous wireless information and power transfer (SWIPT) for the two-way relay transmission network, in which two resources reciprocate communication together over a power collecting relay is considered. By examining the time-switching (TS) relay receiving structure, the TS-based two-way relaying (TS-TWR) protocol was also introduced in **[57]**.
In those cases, a view of SWIPT networks with a special concentration on the hardware performance of rectifying circuits and real techniques which get the SWIPT in the areas of the time, space, energy, the antennas as well as the profits of a potential implementation of the SWIPT techniques in advanced information systems in the context of the source distribution and cooperative knowledge wireless systems was presented in **[58- 60]**.
Moreover, a cognitive wireless network with one primary user (PU) and

one secondary user (SU) and their transmitters operate with TSR is considered. The SU, which collects the power solely from the surrounding wireless signals, employs a save-then-transmit protocol. In that way, a scenario, the SUs maximal cooperation strategic method, called, maximal decision (to decide to work with the PU or not) and the maximal act (to consume how much time on the power collection and to distribute how much energy for the cooperative relay) is studied by previous works as in **[61- 65]**.
On the other hand, an amplify-and-forward (AF) relaying system, in that, the power-constrained relay node, which collected the power from the receiving RF signal, utilized that collected power to transmit the source information to the target, is studied. Relied on the time switching and power splitting receiving structures, two relaying protocols: i) the time switching based relaying (TSR) protocol and ii) the power splitting-based relaying (PSR) protocol are suggested, to collect the required energy to support the forwarding by the relay. Promoted by a model based on the classical cognitive radio (CR) system, an unprecedented way for the radio networks existing at the same time where the lower-energy mobiles in a second system, named, the secondary transmitters (STs), collects the surrounding RF energy from transferring by the transceiver operating neighboring places in the main system, named, primary transmitters (PTs), whereas occasionally accessing the spectrum authorized to PTs is studied. A random-geometry model, in which PTs and STs are allocated as the independent homogeneous Poisson point processes (HPPPs) and communicated with their potential transceivers at the familiar spaces, was proposed in **[31**; **66**; **68-72]**.
In fact, the authors in **[52]** indicated that the full-duplex mode is an attractive choice for fixed relays, provided that the loop interference power is maintained at a tolerable level. In addition, the authors in **[53]** presented the power allocation strategy to maximize the sum-rate of the FD-two-way relaying system under the realistic residual self-interference (RSI).
Recently, few research trends have been conducted in the FD relay system in the context of the SWIPT scheme. In **[51]**, the throughput is analyzed for three relay control schemes, including the maximum relay, optimal relay, and target relay. Analytical expressions for the outage probability and ergodic capacity are also presented for these considered relays control schemes. However, no work related to the optimal throughput has been considered for the application of a one-way FD relay in systems with RF energy harvesting.
Therefore, in this part, we analyze the outage probability and the throughput of full-duplex relaying with the novel ability of the simultaneous energy harvesting and information transfer. Based on these analytical expressions, the best model for optimal energy efficiency is given.
Our contribution in this part is to find out the optimal time fraction α_{max} value. From this result, we can recommend an optimal model for energy harvesting full-duplex relaying networks and prove that it satisfies the conditions for deployment in future cellular networks.

5.2.1 Optimal point for throughput

By simple replacement from Eq. (5.10), we get new formula as

$$\gamma_D = \frac{\gamma_{SD}\Omega\alpha(1-\alpha)}{(1-\alpha)^2 + \Omega^2\alpha^2\gamma_{LI}\gamma_{SD} + \sigma^2\eta\alpha\gamma_{LI}(1-\alpha)}, \tag{5.16}$$

or $\gamma_D = \frac{a_1\alpha(1-\alpha)}{a_2\alpha^2+a_3\alpha+1}$.
with

$$\begin{cases} a_1 = \gamma_{SD}\Omega \\ a_2 = 1 + \Omega^2\gamma_{LI}\gamma_{SD} - \sigma^2\Omega\gamma_{LI}, \\ a_3 = 2 + \sigma^2\Omega\gamma_{LI} \end{cases} \tag{5.17}$$

and

$$\gamma_{SD} = \frac{P_s|h|^2|g|^2}{d_1^m d_2^m \sigma^2} = SIN_S \frac{|h|^2|g|^2}{d_1^m d_2^m}, \tag{5.18}$$

where $SIN_S = \frac{P_s}{\sigma^2}$, $\gamma_{LI} = \frac{|\tilde{\tilde{f}}|^2}{\sigma^2}$. We find α to maximize SNR, subject to $0 < \alpha < 1$, taken the fact that $\gamma_D(\alpha)$ is a concave function. The optimal value can be found by solving the equation.

$$\frac{\partial\gamma}{\partial\alpha} = 0. \tag{5.19}$$

After some manipulations, we get:

$$\begin{cases} \alpha_1 = \frac{-1+\sqrt{1+a_2+a_3}}{a_2+a_3}, \\ \alpha_2 = \frac{-1-\sqrt{1+a_2+a_3}}{a_2+a_3}, \end{cases} \tag{5.20}$$

and see that only α_1 satisfies the condition $0 < \alpha < 1$. By substituting α_1 into Eq. (5.16), we obtain:

$$\begin{aligned} &\gamma_{D\max} = \frac{C_1C_2}{A_1+B_1}, \\ &where \\ &\begin{cases} A_1 = (3 + \Omega^2\gamma_{LI}\gamma_{SD})A_2. \\ A_2 = ((1 + \Omega^2\gamma_{LI}\gamma_{SD} - \sigma^2\Omega\gamma_{LI})(-1 + \sqrt{3 + \Omega^2\gamma_{LI}\gamma_{SD}}). \\ B_1 = (2 + \sigma^2\Omega\gamma_{LI})(-1 + \sqrt{3 + \Omega^2\gamma_{LI}\gamma_{SD}}) + B_2. \\ B_2 = 3 + \Omega^2\gamma_{LI}\gamma_{SD})). \\ C_1 = \gamma_{SD}\Omega(-1 + \sqrt{3 + \Omega^2\gamma_{LI}\gamma_{SD}}). \\ C_2 = (4 + \Omega^2\gamma_{LI}\gamma_{SD} - \sqrt{3 + \Omega^2\gamma_{LI}\gamma_{SD}}). \end{cases} \end{aligned} \tag{5.21}$$

5.2.2 Numerical Results

In this section, we use the derived analytical results to plot the outage probability, the optimal throughput, the optimal energy harvesting time. We set the source transmission rate $R = 3$ (bps/Hz), and hence the outage SINR threshold is given by $Z = 2^R - 1$. The energy harvesting efficiency is set to be $\Omega = 0.4$ (eliminate Fig. (5.7), Fig. (5.8)), $\sigma^2 = 0.1$ (exclude Fig. (5.9)), the path loss exponent is set to be $m = 3$. For simplicity, we set the distance $d_1 = d_2 = 1$ (exclude Fig. (5.5) and Fig. (5.6)). Also, we set $\lambda_s = \lambda_d = 1; \lambda_r = 0.1$, unless it is stated in different special cases. As we can observe, the analysis curves match perfectly with simulation curves.

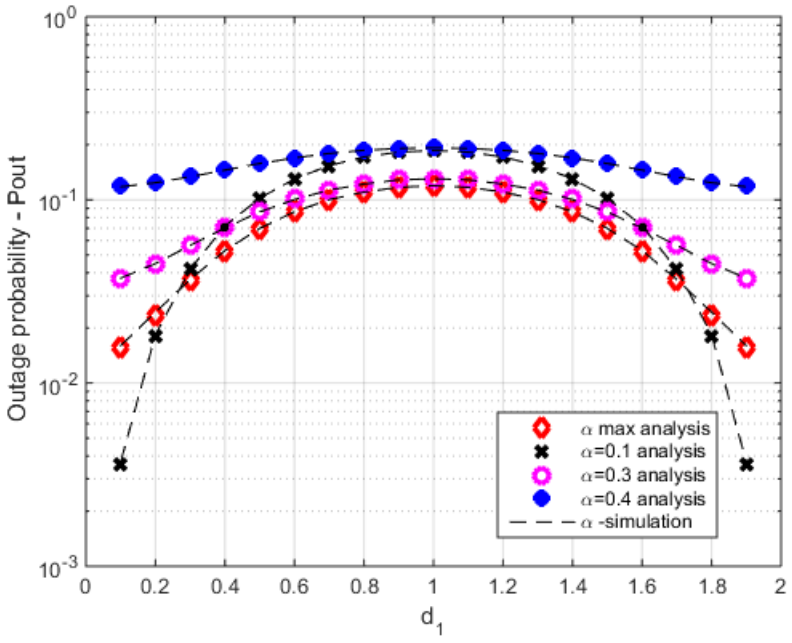

FIGURE 5.5: Outage probability of FD energy-aware relaying network versus distance.

From Fig. (5.5), the outage probability varies for different scenarios of time factor α values. The outage probability is minimized at approximately $\alpha = \alpha_{\max}$. Whenever α is as smaller than α_{max}, the higher the outage probability is. And the same thing happens when $\alpha > \alpha_{\max}$. In Fig. (5.6), it is clear that the throughput at $\alpha \leq 0.1$ is better than that of $\alpha_{\max}$. Of course, $\alpha_{\max}$ is the best value satisfying maximal SNR and remaining the acceptable outage probability when we employ this model.
In the above figures, we can see that the outage probability increases when d_1 increases and gets the maximum value at the midway point. The closer to the resource node the relay is, the smaller the outage probability gets. The thing happens reversely to the throughput. So the closer resource the relay locates, the better performance we get. In Fig. (5.7), the smaller Ω, the bigger outage probability, and this outage probability decreases when Ω increases. Moreover, we had seen that α affects to the outage probability, the smaller α is, the bigger outage probability we have. For the throughput, we have the opposite result in Fig. (5.8).
In general, we can see that with α smaller than $\alpha_{\max}$, its throughput is better than that of $\alpha_{\max}$. It is believed that because when α is as smaller, as bigger the information quantity is sent to the destination but its outage probability is very high, so that the operation of the system may be stopped at a higher level. The second reason is that when α is smaller, the necessary energy that is harvested by the relay does not have enough power to transmit the signal to the destination node. So, considering all the things, we find one thing that the model has the best performance for both maximal SNR and optimal throughput only with $\alpha_{\max}$.
The same scenarios occur when we investigate the outage probability and the throughput with respect to parameter σ, in Fig. (5.9). The bigger σ, the

bigger outage probability and the smaller throughput. Here, there is a little different thing, α is smaller or bigger than $\alpha_{\max}$, the bigger the outage probability is but when $\alpha \leq 0.1$, its throughput is better than that of $\alpha_{\max}$.

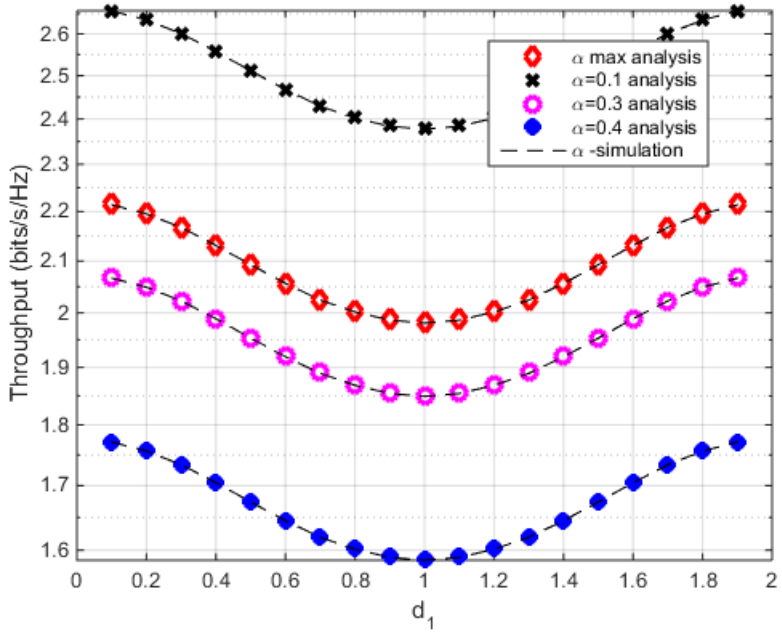

FIGURE 5.6: Throughput of FD relaying versus distance.

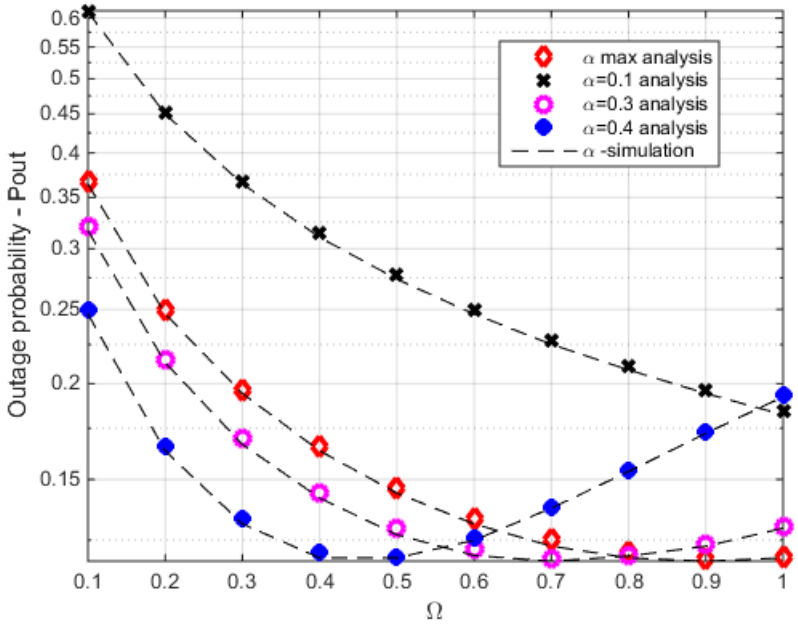

FIGURE 5.7: Outage probability of FD relaying network versus Ω.

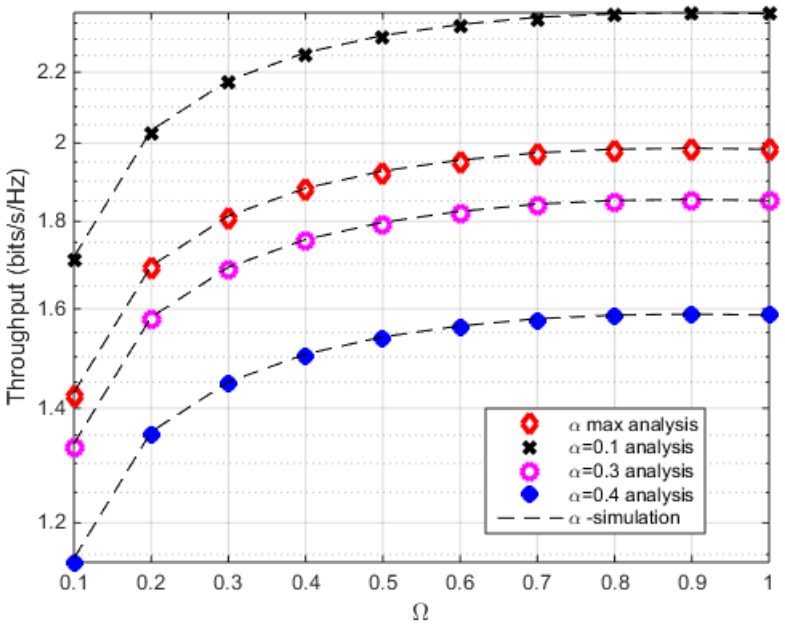

FIGURE 5.8: Throughput of FD relaying versusΩ.

In this part, we have proposed a full-duplex relaying network with wireless energy harvesting and information transfer protocol, where an energy-constrained relay node harvests energy from the received RF signal and uses that harvested energy to forward the source signal to the destination in delay-limited mode. In order to determine the achievable outage probability and throughput, the analytical expressions for the outage probability and throughput following the optimal value of the energy harvesting time in AF scheme of TSR protocol can be found by the simulation. As a result, we can see that the model deployed with $\alpha_{\max}$ becomes the optimal model that achieves the best performance.

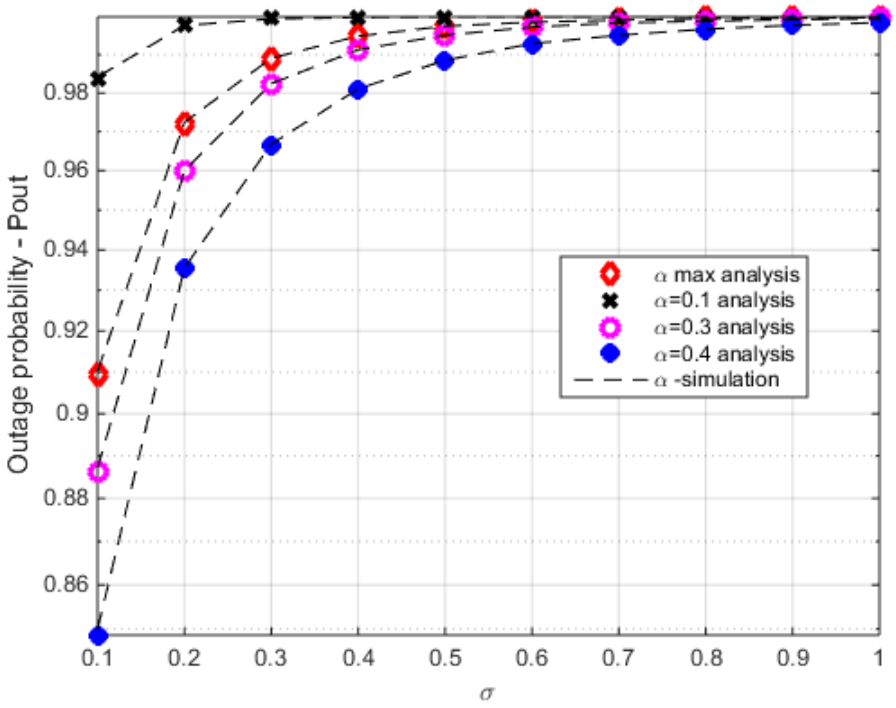

FIGURE 5.9: Outage probability of FD relaying network versus σ.

5.3 A Performance Analysis of AF and DF Mode in Energy Harvesting Full-Duplex Relay

In recent years, several radio system applications that require long lifetime are facing with an obstructive challenge on energy consumption. In order to determine the throughput, a delay-limited transmission mode is usually used to derive analytical expressions for outage probability and throughput. The simultaneous wireless information and power transfer (SWIPT) for two-way relaying has been introduced, in which two resources communicate together over a power-collecting relay. By examining the time switching relay (TSR) receiving structure, the TS-based two-way relaying (TS-TWR) protocol is introduced **[57- 59; 61]**.

There has been researching that deeply studied the interference from secondary uses (SUs) to primary receivers (PTs) and from PTs to SUs in cognitive radio networks. The secondary users are not only able to transmit a packet on a licensed channel to a primary user when the selected channel is idle or occupied by the primary user but also able to harvest RF (radio frequency) energy from the primary users' transmissions when the channel is busy **[31; 33; 63; 64]**.

In another situation, we investigate a decode-and-forward (DF) amplify-and forward (AF) relaying system relied on radio power collection. The power-constrained relay node early collects power over radio-frequency (RF) signals from the source node **[68; 70; 79]**.

5.3.1 DF mode

With DF, the relay decodes signal before re-transmitting it. So the transmitted signal from the relay can be expressed as follows.

$$x_R(i) = \begin{cases} Ky_R[i-\tau] \quad with\ AF\,, \\ \sqrt{\frac{P_R}{P_S}}x_S[i-\tau] \ \ with\ DF, \end{cases} \tag{5.22}$$

where τ accounts for the time delay occurred by relay processing.

By substituting Eq. (5.22), into Eq. (5.7), we get the received signal at the destination node as

$$y_{DFD} = \frac{g}{\sqrt{d_2^m}}\left(\sqrt{\frac{P_R}{P_S}}x_R(i-\tau)\right) + n_D. \tag{5.23}$$

Through some simple calculations, we get a new formula as

$$\gamma_{DF}^{FD} = \min\left(\frac{1}{\rho|\overset{\prec}{f}|^2}, \frac{\rho P_S|h|^2|g|^2}{d_1^m d_2^m \sigma^2}\right). \tag{5.24}$$

Proposition 2:
The outage probability of the energy-harvesting-enabled two-way full-duplex relaying with DF protocol is derived as

$$P_{out}^{DFO} = 1 - \left(1 - e^{\frac{1}{\rho\lambda_r Z}}\right)\left(2\sqrt{\frac{\sigma^2 d_1^m d_2^m Z}{\rho\lambda_s\lambda_d P_S}}\right) K_1\left(2\sqrt{\frac{\sigma^2 d_1^m d_2^m Z}{\rho\lambda_s\lambda_d P_S}}\right). \tag{5.25}$$

Proof:
The cumulative distribution function of x is computed by

$$F_x(b) = \Pr(x \le b) = 1 - 2\sqrt{b/\lambda_s\lambda_d}K_1\left(2\sqrt{b/\lambda_s\lambda_d}\right), \tag{5.26}$$

and y can be modeled with the probability distribution function $f_y(c) = (1/\lambda_r)\, e^{(-c/\lambda_r)}$.
We define $x = |h|^2|g|^2$ and $y = \left|\overset{\prec}{f}\right|^2$. From Eq. (5.24), we get:

$$P_{out}^{FDF} = Pr\left(\min\left(\frac{1}{\rho y}, \frac{\rho P_S x}{d_1^m d_2^m \sigma^2}\right) \le Z\right). \tag{5.27}$$

Then

$$P_{out}^{FDF} = 1 - Pr\left(\frac{1}{\rho y} \ge Z\right)\Pr\left(\frac{\rho P_S x}{d_1^m d_2^m \sigma^2} \ge Z\right), \tag{5.28}$$

where $Pr\left(\frac{1}{\rho y} \ge Z\right) = Pr\left(\frac{1}{\rho Z} \ge y\right) = \int\limits_0^{\frac{1}{\rho Z}} f_y(t)dt = \frac{1}{\lambda_r}\int\limits_0^{\frac{1}{\rho Z}} e^{-\frac{t}{\lambda_r}}dt$,
and $\Pr\left(\frac{\rho P_S x}{d_1^m d_2^m \sigma^2} \ge Z\right) = 1 - \Pr\left(x \le \frac{Z d_1^m d_2^m \sigma^2}{\rho P_S}\right) = 1 - F_x\left(\frac{Z d_1^m d_2^m \sigma^2}{\rho P_S}\right)$.

Based on Eq. (5.26), we have a desired result after some manual calculations and then the Proposition 2 is got through some simple manipulations.

5.3.2 Numerical results

In this section, we employ the derived results from analysis to offer perception into the variety of design options. The energy harvesting efficiency is set to be $\eta = 1$, the path loss exponent is set to be $m = 3$. For simplicity, we set $\lambda_s = \lambda_d = 1; \lambda_r = 0.1$ and $d_1 = d_2 = 1$ (except Fig. (5.12), Fig. (5.13)) as well as $\sigma = 1$ (except Fig. (5.10) and Fig. (5.11)).

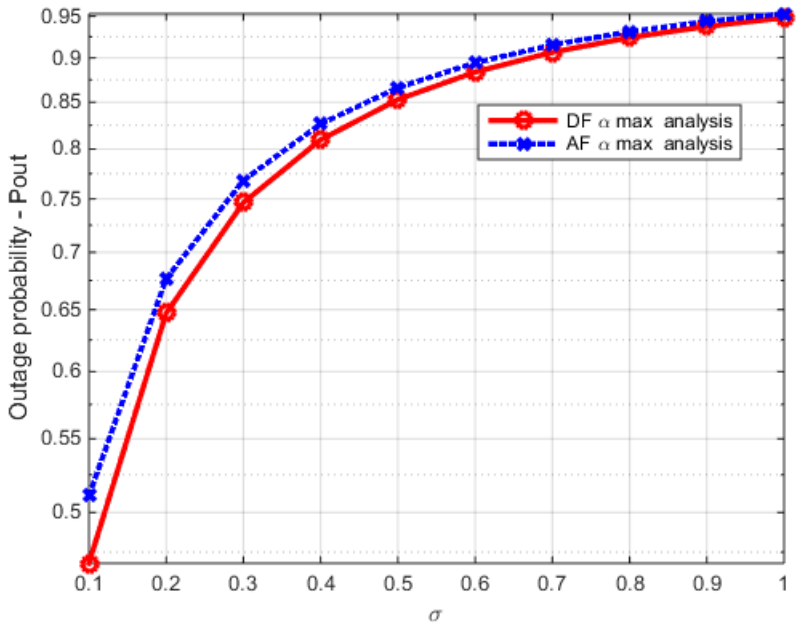

FIGURE 5.10: Outage probability of AF and DF relaying versus σ.

In Fig. (5.10) and Fig. (5.11), the outage probability of the DF model is still better than the AF model but its throughput is worse than AF. This is due to noise at the relay node that has an impact on system performance.
The same thing happens in Fig. (5.12) and Fig. (5.13), as bigger σ, as worse the outage probability of two models gets. We can see clearly that the outage probability of the DF model is better than that of the AF model, slightly and its throughput is better than, too. This is easy to explain because of noise at the relay node, which has an impact on system performance.

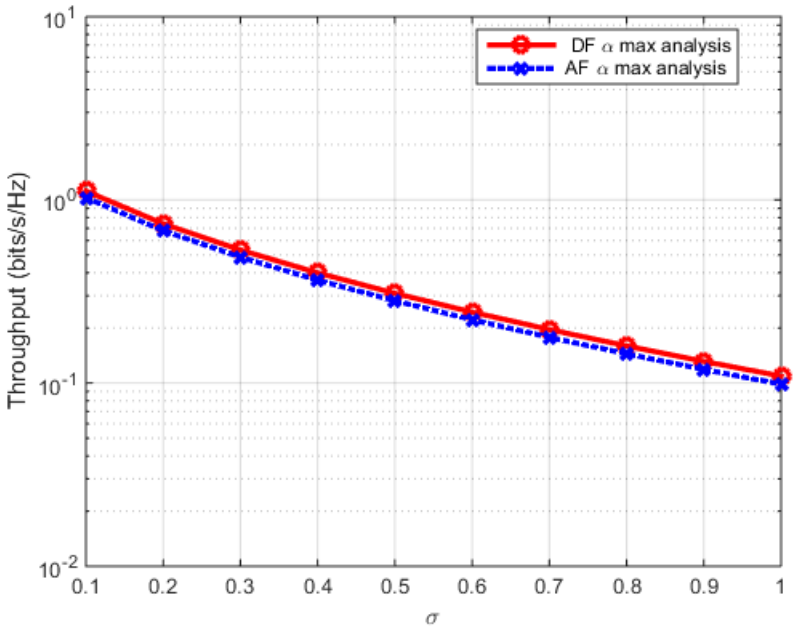

FIGURE 5.11: Throughput of AF and DF relaying versus σ.

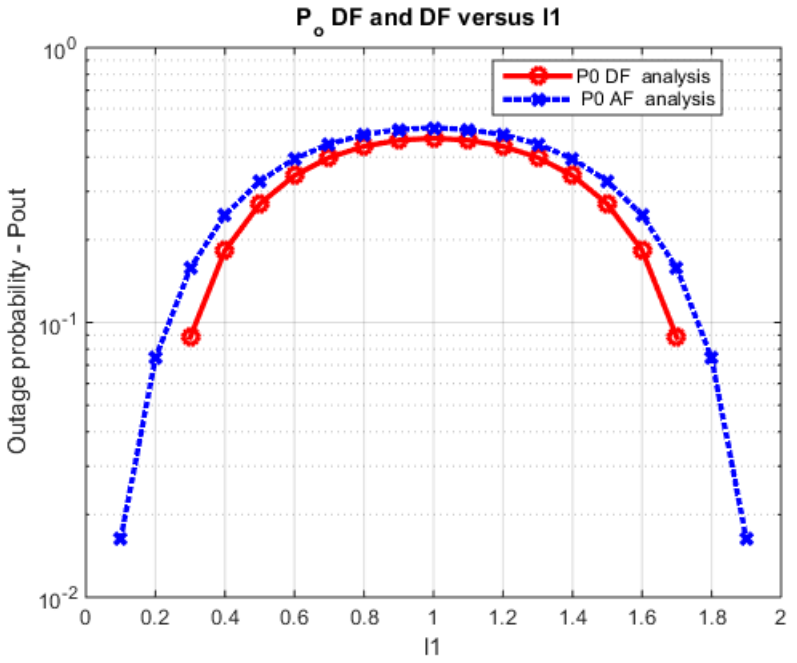

FIGURE 5.12: Outage probability of AF and DF model versus distant.

In this part, the mathematical and numerical analysis have shown practical insight of full-duplex relaying system in term of the effect of different system parameters on the performance of wireless energy collecting and information processing system, which employs AF and DF relay modes. The throughput results in this paper account for the upper bound on the realistically attainable throughput. Moreover, we also find that the AF model

outperforms the DF model in the delay-limited scheme of full-duplex relaying network.

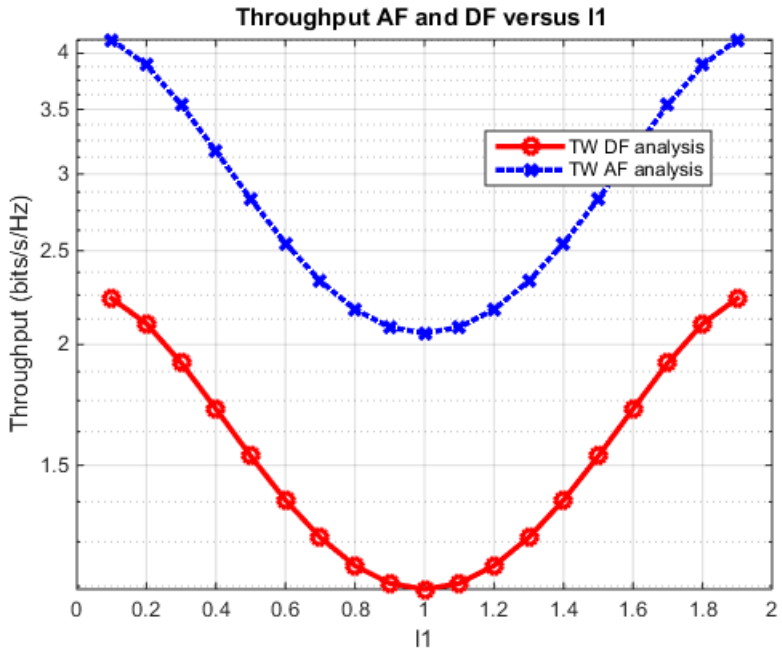

FIGURE 5.13: Throughput of AF and DF model versus distant.

5.4 A Performance Analysis of a Propagation Two-Hop Model in the Cooperative Relaying Network

Using the physical model in life, at present, brings a lot of benefits, especially in the communication area. The EH protocol with a two-hop model has emerged as a promising suitable technology with wireless cooperation as well as the sensory systems to operate in the surrounding environment with the technical and economic limitations. The employment of the energy harvesters, instead of the normal power sources, in wireless cooperative communication, was considered in **[57; 72]**. For the aim of the presentation, the basic three-node Gaussian relay channel with the relaying system, in which the source and relay nodes transfer the data with the energy drawn from the energy-collecting sources is investigated by the authors in **[37; 58]**, where an efficient secure relay beamforming (SRB) algorithm to firstly gets the time fraction rates in an allocated manner and after that interactively adjust to the transfer beam and the AF factors, is also devised in **[69; 70]**. Furthermore, the RF energy harvesting technology is a promising model to keep the operations of the wireless networks. In cognitive radio systems, a second user can be installed with the RF energy harvesting capacity **[29; 61]**. Such a network where the second user can make the channel access to transmit a packet or to harvest the RF energy when the selected channel is idle or occupied by the first user is also investigated in **[62; 63]**, respectively. In this part, we consider a wireless two-hop relaying system employing TSR protocol to build a simultaneous wireless power and information transfer (SWIPT) scheme. To optimize the outage probability and to maximize

the throughput, we use a numerical method to study system performance. Here, it can be seen clearly that the DF model outperforms that of the AF model.

5.4.1 Network Model

Our radio TSR system has two hops, in the first hop, a source, named, S, transfers its information to a relay, named, R. In the next, the relay transmits its received signal to the destination, named, D. Assuming that there is a great distance between S and D, so there is no direct link connecting S and D. A relay operating in TSR scheme uses the collected energy to transfer the information to the destination, as given in Fig. (5.14), the distance between $S - R$ denoted by d_1, and the distance between $R - D$ denoted by d_2.

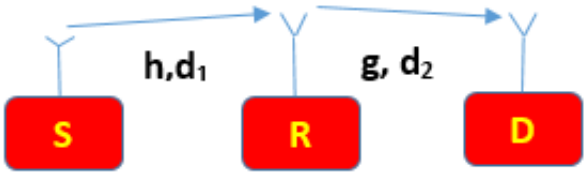

FIGURE 5.14: Throughput of AF and DF model versus distant.

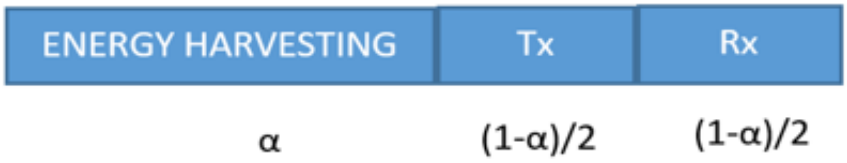

FIGURE 5.15: The parameters of TSR protocol.

As shown in the TSR protocol proposed in Fig. (5-15), the propagation process has two slots. For the first slot, the energy transmits from S to R during a time interval of $\alpha T, (0 < \alpha < 1)$ and for the remaining time slot, $(1 - \alpha) T$ is employed to transmit data, $(1 - \alpha) T/2$ for the information transfer from S to R, another $(1 - \alpha) T/2$ for information transmission from R to S. Here, α is a time-switching factor and T is the duration of the entire signal block.

During the energy harvesting phase, the relay receiving signal at the relay is:

$$y_R = \sqrt{\frac{P_S}{d_1^m}} h x_S + n_R, \tag{5.29}$$

where P_S is the source transmission energy, n_R is the additive white Gaussian noise coefficient at R with zero-mean and variance of σ_R^2.
The harvested power at the relay is given by **[82]**

$$E_h = \eta \alpha T \frac{P_S |h|^2}{d_1^m}, \tag{5.30}$$

where m is the exponential path loss factor, η is the power conversion factor, and h, g are the channel gain factors between the source-relay and the relay-destination link.
In the information transfer phase, assume that S transfers the signal x_S to R and R forwards the signal x_R to D. Both signals have unit energy and zero–mean, i.e., $E\left[|x_j|^2\right] = 1$ and $E[x_j] = 0,\ j = S, R$, respectively. And then the power transmitted by R is given as **[83]**

$$P_R = \frac{E_h}{(1-\alpha)\,T/2} = 2\mu P_S \frac{|h|^2}{d_1^m}, \tag{5.31}$$

where $\mu = \frac{\alpha\eta}{1-\alpha}$.
For AF scheme, we have:

$$x_R = H y_R, \tag{5.32}$$

where H is an amplification coefficient determined by

$$H = \sqrt{\frac{P_R}{\frac{P_S}{d_1^m}|h|^2 + \sigma^2}}. \tag{5.33}$$

Then, we get the received signal at destination as:

$$y_D = \frac{g}{\sqrt{d_2^m}} x_R + n_D. \tag{5.34}$$

For DF scheme, we get:

$$x_R = \sqrt{\frac{P_R}{P_S}} x_R(i-\tau). \tag{5.35}$$

Following **[20]**, we have:

$$y_D = \frac{g}{\sqrt{d_2^m}} \left(\sqrt{\frac{P_R}{P_S}} x_R(i-\tau) \right) + n_D, \tag{5.36}$$

where n_D is the additive white Gaussian noise at the destination node with zero-mean and variance of $\sigma_D^2 = \sigma_R^2 = \sigma^2$, for simplicity.
On the other hand, the instantaneous received SINR at D through R is calculated as

$$\gamma = \frac{E\left\{|signal|^2\right\}}{E\left\{|noise|^2\right\} + E\left\{|RSI|^2\right\}}. \tag{5.37}$$

So, through some simple calculations, we obtain:

$$\gamma_{AF} = \frac{\frac{P_S|h|^2 P_R|g|^2}{d_1^m d_2^m \sigma^2}}{\frac{P_S|h|^2}{\sigma^2 d_1^m} + \frac{P_R|g|^2}{d_2^m \sigma^2} + 1}, \tag{5.38}$$

and

$$\gamma_{DF} = \min\left(\frac{P_S|h|^2}{d_1^m \sigma^2}, \frac{2\mu P_S |h|^2 |g|^2}{d_1^m d_2^m \sigma^2} \right). \tag{5.39}$$

5.4.2 Outage Probability and Throughput Analysis

In this section, we investigate the outage probability and the throughput of two-hop relaying with energy harvesting and information transfer. Based on analytical expressions, the outage probability and the throughput of this model are extracted and the best model for the energy harvesting-based relaying network is also obtained.

The Outage probability analysis

The outage probability of the two-hop relaying system in delay-limited mode is computed as

$$P_{out} = \Pr\left(\gamma \leq Z\right), \tag{5.40}$$

where R is the transmission rate and $Z = 2^R - 1$.
Proposition 3:
The outage probability of the energy harvesting enabled AF relay is extracted as

$$\begin{aligned} P_{AF} &= \Pr\left\{ \frac{\frac{P_S|h|^2 P_R|g|^2}{d_1^m d_2^m \sigma^2}}{\frac{P_R|g|^2}{\sigma^2 d_2^m} + \frac{P_S|h|^2}{d_1^m \sigma^2} + 1} \leq Z \right\} \\ &= 1 - \tfrac{1}{\lambda_S} \int_{Z/P_S}^{\infty} \exp\left(-\frac{x}{\lambda_S} - \frac{Z(\frac{xP_S}{\sigma^2 d_1^m} + 1)}{\lambda_D(\frac{2\mu P_S^2 x^2}{d_1^m d_2^m \sigma^2} - \frac{2\mu Z P_S x}{d_1^m d_2^m \sigma^2})} \right) dx. \end{aligned} \tag{5.41}$$

Proof:
We denote $x = |h|^2$ and $y = |g|^2$. Based on statistical property of *cdf* and *pdf* $f_y(b) = (1/\lambda_r)\, e^{(b/\lambda_r)}$ and $F_{|h|^2}(b) = \Pr\left(|h|^2 \leq b\right) = 1 - e^{\frac{-b}{\lambda_h}}$, and from Eq. (8.423.1) in **[49]**, Proposition 3 is obtained after some simple manipulations.

Assume that λ_h, λ_g are the mean of the exponential random variable $|h|^2, |g|^2$ and the channel gains $|h|^2, |g|^2$ are the independent and identically distributed (i.i.d.) exponential random variables.
Proposition 4:
The outage probability of the energy harvesting enabled DF relay is expressed as:

$$P_{DF} = 1 - e^{\frac{\sigma^2 d_1^m z}{\lambda_s P_S} - \frac{d_1^m}{2\lambda_d \mu}} - \frac{1}{\lambda_d} \int_0^{\frac{d_2^m}{2\mu}} e^{\frac{\sigma^2 d_1^m d_2^m z}{2\mu \lambda_s P_S x}} e^{-\frac{x}{\lambda_d}} dx. \tag{5.42}$$

Proof:
From Eq. (5.39), Eq. (5.40), we get:

$$P_{DF} = \Pr\left(\frac{P_S|h|^2}{d_1^m \sigma^2} \min\left(1, \frac{2\mu|g|^2}{d_2^m}\right) \leq Z \right). \tag{5.43}$$

For the time being, from conditioning on $y = \min\left(1, \frac{2\mu|g|^2}{d_2^m}\right)$, we have $P_{DF} = 1 - e^{\frac{\sigma^2 d_1^m Z}{\lambda_s P_S y}}$. Averaging over y provides the expected result.

The throughput analysis

In Proposition 3 and Proposition 4, the outage probabilities of two models are investigated. In the delay-limited transmit protocol, the transmitter propagates information at a fixed transmission rate R bits/sec/Hz and $(1-\alpha)T$ is the effective information time. So, the throughput of the two-hop system is given as:

$$\tau = (1 - P_{out})\, R \frac{(1-\alpha)}{2}. \tag{5.44}$$

Unhappily, it is difficult to draw out the maximal throughput mathematically, but we can reach that value by the numerical method as illustrated in the next section.

5.4.3 Numerical Results

In this section, we employ the derived analytical results to study the outage probability as well as throughput of two models. We set the source transmission rate $R = 3\ (bps/Hz)$, $\alpha = 0.3$ (except for Fig. (5.16)). The energy efficiency coefficient is set to be $\eta = 0.4$ (except for Fig. (5.18)), the path loss exponent factor is set to be $m = 3$. For simplicity, we set the distance $d_1 = d_2 = 1$ (except for Fig. (5.17)). Also, we set $\lambda_s = \lambda_d = 1; \lambda_r = 0.1$ and $P_S(dB) = 10$, $\sigma^2 = 0.1$. These factors are chosen because they give the best asymptotic curves.

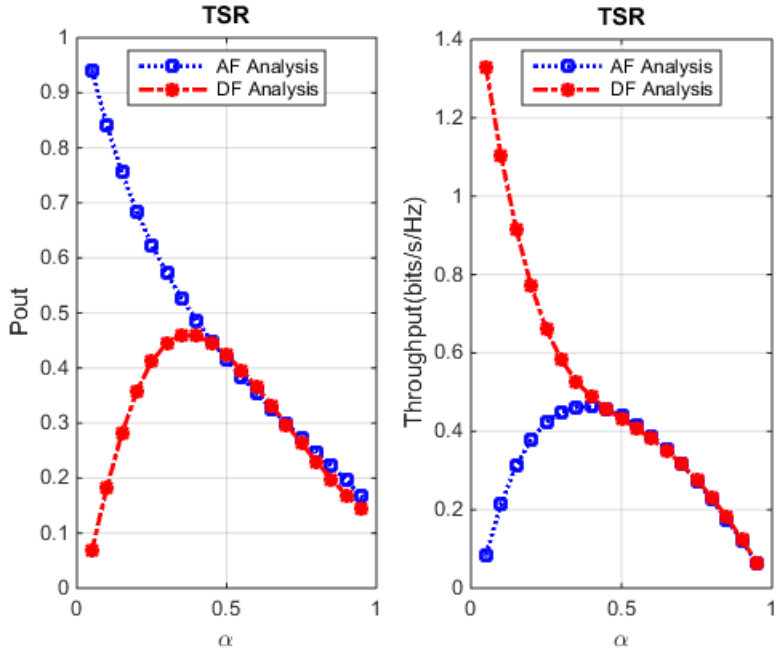

FIGURE 5.16: The outage probability and throughput of AF and DF model versus α.

Fig. (5.16) reveals that the time-switching factor affects system performance. When α changes form 0 to 1, the outage probability and throughput of two models also change. In this case, when $\alpha \leq 0.4$, the DF outage probability is better than that of the AF model but when $\alpha \geq 0.4$, the curves of two

models overlap. In both cases, the DF throughput is always better than that of the AF model. This is proven that as big α, as much information to send to the destination. This helps them to overcome the effect of the noise.

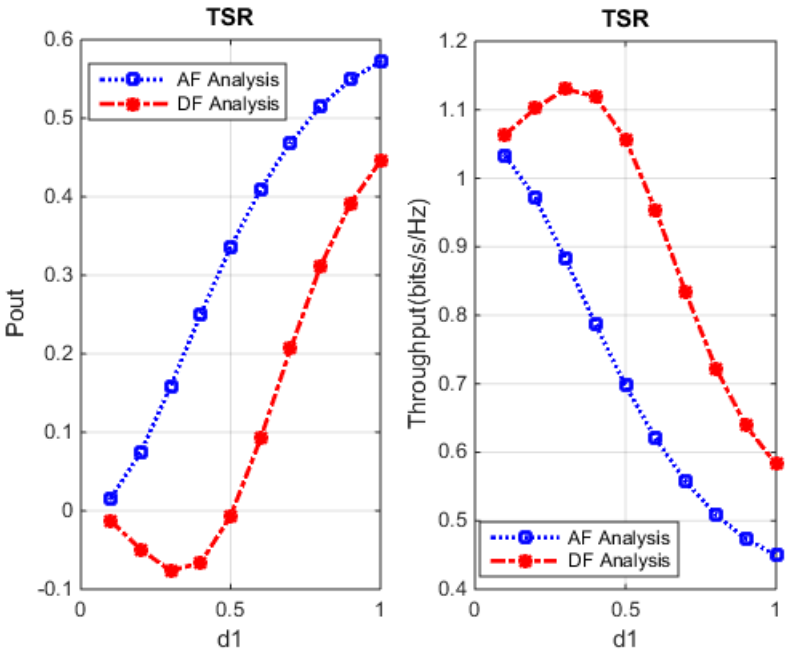

FIGURE 5.17: The outage probability and throughput of AF and DF model versus d_1.

Fig. (5.17) displays the outage probability and throughput of two models versus the relay position. In the evaluation, we set $d_1 + d_2 = 2$, and d_1 varies from 0 to 2. As described in Fig. (5.17), for both models, the best outage probability is attained. Therefore, the relay is put close to the source or destination to achieve the optimal outage probability. Two suggested models have the worst outage probability at midway. Moreover, Fig. (5.17) shows that the DF model gets the better outage probability performance that of the AF model. Otherwise, the throughput of the DF model outperforms that of the AF one, it has the optimal value near the midway between S and R. This is easy to understand because the noise near the relay has an impact on system performance.

It can be shown in Fig. (5.18) that η has an impact on the outage probability and throughput of both models. When $\eta \leq 0.65$, the DF throughput and outage probability are better than that of the AF model. But as $\eta \geq 0.65$, the interesting thing occurs, i. e, the curves of their outage probability and throughput nearly coincide together. It is easy to explain because the bigger η is the more power at the relay helps them to send information to the destination easily, not affected by noise.

In this part, we have investigated two-hop relaying systems with the radio energy harvesting and information transfer protocol, in which an energy-constrained relay node harvests the energy from the received RF signal and employs that harvested power to forward the information to the destination. Hereby, their operation is compared. To determine the best model, the analytical expressions for the outage probability and throughput in TSR

protocol can be found by the simulation approach. As expected, through simulations, it is known that the DF model outperforms AF one in a two-hop relaying network, and the DF relaying system could normally improve the throughput performance.

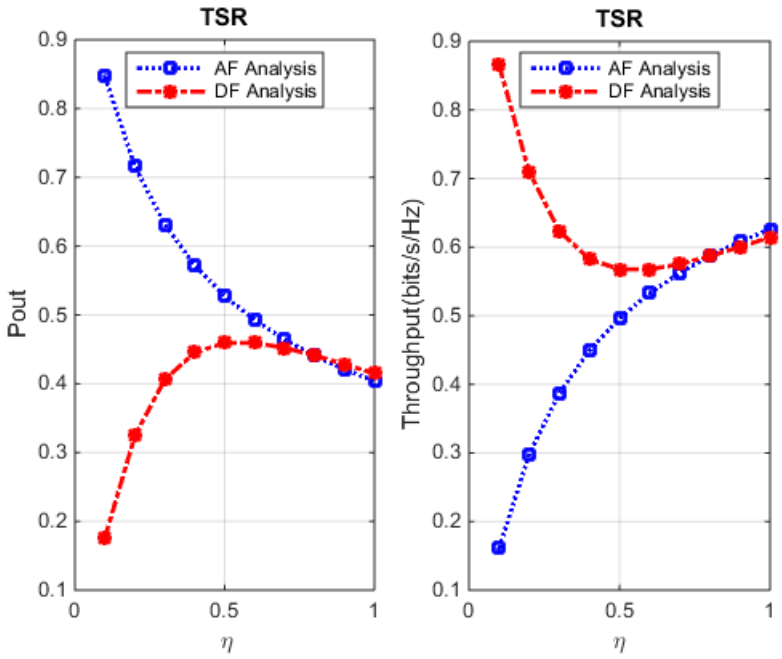

FIGURE 5.18: The outage probability and throughput of AF and DF model versus η.

5.5 Summary

In this chapter, the performance of EH for the FD relaying network with various antenna configurations and transmission protocols, including TSR and PSR EH protocols as well as AF and DF relaying strategies, was investigated. Specifically, with the deployment of a low-complexity EH model and the achievement of optimal TS ratio, the relay could operate continuously without battery replacement or being charged by using the energy collected from the received signal. Regarding system performance analysis, we provided the close-form expressions for OP and throughput in the above-mentioned protocols. On the other hand, a comparison between analytical and simulation results is conducted. Our simulation results matched well with the exact expressions for OP. In addition, we also provided insights into the impact of several parameters, i.e., the position of the relay, TS ratio, PS ratio, the energy conversion factor on the system OP, and throughput.

6 Study of energy harvesting performance in full-duplex relay networks with various antenna configurations at relay

This chapter shows the details of what have been carried out to achieve Aim 2 in Chapter 4. I also conduct the performance analysis of EH FD relaying system in two different antenna configurations here. For the first antenna configuration, the relay node uses one antenna to harvest energy from the source node and another antenna to forward the information signal to the destination. For the second configuration, both antennas at relay nodes are employed to harvest energy from the sources during the EH phase, but during the information transfer, only one is used to receive information from the source while the other antenna is used to forward that information to the destination. For both cases, analytical expressions are derived for outage probability and throughput of the system. The impact of different parameters such as the position of the relay, noise level at the relay and destination, energy conversion factor, and TSR or PSR parameters on the system performance are also studied in detail **[TNK08**; **TNK09**; **TNK21]**. To enhance the transmission efficiency, multiple-antenna configuration and antenna selection algorithms are applied **[TNK03**; **TNK05**; **TNK06**; **TNK16**; **TNK17]**. Besides, three diversified techniques are considered in my dissertation to better exploit the best quality from MIMO communications: TZF, RZF, and MRC **[TNK04]**.

6.1 A Performance Analysis in Energy Harvesting Full-Duplex Relay with two antennas

In recent times, the radio system applications required longer lifetime activities, so there is an impediment challenge on energy consumption. The simultaneous wireless information and power transfer (SWIPT) for system-decoded duplex relay model has been investigated from an information theory viewpoint, in which two sources exchange information via energy harvested. By considering the time -switching relay (TSR) mechanism, the TS-based two-way relaying (TS-TWR) protocol has been given by the authors in **[31**; **57-59]**.

Next, in **[61**; **63**; **64**; **68]**, careful researches have been conducted on the noise from secondary uses (SUs) to primary receivers (PTs) and from PTs to SUs. In cognitive radio networks, the secondary users are not only able to transfer a packet on a channel licensed to a primary user when the selected

channel is idle or taken place by the primary user but also harvest RF (radio frequency) energy from the primary users' transmissions when the channel is busy.
Alternatively, in **[33**; **70**; **79]** the energy-constrained relay node early that harvests energy over the radio-frequency (RF) signals sent by the source node has been investigated.
In this part, we study a decode-and-forward (DF) and amplify-and forward (AF) relaying systems based on radio energy harvesting and then compare the performances. From that, we select a proper model to use depending on specific conditions to obtain the best benefit.

6.1.1 System model

This section shows the Time Switching Relaying (TSR) protocol and investigates the expressions for the outage probability and throughput, which are derived for the delay-limited transmission mode. Here, we consider the case in which two antennas at relay collect energy at the same time in the energy harvesting stage.

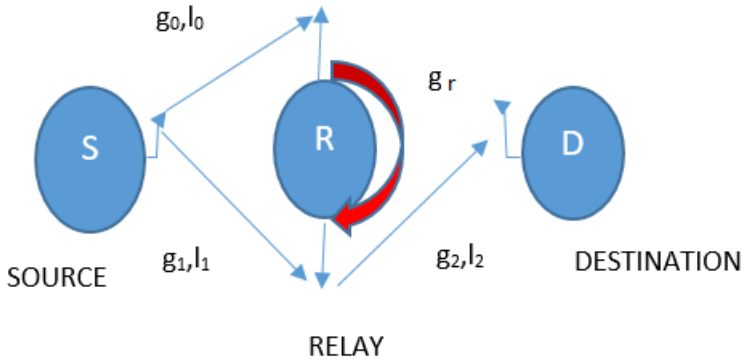

FIGURE 6.1: System model of one way full-duplex relaying.

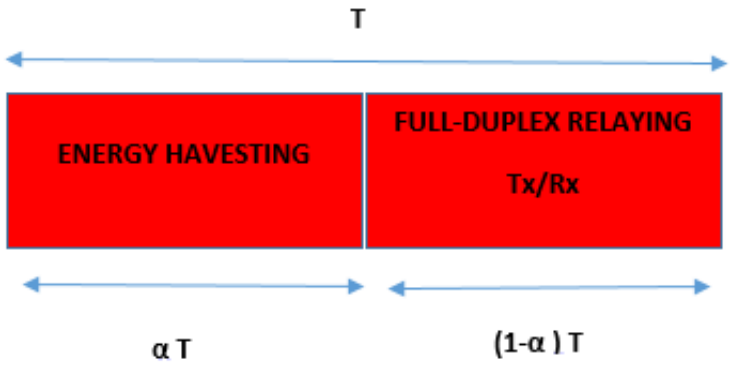

FIGURE 6.2: The parameters of TSR protocol.

As in Fig. (6.1), a proposed model has three nodes. We denote the source node by S, the destination node by D, and the relay node by R. Two antennas are set up at each node, one antenna is used for the signal transmission and another one is used for the signal reception. The relay is assumed to

be power-constrained equipment, so it could collect energy from the source signals, and utilizes that power to transmit the information to the destination. Terms g_0, g_1, and g_2 respectively represent the block-fading channel gain from the source to the two-antennas relay and the relay to the destination. Besides, terms l_0, l_1, and l_2 denote the distances from the source to the two-antennas relay and from the relay to the destination, respectively. For simplification, we assume $l_0 = l_1$. The system mode for TSR protocol is shown in Fig. (6.2).

The information process is divided into two stages. At first, the energy is transferred from the source to the relay within an interval of $\alpha T, (0 < \alpha < 1)$, and the remainder, $(1-\alpha)\,T$ is employed to convey the information with α is a time switching factor and T is the duration of on a transmission block as in **[83]**. During the energy harvesting stage, the received signal at the relay node can be expressed as

$$y_R = \sqrt{\frac{P_S}{l_1^m}} \begin{pmatrix} g_0 \\ g_1 \end{pmatrix} x_S + n_R, \tag{6.1}$$

where P_S is the source transmit power while m is the path loss exponent.
In this work, we assume a normalized path loss model to show the path loss degradation effects on system performance. For simplicity, n_R and n_D are zero mean additive white Gaussian noise (AWGN) with variance N and $E\left\{n_R n_R^\dagger\right\} = NI$ with I is the identity matrix. Regarding the radio energy harvested at the relay, we get:

$$E_h = \eta\alpha T \frac{P_s(|g_1|^2 + |g_0|^2)}{l_1^m}, \tag{6.2}$$

where η is the energy conversion efficiency.
In the information transfer phase, the following **[83]**, we assume that the source node transfers the information signal x_S to R and R forwards the signal x_R to the destination. The unit energy and zero mean are assumed, i.e., $E\left[|x_S|^2\right] = 1$, $E\left[|x_R|^2\right] = 1$ and $E\left[x_S\right] = 0$, $E\left[x_R\right] = 0$. So, we receive the signal at the relay under the self-interference as:

$$y_R = \sqrt{\frac{P_S}{l_1^m}} x_S(g_1 + g_0) + \overleftarrow{g}_r + n_R, \tag{6.3}$$

where $\overleftarrow{g}_r$ is the residual self-interference (RSI) component at R.
In this part, we investigate both AF and DF schemes in the duplex relaying system. In the AF model, the relay magnifies signal with an amplification factor:

$$K^{-1} = \sqrt{\frac{P_S}{l_1^m}(|g_1|^2 + |g_0|^2) + P_R\left|\overleftarrow{g}_r\right|^2 + N}. \tag{6.4}$$

For DF model, the relay decodes signal then re-transmits it to the destination. Hence, it can be better expressed as follows:

$$x_R(i) = \begin{cases} K\, y_R[i-\tau] & \text{with AF}, \\ \sqrt{\frac{P_R}{P_S}} x_S[i-\tau] & \text{with DF}, \end{cases} \tag{6.5}$$

where τ accounts for the time delay due to relay processing.
It is worth seeing that R uses all of the harvested energy to assist the activity for the next transmission, so P_R is given by

$$P_R = \frac{E_h}{(1-\alpha)\,T} = \rho P_S \frac{(|g_1|^2 + |g_0|^2)}{l_1^m}, \tag{6.6}$$

where ρ is denoted as $\rho = \frac{\alpha\eta}{1-\alpha}$. Therefore, the received signal at the destination can be expressed as

$$y_D(k) = \frac{g_2}{\sqrt{l_2^m}} x_r[k] + n_D[k]. \tag{6.7}$$

For AF, we have:

$$y_D\,(k) = \underbrace{\frac{g_2}{\sqrt{l_2^m}} K \sqrt{P_R} \frac{g_1\sqrt{P_S}}{\sqrt{l_1^m}} x_S}_{signal} + \underbrace{\frac{g_2}{\sqrt{l_2^m}} K \sqrt{P_R} \overset{\prec}{g}_r x_R}_{RSI} + \underbrace{\frac{g_2}{\sqrt{l_2^m}} K \sqrt{P_R} n_R + n_D}_{noise}. \tag{6.8}$$

With DF, we obtain:

$$y_D(t) = \sqrt{P_R} g_2 x_S(t-\tau) + n_D(t). \tag{6.9}$$

In the previous results, we determine the instantaneous received SINR at D over R as

$$\gamma = \frac{E\left\{|signal|^2\right\}}{E\left\{|noise|^2\right\} + E\left\{|RSI|^2\right\}}. \tag{6.10}$$

We get:

$$\gamma_{AF} = \frac{\frac{P_S |g_1|^2 |g_2|^2}{l_1^m l_2^m \left|\overset{\prec}{g}_r\right|^2}}{\frac{N|g_1|^2}{\rho P_R (|g_0|^2 + |g_1|^2)\left|\overset{\prec}{g}_r\right|^2} + \frac{\rho P_S (|g_0|^2 + |g_1|^2)|g_2|^2}{l_1^m l_2^m} + N}. \tag{6.11}$$

Assume that the channel gains $|g_0|^2, |g_1|^2, |g_2|^2$ are independent and identically distributed (i.i.d.) exponential random variables.

6.1.2 The Outage Probability and Throughput Analysis

In this section, we compare the outage probability and throughput of the full-duplex relaying with energy harvesting and information transmission using AF and DF modes. Based on that analytical expressions, we can easily see that some factors have an impact on the performance of the system and we can suggest using this method to deploy them in different situations.

The outage probability analysis

The outage probability of FD relaying network in the delay-limited mode is computed in **[83]**

$$P_{out} = \Pr\left(\gamma \leq H\right), \tag{6.12}$$

where R is a target rate and $H = 2^R - 1$.

Proposition 5:

The outage probability of the one way full-duplex relay network with energy harvesting and AF protocol is given as

$$P_{out}^{AF} = 1 - \int_{\rho H}^{\infty} 2\frac{Nl_1^m l_2^m H\left(\frac{t}{\rho}+1\right)}{\lambda_s\lambda_d\left(tP_S - \rho P_S H\right)} K_2\left(2\sqrt{2\frac{Nl_1^m l_2^m H\left(\frac{t}{\rho}+1\right)}{\lambda_s\lambda_d\left(tP_S - \rho P_S H\right)}}\right) B(t), \tag{6.13}$$

where $B(t) = (\lambda_r - (\lambda_r - \frac{1}{t})e^{-\frac{1}{\lambda_r t}}dt$, and $\lambda_s, \lambda_d, \lambda_r$ are the mean value of the exponential random variables $g_0, g_1, g_2, \overset{\prec}{g}_r$, respectively and $K_2(x)$ is Bessel function defined as Eq. (8.423.1) in **[91]**.

Proof:

We denote $U = \frac{X+Y}{Y}$ and $V = X + Y$ with $X = |g_0|^2$ and $Y = |g_1|^2$, where U and V are established independent random variables. Interestingly, the joint distribution function of X and Y is expressed as:

$$f_{X,Y}(x,y) = \frac{1}{\lambda_S^2} e^{-\frac{x+y}{\lambda_S}}, \tag{6.14}$$

and on the other hand, we see that $X = UV$ and $Y = V(1-U)$. Using Jacobian transformer (U,V) back to (X,Y),

$$f_{U,V}(u,v) = \frac{v}{\lambda_S^2} e^{-\frac{v}{\lambda_S}}.$$

So we can see clearly that U and V are independent, and U is following the uniform distribution with *pdf*: $f_U(u) = 1, 0 \le U < 1$ and V is following the gamma distribution with *pdf*:

$$f_V(v) = \frac{v}{\lambda_S^2} e^{-\frac{v}{\lambda_S}}.$$

At last, let $W = V|g_2|^2$ and $T = \frac{U}{|\overset{\prec}{g}_r|^2}$, $F_W(w) = 2\frac{w}{\lambda_S\lambda_D}K_2(2\sqrt{\frac{w}{\lambda_S\lambda_D}})$, $F_T(t) = \lambda_r t(1 - e^{-\frac{1}{\lambda_r t}})$ is got. From the statistical property of W and T, we get:

$$P_{out}^{AF} = \Pr(\gamma_{AF} \le H) = \begin{cases} \Pr\left(W \le \frac{\frac{TH}{\rho}+H}{\frac{TP_S}{Nl_1^m l_2^m} - \frac{H\rho P_S}{Nl_1^m l_2^m}}\right), & T > \rho H. \\ 1, & T < \rho H. \end{cases} \tag{6.15}$$

We have an expected result after some simple manipulations.

Proposition 6:

The outage probability of the full-duplex relay network with energy harvesting and DF protocol is given as:

$$P_{out}^{DF} = 1 - (1 - \rho\lambda_r H(1 - e^{\frac{-1}{\rho\lambda_r H}})) \times (\int_{\rho H}^{\infty} \frac{2l_1^m l_2^m HN}{\lambda_s\lambda_d\rho P_S H} \times K_2\left(2\sqrt{\frac{l_1^m l_2^m HN}{\lambda_s\lambda_d\rho P_S H}}\right). \tag{6.16}$$

Proof:

Based on:

$$P_{out}^{DF} = Pr\left\{\min\left\{\frac{T}{\rho}, \frac{\rho P_S W}{l_1^m l_2^m N}\right\} \le H\right\} = 1 - Pr(T \ge \rho H)\Pr(W \ge \frac{l_1^m l_2^m NH}{\rho P_S}),$$

and from the previous result, we get the desired result after some manual calculations.

The Optimal throughput analysis

As we can see in Proposition 5 and Proposition 6, the outage probability of the considered model is a function of the distance and noise power N. In the delay-limited transmission mode, the transmitter is communicating at a fixed transmission rate R bits/sec/Hz and $(1-\alpha)T$ is the effective information transfer time. Hence, the throughput of the system is given as:

$$\tau = (1 - P_{out})\, R \frac{(1-\alpha)\,T}{T}. \tag{6.17}$$

Unfortunately, it is hard to derive the optimal throughput mathematically, but we can get this value by using the numerical method as presented in the next part.

6.1.3 Simulation results

In this section, we employ the results from the derived analysis to offer the perception of a variety of design options. The energy switching efficiency is set to be $\eta = 1$, $SNR = \frac{P_S}{N} = 1dB$, the path loss exponent is set to be $m = 3$, the time fraction coefficient α is 0.3, the target transmission rate is $R = 3\ (bps/Hz)$. For simplicity, we set $\lambda_s = \lambda_d = 1; \lambda_r = 0.1$ and $l_1 = l_2 = 1$ (except for Fig. (6.3), Fig. (6.4)) as well as $N = 0.3$ (except for Fig. (6.5) and Fig. (6.6)). The reason we use these values is simply that if other values are fixed, these will be the best parameters to make the curves corresponding to two models asymptotic together.

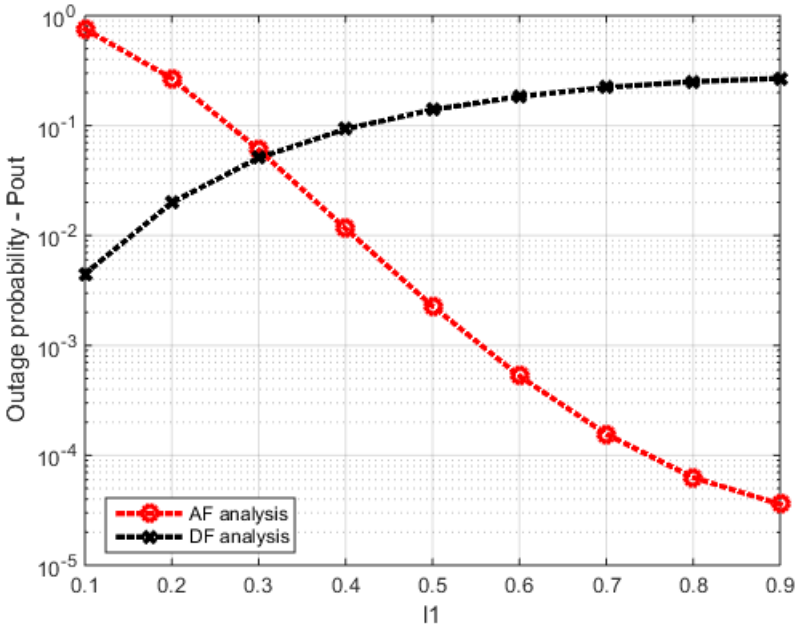

FIGURE 6.3: Outage probability of AF and DF model versus distance.

As we can see from Fig. (6.3) and Fig. (6.4), the outage probability of the AF model is better than that of DF model and its throughput is better, too. As close to the middle, the outage probability of DF model is gradually increasing but its throughput is decreasing. The nearer it gets to the S node, the better the DF model is than that of the AF one but as the distance increases, the contrary happens. This is easy to understand because the noise had affected the system performance.
Furthermore, from the curves in Fig. (6.3) and Fig. (6.4), we get the cross-over of two models at $l_1 = 0.3$. The same thing happens in Fig. (6.5) and Fig. (6.6), i.e., at a low noise regime, the outage probability of DF model is still better than AF, but at a high noise regime, the AF model is better than that of the DF model, and we have the cross-over at $\sigma = 0.35$. This is because the noise at the relay node has affected its performance. As a consequence, we can see that it depends on each practical situation that we deploy a proper model to achieve the best results.
In this part, the mathematical analysis has shown practical insights into the effect of different system parameters on the performance of the wireless energy harvesting and information transfer employing AF and DF relay nodes. Another interesting thing, the throughput results in this paper represent the upper bound on the realistically attainable throughput. Moreover, we also find that the DF model outperforms that of the AF one when the relay is deployed near the S node, i.e., $l_1 \leq 0.3$ or every place has $N \leq 0.35$. Otherwise, the AF model outperforms the DF model in delay-limited scheme of full-duplex relaying networks. So, depending on the perfect equipment as well as the position we have, we can decide to deploy the proper model to get the best benefit.

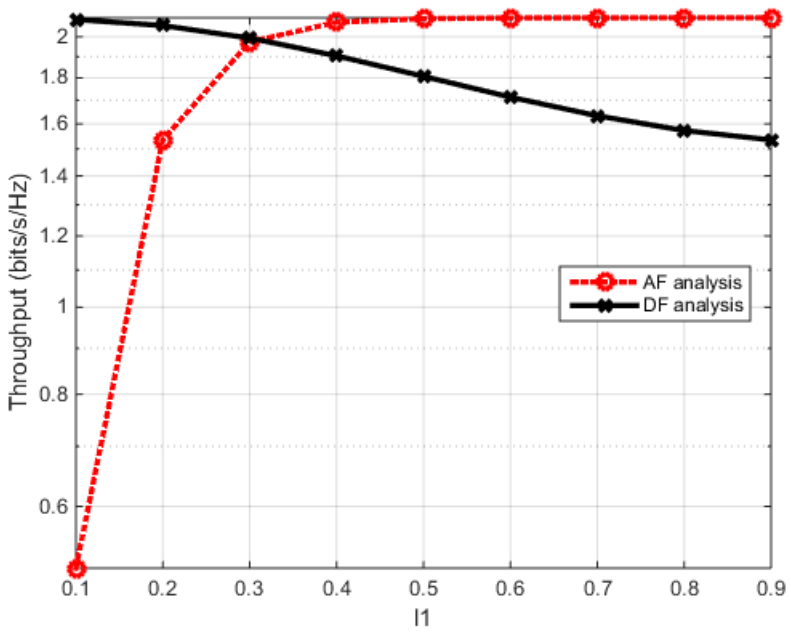

FIGURE 6.4: Throughput of AF and DF model versus distance.

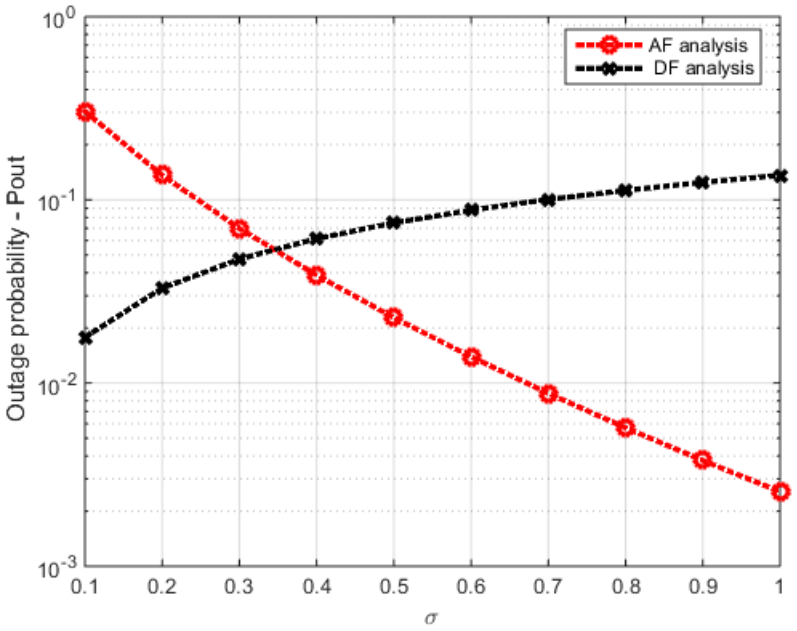

FIGURE 6.5: Outage probability of AF and DF model versus N.

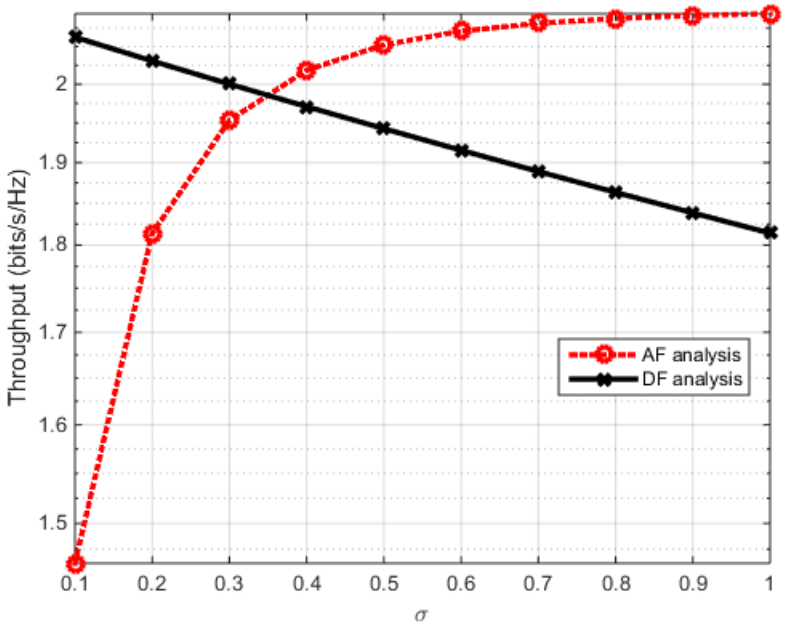

FIGURE 6.6: Throughput of AF and DF model versus N.

6.2 A Performance Analysis in The One-Way Full-Duplex Relaying Network

Energy harvesting (EH) approach based on surrounding radio frequency (RF) has lately become the advanced approach to prolong the lifetime of signals wireless systems.

The authors in **[59; 60; 92; 93]** have studied the problem of throughput optimization in a two-stage energy harvesting in the AF relay network. It is considered the harvested energy and the fading of system are available.
Moreover, the energy-constrained relay node position matter in an energy-harvesting network in which the energy harvesting ability of the candidate positions is given a priority. The object is to deploy a minimal number of relay nodes, to get connected while making sure that the relay nodes collect a considerable amount of surrounding energy as in **[31; 33; 94; 95]**.
On the other hand, express in for the outage probability of the relay supported cognitive system is derived subject to the following energy-constr -aints: 1) maximum energy that the source and the relay in the SU system can transfer from the collected power, 2) the peak interference power from the source and the relay in the SU system at the primary user (PU) system, and 3) noise energy of the PU system at the relay-assisted SU system, as the authors took out in **[61 - 64]**.
Therefore, in this part, we study the outage probability and throughput of the full-duplex relaying network with a new ability of energy harvesting and information transfer. Based on the analytical expressions, outage probability and throughput are investigated, and depending on the specific situation, we can select the proper model to get the best outcomes.

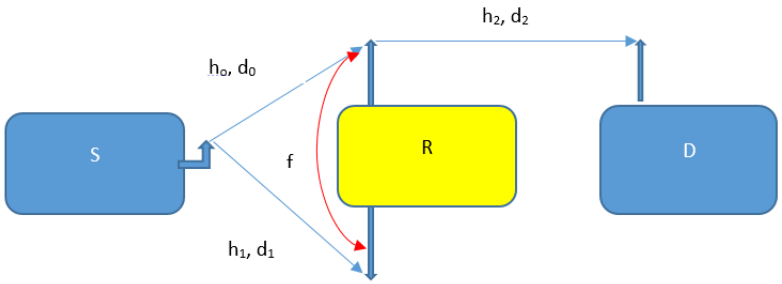

FIGURE 6.7: System model of one way full-duplex relaying.

6.2.1 The System Model

As shown in Fig. (6.7), we propose an AF cooperative relaying system, where the information is transmitted from the source node, S, to the target node, D, via an energy-constrained intermediate relay node, R. All nodes are set up with two antennas, one for transmitting the information, another for receiving data. Assume that there is no direct link between the source and the destination node so that AF relay supports the communication between source and destination. Firstly, the AF relay collects energy from the source signal. After that, it employs the collected energy to forward the information to the destination. The distances between $S \rightarrow R$ of two antennas and $R \rightarrow D$ are denoted by d_0, d_1 and d_2, respectively.
Assume that the residual self-interference (RSI) channel at R, denoted by f, still exists because the interference cancellation mechanism is not perfect.
The model utilized in this study is Time Switching Relaying (TSR) protocol as illustrated in Fig. (6.8).

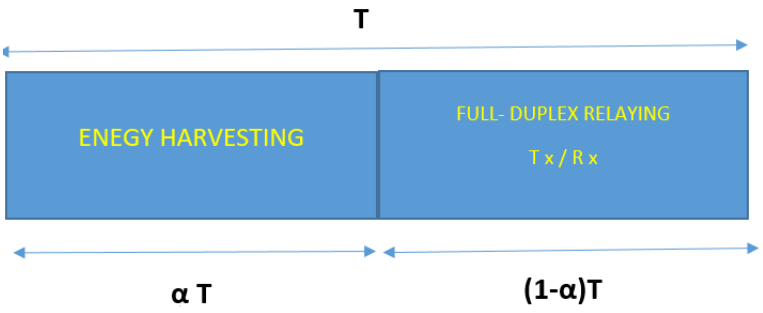

FIGURE 6.8: Illustration of the parameters of TSR protocol.

From Fig. (6.8), we can see that there are two phases to process the information. First, the energy is transmitted from the source to the relay during an interval of length $\alpha T, (0 < \alpha < 1)$ and next, an interval of length $(1-\alpha)T$ is used to transfer information, where α is a time switching factor, and T is the duration of transmission block.
In the energy harvesting phase, at the relay, we get the received signal as

$$y_R = \sqrt{\frac{P_S}{d_0^m}} h_0 x_S + n_R, \tag{6.18}$$

where P_S is source transmit power, n_R is the additive white Gaussian noise at R with the variance of σ_r^2 and zero-mean. In this paper, we study two antennas configurations at R.

Only One Antenna Is Used to Collect Energy, Another Is Used for Transferring Information

Following **[31]**, the harvested energy at the relay is given as

$$E_h = \eta \alpha T \frac{P_s |h_0|^2}{d_0^m}, \tag{6.19}$$

where m is denoted the path loss exponent, η is the energy conversion efficiency, the channel gains are h_0, h_1, h_2 as in Fig. (6.7). Assume that x_S is the signal transmitted from S to R and x_R is the signal transmitted from R to the destination. For simplicity, we assume they have the unit energy and zero–mean, i.e., $E\left[|x_j|^2\right] = 1$ and $E[x_j] = 0$, $j \in \{S, R\}$, respectively. we can write the signal at the relay as in **[83]**:

$$y_R = \sqrt{\frac{P_S}{d_0^m}} x_S h_0 + f x_R + n_R. \tag{6.20}$$

Now, assume that y_R is received at R and in the next time slot, R uses the harvested energy to amplify y_R. So, x_R is written as:

$$x_R = K_O \sqrt{P_R} y_R, \tag{6.21}$$

where K_O is the amplification factor at R.
Following **[41]**, we have:

$$K_O^{-1} = \sqrt{\frac{P_S}{d_0^m} |h_0|^2 + P_R |f|^2 + \sigma_r^2}. \tag{6.22}$$

Because R uses all harvested energy and to assist the next information transfer, P_R can be expressed as:

$$P_R = \frac{E_h}{(1-\alpha)\,T} = \mu P_S \frac{|h_0|^2}{d_0^m}, \tag{6.23}$$

where $\mu \cong \frac{\alpha\eta}{1-\alpha}$ and

$$y_D = \frac{h_2}{\sqrt{d_2^m}} x_R + n_D, \tag{6.24}$$

where n_D is the Gaussian noise at D with variance of $\sigma_d^2 = \sigma_r^2 = N$ and zero-mean.

By substituting Eq. (6.21), Eq. (6.31), Eq. (6.32) into Eq. (6.30), we get:

$${y^0}_D = \underbrace{\frac{h_2}{\sqrt{d_2^m}} K_O \sqrt{P_R} \frac{h_0\sqrt{P_S}}{\sqrt{d_0^m}} x_S}_{signal} + \underbrace{\frac{h_2}{\sqrt{d_2^m}} K_O \sqrt{P_R} f x_R}_{RSI} + \underbrace{\frac{h_2}{\sqrt{d_2^m}} K_O \sqrt{P_R} n_R + n_D}_{noise}. \tag{6.25}$$

On the other hand, the instantaneous received SINR at S over R is calculated as

$$\gamma = \frac{E\left\{|signal|^2\right\}}{E\left\{|noise|^2\right\} + E\left\{|RSI|^2\right\}}. \tag{6.26}$$

After some simple calculations, a new formula is obtained:

$$\gamma^O = \frac{\frac{P_S|h_0|^2 P_R|h_2|^2}{d_0^m d_2^m P_R|f|^2}}{\frac{NP_S|h_0|^2}{P_R|f|^2 d_0^m} + \frac{P_R|h_2|^2}{d_2^m} + N}, \tag{6.27}$$

where the channel gains $|h_0|^2$ and $|h_2|^2$ are independent and identically distributed (i.i.d.) exponential random variables.

Both Antennas Are Utilized to Harvest energy, But Only One Is Used to Transmit The Information

Similar to the previous section, terms d_1, and h_1 denote the distance from the source to the relay as well as the fading channel gain of a link between the source and the remaining antenna at the relay. For simplicity, we assume $d_0 = d_1$, and $E\left\{n_R n_R^\dagger\right\} = NI$ where I is the identity matrix. The received signal at the relay can be written as

$$y_R = \sqrt{\frac{P_S}{d_0^m}} \begin{pmatrix} h_0 \\ h_1 \end{pmatrix} x_S + n_R, \tag{6.28}$$

and

$$E_h = \eta\alpha T \frac{P_s(|h_0|^2 + |h_1|^2)}{d_0^m}. \tag{6.29}$$

So, the signal at R can be rewritten as:

$$y_R = \sqrt{\frac{P_S}{d_0^m}} x_S (h_0 + h_1) + f x_R + n_R, \tag{6.30}$$

with

$$K_T^{-1} = \sqrt{\frac{P_S}{d_0^m}(|h_0|^2 + |h_1|^2) + P_R|f|^2 + N}, \tag{6.31}$$

and

$$P_R = \frac{E_h}{(1-\alpha)\,T} = \mu P_S \frac{(|h_0|^2 + |h_1|^2)}{d_0^m}. \tag{6.32}$$

By substituting Eq. (6.21), Eq. (6.31), Eq. (6.32) into Eq. (6.30), after some calculations, we obtain:

$$y^T{}_D = \underbrace{\frac{h_2}{\sqrt{d_2^m}} K_T \sqrt{P_R} \frac{h_0\sqrt{P_S}}{\sqrt{d_0^m}} x_S}_{signal} + \underbrace{\frac{h_2}{\sqrt{d_2^m}} K_T \sqrt{P_R} f x_R}_{RSI} + \underbrace{\frac{h_2}{\sqrt{d_2^m}} K_T \sqrt{P_R} n_R + D}_{noise}, \tag{6.33}$$

where $D = n_d$. Of course, a new formula can be obtained from Eq. (6.26) and Eq. (6.33)

$$\gamma^T = \frac{\frac{P_S|h_0|^2|h_2|^2}{d_0^m d_2^m |f|^2}}{\frac{N|h_0|^2}{\mu P_R(|h_1|^2+|h_0|^2)|f|^2} + \frac{\mu P_S(|h_1|^2+|h_0|^2)|h_2|^2}{d_0^m d_2^m} + N}. \tag{6.34}$$

6.2.2 Outage Probability and Throughput Analysis

In this section, we consider the outage probability and throughput of full-duplex relaying which employs energy harvesting and information transfer. Based on analytical results, the outage probability and throughput of two models are given. Next, we can find which model is better than the other to apply them properly.

Outage Probability Analysis

The FD relaying network outage probability is computed in **[48]**

$$P_{out} = \Pr\left(\gamma \le Z\right), \tag{6.35}$$

where we define R as the target transmission rate and $Z = 2^R - 1$.
Proposition:
The single-antenna outage probability is found as:

$$P_{out}^O = \Pr\left\{\frac{\frac{P_S|h_0|^2 P_R|h_2|^2}{d_0^m d_2^m P_R|f|^2}}{\frac{NP_S|h_0|^2}{P_R|f|^2 d_0^m} + \frac{P_R|h_2|^2}{d_2^m} + N} < Z\right\} = 1 - \int_0^{1/\mu Z} 2\sqrt{\frac{d_0^m d_2^m Z\left(\frac{N}{\mu}+Ny\right)}{\lambda_s\lambda_d(P_S - \mu P_S Z y)}} \times K_1\left(2\sqrt{\frac{d_0^m d_2^m Z\left(\frac{N}{\mu}+Ny\right)}{\lambda_s\lambda_d(P_S-\mu P_S Z y)}}\right) \frac{1}{\lambda_r} e^{-\frac{y}{\lambda_r}} dy, \tag{6.36}$$

where $\lambda_s, \lambda_d, \lambda_r$ are the mean value of the exponential random variables $h_0, h_1, h_{2,}, f$, respectively and $K_1(x)$ is Bessel function defined as Eq. (8.423.1) in **[49]**.
Proof:
We define $x = |h_0|^2|h_2|^2$ and $y = |f|^2$, then we obtain:

$$P_{out}^O = \begin{cases} \Pr\left\{x < \frac{d_0^m d_2^m Z\left(\frac{N}{\mu}+Ny\right)}{P_S - \mu P_S Z y}\right\}, & y < \frac{1}{\mu Z}. \\ 1, & y > \frac{1}{\mu Z}. \end{cases} \tag{6.37}$$

The cumulative distribution function of x can be calculated easily by

$$F_x(a) = \Pr(x < a) = 1 - 2\sqrt{a/\lambda_s\lambda_d}K_1\left(2\sqrt{a/\lambda_s\lambda_d}\right), \tag{6.38}$$

and y can be described with probability distribution function
$f_y(b) = (1/\lambda_r)\, e^{(b/\lambda_r)}$. Finally, the Proposition is obtained through some simple calculations.

Proposition:
The outage probability of the two-antenna protocol is derived as:

$$P_{out}^T = 1 - \int_{\mu Z}^{\infty} 2\frac{Nd_0^m d_2^m Z\left(\frac{t}{\mu}+1\right)}{\lambda_s\lambda_d\left(tP_S - \mu P_S Z\right)} K_2\left(2\sqrt{2\frac{Nd_0^m d_2^m Z\left(\frac{t}{\mu}+1\right)}{\lambda_s\lambda_d\left(tP_S - \mu P_S Z\right)}}\right) B(t), \tag{6.39}$$

where $B(t) = (\lambda_r - (\lambda_r - \frac{1}{t})e^{-\frac{1}{\lambda_r t}}\, dt$

Proof:
We define $M = \frac{X+Y}{Y}$ and $N = X + Y$ when $X = |h_0|^2$ and $Y = |h_1|^2$. So, M and N are also random variables. We can express the joint distribution function of X and Y as:

$$f_{X,Y}(x,y) = \frac{1}{\lambda_S^2} e^{-\frac{x+y}{\lambda_S}}. \tag{6.40}$$

Alternatively, we find that $X = MN$ and $Y = N(1-M)$.
By utilising Jacobian transformer (M, N) on to (X, Y), we get

$$f_{M,N}(m,n) = \frac{n}{\lambda_S^2} e^{-\frac{n}{\lambda_S}}.$$

We can see clearly that M and N are independent, and M is following the uniform distribution with *pdf* $f_M(m) = 1, 0 \le M < 1$ and N is following the gamma distribution with *pdf*,

$$f_N(n) = \frac{n}{\lambda_S^2} e^{-\frac{n}{\lambda_S}}.$$

Finally, let $W = N|g_2|^2$ and $T = \frac{M}{|f|^2}$, we easily obtain:
$F_W(w) = 2\frac{w}{\lambda_S\lambda_D}K_2(2\sqrt{\frac{w}{\lambda_S\lambda_D}})$, $F_T(t) = \lambda_r t(1 - e^{-\frac{1}{\lambda_r t}})$.
From the statistical property of W and T, we have:

$$P_{out}^T = \Pr\left(\gamma^T \le Z\right) = \Pr\left(W \le \frac{\frac{TZ}{\mu} + Z}{\frac{TP_S}{Nd_0^m d_2^m} - \frac{Z\mu P_S}{Nd_0^m d_2^m}}\right), T > \mu Z, \tag{6.41}$$

The expected result is achieved after some simple manipulations.

Optimal Throughput Analysis

Following the above Proposition, the outage probability of two models, where the relay harvests energy from the source signal and employs that energy to amplify and forward the signal to the destination is a function of the energy harvesting time factor α, and changes when α raises from 0 to 1. In the delay-limited transmission mode, the transmitter communicates

at a fixed transmission rate $R(bits/sec/Hz)$ and $(1-\alpha)T$ is the effective transmission time. So, the throughput of the system is defined as in **[31]**:

$$\tau = (1 - P_{out})\, R\, (1 - \alpha)\,. \tag{6.42}$$

Unfortunately, it is hard to get the maximal throughput mathematically, but we can get it by using numerical algorithms as introduced in the following section.

6.2.3 Numerical Results

In this section, we utilize the derived analytical results to find the optimal outage probability and throughput. We put the source transfer rate $R = 3\,(bps/Hz)$. The energy conversion efficiency is set to be $\eta = 0.4$ (except for Fig. (6.17), Fig. (6.18)), the $SNR = \frac{P_s}{N} = 5\ dB$, the path loss exponent is set to be $m = 3$. For simplicity, we set the distance $d_0 = d_2 = 1$ (except for Fig. (6.9), Fig. (6.10)). Also, we set $\lambda_s = \lambda_d = 1; \lambda_r = 0.1$, the noise power $N = 0.1$ (except for Fig. (6.11), Fig. (6.12)), as well as the time switching factor α is set to 0.3 (except for Fig. (6.15), Fig. (6.16)).

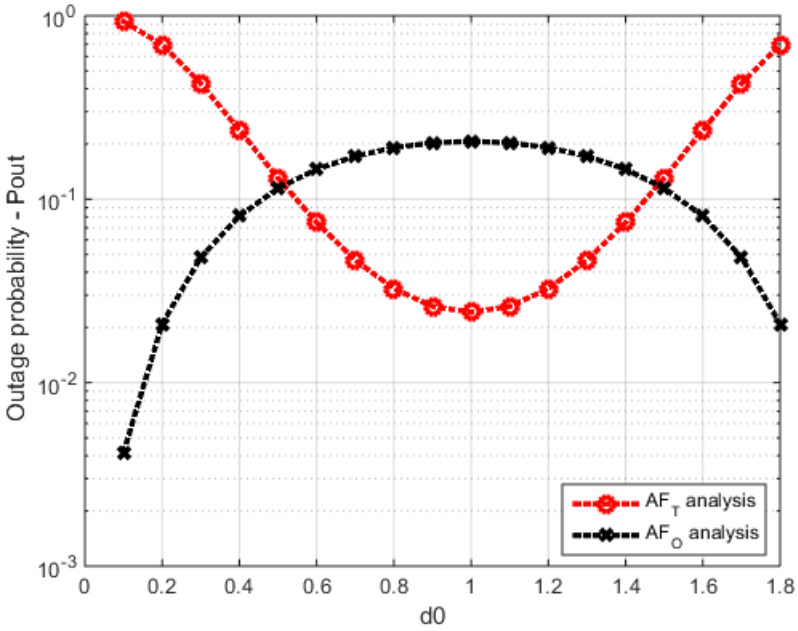

FIGURE 6.9: Outage probability of AFT and AFO model versus distance.

It can be seen from Fig. (6.9) that the outage probability of the single-antenna model decreases when relay position is far away from the source and it gets the worst value at the midway between S and R. But for two-antenna configuration, the contrary thing happens. it means as far the source is, as good its outage probability gets. And it obtains the optimal value at the midway. The outage probability of single-antenna configuration is better than that of two-antenna configuration for $d_0 \leq 0.5$ or ≥ 1.5, but for $d_0 \geq 0.5$ or ≤ 1.5, things are reversed. It is easy to understand because the farther the relay is from the source or the destination, the smaller the transmit power is. So,

the two antennas can collect more energy to make the information transfer easier. But, if the transfer energy is big, i.e., the relay is near to the source or the destination, the redundant amount of energy is harvested, which is harmful because it makes the powerful loop back interference, this leads to the degrade of system performance. There is a cross over at $d_0 = 0.5$ or $d_0 = 1.5$ and at these points, the outage probability of two models is equal.

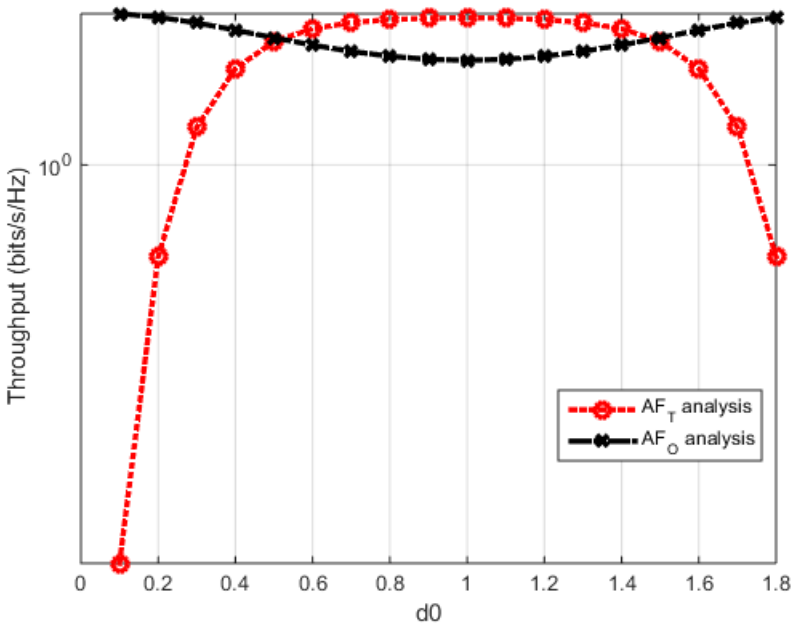

FIGURE 6.10: Throughput of AFT and AFO model versus distance.

This is compatible with Fig. (6.10), meaning that at any point that a model has its the outage probability better than, its throughput is better than the other, too. Here, we also have the intersection point of two models being the same as the previous figure. As analysed, when the delay is close to the source or the destination, the performance of a simple-antenna configuration is better than that of two-antenna one. When the relay is far from the source or the destination, the two-antennas mode configuration takes advantage of the other.
Fig. (6.11), Fig. (6.12) reveal that the outage probability and throughput of the two-antenna configuration are better than that of single-antenna configuration. When σ increases, the performance of two-antenna configuration is enhanced, while the performance of single-antenna configuration is degraded.
As your observation, Fig. (6.13) examines the impact of the rate R on the outage probability of two models. When R increases, the outage probabilities of two antennas model decrease. However, the contrary situation happens with a single-antenna configuration. This happens because when R increases, more energy is harvested by the relay, which affects the performance. It is noted that two-antenna configuration is normally better than that of single-antenna configuration.

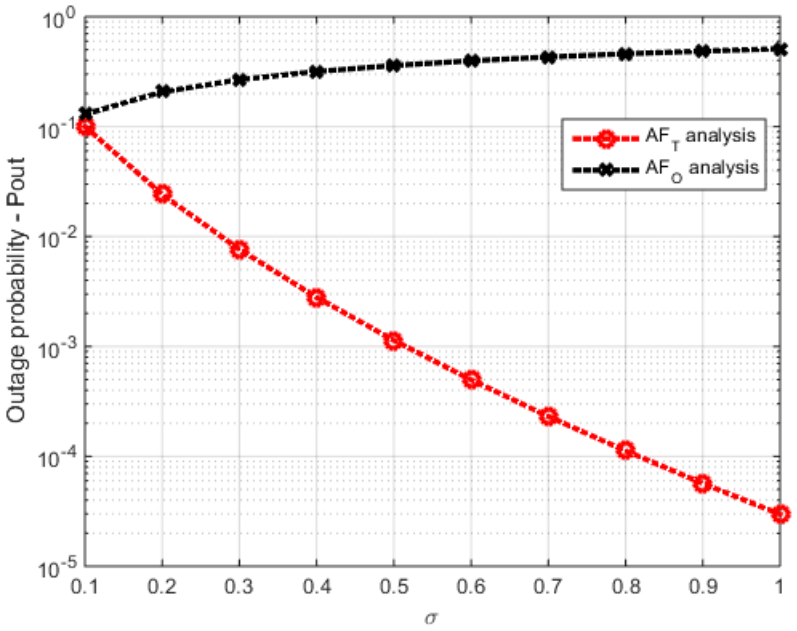

FIGURE 6.11: Outage probability of AFT and AFO model versus N.

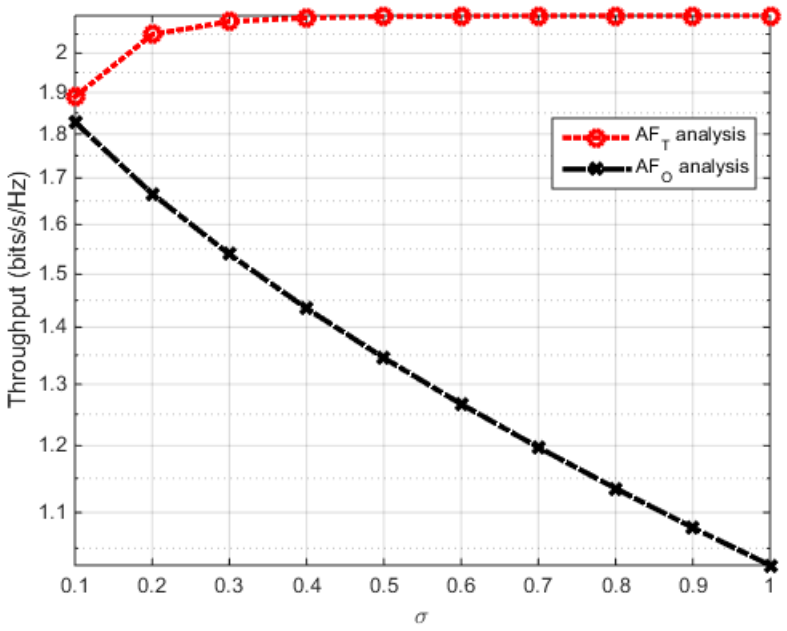

FIGURE 6.12: Throughput of AFT and AFO model versus N.

In practice, Fig. (6.14) gives us the fact that intuitively, according to Eq. (6.45), the smaller the transfer rate is, the smaller the throughput is. When the transfer rate is big, the outage probability raises dramatically, which again decreases the throughput. So, for certain transfer energy, there is an existence of a transfer rate that provides the optimal throughput.

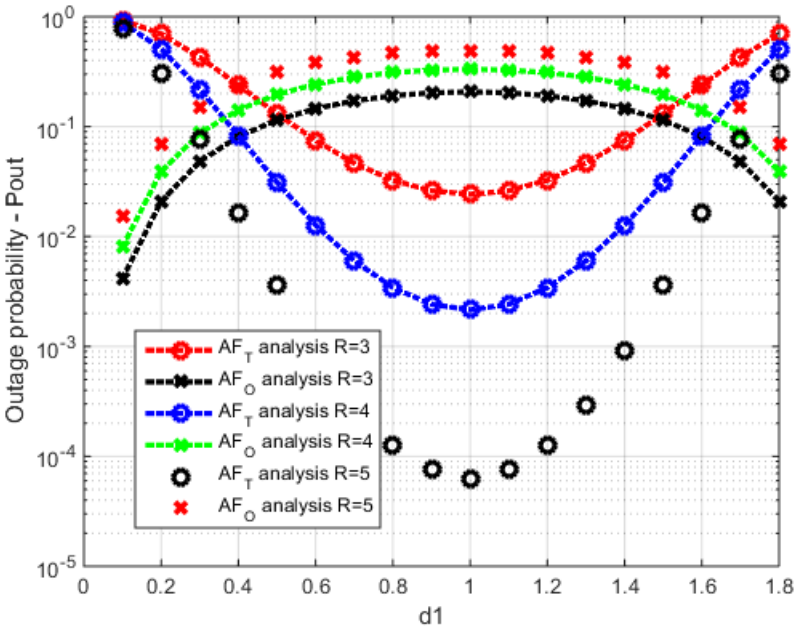

FIGURE 6.13: Throughput of AFT and AFO model versus R.

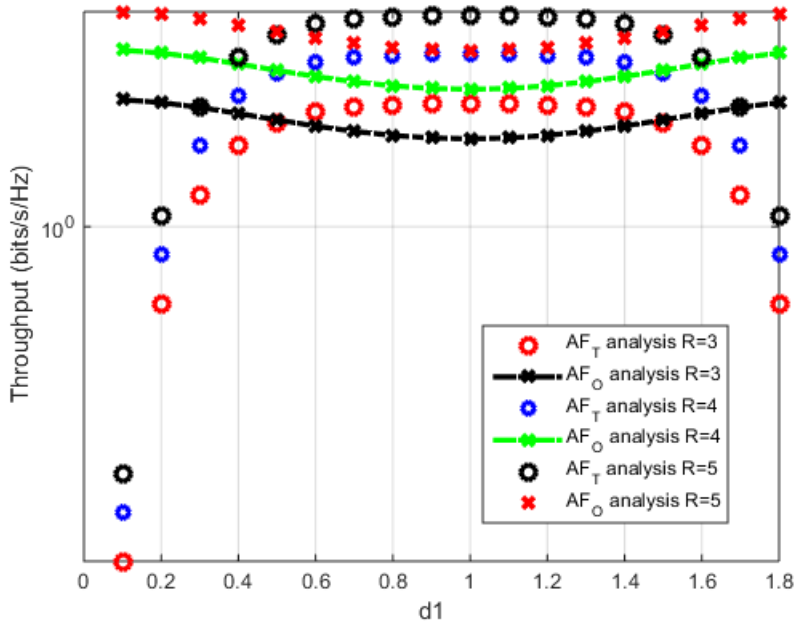

FIGURE 6.14: Throughput of AFT and AFO model versus R.

Pleasantly, we find that the optimal transfer rate of the two-antenna configuration is better than that of the single-antenna configuration. This could be explained easily because the loop back interference in two-antenna configuration and the more harvested energy help it achieve better outage and throughput performance than that of a single-antenna configuration for any fixed transfer rate.

Furthermore, Fig. (6.15) shows the outage probability curves versus the time switching factor α. For two-antenna configuration, the smaller α is, the better its outage probability gets. But as observed, the single-antenna outage probability has a reverse trend.

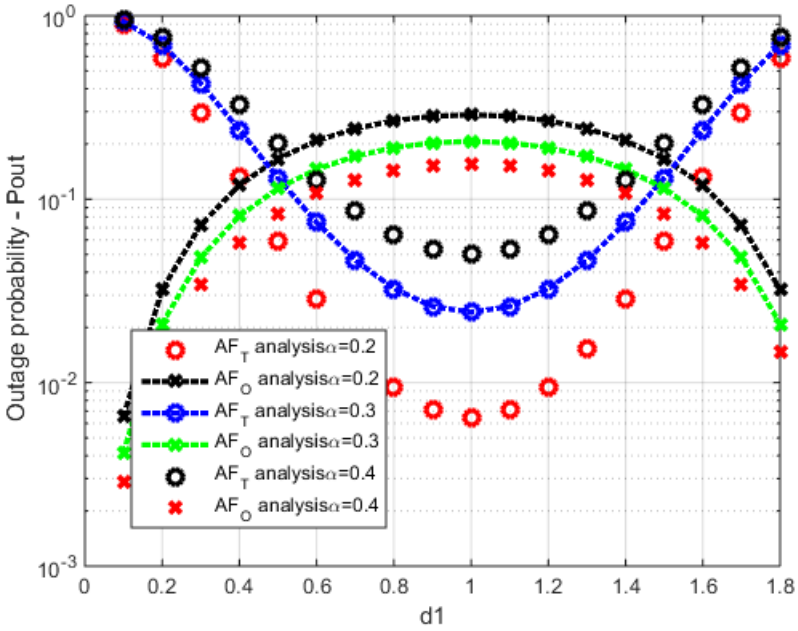

FIGURE 6.15: Throughput of AFT and AFO model versus α.

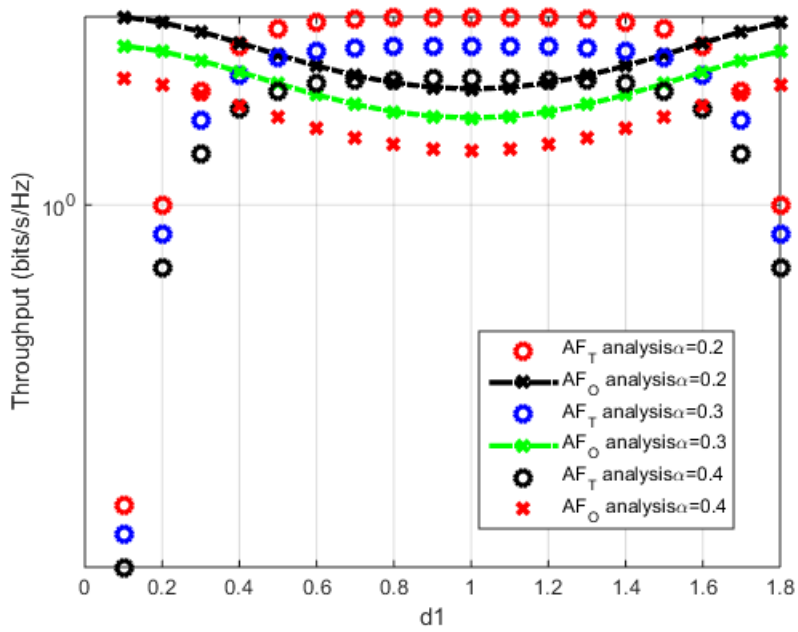

FIGURE 6.16: Throughput of AFT and AFO model versus α.

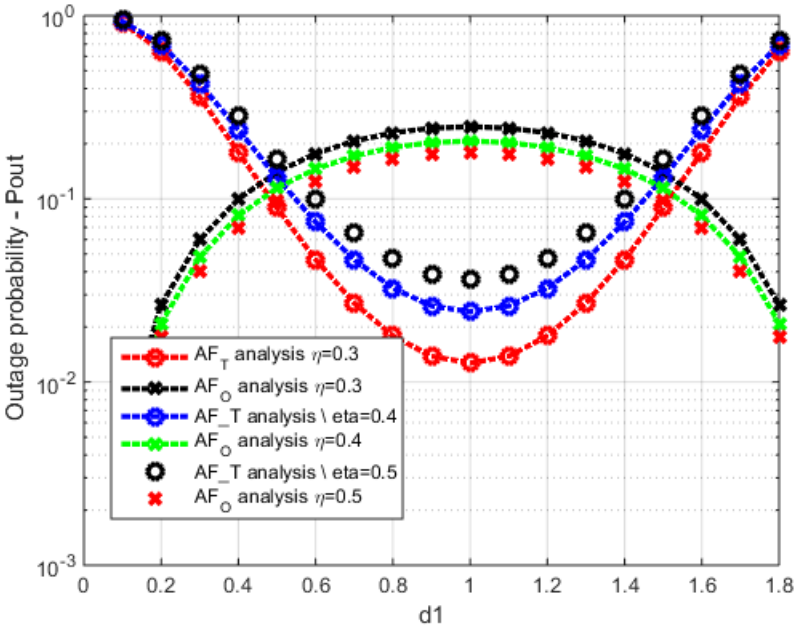

FIGURE 6.17: Throughput of AFT and AFO model versus η.

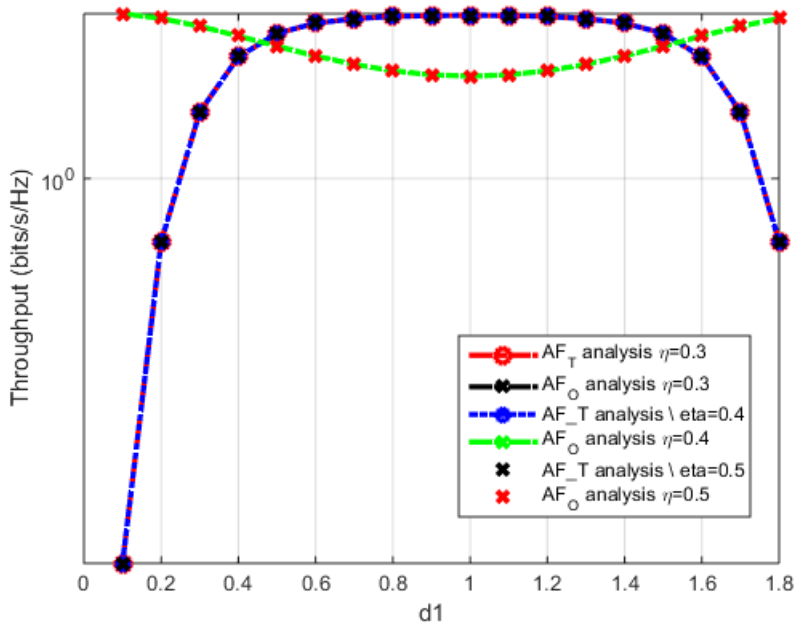

FIGURE 6.18: Throughput of AFT and AFO model versus η.

And as we can see in Fig. (6.16), the throughput of the two-antenna configuration matched the analysis beforehand. The throughput of singe-antenna is different, it gets a better performance when α are smaller. This is because when the values of α is small, there is more time for information transfer. So, smaller values of throughput are got at the destination node because its outage probability increases very much, i.e., the system may stop easily.

As a result, it is noted that the two-antenna configuration outperforms the single-antenna configuration. Furthermore, from the curves of Fig. (6.17), the smaller η is, the greater but the outage probability of two-antenna configuration gets but the reserve thing happens with the single-antenna configuration. An illustrated 1n Fig. (6.18), we can see an interesting thing that their throughput is unchanged. It is easy to know because the noise at the relay impacted on their performances. As a consequence, depending on each practical situation, we can deploy a proper model to achieve the best results. In this part, we have investigated the outage probability and throughput of FD relaying system with RF energy harvesting. Depending on the number of antennas employed at the relay in the energy harvesting stage, two different models have been considered. In both two cases, analytical expressions were derived for outage probability and throughput of network. Based on that, the performance of two models depends on the time switching factor, the noise power, the relay position, the transfer rate as well as the energy conversion efficiency was studied. It was illustrated that using both antennas for energy harvesting is always profitable, and the throughput is higher when source transferred energy is small.
Furthermore, comparing two configurations, our results imply that the two-antenna configuration can really promote the network throughput with the previously considered cases. So, it is a promising solution for executing the future RF energy harvesting cooperative networks.

6.3 A Performance Analysis of DF Model in the Energy Harvesting Half-duplex and Full-Duplex Relay Networks

The EH structure has been developed as a promising method, which is suitable for the radio cooperative network as well as the sensor systems to operate in the ambient environment that has limited resources. The application of energy collectors, which can replace the normal power sources, in wireless cooperative communication has also been considered. For the illustrative purpose, the basic three-node Gaussian relay channel with DF relaying, in which the source and relay nodes transmit the information using the energy harvested from the EH sources has been investigated in **[33**; **78**; **96**; **97]**.
Moreover, the technology of radio frequency energy collecting is a worth-expecting model to sustain the activities of the wireless networks. For instance, in a cognitive radio network, a secondary user can be equipped with the RF energy harvesting function. Such a network where the secondary user can access the channel to transmit information or to collect RF energy when the selected channel is available or being used by the primary user, respectively, has also been studied in **[57**; **59**; **60]**.
In practice, the authors in **[61**; **88]** had given the problem of energy-constrai -ned relay node in an energy-harvesting network and then solved it.
On the other hand, the transmission of energy and information from the source node to the relay node is executed by two methods, i) the TSR and ii) the power splitting-based relaying (PSR). It has also been considered in **[38**; **82]**, too.
The authors in **[80**; **89]** considered the employment of collective energy, in

place of traditional power sources, in wireless communication systems. The classic three-node Gaussian relay channel with decode-and-forward (DF) relaying, in which the source and relay nodes transfer using energy harvested from energy-harvesting sources has been studied.
Furthermore, a wireless-energized cooperative communication system comprising one hybrid access-point (AP), one source, and one relay has been investigated. In contrary to common cooperative networks, the source and relay in this considered network do not have their own power supply. They must rely on energy collected from the source signals for their information transmission as in **[76; 77; 85; 87]**.
On the other hand, an energy collecting cognitive radio (CR) network that operates in a slotted scheme, where the secondary user (SU) does not have power supply and is used energy harvested from the surroundings, was examined. The SU can only employ either energy collecting, spectrum sensing or information transfer at a time because of hardware restriction such that a time frame is partitioned into three non-overlapping parts, as the authors revealed in **[62- 64]**.
So, in this paper, we consider the outage probability and throughput of the full-duplex (FD) relaying network with a new capacity of energy collecting and information transfer. Based on the analytical expressions, their outage probability and throughput are studied from that depending on each practical condition, we can employ which model to achieve the most profit.
In this section, we examine a radio HD relaying and FD relaying system applying TSR protocol to perform the simultaneous wireless information and power transfer (SWIPT) scheme in order to optimize the outage probability and throughput.
The main content of this section is summarized. By comparing two techniques of FD and HD relaying, our results show that based on the method we used, we could evaluate the impact of the relay to determine optimal outage probability and maximal throughput for an appropriately optimized network.

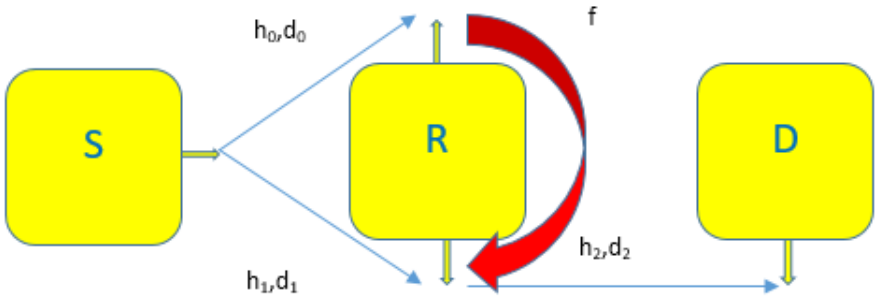

FIGURE 6.19: The Frame diagram of TSR system.

6.3.1 Network Model

As observed in Fig. (6.19), we study a DF cooperative system, where the data is transferred from the source node, called, S, to the destination node, called, D, through an immediate relay node, R. Every node has two antennas, one for transmitting the information, the rest for receiving information. Assuming that between S and D, there does not exist of the contact link, due

to the far distance. Therefore, that DF relay helped the direct connection between them. In the beginning, the DF relay harvests energy from the source signal, and then, that collected energy is used to forward the information to the destination d_0, d_1 and d_2 are denoted for the distance between $S \rightarrow R$ (two-antennas) and $R \rightarrow D$.

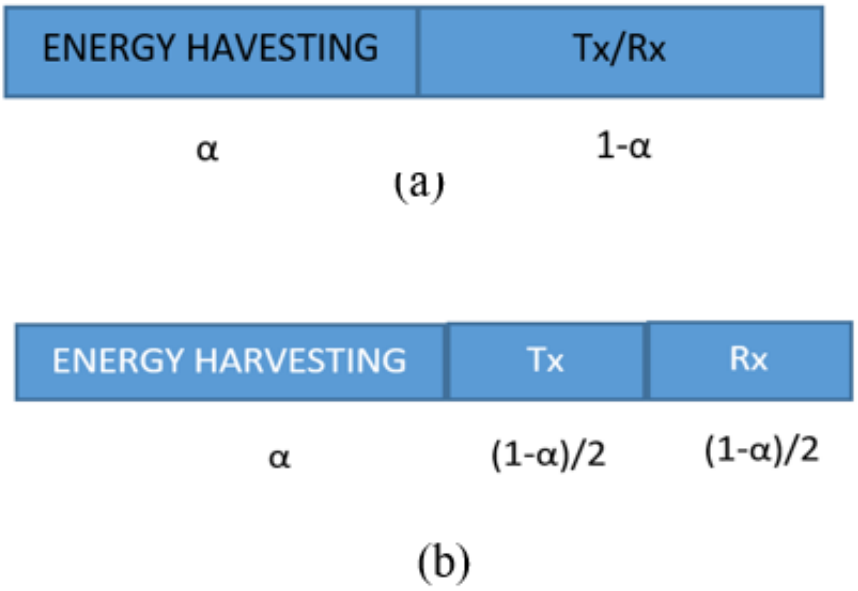

FIGURE 6.20: Illustration of the parameters of TSR protocol: (a) The full-duplex model, (b) The half-duplex model.

Assuming that due to the imperfect interference cancellation structure is perfected, the residual self-interference (RSI) channel at R exists and is denoted by f. With the TSR model in Fig. (6.20), the communication procedure is split into two stages. At first, energy is transmitted from the source and the relay in an interval of $\alpha T, (0 < \alpha < 1)$ and in the second stage, in the case of the full-duplex model, the remaining time $(1-\alpha)\,T$ is used to transmit data, and in the case of the half-duplex, an interval of $(1-\alpha)\,T/2$ for the data receiving at the relay and the remaining time of length $(1-\alpha)\,T/2$ is used for transferring information from R to D in which α is time switching factor and T is the duration of one transmission block.

6.3.2 The Full-Duplex Relaying Model

In this section, two-antenna configuration at R are investigated.

Only One Antenna Is Utilized to Harvest Power, The Other Is Utilized to Transmit Information

From the energy harvesting scheduling, the received data at the relay is given as:

$$y_{RFD} = \sqrt{\frac{P_S}{d_1^m}} h_1 x_S + n_R, \tag{6.43}$$

where P_S is source transmitted energy, n_R is the additional white Gaussian noise at R with zero-mean and variance of σ_R^2.
The harvested energy at the relay is given by **[82]**:

$$E_h = \eta\alpha T \frac{P_S|h_1|^2}{d_1^m}, \tag{6.44}$$

where m is the path loss exponent, η is the energy conversion efficiency, h_0, h_1, h_2 are the channel gain factors of the source-relay (two-antenna) link and the relay-destination link, respectively.
In the information transfer phase, suppose that the source node transmits signal x_S to R and R return the data x_R to the destination node. These signals are assumed to have unit energy and zero–mean, i.e., $E\left[|x_j|^2\right] = 1$ and $E[x_j] = 0$, x_j, $j \in \{S, R\}$ as in **[83]**. So, the received data at the relay under residual self-interference is given as

$$y_{RFD} = \sqrt{\frac{P_S}{d_1^m}} x_S h_1 + f x_R + n_R. \tag{6.45}$$

It is widely known all energy harvested is used to support the information in the next stage, so the transmit power by relay is given by

$$P_{RFD} = \frac{E_h}{(1-\alpha)T} = \rho P_S \frac{|h_1|^2}{d_1^m}, \tag{6.46}$$

where ρ is defined as $\rho = \frac{\alpha\eta}{1-\alpha}$.
Then, we get the signal at the destination node:

$$y_{DFD} = \frac{h_2}{\sqrt{d_2^m}} x_R + n_D, \tag{6.47}$$

where n_D is the additional white Gaussian noise at destination node with zero-mean and variance of $\sigma_D^2 = \sigma_R^2 = \sigma^2$, for simplicity. Following **[38]**, we have:

$$x_{RFD} = \sqrt{\frac{P_R}{P_S}} x_R(i-\tau). \tag{6.48}$$

By substituting Eq. (6.46), Eq. (6.48) into Eq. (6.47), we get the received signal at the destination node as

$$y_{DFD} = \frac{h_2}{\sqrt{d_2^m}} \left(\sqrt{\frac{P_R}{P_S}} x_R(i-\tau) \right) + n_D. \tag{6.49}$$

Through some simple calculations, we get the new formula as:

$$\gamma_{DF}^{FDO} = \min\left(\frac{1}{\rho|f|^2}, \frac{\rho P_S |h_1|^2 |h_2|^2}{d_1^m d_2^m \sigma^2} \right). \tag{6.50}$$

Assume that the channel gains $|h_0|^2, |h_1|^2, |h_2|^2$ are independent and identically distributed (i.i.d.) exponential random variables.

Both Antennas Are Used to Collect Energy, But Only One Is Utilized to Transfer The Information

Same as previous section, terms d_0, and h_0 denote the distance from the source to the relay as well as the fading channel gain of the receiving antenna at the relay. To simplify the issue, we assume: $d_0 = d_1$, and $E\left\{n_R n_R^\dagger\right\} = \sigma^2 I$ where I is identity matrix. The received signal at the relay can be found as

$$y_R = \sqrt{\frac{P_S}{d_1^m}} \begin{pmatrix} h_0 \\ h_1 \end{pmatrix} x_S + n_R, \tag{6.51}$$

and

$$E_h = \eta\alpha T \frac{P_s(|h_0|^2 + |h_1.|^2)}{d_1^m}. \tag{6.52}$$

So, the signal at R can be rewritten as

$$y_R = \sqrt{\frac{P_S}{d_1^m}} x_S(h_0 + h_1) + f x_R + n_R, \tag{6.53}$$

where

$$P_R = \frac{E_h}{(1-\alpha)\,T} = \rho P_S \frac{(|h_0|^2 + |h_1|^2)}{d_1^m}. \tag{6.54}$$

By using Eq. (6.49), a new formula can be obtained:

$$\gamma_{DF}^T = \min\left\{\frac{|h_1|^2}{\rho|f|^2(|h_1|^2 + |h_0|^2)}, \frac{\rho P_S(|h_1|^2 + |h_0|^2)|h_2|^2}{d_1^m d_2^m \sigma^2}\right\}. \tag{6.55}$$

6.3.3 The Half-duplex Relaying

Equivalent to the full-duplex model, in the half-duplex, we have:

$$y_{RHD} = \sqrt{\frac{P_S}{d_1^m}} h_1 x_S + n_R, \tag{6.56}$$

and

$$P_{RHD} = 2\rho P_S \frac{|h_1|^2}{d_1^m}. \tag{6.57}$$

After that, the received data at the destination is given as

$$y_{DHD} = \frac{h_2}{\sqrt{d_2^m}} x_R + n_D. \tag{6.58}$$

By the same calculation method as above, we get:

$$\gamma_{DF}^{HD} = \min\left(\frac{P_S|h_1|^2}{d_1^m \sigma^2}, \frac{2\rho P_S |h_1|^2 |h_2|^2}{d_1^m d_2^m \sigma^2}\right). \tag{6.59}$$

So, we examine the outage probability and the throughput of the half-duplex and full-duplex relaying networks with simultaneous energy collecting and information transmission. Based on analytical expressions, the outage probability and throughput of two models are investigated thoroughly.

The Outage Probability Analysis

The outage probability of the relaying system in the delay-limited transmission mode is computed as

$$P_{out} = \Pr\left(\gamma \leq Z\right), \tag{6.60}$$

where R is the target transmission rate and $Z = 2^R - 1$.
Proposition:
The outage probability of the energy harvesting enabled one-way full-duplex relay network with DF protocol is derived as:

$$P_{out}^{DFO} = 1 - \left(1 - e^{\frac{1}{\rho\lambda_r Z}}\right)\left(2\sqrt{\frac{\sigma^2 d_1^m d_2^m Z}{\rho\lambda_s\lambda_d P_S}}\right) K_1\left(2\sqrt{\frac{\sigma^2 d_1^m d_2^m Z}{\rho\lambda_s\lambda_d P_S}}\right), \tag{6.61}$$

where λ_s, λ_d, λ_r are the mean values of the exponential random variables h_1, h_2, f, respectively and $K_1(x)$ is the Bessel function denoted as Eq. (8.423.1) in **[49]**.
Proof:
The cumulative distribution function of x is computed by

$$F_x(b) = \Pr\left(x \leq b\right) = 1 - 2\sqrt{b/\lambda_s\lambda_d} K_1\left(2\sqrt{b/\lambda_s\lambda_d}\right), \tag{6.62}$$

and y can be modeled with the probability distribution function $f_y(c) = (1/\lambda_r)\, e^{(-c/\lambda_r)}$.
We define $x = |h_1|^2 |h_2|^2$ and $y = |f|^2$, from Eq. (6.50), Eq. (6.60), we get:

$$P_{out}^{DFO} = Pr\left(\min\left(\frac{1}{\rho y}, \frac{\rho P_S x}{d_1^m d_2^m \sigma^2}\right) \leq Z\right). \tag{6.63}$$

Then

$$P_{out}^{FDF} = 1 - Pr\left(\frac{1}{\rho y} \geq Z\right) \Pr\left(\frac{\rho P_S x}{d_1^m d_2^m \sigma^2} \geq Z\right), \tag{6.64}$$

where $Pr\left(\frac{1}{\rho y} \geq Z\right) = Pr\left(\frac{1}{\rho Z} \geq y\right) = \int\limits_0^{\frac{1}{\rho Z}} f_y(t)dt = \frac{1}{\lambda_r}\int\limits_0^{\frac{1}{\rho Z}} e^{-\frac{t}{\lambda_r}} dt$,
and $\Pr\left(\frac{\rho P_S x}{d_1^m d_2^m \sigma^2} \geq Z\right) = 1 - \Pr\left(x \leq \frac{Z d_1^m d_2^m \sigma^2}{\rho P_S}\right) = 1 - F_x\left(\frac{Z d_1^m d_2^m \sigma^2}{\rho P_S}\right)$.
Based on Eq. (6.62), we obtain our desired result after some algebras, then the proof of Proposition is computed
Proposition:
The outage probability of the two-antennas protocol is given as:

$$P_{out}^{DFT} = 1 - (1 - \rho\lambda_r Z(1 - e^{\frac{-1}{\rho\lambda_r Z}})) \times (\frac{2 d_1^m d_2^m ZN}{\lambda_s\lambda_d\rho P_S}) \times K_2\left(2\sqrt{\frac{d_1^m d_2^m ZN}{\lambda_s\lambda_d\rho P_S}}\right), \tag{6.65}$$

where $K_2(x)$ is Bessel function denoted as (8.423.1) in **[49]**.
Proof:
We denote $M = \frac{X+Y}{Y}$ and $N = X + Y$ with $X = |h_0|^2$ and $Y = |h_1|^2$, where M and N are built independent random variables. Now, we can illustrate the joint distribution function of X and Y as:

$$f_{X,Y}(x, y) = \frac{1}{\lambda_S^2} e^{-\frac{x+y}{\lambda_S}}, \tag{6.66}$$

alternatively, we see that $X = MN$ and $Y = N(1-M)$. Employing Jacobian transformer (M, N) on to (X, Y),

$$f_{M,N}(m,n) = \frac{n}{\lambda_S^2} e^{-\frac{n}{\lambda_S}}. \tag{6.67}$$

It is obvious that M and N are independence, and M is set to follow the uniform distribution with pdf, $f_M(m) = 1, 0 \leq M < 1$, and N is set up following the gamma distribution with pdf:

$$f_N(n) = \frac{n}{\lambda_S^2} e^{-\frac{n}{\lambda_S}}. \tag{6.68}$$

At last, let $W = N|h_2|^2$ and $T = \frac{M}{|f|^2}$, it is easy to get:
$F_W(w) = 2\frac{w}{\lambda_S \lambda_D} K_2(2\sqrt{\frac{w}{\lambda_S \lambda_D}})$, $F_T(t) = \lambda_r t(1 - e^{-\frac{1}{\lambda_r t}})$. From the statistical property of W and T, we obtain:

$$P_{out}^{DFT} = Pr\left\{\min\left\{\frac{T}{\rho}, \frac{\rho P_S W}{d_1^m d_2^m \sigma^2}\right\} \leq Z\right\} = 1 - Pr(T \geq \rho Z)\Pr(W \geq \frac{d_1^m d_2^m \sigma^2 Z}{\rho P_S}). \tag{6.69}$$

A desired result is achieved after some uncomplicated manipulations.
Proposition:
The outage probability of HD DF relaying networks is given by

$$P_{out}^{HDF} = 1 - e^{\frac{\sigma^2 d_1^m z}{\lambda_s P_S} - \frac{d_1^m}{2\lambda_d \rho}} - \frac{1}{\lambda_d} \int_0^{\frac{d_2^m}{2\rho}} e^{\frac{\sigma^2 d_1^m d_2^m z}{2\rho \lambda_s P_S t}} e^{-\frac{t}{\lambda_d}} dt. \tag{6.70}$$

Proof:
From Eq. (6.59), Eq. (6.60), we get:

$$P_{out}^{HDF} = \Pr\left(\frac{P_S|h_1|^2}{d_1^m \sigma^2} \min\left(1, \frac{2\rho|h_2|^2}{d_2^m}\right) \leq Z\right). \tag{6.71}$$

For the time being, by conditioning on $t = \min\left(1, \frac{2\rho|h_2|^2}{d_2^m}\right)$, we have $P_{out}^{HDF} = 1 - e^{\frac{\sigma^2 d_1^m Z}{\lambda_s P_S t}}$. Averaging over t supplies the expected result.

The throughput analysis

In the above Proposition, the outage probability of two models, in which the relay collects energy from the source data and utilizes that energy to decode and transmit the information to the destination is a function of the energy harvesting time factor α and varies when α raises from 0 to 1. In the delay-limited transmission mode, the transmitter is sending at a fix rate R bits/sec/Hz and $(1-\alpha)T$ is the effective communication time. So, the throughput of the FD model is given as

$$\begin{cases} \tau_{DF}^O = \left(1 - P_{out}^{DFO}\right) R(1-\alpha). \\ \tau_{DF}^T = \left(1 - P_{out}^{DFT}\right) R(1-\alpha). \end{cases} \tag{6.72}$$

Also, the throughput of the HD system is given as

$$\tau_{HD} = \left(1 - P_{out}^{HDF}\right) R\frac{(1-\alpha)}{2}. \tag{6.73}$$

Unfortunately, it is difficult to calculate the maximal throughput mathematically, but we can achieve such value by the numerical analysis as demonstrated in the next part.

6.3.4 Numerical Results

In this part, by using Matlab, we visualize the critical results in investigation of outage probability as well as throughput of two DF models. We fix the source transmission rate $R = 3$ (bps/Hz) (except for Fig. (6.27), Fig. (6.28), Fig. (6.33), Fig. (6.34)), $\alpha = 0.3$ (except for Fig. (6.35), Fig. (6.36)) and so the outage SINR threshold is given by $Z = 2^R - 1$. The energy conversion efficiency is fixed to be $\eta = 0.4$ (except for Fig. (6.23), Fig. (6.24)), the path loss exponent is fixed to be $m = 3$. For simplicity, we set the distance $d_1 = d_2 = 1$ (except for Fig. (6.21), Fig. (6.22), Fig. (6.29), Fig. (6.30)). Also, we set $\lambda_s = \lambda_d = 1; \lambda_r = 0.1$ and $P_S(dB) = 20$, $\sigma^2 = 0.1$ (except for Fig. (6.25) and Fig. (6.26), Fig. (6.31), Fig. (6.32)). These values are chosen because they make curves nearly asymptotic together.

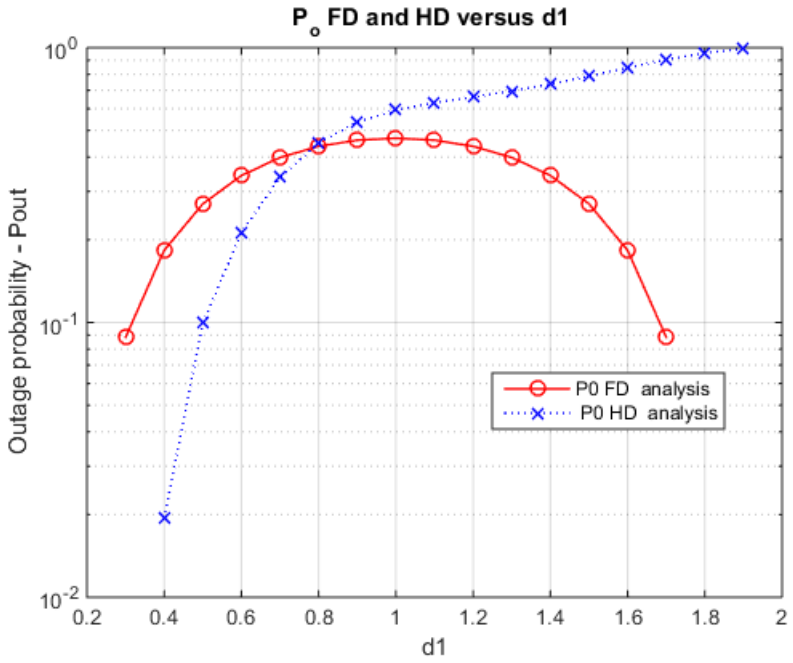

FIGURE 6.21: The outage probability of FD and HD model versus d_1.

Fig. (6.21) shows the outage probability concerning with respect to the relay position. In the simulation, we assume $d_1 + d_2 = 2$, and d_1 varies from 0 to 2. As shown in Fig. (6.21), the best outage probability is got when the relay is located near to the source or destination of the FD model. The suggested FD model gets the worst outage probability at midway. Furthermore, in Fig. (6.21) implies that half-duplex mode gets the outage probability better than that of the FD model when $d_1 \leq 0.6$, i.e., the relay is deployed close to the source. Otherwise, when $d_1 \geq 0.6$, the outage performance of FD mode is better than that of the HD model. Their curves have the intersection at $d_1 = 0.6$. This is uncomplicated to explain because when d_1 increases, d_2 decreases and from Eq. (6.61), Eq. (6.70), we get this result.
As observed in Fig. (6.22), the throughput of full-duplex mode is greater than that of the half-duplex one, as its outage probability is less than that of HD one. We have this fact: when d_1 increases, P_{RHD} and P_{RFD} decrease, P_{out}^{HD} and P_{out}^{FD} decrease but not enough to make τ_{HD} better than τ_{FD}, as

described in Eq. (6.72) and Eq. (6.73).

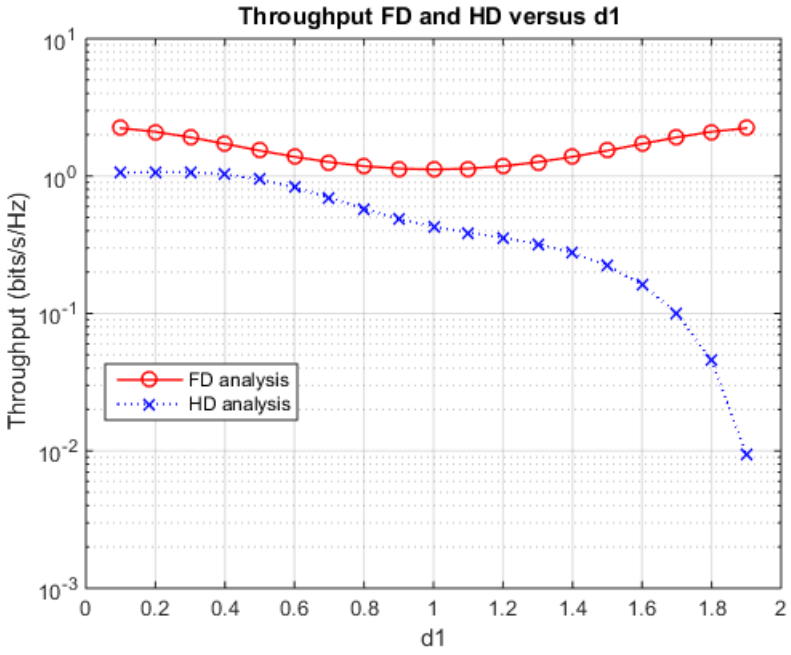

FIGURE 6.22: The throughput of FD and HD model versus d_1.

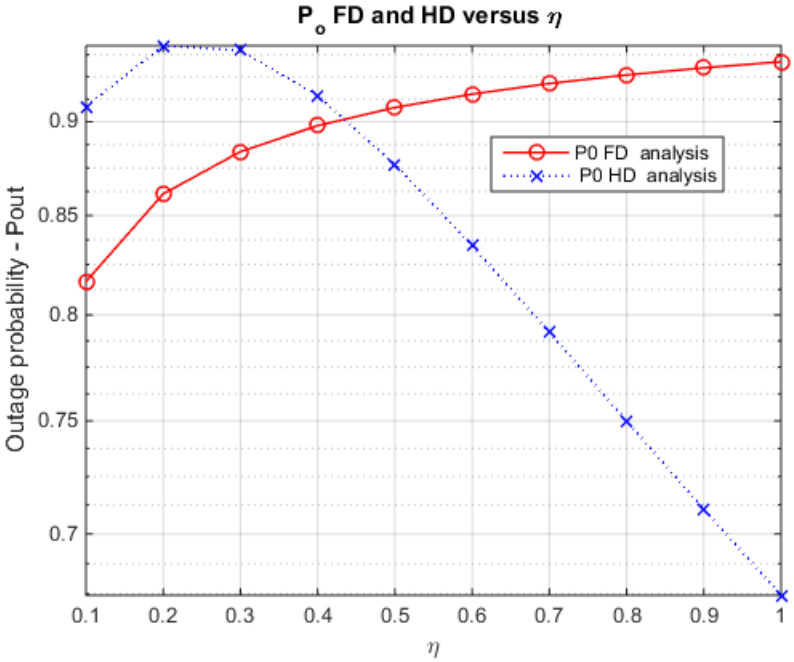

FIGURE 6.23: The outage probability of FD and HD model versus η.

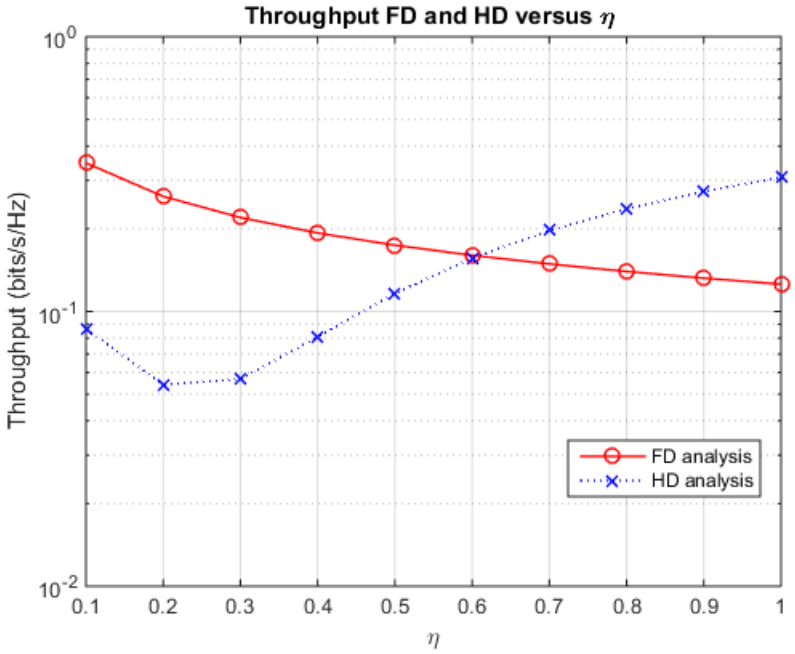

FIGURE 6.24: The throughput of FD and HD model versus η.

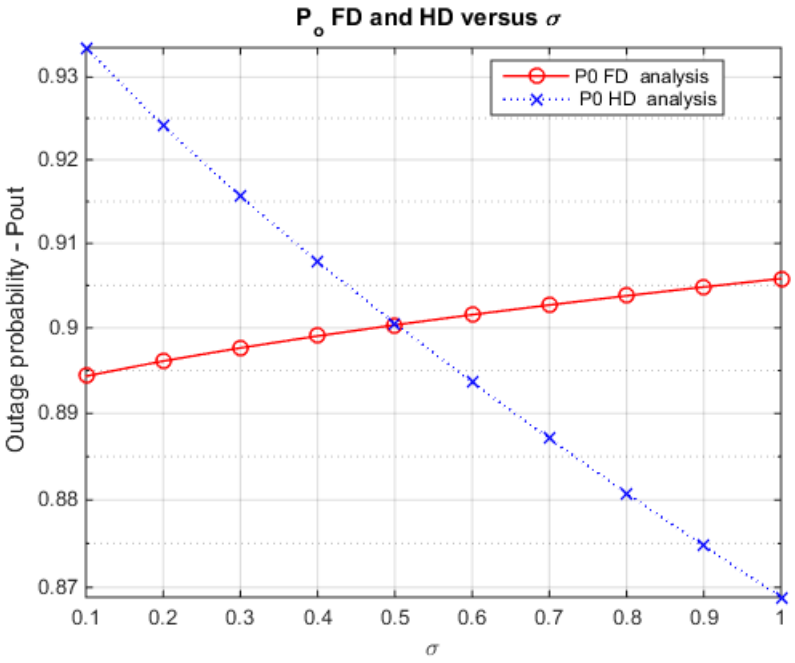

FIGURE 6.25: The outage probability of FD and HD model versus σ.

As described in Fig. (6.23), Fig. (6.24), η can affect the outage probability and throughput of both models. In Fig. (6.23), when $\eta \leq 0.2$, the higher the η is, the worse the HD outage probability gets. This model achieves the worst value as $\eta \in (0.2, 0.3)$. If η prevails over this space, the higher the η is, the better the HD outage probability turns out. Meanwhile, for bigger η, the FD outage probability is worse. This problem is not hard to explain. When

η is big, more power is used to transfer the signal to the destination, so the HD outage probability gets the better. On the contrary, for FD mode, high power at the relay makes the noises operation. Hence its outage probability turns worse.

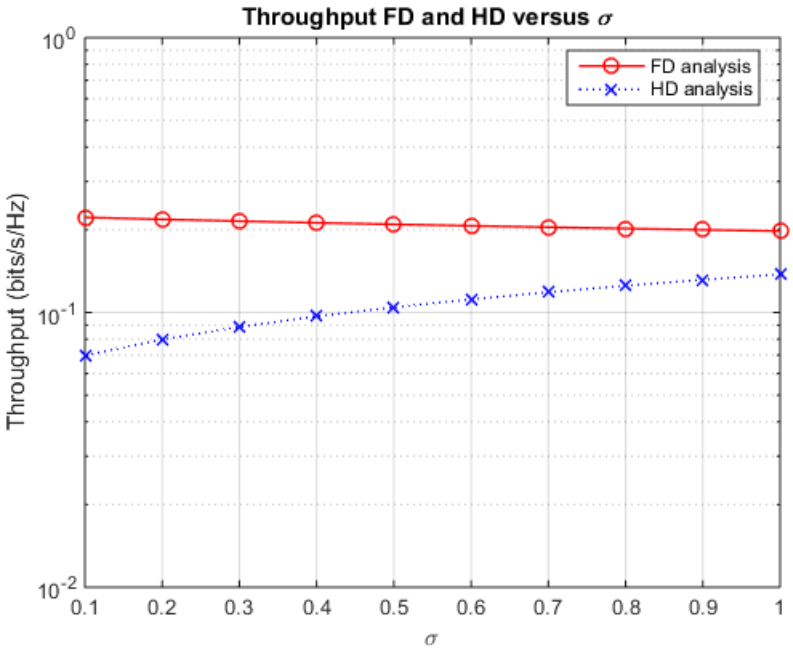

FIGURE 6.26: The throughput of FD and HD model versus σ.

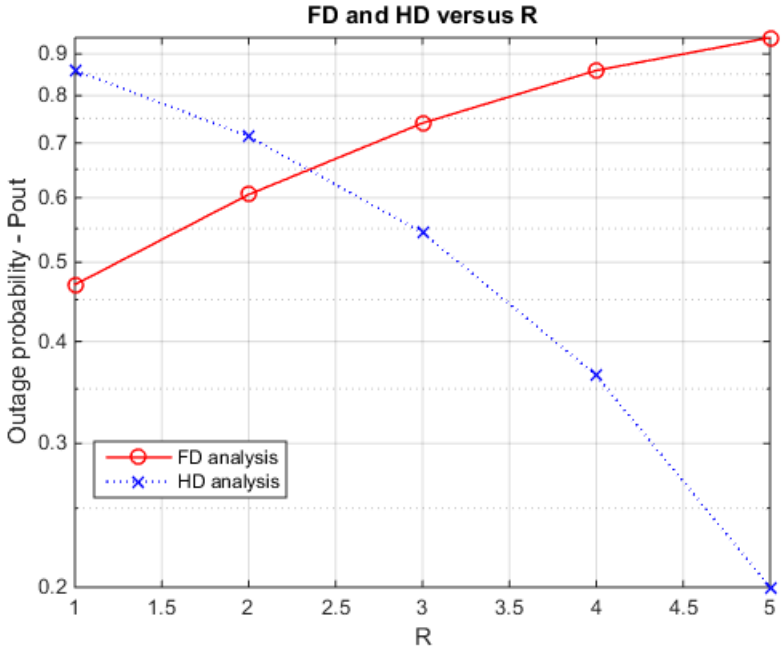

FIGURE 6.27: The outage probability of FD and HD model versus R.

This matter is illustrated in Fig. (6.24), the higher η, the better the HD

throughput gets, but for FD mode, the circumstance is reserved. It is observable that two models have the intersection point at $\eta = 0.6$.
Fig. (6.25), Fig. (6.26) expose that the loop back interference has an effect on system performance. In this case, when $\sigma \leq 0.5$, the FD outage probability is better than one of the HD modes. When $\sigma \geq 0.5$, everything occurs differently. In both cases, the FD throughput is always better than that of the HD model. This also proves that the noise at the relay has a huge effect on system operation.

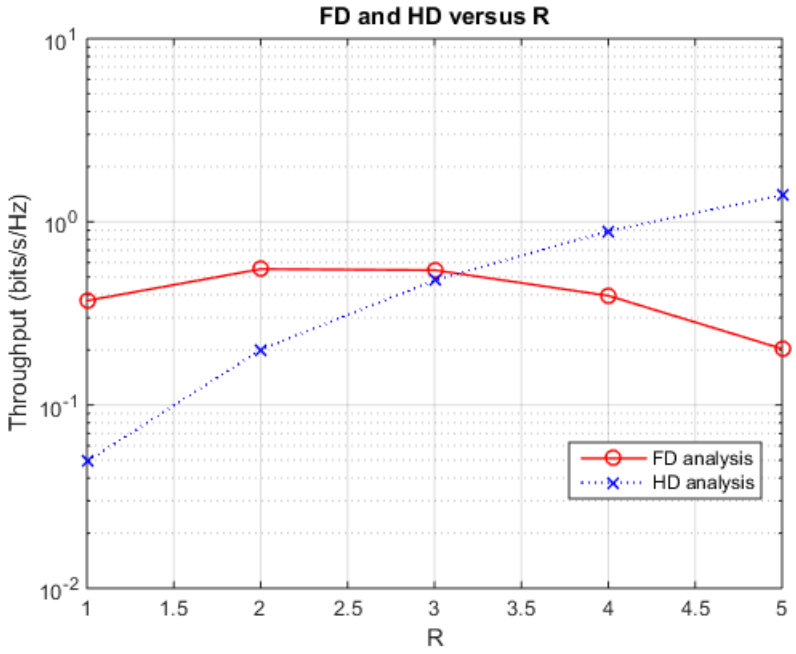

FIGURE 6.28: The throughput of FD and HD model versus R.

Besides, Fig. (6.27), Fig. (6.28) show the plots of outage probability and throughput of two modes versus the achievement rate R. As we can see in Fig. (6.27), as higher R, the outage probability of the FD model is downward, meanwhile, the HD outage probability is increasing. When $R \leq 2$, the FD outage probability is better than the HD one, but this is reserved as $R \geq 2$. Eq. (6.61), Eq. (6.70), Eq. (6.72), Eq. (6.73) verify this each.
On the other hand, Fig. (6.28) is also suitable for the above issue, it means the better outage probability gets, the better the throughput obtains. We have the crossover of their throughput at $R = 3$.
It can be seen from Fig. (6.29), the outage probability of one model decreases when relay position is as far away from the source, and it gets the worst value at the midway between S and D. The outage probability of simple-antenna configuration is better than that of two-antennas configuration when $d_1 \leq 0.25$ or ≥ 1.75. But when $d_1 \geq 0.25$ or ≤ 1.75, this is on reserve. It is easy to explain because the farther the relay is from the source or the destination, the smaller the transmit power is. So, the two-antenna configuration can harvest more energy to carry out the information transfer, easily. But, if the transmit energy is large, i.e., the relay is close to the source or the destination, an unwanted amount of energy is collected, which is

harmful because it creates a strong loop back interference, which reduces the system performance.

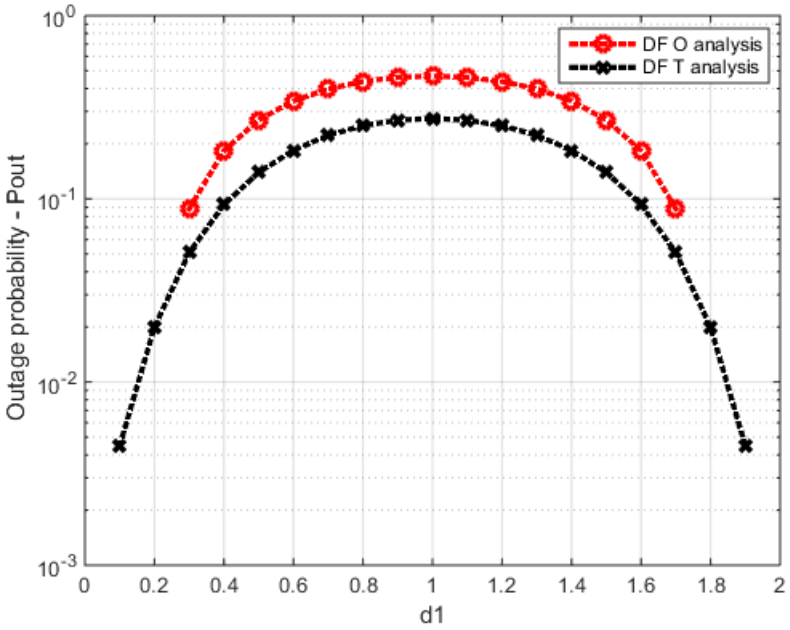

FIGURE 6.29: Outage probability of DFT and DFO model versus d_1.

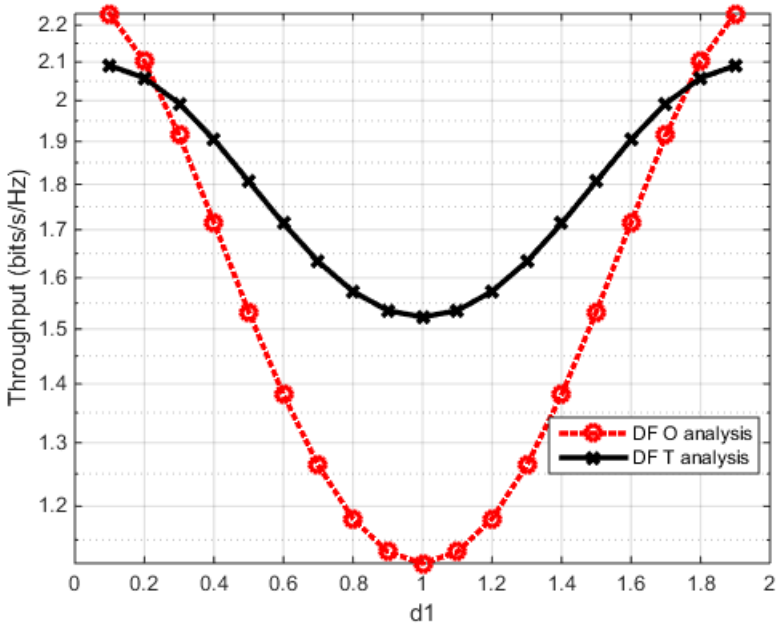

FIGURE 6.30: Throughput of DFT and DFO model versus d_1.

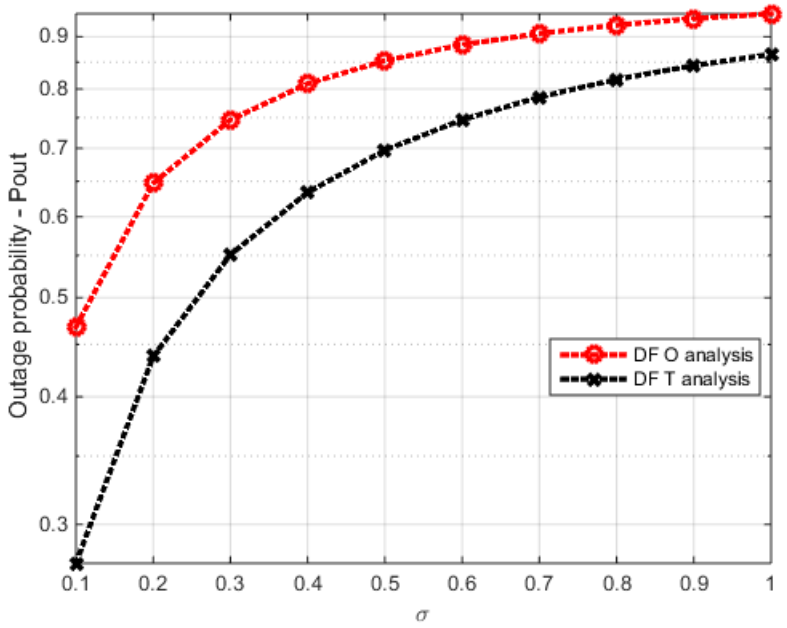

FIGURE 6.31: Outage probability of DFT and DFO model versus σ.

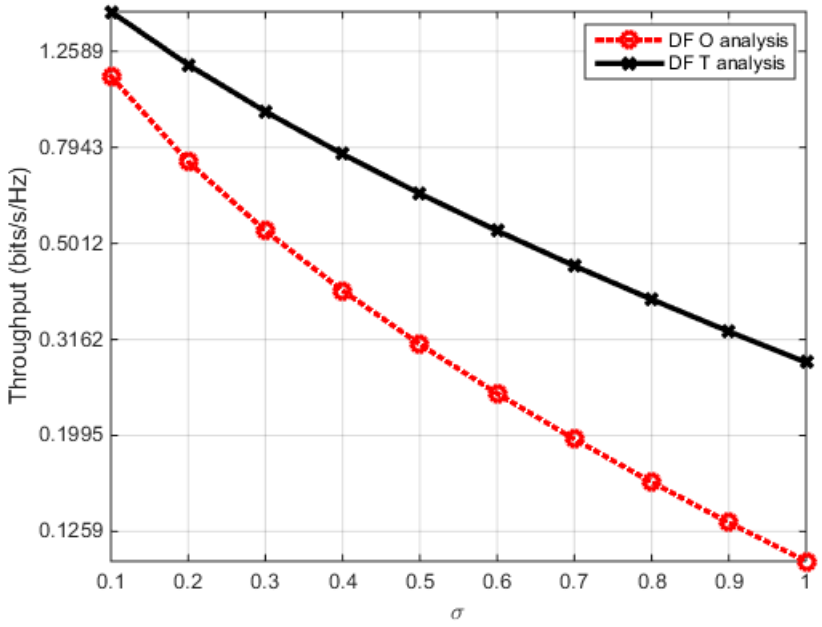

FIGURE 6.32: Throughput of DFT and DFO model versus σ.

Fig. (6.30) shows that where the outage probability of the FD mode is better than, their throughput is better than the throughput of HD mode, too. As observed, when the relay is close to the source or the destination, performance of simple-antenna configuration is better than that of two antennas one, as the relay is far from the source or the destination, the two-antenna one outperforms the other one. Fig. (6.31), Fig. (6.32) show that the outage

probability and throughput of two-antenna configuration are better than that of single-antenna configuration. The bigger σ, the worse their performance. They get the worst value when noise is at the greatest point. This is easy to understand because a higher noise level, can make more harmful power, which causes interference to the transmission signal.

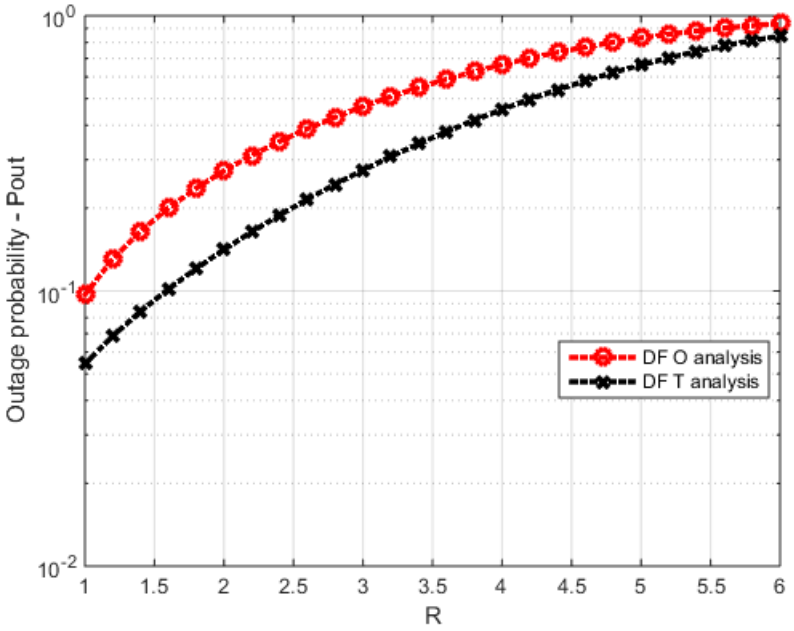

FIGURE 6.33: Outage probability of DFT and DFO model versus R.

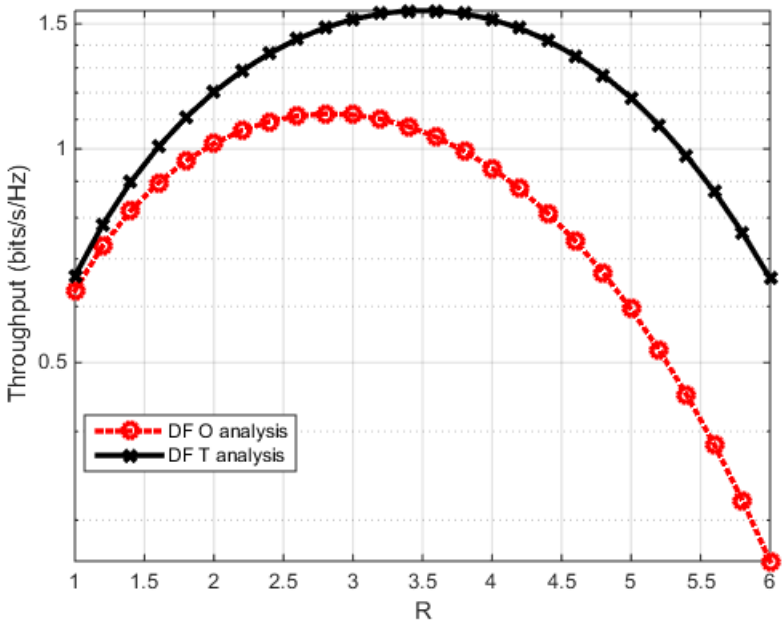

FIGURE 6.34: Throughput of DFT and DFO model versus R.

Moreover, Fig. (6.34) leads to the fact that visually, smaller transfer rate, is corresponding to smaller throughput; it gets the best value at $R = 3$. When the transmission rate ≥ 3, the outage probability raises dramatically, which again decreases the throughput. Easily, we note that the throughput of the two-antenna configuration is better than that of the simple-antenna configuration. This could be explained easily because of the loop back interference in two-antenna configuration and more transmission energy makes attaining the better outage probability and throughput performance than that of single-antenna configuration for any fixed transmission rate.

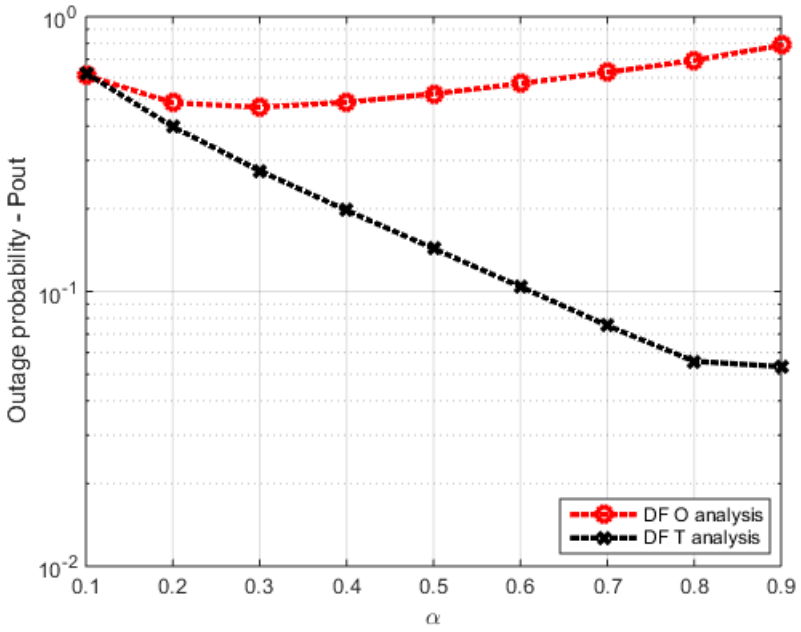

FIGURE 6.35: Outage probability of DFT and DFO model versus α.

As observed, Fig. (6.35), which affects the curves change depending on the time switching factor α, which affects the performance of systems. When $\alpha = 0.2$, for single-antenna configuration, the bigger α is, the worse outage probability gets. It gets the best value at $\alpha = 0.2$. However, for two-antenna configuration, as much α as good its outage probability gets. It is also no difficult to understand, the noise they get to convert a greater amount of energy, which is enough to help it to overcome the drawback of the power splitting initially.
As we can see in Fig. (6.36), the throughput of the two-antenna configuration matches the analysis as mentioned for Fig. (6.35), and the throughput of single-antenna configuration does, either. It gets the best value when $\alpha = 0.2$. For the two-antenna configuration, the best value obtained at $\alpha = 0.3$. As a result, it is noted that the two-antenna configuration outperforms that of a single-antenna configuration.

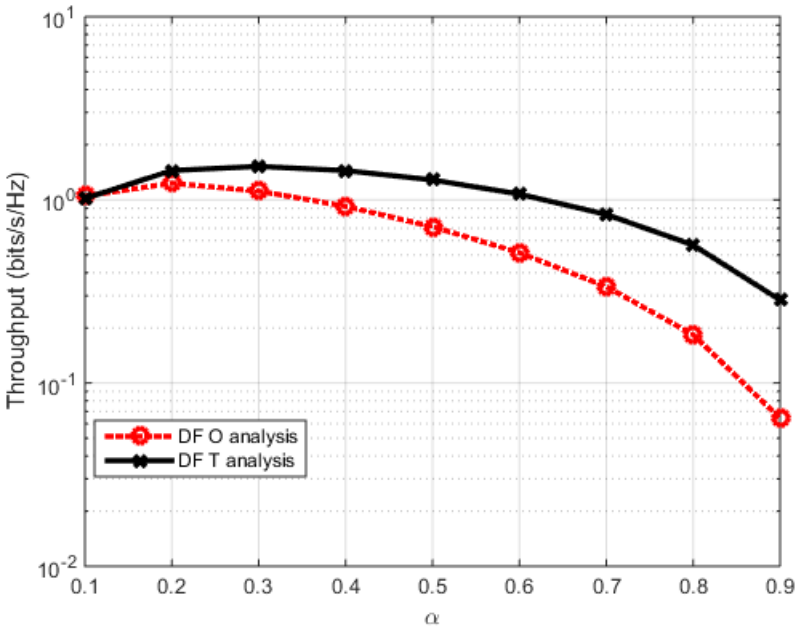

FIGURE 6.36: Throughput of DFT and DFO model versus α.

In this part, we make the comparison between the half-duplex and full-duplex relaying networks with radio energy harvesting and data exchange protocol, in which a power-constrained relaying node harvests energy from the received RF signal and utilize that energy to decode and transmit the data to the destination. Thus, their operation is also compared. To recognize the best communication scheme, the analytical expressions for outage probability and throughput in TSR protocol can be derived and then verified by the Matlab simulation.
As expected, the simulations show that the full-duplex mode outperforms the half-duplex one in some cases. In another case, the HD relaying system could be better than that of the FD one. Also, we see that the performance of the two-antenna configuration is better than that of a single-antenna configuration. So, based on our practical circumstance, we can determine which model should be used to achieve the best benefit. The numerical analysis in this article has also provided a practical vision to the impact of various system parameters on the performance of wireless energy harvesting and information transfer using DF relays nodes.

6.4 Analysis of MRT/MRC Diversity Techniques to Enhance the Detection Performance for MIMO Signals in Full-Duplex Wireless Relay Networks with Transceiver Hardware Impairment

In recent years, multiple-input multiple-output (MIMO) communication systems have greatly attracted attention in both academia and industry because of their capability to boost up the system capacity **[97]**. In MIMO systems, multiple radio frequency (RF) signals are transmitted and received,

thus hardware deployment and signal processing of these systems are very complicated, especially for small-device mobile users. To tackle this issue, maximal ratio transmission (MRT) at the transmitter and maximal ratio combining (MRC) at the receiver have been proposed in literature such as **[98**; **99]**. These diversity techniques were considered as optimal or sub-optimal solutions to improve the detection capability of MIMO RF signal chains. MRT/MRC techniques can significantly enhance the system performance to reach the full diversity order of MIMO systems. Please be noticed that, besides the MRT technique, transmit antenna selection (TAS) is also usually applied at the transmitter. However, the reports in **[99**; **100]** demonstrated that MRT provides maximum array gain when TAS only provides some array gain, but not necessarily maximum. Furthermore, at the receiver, MRC has the best performance among different combining techniques such as selection combining (SC), threshold combining (TC), switch and stay combining (SSC) and equal-gain combining (EGC) **[98- 101]**. Therefore, the usage 0f the MRT/MRC techniques becomes popularly in MIMO communications.

On the other hand, the demand of big data exchanging in the context of the Internet of things (IoT) devices and the Industry Revolution 4.0 has triggered the emerging of various solutions to increase the system capacity such as in-band full-duplex (FD) **[102]**, non-orthogonal multiple access (NOMA) **[103**; **104]**, or millimeter-wave communications **[105**; **106]**. Because FD devices can transmit and receive signals simultaneously on the same frequency band, thus, they can help double the system capacity compared to half-duplex (HD) systems. Therefore, using the FD technique in MIMO systems is inevitable for modern wireless networks, such as the fifth-generation (5G) and beyond **[107]**.

The main drawback of FD communication is the existence of self-interference (SI), caused by the dominance of the power level of the transmitted signal over the received signal at the FD node. To overcome this drawback, a vast variety of self-interference cancellation techniques for full-duplex systems have been proposed **[39**; **109]**. The recent reports on MIMO-FD systems have also investigated the system performance in case of imperfect self-interference cancellation (SIC) at the FD devices **[110- 116]**. The topic of MIMO full-duplex communication has been well studied in the literature, not only about the advanced algorithms and detectors to enhance the overall performance but also on the various channel and hardware conditions, including ideal hardware (ID) and hardware impairment (HI). In **[110]**, the performance of the MIMO-FD system with perfect hardware using amplify-and-forward (AF) FD relay (FDR) has been analyzed in terms of outage probability (OP) and ergodic capacity under the existence of co-channel interference. Their results demonstrated that although the MIMO-FD system suffers from co-channel interference, the FD technique can improve the system performance, especially the capacity, compared to the HD communication mode. In **[111]**, spatial modulation (SM) technique was introduced for MIMO-FDR systems. Through mathematical analysis, the authors derived the average error-probability of signal detection under the impact of RSI at the FDR.

It is also noted that, in practical wireless communication systems, the HI

due to the imperfect transceiver hardware cannot be avoided, especially in the average-quality hardware components. Various works in the literature demonstrated that HI could not be avoided in wireless systems, especially for low-cost devices such as relays **[117]**. There are several types of HI, such as phase oscillator noise, amplifier non-linearity, in-phase/quadrature imbalance, quantization error **[118- 121]**. Large efforts have been made to mitigate the HI via compensation schemes at both the transmitter and receiver using analog and digital signal processing. However, measurement results after all compensation schemes in **[115**; **118-124]** showed that the residual impairments still exist as an additive distortion noise source. The work in **[40]** considered the MIMO-FD system with imperfect hardware, in which transmit and receive beamforming are applied to combat against the hardware noise. The achievable sum-rate has been obtained from this analysis. Other works such as **[114-116]** also analyzed the impact of the HI on the spectral efficiency **[114]** or the achievable sum-rate **[115**; **116]** of MIMO-FD systems. These results, however, do not benchmark with the case of perfect hardware to clearly indicate the effect of HI.

As the aforementioned works, MIMO-FD systems have been considered in a variety of scenarios such as in **[40**; **110**; **111**; **114- 116**; **125]** for both ideal and imperfect hardware, however, most of these works only investigated the case that multiple antennas were deployed at the FDR, not at the source and the destination, i.e., source and destination were single-antenna devices. On the other hand, due to the complexity of MIMO-FD systems, mathematical derivations were focused only on the achievable sum-rate or capacity of the system. The other expressions such as the OP and symbol error rate (SER) were not obtained, especially for the case of HI. In addition, using multiple antennas at the source and the destination may significantly improve the system performance, thanks to the support of diversity techniques and signal processing algorithms, including MRT/MRC. However, this idea was not fully investigated in previous works.

To tackle the above problems as well as provide an insightful view of MIMO-FDR systems under HI condition, we consider in this paper the performance of the MIMO-FDR systems under the effect of both HI and RSI. Unlike previous works, we successfully derive the exact closed-form mathematical expressions of OP, system throughput, and SER of the considered system. From our results, we can easily obtain the OP, throughput and SER expressions of the MIMO-FDR system with perfect hardware and perfect SIC. So that the system performance of the MIMO-FDR system in the case of two imperfect factors can be compared with that in the case of none or one imperfect factor. On the other hand, we indicate the data transmission rates which are suitable for the considered MIMO-FDR system with the presence of HI. The suggestions for proper usage of the transmit power to save the energy for the MIMO-FDR system with HI are also derived from our analysis. It is also noted that, in literature, besides the Rayleigh fading channel model, the Weibull, Nakagami-m, the $\eta - \mu$, $\kappa - \mu$ and the double fading models have been investigated for wireless communication systems **[126-128]**. However, in the paper, we focus on the effects of the HI and RSI on the OP, throughput and SER with MRT/MRC techniques, which creates more complexity in the analysis. Thus, for current work, we just considered

the Rayleigh fading channel model in our analysis. In summary, the contributions of the paper are listed as follows.

– We derive the system and signal detection model using MRT/MRC techniques for MIMO-FDR under HI at all nodes. We aggregate the HI at the transmitters and the receivers for consideration. Based on that the signal-to-interference-plus-noise-and-distortion ratio (SINDR) of the MIMO-FDR system with HI and RSI is derived for DF relaying strategy at the FDR node.

– We successfully obtain the exact closed-form expressions of outage probability, system throughput, and the symbol error rate of the proposed the MIMO-FDR system under the impact of the HI and RSI over Rayleigh fading channel. From these expressions, we can easily obtain the expressions of the MIMO-FDR system or/and the MIMO-HDR systems with perfect hardware as a special case; and they can serve as a benchmark to evaluate the effect of HI. The correctness of our analysis is confirmed by Monte-Carlo simulations.

– We analyze the OP, system throughput and SER of the MIMO-FDR system with HI and compare them to the corresponding values in the MIMO-FDR system with ideal hardware. It is seen that HI has a strong impact on the performance of MIMO-FDR systems, especially at high data transmission rate regime. Thus, under the HI, the MIMO-FDR system is most suitable for low or moderate data transmission rates because the impact of HI and RSI becomes stronger for higher data transmission rates. The combination of HI and RSI can create an error floor for the proposed system, i.e., we cannot reduce the OP or SER less than some lower bounds. It can be implied that due to the error floor, we should use suitable transmission power to save the energy for the MIMO-FDR system with HI. In other words, based on certain values of the HI and RSI levels of the proposed system, we can choose suitable data transmission rates and transmission power for maintaining the performance and power efficiency of the proposed system.

The rest of the paper is organized as follows. The system and signal models of the MRT/MRC MIMO-FDR system with HI are presented in Section 6.4.1. Then, the system performance in terms of OP and SER is derived in Section 6.4.2. Numerical results and discussion are provided in detail in Section 6.4.3. For reading convenience, a summary list of the frequently used mathematical notations is given in Table [6.1].

6.4.1 System Model

Fig. 6.37 presents the block diagram of the MIMO-FDR system under HI, where the source (S) has M transmit antennas communicates with the destination (D) that has N receive antennas via the assistance of a relay (R), which is equipped with two antennas, one for transmitting and the other for receiving. Similar to **[114]**, we assume that the antenna spacing is sufficiently large so that the channels are spatially uncorrelated. We also assume that the hardware impairments are uncorrelated among antennas. As presented in Fig. 6.37, S and D are HD devices while R is the FD device, thus R can simultaneously transmit and receive signals in the same frequency band. As a result, the self-interference (SI) from transmit antenna to receive

TABLE 6.1: List of the frequently used mathematical notations.

Notation	Description
$P_{\mathrm{S}}, P_{\mathrm{R}}$	The average transmit power of S and R
$\Pr\{\mathcal{A}\}$	The probability of an event $\mathcal{A}$
$\mathcal{P}_{\mathrm{out}}$	Outage probability
$F(.)$	Cumulative distribution function (CDF)
$f(.)$	Probability density function (PDF)
$\mathcal{CN}(\mu, \sigma^2)$	Complex Gaussian distribution with mean μ and variance of σ^2
$\mathbb{E}\{\cdot\}$	The expectation operator
G	Complexity-accuracy trade-off parameter
$\mathbf{h}_{\mathrm{SR}}, \mathbf{h}_{\mathrm{RD}}$	The channel vector of S–R and R–D links
η	Noise caused by hardware impairments
k	The HI level
l	The RSI level
M	The number of transmit antennas of S
N	The number of receive antennas of D
SER	Symbol error rate

antenna of R is generated unintentionally. To reduce the SI power in order to improve system performance, all self-interference cancellation (SIC) techniques such as passive suppression and active cancellation are applied at R. It is also noted that although amplified-and-forward (AF) protocol may be simpler to implement than decode-and-forward (DF) protocol, DF relaying usually offer better performance than AF relaying **[130]**. In this paper, the proposed system is affected by various negative factors, including HI and RSI. Thus, DF relaying should be selected to improve system performance.

Furthermore, in the paper, we assume that perfect channel state information (CSI) is available at all nodes in the system. Before signal transmission, channel estimation is performed by using pilot symbols. At the transmitter S, pilot symbols are sent by M transmit antennas, and the received signals at R from M transmit antennas of S are monitored. Then, R feeds back the transmit weights related to the transmit antennas as well as the instantaneous SINDRs at R without feedback error or delay. Based on that, the weights for M transmit antennas of S are fully calculated for the MRT technique **[99- 101**; **131]**. Similarly, we obtain the weights for the MRC technique at the receiver D. These assumptions may not fully reflect the practical MIMO-FDR system behavior, however, we focus on mathematical analysis by deriving the exact closed-form expressions of OP, throughput and SER of the considered system under the impact of HI and RSI. For this reason, we think that it is reasonable to assume the knowledge of all channels at the transceivers.

It is obvious that the transmitted and received signals of the MIMO-FDR system with HI are different from the ideal system. For example, at the transmitter, e.g., at R, the transmitted signal is only x_{R} in the case of the ideal system while it is $x_{\mathrm{R}} + \eta_{\mathrm{R}}^{\mathrm{t}}$ for the imperfect-hardware MIMO-FDR

system, where $\eta_{\mathrm{R}}^{\mathrm{t}}$ denotes the noise due to HI at the transmitter. It is similar for the receivers, e.g., at R, the term $\eta_{\mathrm{R}}^{\mathrm{r}}$ is added due to the receiver HI, where $\eta_{\mathrm{R}}^{\mathrm{r}}$ denotes the noise caused by the receiver at R. Similar model is used for the transmitter S and the receiver D, i.e., the terms η_i^{t} are added at ith transmit antenna of S ($i = 1, 2, ..., M$) and the terms η_j^{r} are added at jth receive antenna of D ($j = 1, 2, ..., N$).

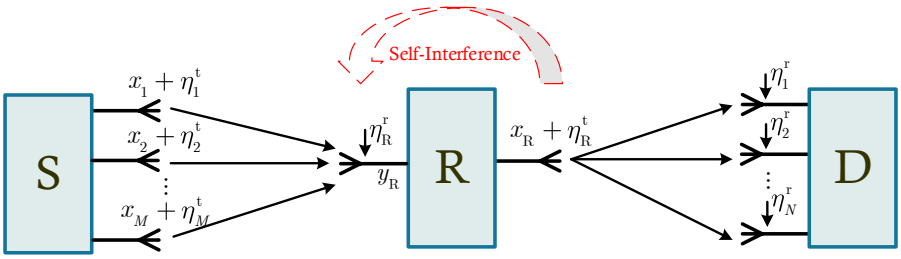

FIGURE 6.37: Block diagram of the MIMO-FDR system with HI.

The received signals at R is computed as

$$y_{\mathrm{R}} = \mathbf{h}_{\mathrm{SR}}(\mathbf{x}_i + \boldsymbol{\eta}_i^{\mathrm{t}}) + \eta_{\mathrm{R}}^{\mathrm{r}} + h_{\mathrm{RR}}(x_{\mathrm{R}} + \eta_{\mathrm{R}}^{\mathrm{t}}) + z_{\mathrm{R}}, \tag{6.74}$$

where $\mathbf{h}_{\mathrm{SR}} = [h_{1\mathrm{R}}\ h_{2\mathrm{R}}\ ...\ h_{M\mathrm{R}}]$ is the channel vector from M transmit antennas of S to the receive antenna of R, $i = 1, 2, ..., M$; $\mathbf{x}_i = [x_1\ x_2\ ...\ x_M]^T$ is the transmitted signal vector from M transmit antennas of S; $\boldsymbol{\eta}_i^{\mathrm{t}} = [\eta_1^{\mathrm{t}}\ \eta_2^{\mathrm{t}}\ ...\ \eta_M^{\mathrm{t}}]^T$ is HI noise vector that caused by the transmitter impairment; h_{RR} is the SI channel from the transmit antenna to receive antenna of R; x_{R} is intended transmitted signal at R; $\eta_{\mathrm{R}}^{\mathrm{t}}$ and $\eta_{\mathrm{R}}^{\mathrm{r}}$ are the HI noises due to the transmitter and the receiver of R, respectively; z_{R} is Gaussian noise at R which has zero mean and variance of σ_{R}^2, e.g., $z_{\mathrm{R}} \sim \mathcal{CN}(0, \sigma_{\mathrm{R}}^2)$. Notice that the HI noises due to the physical transceiver imperfection are caused by many factors. At the transmitters, HI may be caused by in-phase/quadrature (I/Q) imbalance, high power amplifier (HPA) non-linearity and phase oscillator noise **[122; 123; 132; 133]**. At the receivers, the hardware imperfection of low noise amplifier (LNA) and filters may distort the received signals **[123; 133]**. Various compensation algorithms have been proposed to mitigate the transceiver HI, however, the residual impairment always exists in the system **[115; 122; 123; 134]**. It is assumed that after applying compensation algorithms, the residual HI noise is Gaussian distributed, e.g., $\boldsymbol{\eta}_i^{\mathrm{t}} \sim \mathcal{CN}(0, (k_{\mathrm{S}}^{\mathrm{t}})^2 \frac{P_{\mathrm{S}}}{M})$, $\eta_{\mathrm{R}}^{\mathrm{t}} \sim \mathcal{CN}(0, (k_{\mathrm{R}}^{\mathrm{t}})^2 P_{\mathrm{R}})$ for the transmitters S and R, respectively and $\eta_{\mathrm{R}}^{\mathrm{r}} \sim \mathcal{CN}(0, \|\mathbf{h}_{\mathrm{SR}}\|^2 (k_{\mathrm{R}}^{\mathrm{r}})^2 \frac{P_{\mathrm{S}}}{M})$ for the receiver R. Herein, $k_{\mathrm{S}}^{\mathrm{t}}$, $k_{\mathrm{R}}^{\mathrm{t}}$, and $k_{\mathrm{R}}^{\mathrm{r}}$ denote the HI levels at the transmitters S, R and the receiver R, respectively; $\frac{P_{\mathrm{S}}}{M}$ is the average transmission power per antenna of S and P_{R} is the average transmission power of R. It can be seen from Eq. (6.74) that the term $h_{\mathrm{RR}}(x_{\mathrm{R}} + \eta_{\mathrm{R}}^{\mathrm{t}})$ is the SI before applying various SIC techniques. As mentioned above, all SIC techniques for FD devices, which include passive suppression and active cancellation are applied at the FDR of the hardware-impairment MIMO-FDR (HI-MIMO-FDR) system. First, in the passive suppression, R may use directional isolation, absorptive shielding, and cross-polarization to reduce SI power **[135; 136]**. Thanks to the separate antennas for signal transmission and reception, R can use advanced

interference isolation techniques in the propagation domain to better reduce the SI leakage. Then, in active cancellation, the analog and digital signal processing methods are applied at R. We assume that the FD device can exploit the architectures for SIC in analog and digital domains such as in **[106**; **107**; **109]**. By estimating the SI channel, R can subtract the SI signal from the received signal, especially in digital domain cancellation **[39**; **109**; **110]**. In fact, R definitely knows the transmit signal x_{R}, so by using the results of SI channel estimation of h_{RR}, it can apply digital processing methods to subtract the SI from the received signals **[39**; **109**; **136]**. However, SI cannot be removed completely due to the imperfect hardware and imperfect SI channel estimation **[136**; **138]**. Therefore, the residual SI still exists in FDR device. In fact, the RSI at FDR (denoted by I_{R}) can be modeled as Gaussian distributed random variable with zero mean and variance of γ_{RSI}, i.e., $I_{\mathrm{R}} \sim \mathcal{CN}(0, \gamma_{\mathrm{RSI}})$, where $\gamma_{\mathrm{RSI}} = l^2 P_{\mathrm{R}}$ with l denotes the SIC capability of FDR device **[136**; **139- 141]**.

Now, Eq. (6.74) can be rewritten as

$$y_{\mathrm{R}} = \mathbf{h}_{\mathrm{SR}}(\mathbf{x}_i + \boldsymbol{\eta}_i^{\mathrm{t}}) + \eta_{\mathrm{R}}^{\mathrm{r}} + I_{\mathrm{R}} + z_{\mathrm{R}}. \tag{6.75}$$

Then, R decodes the received signal and forwards it to D. The received signal at D is expressed as

$$\mathbf{y}_{\mathrm{D}} = \mathbf{h}_{\mathrm{RD}}(x_{\mathrm{R}} + \eta_{\mathrm{R}}^{\mathrm{t}}) + \boldsymbol{\eta}_j^{\mathrm{r}} + \mathbf{z}_{\mathrm{D}}, \tag{6.76}$$

where $\mathbf{h}_{\mathrm{RD}} = [h_{\mathrm{R}1}\ h_{\mathrm{R}2}\ ...\ h_{\mathrm{R}N}]^T$ is channel vector from the transmit antenna of R to N receive antennas of D; $\boldsymbol{\eta}_j^{\mathrm{r}} = [\eta_1^{\mathrm{r}}\ \eta_2^{\mathrm{r}}\ ...\ \eta_N^{\mathrm{r}}]^T$ $(j = 1, 2, ..., N)$ is HI noise vector that caused by the receiver impairment at D, i.e., $\boldsymbol{\eta}_j^{\mathrm{r}} \sim \mathcal{CN}(0, \|\mathbf{h}_{\mathrm{RD}}\|^2 (k_{\mathrm{D}}^{\mathrm{r}})^2 P_{\mathrm{R}})$ for the receiver D, where $k_{\mathrm{D}}^{\mathrm{r}}$ denotes the HI level at the receiver D; $\mathbf{z}_{\mathrm{D}}$ is Gaussian noise vector at D with zero mean and variance of σ_{D}^2, i.e., $\mathbf{z}_{\mathrm{D}} \sim \mathcal{CN}(0, \sigma_{\mathrm{D}}^2)$.

Based on Eq. (6.75) and Eq. (6.76), the instantaneous SINDR at R and D (denoted by γ_{R} and γ_{D}, respectively) are computed as

$$\gamma_{\mathrm{R}} = \frac{\|\mathbf{h}_{\mathrm{SR}}\|^2 \frac{P_{\mathrm{S}}}{M}}{\|\mathbf{h}_{\mathrm{SR}}\|^2 (k_{\mathrm{S}}^{\mathrm{t}})^2 \frac{P_{\mathrm{S}}}{M} + \|\mathbf{h}_{\mathrm{SR}}\|^2 (k_{\mathrm{R}}^{\mathrm{r}})^2 \frac{P_{\mathrm{S}}}{M} + \gamma_{\mathrm{RSI}} + \sigma_{\mathrm{R}}^2} = \frac{\|\mathbf{h}_{\mathrm{SR}}\|^2 \frac{P_{\mathrm{S}}}{M}}{T_1}, \tag{6.77}$$

$$\gamma_{\mathrm{D}} = \frac{\|\mathbf{h}_{\mathrm{RD}}\|^2 P_{\mathrm{R}}}{\|\mathbf{h}_{\mathrm{RD}}\|^2 (k_{\mathrm{R}}^{\mathrm{t}})^2 P_{\mathrm{R}} + \|\mathbf{h}_{\mathrm{RD}}\|^2 (k_{\mathrm{D}}^{\mathrm{r}})^2 P_{\mathrm{R}} + \sigma_{\mathrm{D}}^2} = \frac{\|\mathbf{h}_{\mathrm{RD}}\|^2 P_{\mathrm{R}}}{\|\mathbf{h}_{\mathrm{RD}}\|^2 k_{\mathrm{RD}}^2 P_{\mathrm{R}} + \sigma_{\mathrm{D}}^2}, \tag{6.78}$$

where $T_1 = \|\mathbf{h}_{\mathrm{SR}}\|^2 k_{\mathrm{SR}}^2 \frac{P_{\mathrm{S}}}{M} + \gamma_{\mathrm{RSI}} + \sigma_{\mathrm{R}}^2$ and $k_{\mathrm{SR}}^2 = (k_{\mathrm{S}}^{\mathrm{t}})^2 + (k_{\mathrm{R}}^{\mathrm{r}})^2$ denotes the aggregated HI level of both HI at the transmitter S ($k_{\mathrm{S}}^{\mathrm{t}}$) and the receiver R ($k_{\mathrm{R}}^{\mathrm{r}}$); $k_{\mathrm{RD}}^2 = (k_{\mathrm{R}}^{\mathrm{t}})^2 + (k_{\mathrm{D}}^{\mathrm{r}})^2$ denotes the aggregated HI level at both transmitter R ($k_{\mathrm{R}}^{\mathrm{t}}$) and receiver D ($k_{\mathrm{D}}^{\mathrm{r}}$). Since the DF relaying strategy is applied at FDR, the end-to-end SINDR (denoted by γ_{e2e}) of the MIMO-FDR system under HI can be expressed as

$$\gamma_{\mathrm{e2e}} = \min\{\gamma_{\mathrm{R}}, \gamma_{\mathrm{D}}\}, \tag{6.79}$$

where γ_{R} and γ_{D} are given as Eq. (6.77) and Eq. (6.78), respectively.

6.4.2 Performance Analysis

In this section, the performance of the proposed MIMO-FDR system with HI is analyzed through mathematical expressions of OP and SER. First, we derive the exact closed-form expression of OP. Based on this expression, we obtain the CDF of the end-to-end SINDR of the proposed system. Finally, from this CDF, we get the exact closed-form expression of SER.

Outage Probability

The OP of the HI-MIMO-FDR system is calculated as the probability when the instantaneous data transmission rate is lower than the predefined data transmission rate **[142]**. Mathematically, we have:

$$\mathcal{P}_{\text{out}} = \Pr\{\mathcal{R} < \mathcal{R}_0\}, \tag{6.80}$$

where $\mathcal{R} = \log_2(1+\gamma_{\text{e2e}})$ and $\mathcal{R}_0$ are the instantaneous and predefined data transmission rates of the considered system, respectively. As a result, we get the probability as

$$\begin{aligned}\mathcal{P}_{\text{out}} &= \Pr\{\log_2(1+\gamma_{\text{e2e}}) < \mathcal{R}_0\} = \Pr\{\gamma_{\text{e2e}} < 2^{\mathcal{R}_0} - 1\} \\ &= \Pr\{\min\{\gamma_{\text{R}}, \gamma_{\text{D}}\} < \gamma_{\text{th}}\} = \Pr\{(\gamma_{\text{R}} < \gamma_{\text{th}}) \cup (\gamma_{\text{D}} < \gamma_{\text{th}})\}, \\ &= \Pr\{\min\{\gamma_{\text{R}}, \gamma_{\text{D}}\} < 2^{\mathcal{R}_0} - 1\},\end{aligned} \tag{6.81}$$

where $\gamma_{\text{th}} = 2^{\mathcal{R}_0} - 1$ denotes the SINDR threshold. It is noted that the probability in Eq. (6.81) can be expressed as the probability of the event that the outage occurs when $\text{S} \to \text{R}$ link is in an outage, or $\text{S} \to \text{R}$ link is not in an outage but $\text{R} \to \text{D}$ link is in an outage.

By applying **[143]** for the probability of two independent events, $\mathcal{A}$ and $\mathcal{B}$, we have:

$$\Pr\{\mathcal{A} \cup \mathcal{B}\} = \Pr\{\mathcal{A}\} + \Pr\{\mathcal{B}\} - \Pr\{\mathcal{A}\}\Pr\{\mathcal{B}\}. \tag{6.82}$$

The equation Eq. (6.81) can be expressed as

$$\mathcal{P}_{\text{out}} = \Pr\{\gamma_{\text{R}} < \gamma_{\text{th}}\} + \Pr\{\gamma_{\text{D}} < \gamma_{\text{th}}\} - \Pr\{\gamma_{\text{R}} < \gamma_{\text{th}}\}\Pr\{\gamma_{\text{D}} < \gamma_{\text{th}}\}. \tag{6.83}$$

Based on Eq. (6.83), we can derive the OP of the considered MIMO-FDR system under HI as in the following Theorem 1.

Theorem 1. The OP expression of the MRT/MRC MIMO-FDR system under the impact of both HI and RSI over Rayleigh fading channel is expressed as

$$\mathcal{P}_{\text{out}} = \begin{cases} 1 - \exp[\frac{-M\gamma_{\text{th}}(\gamma_{\text{RSI}}+\sigma_{\text{R}}^2)}{\Omega_1 P_{\text{S}}(1-k_{\text{SR}}^2\gamma_{\text{th}})} - G_1 \frac{\gamma_{\text{th}}\sigma_{\text{D}}^2}{\Omega_2 P_{\text{R}}(1-k_{\text{RD}}^2\gamma_{\text{th}})}] \\ \quad \text{if } \gamma_{\text{th}} < \min(\frac{1}{k_{\text{RD}}^2}, \frac{1}{k_{\text{SR}}^2}) \\ 1 \qquad \text{otherwise}, \end{cases} \tag{6.84}$$

where $G_1 = \sum\limits_{i=0}^{M-1}\sum\limits_{j=0}^{N-1} \frac{1}{i!j!}[\frac{M\gamma_{\text{th}}(\gamma_{\text{RSI}}+\sigma_{\text{R}}^2)}{\Omega_1 P_{\text{S}}(1-k_{\text{SR}}^2\gamma_{\text{th}})}]^i [\frac{\gamma_{\text{th}}\sigma_{\text{D}}^2}{\Omega_2 P_{\text{R}}(1-k_{\text{RD}}^2\gamma_{\text{th}})}]^j$, $\Omega_1 = \mathbb{E}\{|h_{1\text{R}}|^2\} = \mathbb{E}\{|h_{2\text{R}}|^2\} = ... = \mathbb{E}\{||h_{M\text{R}}|^2\}$ and $\Omega_2 = \mathbb{E}\{|h_{\text{R}1}|^2\} = \mathbb{E}\{|h_{\text{R}2}|^2\} = ... = \mathbb{E}\{||h_{\text{R}N}|^2\}$ are respectively the average channel gains of S-R and R-D links.

Proof: To derive Eq. (6.84), we first obtain the probabilities $\Pr\{\gamma_{\rm R} < \gamma_{\rm th}\}$ and $\Pr\{\gamma_{\rm D} < \gamma_{\rm th}\}$. Since MRT is used for transmitting signals from S to R, we have:

$$\Pr\{\gamma_{\rm R} < \gamma_{\rm th}\} = \Pr\left\{\frac{\|\mathbf{h}_{\rm SR}\|^2 \frac{P_{\rm S}}{M}}{\|\mathbf{h}_{\rm SR}\|^2 k_{\rm SR}^2 \frac{P_{\rm S}}{M} + \gamma_{\rm RSI} + \sigma_{\rm R}^2} < \gamma_{\rm th}\right\}. \tag{6.85}$$

Now, we rewrite Eq. (6.85) as

$$\Pr\{\gamma_{\rm R} < \gamma_{\rm th}\} = \Pr\left\{\|\mathbf{h}_{\rm SR}\|^2 \frac{P_{\rm S}}{M}(1 - k_{\rm SR}^2\gamma_{\rm th}) < \gamma_{\rm th}(\gamma_{\rm RSI} + \sigma_{\rm R}^2)\right\}. \tag{6.86}$$

When $1 - k_{\rm SR}^2\gamma_{\rm th} \leq 0$, or equivalently, $\gamma_{\rm th} \geq \frac{1}{k_{\rm SR}^2}$ the inequality inside the probability in Eq. (6.86) always holds, due to the fact that $\|\mathbf{h}_{\rm SR}\|^2 \frac{P_{\rm S}}{M}(1 - k_{\rm SR}^2\gamma_{\rm th}) \leq 0$ while $\gamma_{\rm th}(\gamma_{\rm RSI} + \sigma_{\rm R}^2) > 0$. Therefore, we obtain $\Pr\{\gamma_{\rm R} < \gamma_{\rm th}\} = 1$ when $\gamma_{\rm th} \geq \frac{1}{k_{\rm SR}^2}$.

When $1 - k_{\rm SR}^2\gamma_{\rm th} > 0$, i.e., $\gamma_{\rm th} < \frac{1}{k_{\rm SR}^2}$, we can rewrite the probability in Eq. (6.86) as

$$\Pr\{\gamma_{\rm R} < \gamma_{\rm th}\} = \Pr\left\{\|\mathbf{h}_{\rm SR}\|^2 < \frac{M\gamma_{\rm th}(\gamma_{\rm RSI} + \sigma_{\rm R}^2)}{P_{\rm S}(1 - k_{\rm SR}^2\gamma_{\rm th})}\right\}. \tag{6.87}$$

Since $\|\mathbf{h}_{\rm SR}\|^2 = |h_{1\rm R}|^2 + |h_{2\rm R}|^2 + ... + |h_{M\rm R}|^2$, the probability density function (PDF, $f(.)$) and the cumulative distribution function (CDF, $F(.)$) of $\|\mathbf{h}_{\rm SR}\|^2$ are respectively given as **[144]**

$$F_{\|\mathbf{h}_{\rm SR}\|^2}(x) = 1 - \exp\Big(-\frac{x}{\Omega_1}\Big)\sum_{i=0}^{M-1}\frac{1}{i!}\Big(\frac{x}{\Omega_1}\Big)^i, \quad x \geq 0, \tag{6.88}$$

$$f_{\|\mathbf{h}_{\rm SR}\|^2}(x) = \frac{x^{M-1}}{\Omega_1^M \Gamma(M)}\exp\Big(-\frac{x}{\Omega_1}\Big), \quad x \geq 0, \tag{6.89}$$

where $\Gamma(z) \triangleq \int_0^\infty x^{z-1}e^{-x}dx$ is the gamma function **[145]**.

By using Eq. (6.88), Eq. (6.87) can be rewritten as

$$\begin{aligned}
&\Pr\{\gamma_{\rm R} < \gamma_{\rm th}\} = F_{\|\mathbf{h}_{\rm SR}\|^2}\Big(\frac{M\gamma_{\rm th}(\gamma_{\rm RSI} + \sigma_{\rm R}^2)}{P_{\rm S}(1 - k_{\rm SR}^2\gamma_{\rm th})}\Big) = {\rm A}_1 \\
&A_1 = 1 - \exp\Big(-\frac{M\gamma_{\rm th}(\gamma_{\rm RSI} + \sigma_{\rm R}^2)}{\Omega_1 P_{\rm S}(1 - k_{\rm SR}^2\gamma_{\rm th})}\Big)\sum_{i=0}^{M-1}\frac{1}{i!}\Big(\frac{M\gamma_{\rm th}(\gamma_{\rm RSI} + \sigma_{\rm R}^2)}{\Omega_1 P_{\rm S}(1 - k_{\rm SR}^2\gamma_{\rm th})}\Big)^i.
\end{aligned} \tag{6.90}$$

$$\Pr\{\gamma_{\rm R} < \gamma_{\rm th}\} = \begin{cases} A_1 & \text{if } \gamma_{\rm th} < \frac{1}{k_{\rm SR}^2}. \\ 1 & \text{if } \gamma_{\rm th} \geq \frac{1}{k_{\rm SR}^2}. \end{cases} \tag{6.91}$$

By applying all above steps, we can obtain the probability $\Pr\{\gamma_{\rm D} < \gamma_{\rm th}\}$ as

$$\Pr\{\gamma_{\rm D} < \gamma_{\rm th}\} = \begin{cases} 1 - B_1 & \text{if } \gamma_{\rm th} < \frac{1}{k_{\rm RD}^2}, \\ 1 & \text{if } \gamma_{\rm th} \geq \frac{1}{k_{\rm RD}^2}, \end{cases} \tag{6.92}$$

where $B_1 = exp(-\frac{\gamma_{\rm th}\sigma_{\rm D}^2}{\Omega_2 P_{\rm R}(1-k_{\rm RD}^2\gamma_{\rm th})}) \sum\limits_{j=0}^{N-1} \frac{1}{j!}(\frac{\gamma_{\rm th}\sigma_{\rm D}^2}{\Omega_2 P_{\rm R}(1-k_{\rm RD}^2\gamma_{\rm th})})^j$.

Finally, by substituting Eq. (6.91) and Eq. (6.92) into Eq. (6.83), the OP of the MRT/MRC MIMO-FDR system under HI is obtained as in Eq. (6.84). This completes the proof.

System Throughput

Besides the OP, another important parameter for the system performance is system throughput. The system throughput (denoted by $\mathcal{T}_{\rm put}$) of the MRT/MRC MIMO-FDR system under HI is calculated as

$$\mathcal{T}_{\rm put} = \mathcal{R}(1 - \mathcal{P}_{\rm out}), \tag{6.93}$$

where $\mathcal{R}$ is the data transmission rate (bit/s/Hz); $\mathcal{P}_{\rm out}$ is the OP of the considered system which is given as in Eq. (6.84) in Theorem 1.

Symbol Error Rate

According to **[142]**, the SER of the proposed MIMO-FDR system under HI and with coherent detection as receivers is computed as

$$\text{SER} = a\mathbb{E}\{Q(\sqrt{b\gamma_{\rm e2e}})\} = \frac{a}{\sqrt{2\pi}} \int\limits_0^\infty F\Big(\frac{t^2}{b}\Big) \exp\Big(-\frac{t^2}{2}\Big) dt, \tag{6.94}$$

where (a, b) are a pair of parameters which depend on specific modulation type, e.g. $(a, b) = (1, 2)$ for binary phase-shift keying (BPSK) and $(a, b) = (2, 1)$ for 4-quadrature amplitude modulation (4-QAM) modulations; $Q(x) \triangleq \frac{1}{\sqrt{2\pi}} \int\limits_x^\infty \exp\left(-\frac{u^2}{2}\right) du$ is the Gaussian function; $\gamma_{\rm e2e}$ is the end-to-end SINDR and $F(.)$ is the CDF of the SINDR of the considered system. By changing variable $x = \frac{t^2}{b}$, Eq. (6.94) now becomes

$$\text{SER} = \frac{a\sqrt{b}}{2\sqrt{2\pi}} \int\limits_0^\infty \frac{\exp\left(-\frac{bx}{2}\right)}{\sqrt{x}} F(x) dx. \tag{6.95}$$

From Eq. (6.95), we can claim the SER of the MRT/MRC MIMO-FDR system under HI in the following Theorem 2.

Theorem 2. The SER expression of the MRT/MRC MIMO-FDR system under the impact of both HI and RSI over Rayleigh fading channel is expressed as

$$\text{SER} = \tfrac{a}{2} - \tfrac{a\sqrt{b\pi}}{4\sqrt{2}Gk^2} \sum_{i=0}^{M-1} \sum_{j=0}^{N-1} \sum_{g=1}^{G} \frac{\sqrt{1-\phi_g^2}}{i!j!\sqrt{\Delta}} \quad E_1 E_2, \tag{6.96}$$

where $E_1 = \exp(-\frac{b\Delta}{2} - \frac{M(\gamma_{\text{RSI}}+\sigma_{\text{R}}^2)\Delta}{\Omega_1 P_{\text{S}}(1-k_{\text{SR}}^2\Delta)} - \frac{\sigma_{\text{D}}^2\Delta}{\Omega_2 P_{\text{R}}(1-k_{\text{RD}}^2\Delta)})$, $k^2 = \max(k_{\text{SR}}^2, k_{\text{RD}}^2)$, $\Delta = \frac{1}{k^2}\Big(1+\phi_g\Big)$; $E_2 = (\frac{M(\gamma_{\text{RSI}}+\sigma_{\text{R}}^2)\Delta}{\Omega_1 P_{\text{S}}(1-k_{\text{SR}}^2\Delta)})^i(\frac{\sigma_{\text{D}}^2\Delta}{\Omega_2 P_{\text{R}}(1-k_{\text{RD}}^2\Delta)})^j$, G is a complexity-accuracy trade-off parameters **[108]**; $\phi_g = \cos\Big(\frac{(2g-1)\pi}{2G}\Big)$, Ω_1 and Ω_2 are defined as in Theorem 1.

Proof: To derive the SER expression in Eq. (6.96), we first derive the CDF, $F(x)$, to substitute it into Eq. (6.95). From the definition of $F(x)$ in **[142]**, i.e.,

$$F(x) = \Pr\{\gamma_{\text{e2e}} < x\}. \tag{6.97}$$

We can obtain $F(x)$ from the OP of the MRT/MRC MIMO-FDR system under HI by replacing γ_{th} with x in the OP expression. Therefore, we have:

$$F(x) = \begin{cases} 1 - \exp(-\frac{M(\gamma_{\text{RSI}}+\sigma_{\text{R}}^2)x}{\Omega_1 P_{\text{S}}(1-k_{\text{SR}}^2 x)} - \frac{\sigma_{\text{D}}^2 x}{\Omega_2 P_{\text{R}}(1-k_{\text{RD}}^2 x)})E_3 & \text{if } x < \frac{1}{k^2}, \\ 1 \quad \text{if } x \geq \frac{1}{k^2}, \end{cases} \tag{6.98}$$

where $E_3 = \sum_{i=0}^{M-1}\sum_{j=0}^{N-1} \frac{1}{i!j!}(\frac{M(\gamma_{\text{RSI}}+\sigma_{\text{R}}^2)x}{\Omega_1 P_{\text{S}}(1-k_{\text{SR}}^2 x)})^i(\frac{\sigma_{\text{D}}^2 x}{\Omega_2 P_{\text{R}}(1-k_{\text{RD}}^2 x)})^j$.
By substituting Eq. (6.98) into Eq. (6.95), the SER can be calculated as

$$\text{SER} = \frac{a\sqrt{b}}{2\sqrt{2\pi}}[\int_0^{\frac{1}{k^2}} \frac{\exp(-\frac{bx}{2})}{\sqrt{x}}(1-L_1)\,\text{L}_2 dx + \int_{\frac{1}{k^2}}^{\infty} \frac{\exp(-\frac{bx}{2})}{\sqrt{x}}dx], \tag{6.99}$$

where $L_1 = \exp\Big(-\frac{M(\gamma_{\text{RSI}}+\sigma_{\text{R}}^2)x}{\Omega_1 P_{\text{S}}(1-k_{\text{SR}}^2 x)} - \frac{\sigma_{\text{D}}^2 x}{\Omega_2 P_{\text{R}}(1-k_{\text{RD}}^2 x)}\Big)$,
$L_2 = \sum_{i=0}^{M-1}\sum_{j=0}^{N-1} \frac{1}{i!j!}(\frac{M(\gamma_{\text{RSI}}+\sigma_{\text{R}}^2)x}{\Omega_1 P_{\text{S}}(1-k_{\text{SR}}^2 x)})^i(\frac{\sigma_{\text{D}}^2 x}{\Omega_2 P_{\text{R}}(1-k_{\text{RD}}^2 x)})^j$.
Now, we rewrite Eq. (6.99) as

$$\text{SER} = \frac{a\sqrt{b}}{2\sqrt{2\pi}}[\int_0^{\frac{1}{k^2}} \frac{\exp(-\frac{bx}{2})}{\sqrt{x}}dx - \int_0^{\frac{1}{k^2}} \frac{1}{\sqrt{x}}\exp(N_2)N_3 dx + \int_{\frac{1}{k^2}}^{\infty} \frac{\exp(-\frac{bx}{2})}{\sqrt{x}}dx], \tag{6.100}$$

where $N_2 = -\frac{bx}{2} - \frac{M(\gamma_{\text{RSI}}+\sigma_{\text{R}}^2)x}{\Omega_1 P_{\text{S}}(1-k_{\text{SR}}^2 x)} - \frac{\sigma_{\text{D}}^2 x}{\Omega_2 P_{\text{R}}(1-k_{\text{RD}}^2 x)}$,
$N_3 = \sum_{i=0}^{M-1}\sum_{j=0}^{N-1} \frac{1}{i!j!}(\frac{M(\gamma_{\text{RSI}}+\sigma_{\text{R}}^2)x}{\Omega_1 P_{\text{S}}(1-k_{\text{SR}}^2 x)})^i(\frac{\sigma_{\text{D}}^2 x}{\Omega_2 P_{\text{R}}(1-k_{\text{RD}}^2 x)})^j$.
By combining first and last terms in Eq. (6.100), we can rewrite Eq. (6.100) as

$$\text{SER} = \frac{a\sqrt{b}}{2\sqrt{2\pi}}\left[\int_0^{\infty} \frac{\exp(-\frac{bx}{2})}{\sqrt{x}}dx - \int_0^{\frac{1}{k^2}} \frac{1}{\sqrt{x}})A_1 A_2 dx\right], \tag{6.101}$$

where $A_1 = \exp\Big(-\frac{bx}{2} - \frac{M(\gamma_{\text{RSI}}+\sigma_{\text{R}}^2)x}{\Omega_1 P_{\text{S}}(1-k_{\text{SR}}^2 x)} - \frac{\sigma_{\text{D}}^2 x}{\Omega_2 P_{\text{R}}(1-k_{\text{RD}}^2 x)}\Big)$,
$A_2 = \sum_{i=0}^{M-1}\sum_{j=0}^{N-1} \frac{1}{i!j!}(\frac{M(\gamma_{\text{RSI}}+\sigma_{\text{R}}^2)x}{\Omega_1 P_{\text{S}}(1-k_{\text{SR}}^2 x)})^i(\frac{\sigma_{\text{D}}^2 x}{\Omega_2 P_{\text{R}}(1-k_{\text{RD}}^2 x)})^j$.

Now, using Eq. [3.361.2] in **[145]**, the first integral in Eq. (6.101) can be found as

$$\int_0^{\infty} \frac{\exp\left(-\frac{bx}{2}\right)}{\sqrt{x}} dx = \sqrt{\frac{2\pi}{b}}. \tag{6.102}$$

To evaluate Eq. (6.101), we apply the Gaussian-Chebyshev quadrature method **[108]**. In particular, the second integral in Eq. (6.101) can be evaluated as

$$\begin{aligned}
&\int_0^{\frac{1}{k^2}} \frac{1}{\sqrt{x}} \exp\left(-\frac{bx}{2} - \frac{M(\gamma_{\text{RSI}} + \sigma_{\text{R}}^2)x}{\Omega_1 P_{\text{S}}(1 - k_{\text{SR}}^2 x)} - \frac{\sigma_{\text{D}}^2 x}{\Omega_2 P_{\text{R}}(1 - k_{\text{RD}}^2 x)}\right) \\
&\times \sum_{i=0}^{M-1} \sum_{j=0}^{N-1} \frac{1}{i!j!} \left(\frac{M(\gamma_{\text{RSI}} + \sigma_{\text{R}}^2)x}{\Omega_1 P_{\text{S}}(1 - k_{\text{SR}}^2 x)}\right)^i \left(\frac{\sigma_{\text{D}}^2 x}{\Omega_2 P_{\text{R}}(1 - k_{\text{RD}}^2 x)}\right)^j dx \\
&= \frac{\pi}{2Gk^2} \sum_{i=0}^{M-1} \sum_{j=0}^{N-1} \sum_{g=1}^{G} \frac{\sqrt{1 - \phi_g^2}}{i!j!\sqrt{\Delta}} \exp\left(-\frac{b\Delta}{2} - \frac{M(\gamma_{\text{RSI}} + \sigma_{\text{R}}^2)\Delta}{\Omega_1 P_{\text{S}}(1 - k_{\text{SR}}^2 \Delta)} - H_1\right) \\
&\times \left(\frac{M(\gamma_{\text{RSI}} + \sigma_{\text{R}}^2)\Delta}{\Omega_1 P_{\text{S}}(1 - k_{\text{SR}}^2 \Delta)}\right)^i \left(\frac{\sigma_{\text{D}}^2 \Delta}{\Omega_2 P_{\text{R}}(1 - k_{\text{RD}}^2 \Delta)}\right)^j,
\end{aligned} \tag{6.103}$$

where $H_1 = \frac{\sigma_{\text{D}}^2 \Delta}{\Omega_2 P_{\text{R}}(1 - k_{\text{RD}}^2 \Delta)}$, and k, ϕ_g, and Δ are defined as in Theorem 2.

Finally, by substituting Eq. (6.102) and Eq. (6.103) into Eq. (6.101), the SER of the MRT/MRC MIMO-FDR system under HI is obtained as Eq. (6.96) in Theorem 2. The proof is now complete.

6.4.3 Numerical Results and Discussion

TABLE 6.2: Parameters for the system performance evaluation.

Notations	Parameter name	Fixed value	Varying range
SNR	Signal-to-noise ratio	30 dB	$0 \rightarrow 40$ dB
σ^2	Variance of Gaussian noise	1	none
Ω	Average channel gain	1	none
(a, b)	Modulation types	$(2, 1)$	$(1, 2)$
k	HI level	0.15	$0.05 \rightarrow 0.3$
l	RSI level	0.15	$0 \rightarrow 0.3$
M	Number of transmission antennas of S	4	3, 5
N	Number of reception antennas of D	4	5, 3
$\mathcal{R}$	Predefined data transmission rate	1	$1 \rightarrow 4$

In this section, we investigate the performance of the MRT/MRC MIMO-FDR system under the impact of many parameters such as HI and RSI levels. This can be done based on the mathematical expressions in Theorem 1

and Theorem 2 in the previous section. To evaluate the performance degradation due to HI as well as to verify the correctness of our analysis, we also conduct Monte Carlo simulations on the OP and SER of the MIMO-FDR system with ideal hardware (denoted by "ID" on following figures) and with HI (denoted by "HI" on following figures). In our simulations, we set $P_{\mathrm{S}} = P_{\mathrm{R}} = P$; $\sigma_{\mathrm{R}}^2 = \sigma_{\mathrm{D}}^2 = \sigma^2$; $k_{\mathrm{S}}^{\mathrm{t}} = k_{\mathrm{R}}^{\mathrm{r}} = k_{\mathrm{R}}^{\mathrm{t}} = k_{\mathrm{D}}^{\mathrm{r}} = k$. The average channel are normalized to $\Omega_1 = \Omega_2 = 1$ such as in **[140; 141]**. The average SNR is defined as $\mathrm{SNR} = P/\sigma^2$. For ease of reading, we list the parameter values for simulations in Tab. 6.2. It should be better to know that, in a practical system, the transmit power and the HI levels at S, R, and D may be different ($P_{\mathrm{S}} \neq P_{\mathrm{R}}$, $k_{\mathrm{S}}^{\mathrm{t}} \neq k_{\mathrm{R}}^{\mathrm{r}}$, $k_{\mathrm{R}}^{\mathrm{r}} \neq k_{\mathrm{R}}^{\mathrm{t}}$, $k_{\mathrm{R}}^{\mathrm{t}} \neq k_{\mathrm{D}}^{\mathrm{r}}$). Furthermore, the HI level ranges from 0.08 to 0.175 for long term evolution (LTE) system **[112]**.

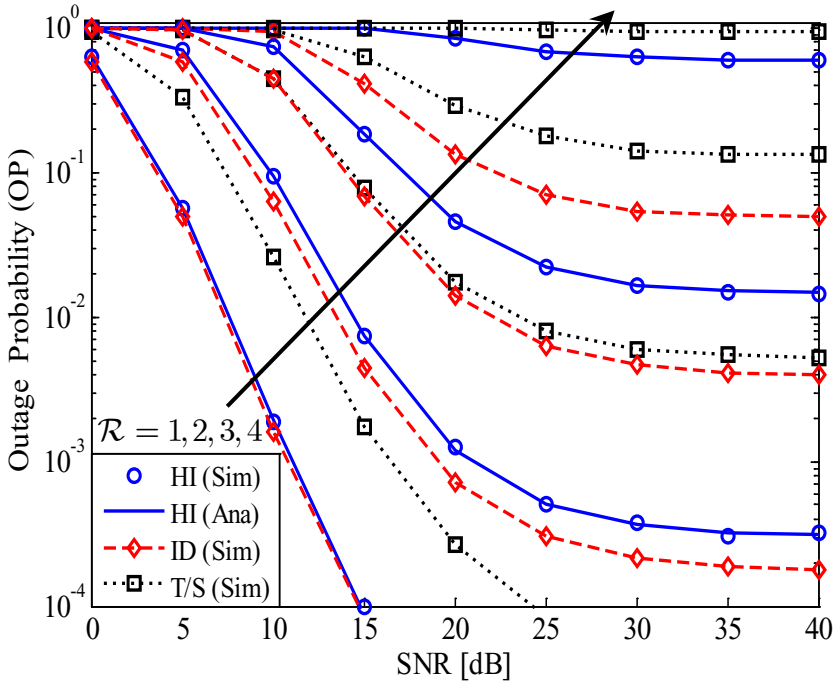

FIGURE 6.38: The OPs of the HI-MIMO-FDR system versus the average SNR with $k = l = 0.15$, $\mathcal{R} = 1, 2, 3, 4$ bit/s/Hz.

Fig. 6.38 illustrates the OPs of the MRT/MRC MIMO-FDR system with HI versus the average SNR in comparison with the OPs of the MRT/MRC MIMO-FDR system with ideal hardware. We use Eq. (6.84) in Theorem 1 to plot the analytical curves of the MIMO-FDR system with HI. It's worth noting that the simulation results perfectly match the analytical ones, which confirms the correctness of our analysis. In addition, we also simulate the OP of the considered system with TAS/SC (denoted by "T/S (Sim)" on Fig. 6.38) to show the benefits of MRT/MRC. For example, when $\mathcal{R} = 1$ bit/s/Hz and the target OP is $\mathrm{OP} = 10^{-4}$, we need to use $\mathrm{SNR} = 15$ dB for MRT/MRC and $\mathrm{SNR} = 25$ dB for TAS/SC. In this case, the benefit of MRT/MRC compared with TAS/SC is 10 dB in SNR. Fig. 6.38 clearly indicates that the impact of HI is stronger at high data transmission rates. For low data transmission rates, e.g., $\mathcal{R} = 1, 2$ bit/s/Hz, the difference between the OPs of the HI and ID MIMO-FDR systems is negligible, especially in the case of $\mathcal{R} = 1$ bit/s/Hz. However, for higher data transmission rates,

e.g., $\mathcal{R} = 3, 4$ bit/s/Hz, that difference becomes big and cannot be ignored. Although both OPs of the HI and ID MIMO-FDR systems reach some outage floors at $\mathrm{SNR} = 40$ dB in the case of $\mathcal{R} = 3$ bit/s/Hz, the MIMO-FDR system OP with the presence of HI can only be as low as $\mathrm{OP} = 15 \times 10^{-3}$ while it can reach $\mathrm{OP} = 4 \times 10^{-3}$ for the ideal hardware case. For higher data transmission rate, such as $\mathcal{R} = 4$ bit/s/Hz, the performance degradation due to HI becomes higher. Therefore, to maintain the OP performance of the MIMO-FDR system in HI condition, it is necessary to regulate the data transmission rate lower than 4 bit/s/Hz.

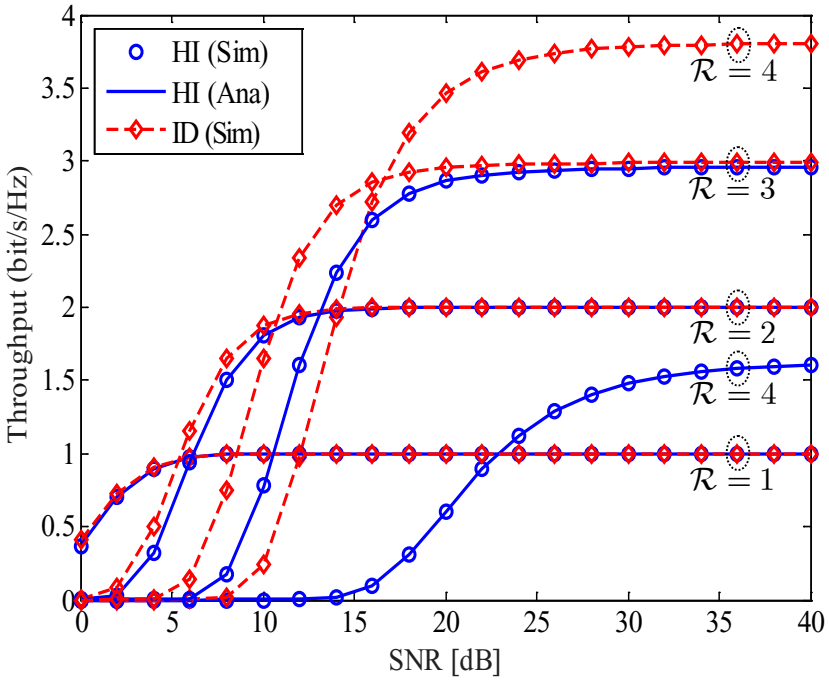

FIGURE 6.39: The system throughput of the HI-MIMO-FDR system with difference data transmission rates.

Fig. 6.39 compares the system throughput of the HI-MIMO-FDR system with that of the ID-MIMO-FDR system, where the system throughput is calculated as Eq. (6.93). It can be observed from Fig. 6.39 that the system throughput of both HI and ID MIMO-FDR systems can reach the target throughput of $\mathcal{R} = 1, 2, 3$ bit/s/Hz. Also, system throughput in both HI and ID cases can achieve similar throughput for $\mathcal{R} = 1, 2, 3$ bit/s/Hz. But for higher data transmission rate, e.g., $\mathcal{R} = 4$ bit/s/Hz, the system throughput of the ID-MIMO-FDR system nearly reaches the target of 4 bit/s/Hz when $\mathrm{SNR} = 40$ dB while the system throughput of the HI-MIMO-FDR system only reaches 1.6 bit/s/Hz. From Fig. 6.38 and Fig. 6.39, we can conclude that when the HI exists in the system, it is necessary to use a low data transmission rate to avoid the performance and throughput degradation for MRT/MRC MIMO-FDR system.

Fig. 6.40 displays the SER plots of the MRT/MRC MIMO-FDR system under HI for two modulation types, e.g., BPSK ($a = 1, b = 2$) and 4-QAM ($a = 2, b = 1$). Besides the SER results for the ID-MIMO-FDR system, we also present the SER plot of the ID-MIMO-HDR system (perfect SIC, $l = 0$, denoted by "ID-HD" on Fig. 6.40) to demonstrate the great impact of RSI

on SER of the proposed system. In Fig. 6.40, the analytical curves are obtained by using Eq. (6.96) in Theorem 2. Similar to OP, SER performance of MRT/MRC MIMO-FDR system is also significantly reduced by HI, especially for higher order modulation such as 4-QAM. Furthermore, compared to the case of perfect SIC ($l = 0$, ID-MIMO-HDR system), the RSI in the case of imperfect SIC ($l = 0.15$, HI-and-ID-MIMO-FDR systems) greatly affects the SER performance of the HI-and-ID-MIMO-FDR systems. We can see that for the ID-MIMO-HDR system, SER goes down and avoids the error floor at a high SNR regime. However, this does not happen in other cases. Specifically, SERs reach the error floor due to the impact of both HI and RSI for the HI-MIMO-FDR system and due to the impact of RSI for the ID-MIMO-FDR system.

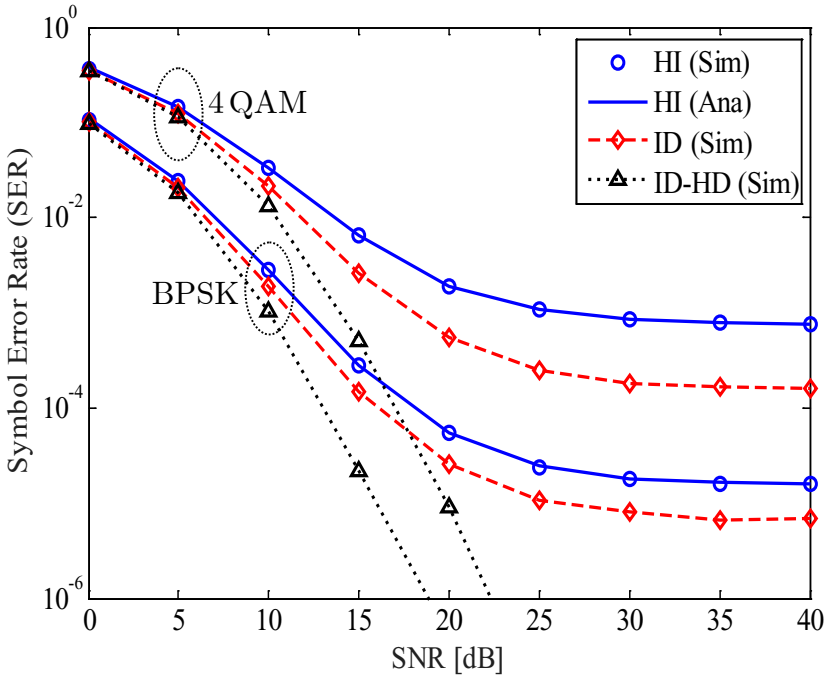

FIGURE 6.40: The SER of the HI-MIMO-FDR system using BPSK and 4-QAM modulation schemes.

Fig. 6.41 demonstrates the impact of RSI on the SER performance of the HI-MIMO-FDR system. In this figure, we set SNR $= 30$ dB. Notice that in the case of $l = 0$, the SER in Fig. 6.41 becomes the SER of the HI-MIMO-HDR system. It is obvious that in the case that the RSI level is small ($l < 0.1$), the difference between two SERs (of HI-and-ID-MIMO-FDR systems) is very large. However, this gap decreases when RSI increases. Particularly, in the case of $l = 0.3$, SERs of the HI-and-ID-MIMO-FDR systems are nearly the same. As a result, when RSI is small, the impact of HI on SER of HI-MIMO-FDR system becomes more significant because the impact of RSI is much smaller than that of HI. However, when RSI is larger, the impact of HI on SER is much less than that of the RSI and can be negligible.
Fig. 6.42 expresses the impact of HI on SER of MRT/MRC MIMO-FDR system for three values of the RSI, i.e., $l = 0.1; 0.15; 0.2$. It is noted that for RSI, we can set $l = 0$ such as in Fig. 6.41, however, we cannot set $k = 0$ due

to the term $\frac{1}{k^2}$ in Eq. (6.96). Therefore, we can obtain the SER of the HI-MIMO-HDR system by replacing $l = 0$ in Eq. (6.96) but we cannot obtain the SER of the ID-MIMO-HDR system or/and ID-MIMO-FDR system from Eq. (6.96) because of the mathematical error occurring if the HI level is set to $k = 0$. Fig. 6.42 indicates that when the HI level ranges in $0.05 \leq k \leq 0.1$, SER increases slowly. Thus, the impact of HI is not significant for this range of HI. However, for a higher value range of HI, e.g., $k > 0.1$, SER rapidly increases, which leads to a stronger impact of HI. It can be concluded that beside applying all effective SIC techniques for FD communications, we need to figure out various methods to suppress HI in the wireless communication system.

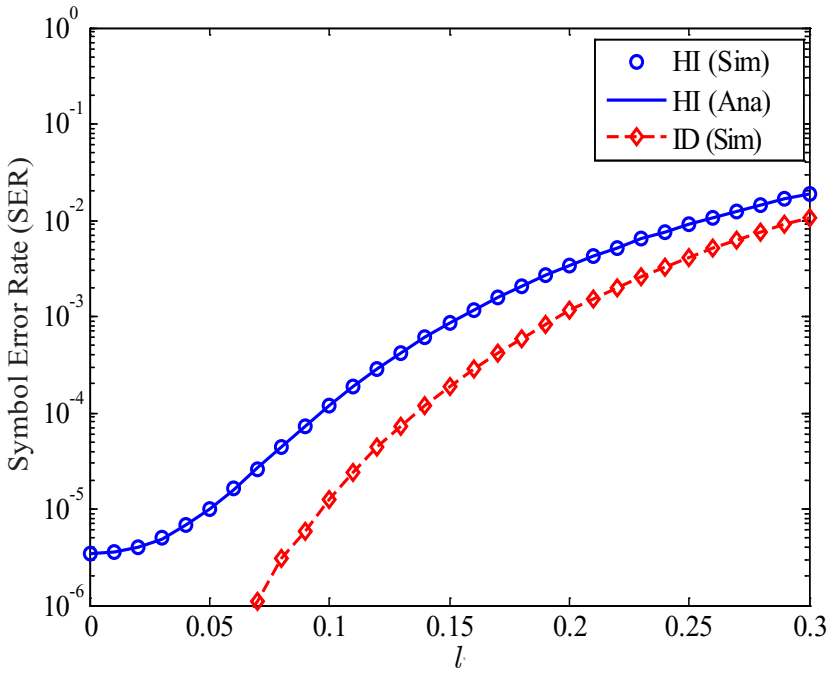

FIGURE 6.41: The impact of the RSI on the SER performance of the HI-MIMO-FDR system using 4-QAM modulation, $k = 0.15$.

In Fig. 6.43, we consider the SER of MRT/MRC MIMO-FDR system under HI in the case that the total number of transmit and receive antennas is a constant, e.g., $M + N = 8$, where M is the number of transmit antennas at S and N is the number of receive antennas at D. For three considered cases, i.e., $(M, N) = (5, 3); (4, 4)$ and $(3, 5)$, SER in the case of $(M, N) = (5, 3)$ is the best while SER in the case of $(M, N) = (3, 5)$ is the worst. These results are reasonable for MRT/MRC MIMO-FDR system under HI. It is because that the MRC technique improves the SER performance compared to MRT technique for the same number of antennas. Therefore, the received signal power at R is usually smaller than that at D, especially for HI case. Due to the imperfect SIC, the RSI can reduce the received signal power at R, hence, we usually have $\gamma_{\mathrm{R}} < \gamma_{\mathrm{D}}$ when $M \leq N$. To resolve this issue, we choose the number of transmit antennas at S greater than the number of receive antennas of D, e.g., $M = 5, N = 3$ to improve the SER performance of our proposed system. MRT/MRC techniques are known as the good solutions

to improve the performance and diversity order of wireless communication systems, thus, applying these techniques for advanced wireless communication systems is essential.

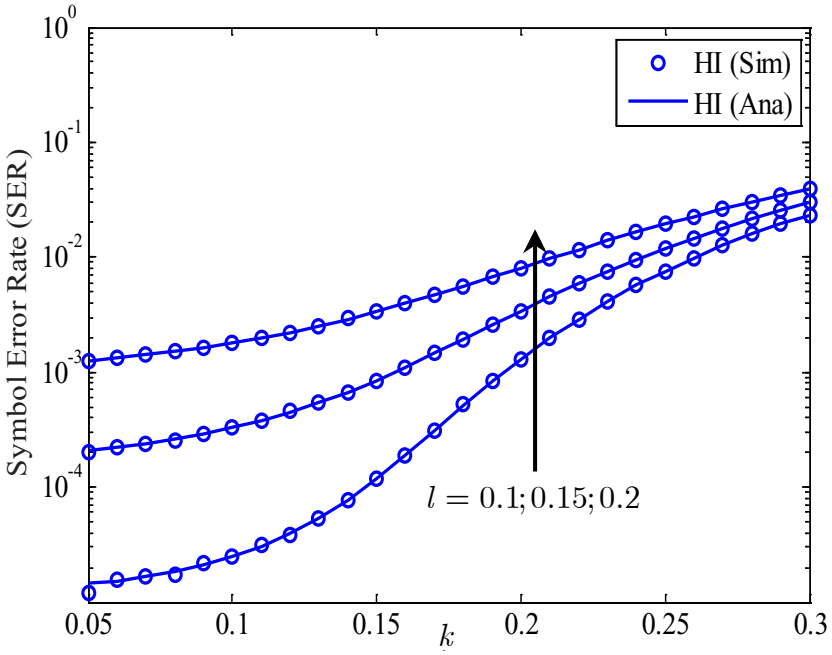

FIGURE 6.42: Impact of the HI on the SER performance of the HI-MIMO-FDR system using 4-QAM modulation for different values of the RSI.

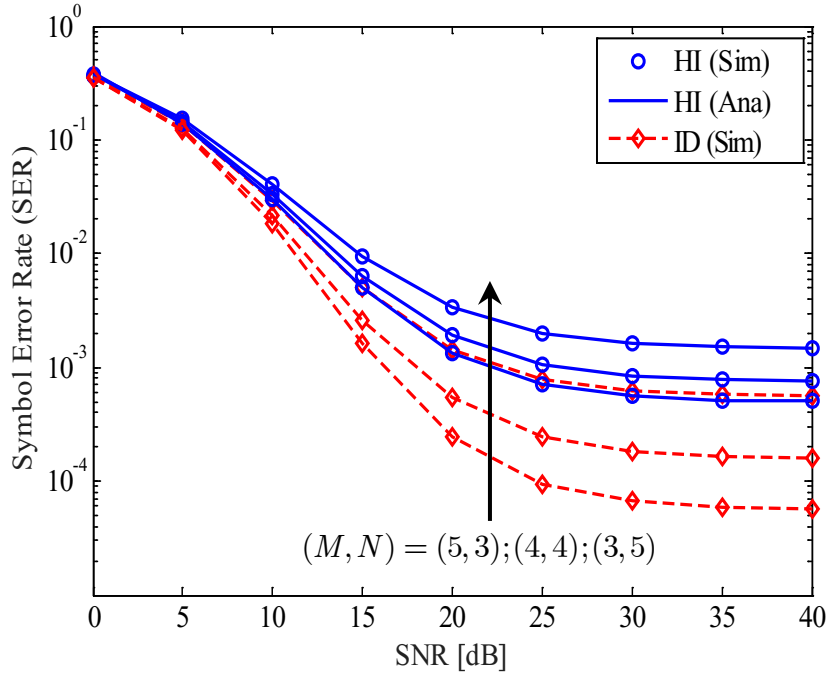

FIGURE 6.43: The SER of the HI-MIMO-FDR system with various number of the transmission and reception antennas, $k = l = 0.15$.

In this paper, we mathematically analyzed the performance of MRT/MRC MIMO-FDR system under the existence of HI and RSI by deriving the analytical expressions of outage probability, throughput, and the symbol error rate of the system. Based on these closed-form expressions, we can investigate the impact of various parameters on the performance of the proposed system under HI and RSI conditions. Numerical results demonstrate that the impact of HI is stronger for a higher data transmission rate system. Where both HI and RSI co-exist in the system, the OP and SER performance of the HI-MIMO-FDR system are lower-bounded by some error floor. Also, the impact of HI is greater when RSI is small and vice versa. Furthermore, by selecting the number of transmit antennas at the source larger than the number of receive antennas at the destination, the system performance can be significantly improved. This work can be extended further by considering the case of correlated antenna channels or by applying other techniques to alleviate the effect of HI such as in **[117]** or **[124]**.

6.5 Summary

In this chapter, we investigated the outage probability and throughput of FD relaying based on RF energy harvesting. Depending on the number of the relay antennas employed in the energy harvesting stage, two configurations were considered: (1) Only one antenna was used to collect energy from the source, while the other was used for information forwarding and (2) Both antennas were exploited to collect energy, while only one of them was applied to the information signal forwarding. In both cases, analytical expressions have been derived for outage probability and throughput of this network. Generally, two-antenna configuration outperforms single-antenna one. In addition, we also proposed multiple-antenna configuration (MIMO communication scheme) with various diversity techniques for EH-based FDRNs and derived the closed-form expression of OP.

7 Analysis of energy harvesting performance for various transmission modes

In this chapter, we continue to extend the performance analysis of FDRNs by studying the performance of the considered system in three transmission modes: instantaneous transmission, delay-limited transmission, and delay-tolerant transmission **[TNK01**; **TNK09]**. I derived the closed-form expressions for OP and throughput of the considered system one more time, and also search for the optimal EH parameter to maximize system throughput. A rigorous comparative analysis for three transmission modes is provided and from this analysis, it is found that the throughput performance in the delay-limited transmission is lower than the one in delay-tolerant transmission modes **[TNK10**; **TNK18- TNK19]**. Monte Carlo simulation results confirmed the analytical results and also provided a better look insight the difference between the performance of AF and DF schemes, in terms of OP and throughput. For my considered model, DF relaying strategy can provide better performance than AF strategy.

7.1 An Instantaneous Transmission Mode Analysis in The Half-Duplex and Full-Duplex Relaying Network

For the instantaneous transmission mode, the optimal time switching factor is updated for each channel realization, which is computed by a centralized entity having access to the global instantaneous CSI. The results reported in this sub-section have also been published.

The system model of full-duplex relay network in consideration is the same as the single-antenna model introduced in the previous section. Hence, we skip the description of the system model here because the instantaneous CSI is known to the relay, we can derive the throughput of the system. The following Propositions state the results for both FD relay networks and HD relay networks for comparison.

The lifetime maintenance of a wireless network by energy harvested has drawn a huge concern from many researchers in recent years. The simultaneous wireless information and power transfer (SWIPT) for the two-way relay transmission from an information theory viewpoint, in which two sources reciprocate communication over a power collecting relay is studied. By examining the time switching (TS) relaying structure, the TS-based two-way relaying (TS-TWR) protocol as well as a secret information model

for the simplex AF relay systems in the availability of several wiretaps are introduced. Different from the popular relay systems, this relay is known as "green", i.e., it is energized by the power collected from the surrounding environment as introduced in **[57; 59; 85; 87]**.

Next, an amplify-and-forward (AF) relaying system is examined by the authors in **[31; 67; 69; 71]**, in which a power-constrained relay node collects the power from the received RF signal and utilizes that collected power to transmit the source information to the target. Based on the time switching and power splitting receiving structures, two relaying protocols i) the TSR protocol and ii) power splitting-based relaying (PSR) protocol are investigated to offer the energy harvesting and information transfer at the relay.

On the other hand, the advantage of this solution lies in the fact that the RF signals can carry energy and information at the same time. Thus, the energy-constrained nodes can scavenge energy and process the information simultaneously as shown in **[21; 22; 90]**.

Now, in this part, we analyze the instantaneous throughput of the half-duplex and full-duplex relaying system with the main ability of energy harvesting and information transfer. Based on the analytical expressions, their throughput performance is studied. Hereby we can conclude which model is better to use them properly and get the most effect.

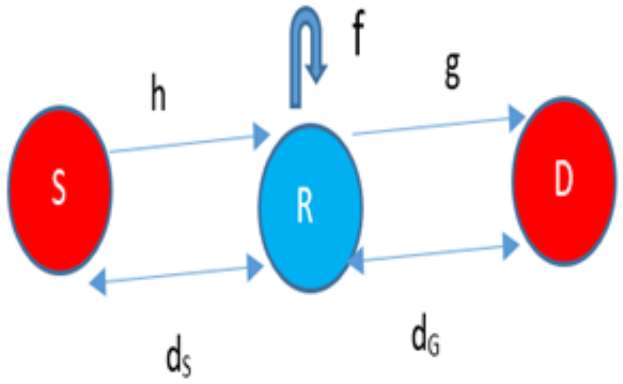

FIGURE 7.1: System model of one way half-duplex and full-duplex relaying network.

7.1.1 System Model

We assume that a three-node network consisting of one source node defined by S, one relay node defined by R, and one destination node defined by D. Fig. (7.1) describes the network model. There is no direct link between the source and the destination and their information can be exchanged through the relay node. Every node is set up with one antenna (the relay operates in FD mode is equipped with two antennas, one for transmission and the other for reception). The source node always has data to transmit. The relay node is not supplied by external energy and must harvest energy from the environment in order to operate. Its operation adopts an energy harvesting architecture and so it can directly convert the harvested energy to electric energy to operate its circuits. Due to the circuit hardware, the energy-constraint relay node can not receive or transmit data and harvest energy

simultaneously. The communication occurs in time basically with frame duration T.

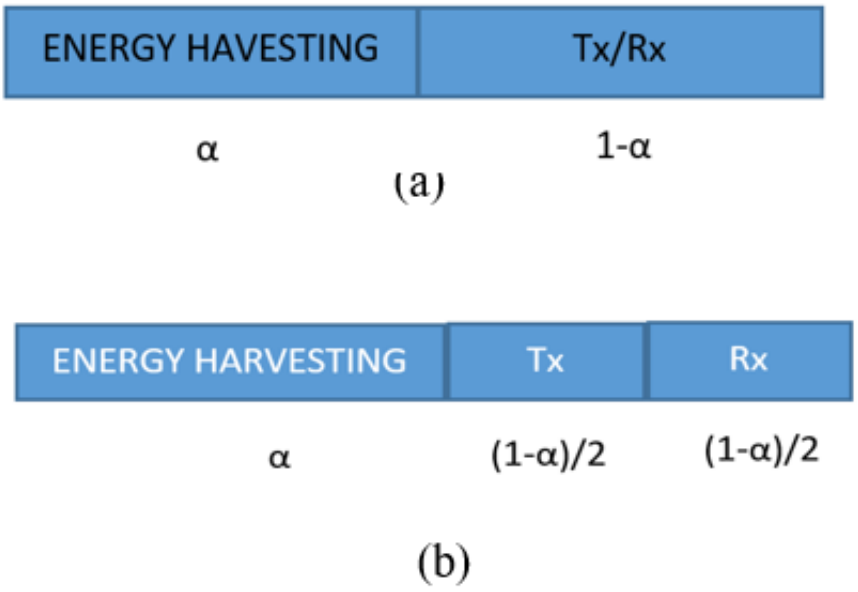

FIGURE 7.2: Time-switching architecture for a. The full-duplex model b. The half-duplex model.

Based on the TSR protocol proposed in Fig. (7.2), the communication process is divided into two phases. In the first phase, energy is transferred from the source to the relay with a duration of $\alpha T, (0 < \alpha < 1)$ and in the second phase, the remaining time, $(1 - \alpha) T$ is used to transmit information (in case full-duplex) or $\frac{(1-\alpha)T}{2}$ for information receiving at the relay, another $\frac{(1-\alpha)T}{2}$ for the information transfer to the destination (in case half-duplex protocol). Here α is the time switching factor.

We assume that all of the harvested energy can only be used for transmission. The relay node employs an AF relaying strategy and can operate either in HD or FD mode. All of the wireless links exhibit fading and additive white Gaussian noise (AWGN). The fading is assumed to be the Rayleigh blocked fading, h, g, and f denoted the exponential channel power gains for the link $S - R$, $R - D$ and $R - R$ (the loop interference from the relay output to the relay input for the case of FD operation).

7.1.2 Full-Duplex Relaying Model

During the power harvesting period, the relay received signal is expressed as

$$y_R = \sqrt{\frac{P_S}{d_S^m}} h x_S + n_a^{[R]} + n_c^{[R]}, \tag{7.1}$$

where $n_a^{[R]}$ is the base-band additive white Gaussian noise (AWGN) due to the receiving antenna at the relay node, $n_c^{[R]}$ is the sampled AWGN due to RF band to base-band signal conversion and the source transmit power is P_S, the additive white Gaussian noise at R with zero-mean and variance of

σ_r^2 is $n_R = n_a^{[R]} + n_c^{[R]}$, and the collected energy at the is found by **[31]**

$$E_h = \eta\alpha T \frac{P_S|h|^2}{d_S^m}, \tag{7.2}$$

where m is the exponential path loss coefficient, the power conversion factor is η.

In the remaining period, suppose that the source node transfers signal x_S to R and R re-transfers signal x_R to the destination node. They have the unit energy and zero mean, $E\left[|x_j|^2\right] = 1$ and $E\left[x_j\right] = 0$, where $j \in \{S, R\}$. So, the relay received signal under the residual self-interference (RSI) source is given as

$$y_R = \sqrt{\frac{P_S}{d_S^m}} x_S h + f x_R + n_R, \tag{7.3}$$

where f is the residual self-interference level at R. We assume R receives y_R and then, R utilizes that harvested energy to amplify and forward y_R. So, the previous received signal, x_R, is:

$$x_R = H y_R, \tag{7.4}$$

where H is the magnification efficiency of R.

Based on the AF relaying model at R, the magnification coefficient is given by

$$H = \sqrt{\frac{P_R}{\frac{P_S}{d_S^m}|h|^2 + P_R|f|^2 + \sigma_n^2}}. \tag{7.5}$$

It is deservedly finding that first, the relay harvests energy then assists the action for the next stage transmission, so P_R is taken by

$$P_R = \frac{E_h}{(1-\alpha)T} = \mu P_S \frac{|h|^2}{d_S^m}, \tag{7.6}$$

where μ is denoted as $\mu = \frac{\alpha\eta}{1-\alpha}$.

After that, the destination received signal is found as:

$$y_D = \frac{g}{\sqrt{d_R^m}} x_R + n_a^{[D]} + n_c^{[D]}, \tag{7.7}$$

where $n_D = n_a^{[D]} + n_c^{[D]}$ is AWGN at the destination node with zero-mean and variance of $\sigma_d^2 = \sigma_r^2 = \sigma^2$, for simplicity.
By substituting Eq. (7.4), Eq. (7.5), Eq. (7.6) into Eq. (7.7), the received signal can be computed as

$$y_D = \underbrace{\frac{g}{\sqrt{d_2^m}} H \frac{h\sqrt{P_S}}{\sqrt{d_S^m}} x_S}_{signal} + \underbrace{\frac{g}{\sqrt{d_R^m}} H f x_R}_{RSI} + \underbrace{\frac{g}{\sqrt{d_R^m}} H n_R + n_D}_{noise}. \tag{7.8}$$

Through some simple substitutions, we get new formula in **[83]**

$$\gamma_{FD} = \frac{\frac{P_S|h|^2 P_R|g|^2}{d_S^m d_R^m P_R|f|^2}}{\frac{\sigma^2 P_S|h|^2}{P_R|f|^2 d_S^m} + \frac{P_R|g|^2}{d_R^m} + \sigma^2}. \tag{7.9}$$

Here, we assume that the channel gains $|h|^2, |g|^2$ are independent and identically distributed (i.i.d.) exponential random variables.

7.1.3 The Half- Duplex Relaying Network

Similar to full-duplex system, in the half duplex one, we obtain:

$$y_{RHD} = \sqrt{\frac{P_S}{d_S^m}} h x_S + n_R, \tag{7.10}$$

and the relay magnifies the input signal by an amplifying factor which is express by

$$H_{HD} = \sqrt{\frac{P_R}{\frac{P_S}{d_S^m}|h|^2 + \sigma^2}}, \tag{7.11}$$

where $P_{RHD} = 2\mu P_S \frac{|h|^2}{d_S^m}$. Next, we get the received signal at the destination as

$$y_{DHD} = \frac{g}{\sqrt{d_R^m}} x_R + n_D. \tag{7.12}$$

By same calculations as above in the full-duplex section, we get:

$$\gamma_{HD} = \frac{\frac{P_S|h|^2 P_R|g|^2}{d_S^m d_R^m \sigma^2}}{\frac{P_S|h|^2}{\sigma^2 d_S^m} + \frac{P_R|g|^2}{d_R^m \sigma^2} + 1}. \tag{7.13}$$

7.1.4 Throughput Analysis

In this section, we investigate the instantaneous throughput of the half-duplex and full-duplex one-way relaying with energy harvesting and information transfer. Based on analytical expressions, the throughput of two models is figured out, and we can evaluate their performance.
In the delay-limited transmission protocol, the transmitter is communicating at a fixed transmission rate $R\ bits/\sec/Hz$ is and $(1-\alpha)T$ is the effective transmission time. So, the throughput of systems are obtained as

$$\tau_{FD} = (1-\alpha)\log_2(1+\gamma_{FD}), \tag{7.14}$$

for FD relaying network, and

$$\tau_{HD} = \frac{(1-\alpha)}{2}\log_2(1+\gamma_{HD}), \tag{7.15}$$

for HD relaying network.

Unluckily, it is hard to extract the instantaneous throughput mathematically, but we can get their performances by simulation as shown in the next section.

7.1.5 Numerical Results

In this section, from the derived analytical results, we compare the instantaneous throughput of two systems. We set the source transmission rate $R = 3\ (bps/Hz)$ (except for Fig. (7.7)), and $Z = 2^R - 1$, the time-switching factor is $\alpha = 0.3$. The energy conversion efficiency is set to be $\eta = 0.2$ (except for Fig. (7.5)), the path loss exponent factor is set to be $m = 3$. For simplicity, we set the distance $d_S = d_R = 1$ (except for Fig. (7.4), d_R is set to

$d_S = 2 - d_R$). Also, we set $\lambda_s = \lambda_d = 1; \lambda_r = 0.1$ and $\sigma^2 = 0.1$ (except for Fig. (7.3)), $SNR = \frac{P_S}{\sigma^2} = 1dB$.

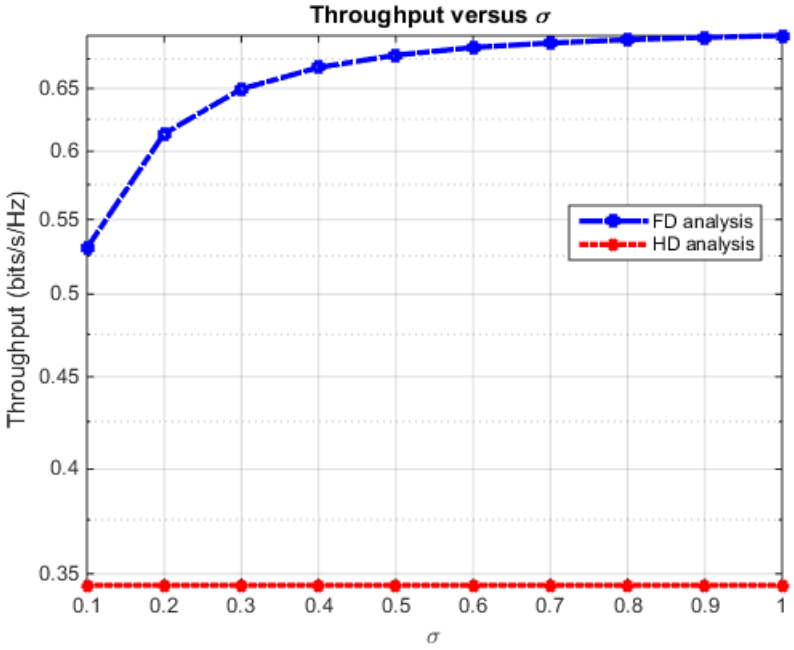

FIGURE 7.3: Instantaneous throughput of HD and FD energy-aware relaying network versus σ.

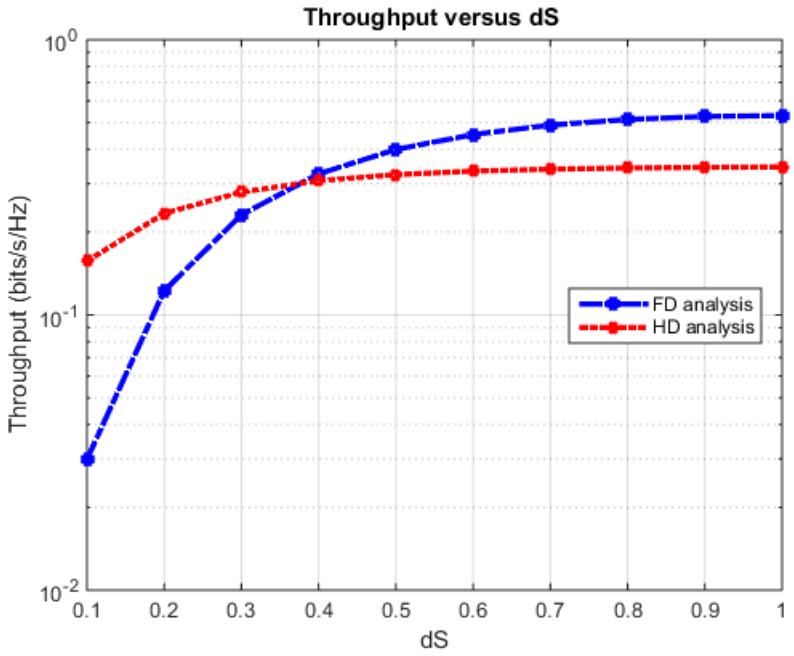

FIGURE 7.4: Instantaneous throughput of HD and FD energy-aware relaying network versus d_S.

It can be seen from Fig. (7.3), when σ increases, the throughput of full-duplex system increases, meanwhile the throughput of half-duplex is constant. This is because σ has a high influence on the performance of FD

systems. Meanwhile, the HD system does not have any factor related to interference, so its throughput is invariant when σ changes.
As we observe the process, Fig. (7.4) proves the impact of the position of a relay on the instantaneous throughput of two systems. The throughput of HD is high when the relay is close to the source node, when the relay is far from the S node, the throughput of the HD model is as smaller than that of the FD model. The throughput of the FD system increases as d_S increases from 0.4 to optimal value, however, it starts decreasing when d_S passes over this value. This is because the higher the value of d_S is, the lower the value of d_R, becomes and this has an impact on system performance.
In Fig. (7.5), we can see clearly that the effect of the energy conversion efficiency on the performances of both systems. The throughput of the FD model is better than that of the HD model. When η is big, the throughput of both models is small, because noise at the relay has dramatic impact. Similarly, for $\eta \geq 0.6$, the throughput of two models is overlap because the bigger the energy conversion efficiency gets, the more energy is harvested at the relay. Therefore, there is more energy in the half-duplex model to used to transfer information to the destination.

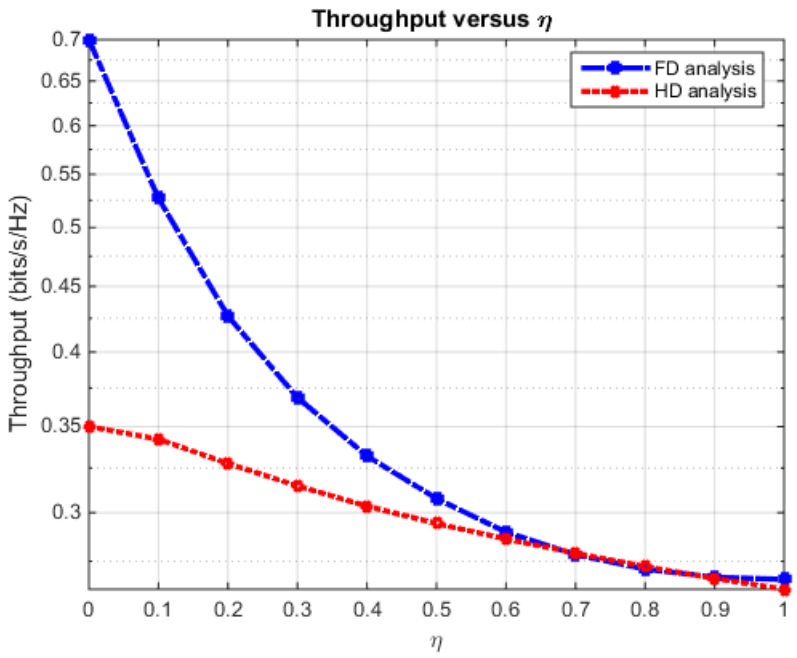

FIGURE 7.5: Instantaneous throughput of HD and FD energy-aware relaying network versus η.

Fig. (7.6) reveals that the factor α has an impact on the throughput of both systems evidently, the higher α is, the smaller their throughput is. This is based on the fact that there is much information transferred to the destination when α decreases, or there is less time using for harvesting energy.

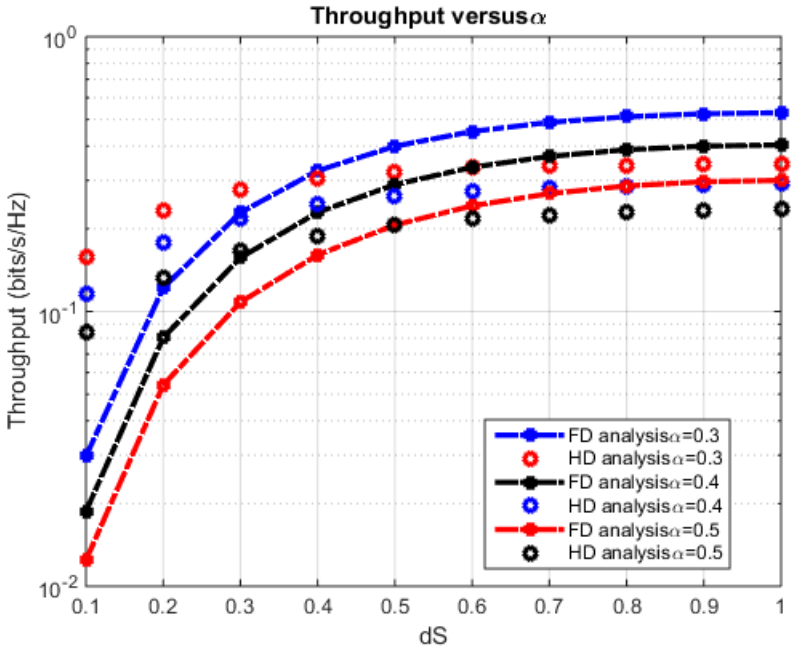

FIGURE 7.6: Instantaneous throughput of HD and FD energy-aware relaying network versus α .

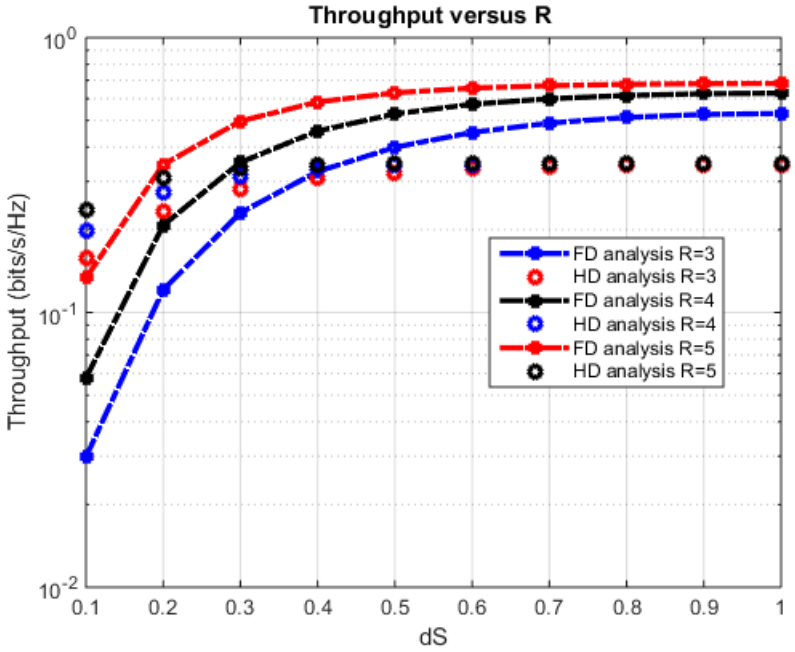

FIGURE 7.7: Instantaneous throughput of FD energy-aware relaying network versus R.

On the other hand, in Fig. (7.7), it can be seen from the curves that affect the target rate on the performance of both systems. The bigger R is, the higher the throughput is because when R is big, more energy is transferred to the destination.
Intuitively, when the transfer rate is small, the throughput is small; when

the transfer rate is large, it again degrades the throughput; so, for special transmitted energy, there exists a transfer rate that gives maximum throughput. Interestingly, we find that the optimal transfer rate for the HD model is also smaller than that of the FD scheme. This could be explained as follows: because the influence of the loop back noise in the FD scheme as well as the doubled transfer energy in the HD scheme have an impact on their performance.
In this part, a half-duplex and full-duplex relaying network with wireless energy harvesting and information transfer protocol are studied, where an energy-constrained relay node collects energy from the received RF signal and utilizes that harvested energy to amplify and forward the information to the destination. In order to verify the instantaneous throughput results. The instantaneous throughput of two systems with TSR protocol can be obtained by simulation.
From that, it has given real insights into the effect of various network parameters on the performance of wireless energy harvesting and information transfer using AF relay nodes.

7.2 An AF Performance Analysis in the Energy Harvesting Relaying Network

The demand for wireless communication techniques in history will be mark -ed by 5G networks delivering massive capacity in recent years. Accompany with these milestones, an issue that is not less important and is a requirement for prolonging the operation is not less important and is a requirement prolonging the operation time of wireless systems, had attracted many researchers in recent years. The common relay selections and energy harvesting models for maximization of the throughput of amplify and forward (AF) relaying communication system in which the source and the relays are equipped with energy harvesting (EH) capability are investigated. An optimization problem that can be solved by the common Bender's analysis was formulated by the authors in **[59; 60; 92; 93]**.

On the other hand, a system in which the second user can realize channel access to transfer a packet or collect radio frequency (RF) power on the chosen channel, free or seized by the first user, was considered. A maximization formulation to get the channel access strategy for the second user to optimize its throughput was proposed in **[31; 33; 61; 94; 95]**.
Moreover, as we can see in **[62- 64]**, the simultaneous wireless information and power transfer (SWPIT) for network-coded two-way relay transmission, in which two resources exchange information with the help of energy harvesting relay was studied point of view. By examining the time switching (TS) relaying protocol, the TS-based two-way relaying (TS-TWR) scheme was also considered.
As a result, in this part, we analyze the outage probability and ergodic capacity as well as throughput of the delay-limited and delay-tolerant schemes in the full-duplex relaying with the novel ability of energy harvesting and information transfer. Hereby, I recommend the optimal model for each situation.

7.2.1 System Model

Let consider a wireless two-hop relaying network with AF protocol as described in Fig. (7.8). The model has three nodes, one source node S, one destination node D, and one relay node R. Each node embraces two antennas, one uses to transfer signal and the other is responsible for the signal receiver. The cooperation relay is assumed to be energy-constrained equipment so that it can collect energy from the source signals, and utilizes that energy to amplify and forward the information to the destination. Assuming that the link between source and destination does not exist by the deep shadowing effect.

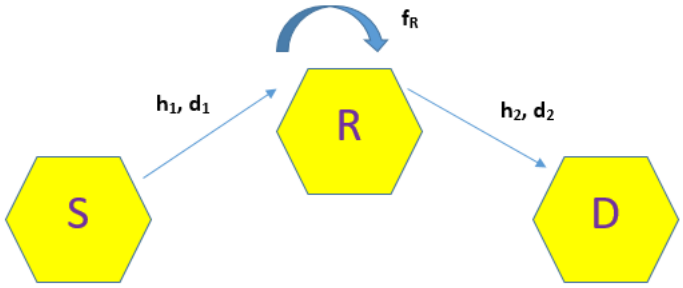

FIGURE 7.8: System model of one way full-duplex relaying.

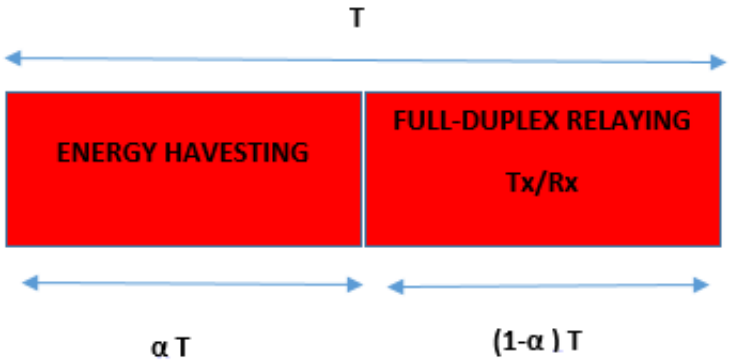

FIGURE 7.9: The parameters of TSR protocol.

The interference cancellation mechanism is not perfect. Definitely, a certain amount of interference still exists. The residual self-interference channel at R is denoted by f_R. Let d_1, d_2 denote the length between $S - R$ link and $R - D$ link. Let h_1, h_2 be the channel gains of $S - R$ and $R - D$ link, respectively. The model employed in this investigation is the Time Switching-based Relaying (TSR) protocol. Its main parameters are illustrated in Fig. (7.9). For the above protocol, the communication process is divided into two phases. In the earlier phase, the energy is transmitted from the resource to the relay during an interval of duration αT, $(0 < \alpha < 1)$ and in the next phase, which has the duration of $(1 - \alpha) T$ is used to convey information. Here, α is the time switching factor and T is the transmission

time for one block. Then, the signal received at the relay is given as

$$y_R = \sqrt{\frac{P_S}{d_1^m}} h_1 x_S + n_R, \tag{7.16}$$

where m is the path loss factor and P_S is the power transmitted by the source, n_R is the additive white Gaussian noise at R with zero-mean and variance of σ_R^2. Evidently, the harvested energy at the relay is determined as

$$E_h = \mu\alpha T \frac{P_s |h_1|^2}{d_1^m}, \tag{7.17}$$

where μ is an energy conversion factor.
In the second phase, assuming that the source node transmits a message signal x_S to R and R forwards signal x_R to the destination. They have unit energy and zero–mean, i.e., $E\left[|x_S|^2\right] = 1$, $E\left[|x_R|^2\right] = 1$ and $E[x_S] = 0$, $E[x_R] = 0$ as in **[83]**. Hence, the received signal at the relay with the presence of residual self-interference now is:

$$y_R = \sqrt{\frac{P_S}{d_1^m}} x_S h_1 + f_R + n_R, \tag{7.18}$$

where f_R is the residual self-interference factor at R. Assume that R receives y_R and employs the harvested energy to amplify y_R. As a result, the amplified signal, x_R, can be written as

$$x_R = G\sqrt{P_R} y_R, \tag{7.19}$$

where G is the amplification factor of R. Based on the AF relaying model at R, G is rewritten as

$$G = \sqrt{\left(\frac{P_S}{d_1^m}|h_1|^2 + P_R|f_R|^2 + \sigma_R^2\right)^{-1}}. \tag{7.20}$$

Given that harvested energy supports activities for the next phase transmission, P_R is expressed by

$$P_R = \frac{E_h}{(1-\alpha)T} = \varphi P_S \frac{|h_1|^2}{d_1^m}, \tag{7.21}$$

where φ is defined as $\varphi = \frac{\alpha\mu}{1-\alpha}$. Finally, we obtain the received signal at the destination as

$$y_D = \frac{h_2}{\sqrt{d_2^m}} x_R + n_D, \tag{7.22}$$

where n_D is the Gaussian noise at the destination with zero-mean and variance of $\sigma_S^2 = \sigma_R^2 = \sigma^2$, for simplicity. By substituting Eq. (7.19), Eq. (7.20), Eq. (7.21) into Eq. (7.22), we get:

$$\mathrm{E}\{|y_D|^2\} = \underbrace{P_s|h_1|^2||h_2|^2(|f_R|^2)^{-1}(d_1^m)^{-1}(d_2^m)^{-1}}_{Signal} + \underbrace{\mathrm{P}_R|h_2|^2(d_2^m)^{-1} + \sigma^2}_{Noise} + \underbrace{P_s|h_1|^2(|f_R|^2)^{-1}(d_1^m)^{-1}\sigma^2(P_R)^{-1}}_{RSI}. \tag{7.23}$$

And, the instantaneous receiving SINR at S is specified in **[31]**

$$\gamma_D = \frac{E\left\{|signal|^2\right\}}{E\left\{|noise|^2\right\} + E\left\{|RSI|^2\right\}}. \tag{7.24}$$

A new formula is achieved after some simple algebras as

$$\gamma_D = \frac{\frac{P_S|h_1|^2 P_R|h_2|^2}{d_1^m d_2^m P_R|f_R|^2}}{\frac{\sigma^2 P_S|h_1|^2}{P_R|f_R|^2 d_1^m} + \frac{P_R|h_2|^2}{d_2^m} + \sigma^2}. \tag{7.25}$$

Assuming that the channel gains $|h_1|^2, |h_2|^2$ are independent and identically distributed exponential random variables.

7.2.2 The Outage Probability and Throughput Analysis

In this section, we study the outage probability and the throughput of full-duplex one-way relaying with energy harvesting and information transfer. Based on analytical expressions, the outage probability and the throughput of the AF delay-limited and AF delay-tolerant schemes are given. Accordingly, we can compare and evaluate them together. It can be seen that their parameters have an impact on system operation. Then, we can suggest which model is appropriate for use.

The outage probability analysis

The outage probability of FD relaying network is reckoned as

$$P_{out} = \Pr\left(\gamma \leq Z\right), \tag{7.26}$$

where R is a transfer rate and $Z = 2^R - 1$.
Proposition:
The outage probability of the AF delay-limited scheme is given as $P_{out}^{DL} = \Pr\left\{\gamma_D < Z\right\} = 1 - A$ and

$$A = \int_0^{1/\varphi Z} 2\sqrt{\frac{d_1^m d_2^m Z\sigma^2\left(\frac{1}{\varphi}+y\right)}{\lambda_s\lambda_d P_S - \varphi P_S Z y}} K_1\left(2\sqrt{\frac{d_1^m d_2^m Z\sigma^2\left(\frac{1}{\varphi}+y\right)}{\lambda_s\lambda_d P_S - \varphi P_S Z y}}\right) \frac{1}{\lambda_r} e^{-\frac{y}{\lambda_r}} dy, \tag{7.27}$$

where $\lambda_s, \lambda_d, \lambda_r$ are the mean value of the exponential random variables h_1, h_2, f_R, respectively and $K_1(x)$ is Bessel function defined by Eq. (8.423.1) in **[49]**.

Proof:
By denoting $x = |h_1|^2|h_2|^2$, $y = |f_R|^2$ and we obtain:

$$P_{out}^{DL} = \begin{cases} \Pr\left\{ x < \frac{d_1^m d_2^m Z\sigma^2\left(\frac{1}{\varphi}+y\right)}{P_S - \varphi P_S Z y} \right\}, & y < \frac{1}{\varphi Z}, \\ 1, & y > \frac{1}{\varphi Z}. \end{cases} \tag{7.28}$$

We can calculate the cumulative distribution function of x as

$$F_x(a) = \Pr(x < a) = 1 - 2\sqrt{a/\lambda_s\lambda_d} K_1\left(2\sqrt{a/\lambda_s\lambda_d}\right), \tag{7.29}$$

and the probability distribution function of y as $f_y(b) = (1/\lambda_r)\, e^{(b/\lambda_r)}$. Finally, the Proposition is easily got after some simple calculations.

Proposition 7:
In the AF delay-tolerant scheme, we have:

$$R_E = \frac{G_{3\ 1}^{1\ 3}\left(\frac{\varphi P_S \lambda_s \lambda_d}{\sigma^2 d_1^m d_2^m}\middle| \begin{matrix}0,1,1\\1\end{matrix}\right)}{\ln 2} + \frac{1}{\lambda_r \ln 2}\int_0^\infty G_{3\ 1}^{1\ 3}\left(\frac{\varphi P_S \lambda_s \lambda_d}{\sigma^2 d_1^m d_2^m}\middle| \begin{matrix}0,1,1\\1\end{matrix}\right) e^{\frac{-y}{\lambda_r}} dy, \tag{7.30}$$

where R_E is the ergodic capacity of the DT system and $G_{p\ q}^{m\ n}(x)$ is Meijer G-function defined by Eq. (9.31) in **[75]**.

Proof:
By denoting $x = |h_1|^2|h_2|^2$, $y = |f_R|^2$, the ergodic capacity can be expressed as:

$$R_E = E\left\{\log_2\left(1 + \frac{\varphi P_S x}{\sigma^2 d_1^m d_2^m}\right)\right\} E\left\{\log_2\left(1 + \frac{\varphi^2 P_S x y}{\sigma^2 d_1^m d_2^m (1+\varphi y)}\right)\right\}. \tag{7.31}$$

Besides, the probability density function (p.d.f.) of x is given by $f_X(x) = \frac{2}{\lambda_s\lambda_d} K_0\left(2\sqrt{\frac{x}{\lambda_s\lambda_d}}\right)$. The first item of Eq. (7.31) can be calculated as

$$\begin{aligned} E\left\{\log_2\left(1 + \frac{\varphi P_S x}{\sigma^2 d_1^m d_2^m}\right)\right\} &= \frac{1}{\lambda_s\lambda_d \ln 2}\int_0^\infty \ln\left(1 + \frac{\varphi P_S x}{\sigma^2 d_1^m d_2^m}\right) K_0\left(2\sqrt{\frac{x}{\lambda_s\lambda_d}}\right) dx \\ &= \frac{1}{\lambda_s\lambda_d \ln 2}\int_0^\infty G_{2\ 2}^{1\ 2}\left(\frac{\varphi P_S x}{\sigma^2 d_1^m d_2^m}\middle| \begin{matrix}1,1\\1,0\end{matrix}\right) \times K_0\left(2\sqrt{\frac{x}{\lambda_s\lambda_d}}\right) dx, \end{aligned} \tag{7.32}$$

and I apply Eq. (8.4.6.5)] in **[49]**, and then use the integral identity Eq. (7.821.3)] in **[49]** to obtain

$$E\left\{\log_2\left(1 + \frac{\varphi P_S x}{\sigma^2 d_1^m d_2^m}\right)\right\} = \frac{G_{3\ 1}^{1\ 3}\left(\frac{\varphi P_S \lambda_s \lambda_d}{\sigma^2 d_1^m d_2^m}\middle| \begin{matrix}0,1,1\\1\end{matrix}\right)}{\ln 2}. \tag{7.33}$$

Similarly, the second item of Eq. (7.31) can be given as

$$E\left\{\log_2\left(1 + \frac{\varphi P_S x y}{\sigma^2 d_1^m d_2^m (1+\varphi y)}\right)\right\} = \frac{G_{3\ 1}^{1\ 3}\left(\frac{\varphi P_S \lambda_s \lambda_d y}{\sigma^2 d_1^m d_2^m (1+\varphi y)}\middle| \begin{matrix}0,1,1\\1\end{matrix}\right)}{\ln 2}. \tag{7.34}$$

Finally, the Proposition 7 is achieved through some simple calculations.

The throughput analysis

In the delay-limited (DL) transmission protocol, the transmitter is transferring at a fixed target rate $Rbits/sec/Hz$ and $(1-\alpha)\,T$ is the effective transmission time. Correspondingly, the throughput in the delay-limited mode is obtained as

$$R_{DL} = (1-\alpha)(1-P_{out}^{DL})R. \tag{7.35}$$

In delay-tolerant (DT) mode, the source transfers at any fixed rate, which is upper limited by the ergodic capacity. When the code word length is big enough compared to the frame time, the code-word knows all the potential realizations of the channel. Thus, the ergodic capacity becomes an appropriate metric. Assume that the residual loop back interference is considered as the Gaussian noise. Therefore, the AF delay-tolerant throughput is as

$$R_{DT} = (1-\alpha)R_E. \tag{7.36}$$

Unfortunately, it is difficult to extract the optimal throughput mathematically, but we can obtain that value by simulation as introduced in the next section.

7.2.3 Numerical Results

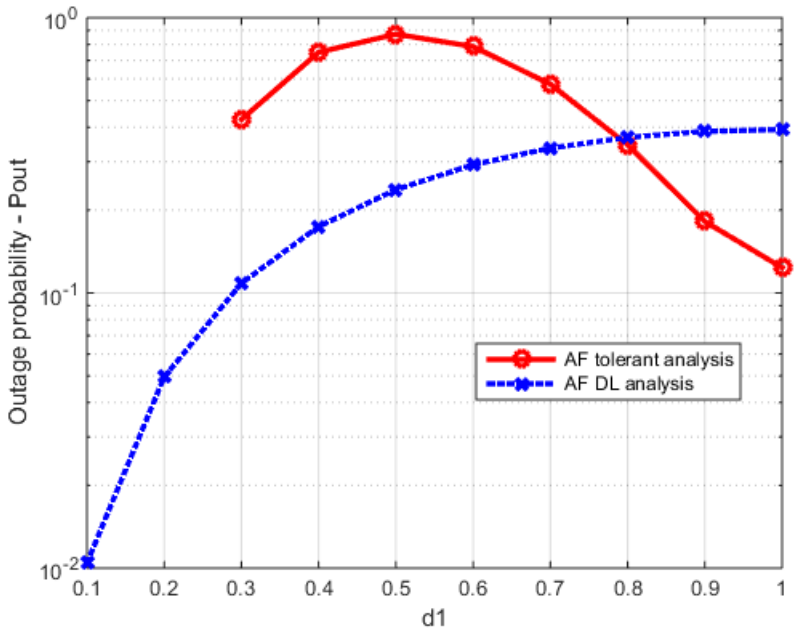

FIGURE 7.10: Outage probability and Ergodic capacity of FD energy-aware relaying network versus distance.

In this section, we use the analytical results to derive the outage probability, the optimal throughput. We set the source transmission rate at $R = 3\ (bps/Hz)$, therefore the outage SINR threshold is given by $Z = 2^R - 1$. The energy conversion efficiency is set to be $\mu = 0.4$ (except for Fig. (7.12), Fig. (7.13)), $\sigma^2 = 0.1$ (except for Fig. (7.14) and Fig. (7.15)), the path loss exponent factor is set to be $m = 3$. For simplicity, we set the distance $d_1 = d_2 = 1$ (except for Fig. (7.10) and Fig. (7.11)). Also,

we set $\lambda_s = \lambda_d = 1; \lambda_r = 0.1$ and the time-switching factor $\alpha = 0.3$, $SNR = \frac{P_s}{\sigma^2} = 2dB$. These are the values that give us the best performance if we fix other parameters.
From Fig. (7.10), the DL outage probability and the DT ergodic capacity are plotted versus the position of relay. The DT ergodic capacity is minimized at midway between the source and relay, it gets the best value near to the relay, i.e., at a certain point that is about 0.3 far away to the source (if the distance is smaller than this one, we do not have the ergodic capacity). This is simple to understand, the DT expressions analyzed is the upper bound in this paper, easily being affected by the transmit power or other interference power. Of course, the closer the relay is to the source, the better its ergodic capacity gets.
Moreover, Fig. (7.10) also reveals that the DL outage probability outperforms that of the DT one. We can see that its outage probability decreases when d_1 increases and gets the worst value at midway between the source and the destination. The closer the relay is to the source node or the destination, the better the outage probability achieves. As $1 \geq d_1 \geq 0.8$, the thing is a difference. In particular, the DT ergodic capacity is better than that of the DL outage probability, and the reason is that more noise at the relay has an impact on the system operation. Two models have a cross-over at $d_1 = 0.8$. Here, the outage probabilities of two models are equal.

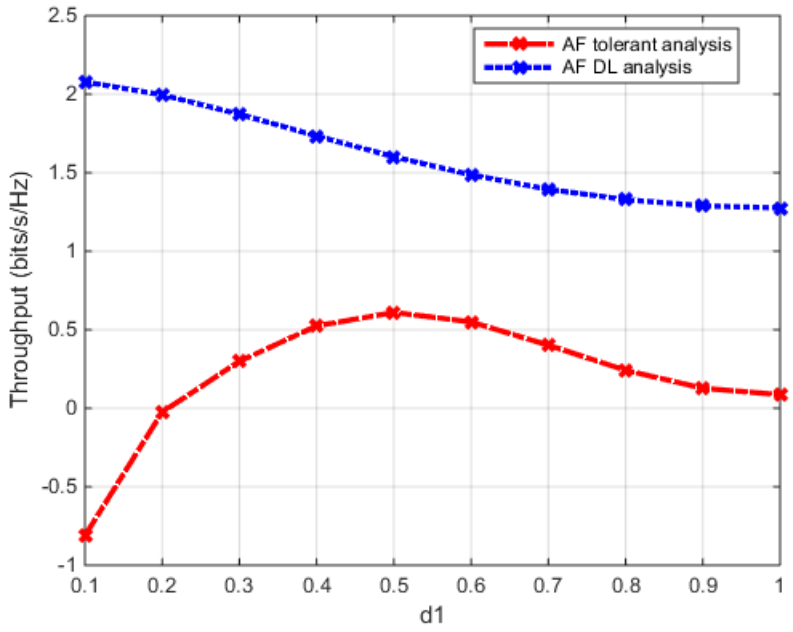

FIGURE 7.11: Throughput of FD relaying versus distance.

Consequently, as observed in Fig. (7.11), the DL throughput is better than that of the DT throughput. The farther the relay is to the source, the smaller the DL throughput gets. It obtains the minimum at the midway. Meanwhile, the ergodic capacity increases and gets the maximal value at the midway between the source and the relay. This is compatible with the above analysis in Fig. (7.10). Although when $1 \geq d_1 \geq 0.8$, the DT ergodic capacity

is better than that of the DL one, but the DL throughput is still better than that of the DT model. It is because the noise at the relay is not big enough to help the DT model to overcome the DL one.
The same scenario occurs when we investigate the outage probability and the ergodic capacity concerning the energy conversion factor μ, in Fig. (7.12). The bigger μ is, the better the outage probability and the ergodic capacity are. Here, when μ is greater than 0.4, the ergodic capacity starts to appear, and it gradually becomes bad. This problem is not hard to explain. When μ increases, energy at the relay increases. It makes the DL model to have more energy to forward information to the destination. However, the more energy at the relay, the more noise impacts on the DT transmission mode.
As a result, Fig. (7.13) shows that, the smaller μ, the smaller the throughput. When μ increases, throughput increases. Moreover, we have seen that μ affects the DT throughput, incredibly. The bigger μ is, the lower DT throughput we have. This confirms that more power to forward the signal, we obtain a high throughput at the destination.

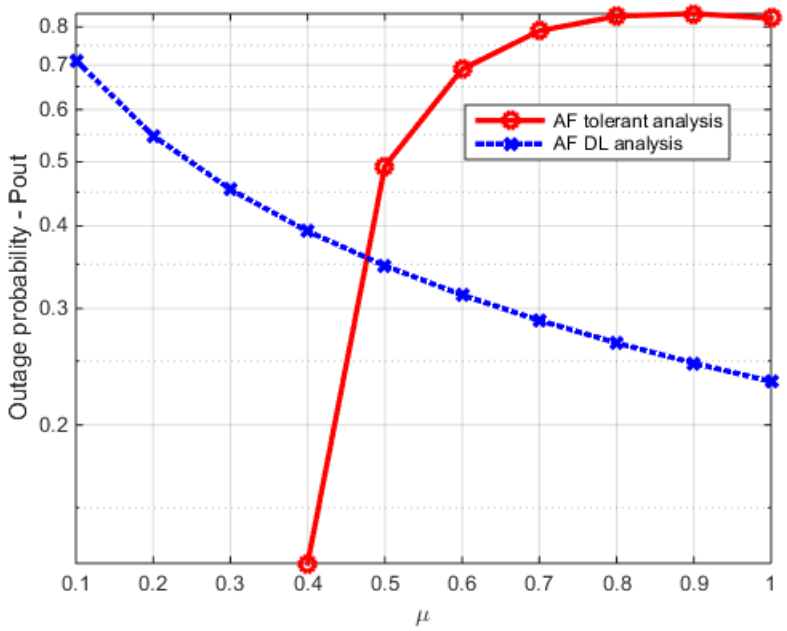

FIGURE 7.12: Outage probability and ergodic capacity of FD energy-aware relaying network versus μ.

A similar trend is observed in Fig. (7.14), for σ is smaller than 0.4 or bigger than 0.6, we do not see egordic capacity (with the same reason as the previous part). The bigger the noise is, The better the ergodic capacity is and the worse the outage probability we have. When $\sigma \in [0.4, 0.5]$, the DT ergodic capacity is worse than that of the DL one for remaining values as things happen contrarily. This scenario demonstrates that noise has an significant impact on system performance. We have the cross over of two transmission modes at $\sigma = 0.5$, while the probabilities of two models are equal.

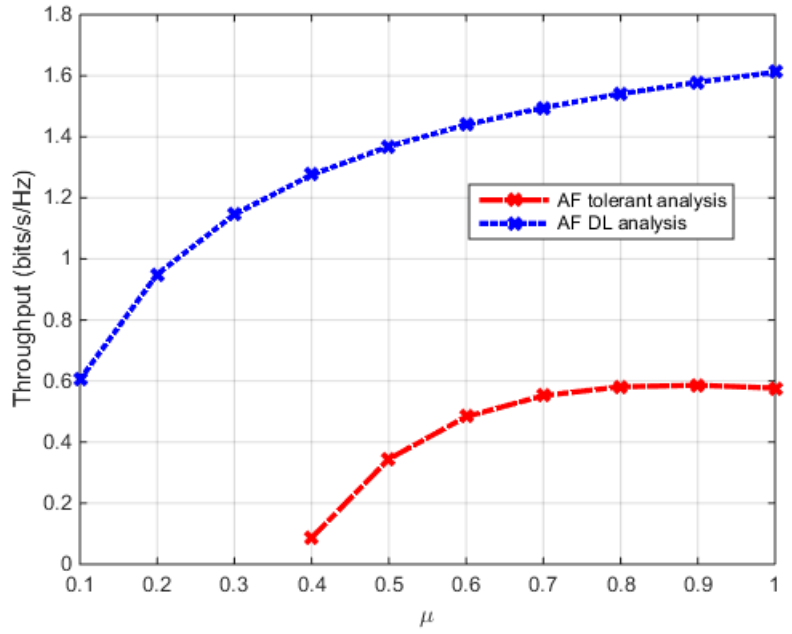

FIGURE 7.13: Throughput of FD relaying versus μ.

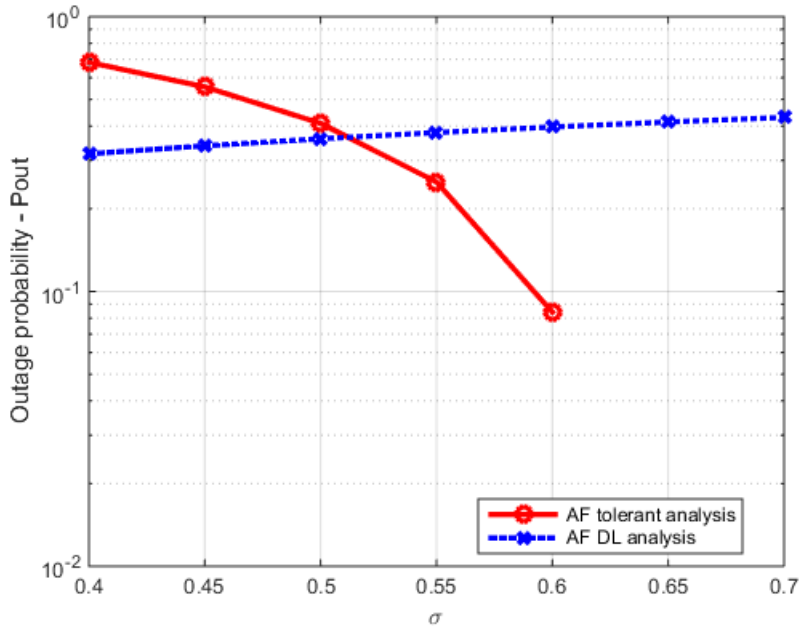

FIGURE 7.14: Outage probability and Ergodic capacity of FD energy-aware relaying network versus σ.

Finally, Fig. (7.15) shows that though σ is small or big, the DL throughput is still better than that of the DT one. One again, it is proven that more noise at the relay leads to the DL mode is better than that of the DT one (the reason for this is the same as above).

In this part, we have investigated a full-duplex relaying network with wireless energy harvesting and information transfer protocol, where an energy-constrained relay node collects energy from the RF signal and employs that collected energy to transmit the information signal to the destination in the DL and DT mode. The analytical expressions of two modes for the TSR protocol can be found by simulation. Here, we can see that the DL mode becomes the better mode if we must select either one of two modes

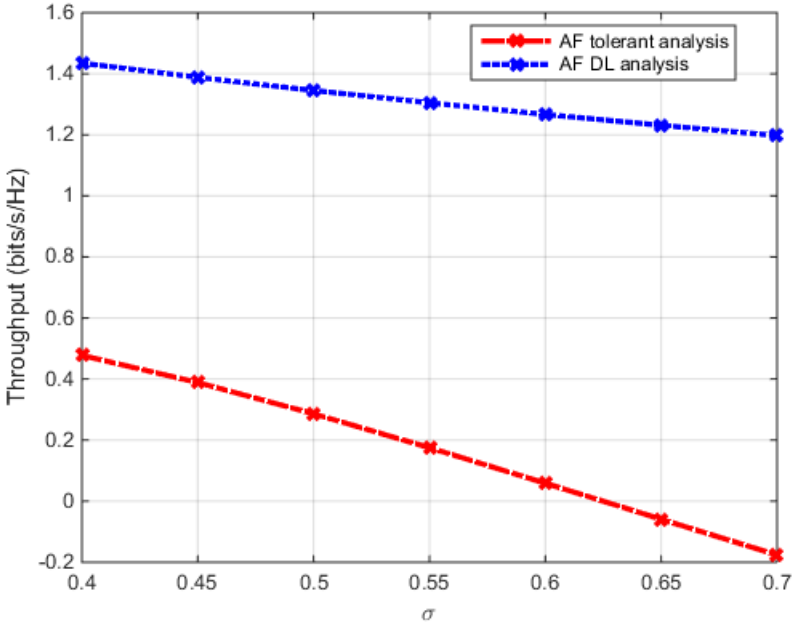

FIGURE 7.15: Throughput of FD relaying versus σ.

7.3 Performance Analysis in the DF Full-Duplex Relay Network

EH method relied on ambient radio frequency (RF) signals has recently provide the advanced method to keep the radio networks survive from leaking of energy.

In this part, performance analysis for underlay cognitive DF relayed systems with the Nth best relay selection model over Nakagami-m fading channels is presented. Both the maximum tolerated interference energy-constraint and the maximum transfer energy limitation were studied in **[67]**. Besides, the utilization of power collectors, in place of normal power resources, in radio cooperative communication was considered by the authors in **[96]**. The influence of hardware impairments in cognitive DF system is standardized. More particularly, the derivation of signal-to-the noise-and-distortion ratio (SNDR) at the relay and destination node of the cognitive DF network are achieved in **[84]**. Among them, a DF relay system relied on radio energy collecting and the energy-constrained relay node, which first collects power over radio-frequency (RF) signals from the source node, was also mentioned in **[33]**.

Moreover, an overview of the simultaneous wireless information and power transfer (SWIPT) especially with a particular concern on the hardware realization of circuits and real technologies that get SWIPT in the respect of time, power, antennas, and space and the profits of a potentiality integration of SWIPT technologies in up-to-date information systems in the context of source deployment and cooperation cognitive wireless systems were talked in **[57; 69]**. On the other hand, a wireless-energized cooperative information system comprising one hybrid access-point (AP), one source, and one relay was investigated. In contrary to normal cooperative networks, in **[77; 85]**, the source and relay in the considered system have no power supply.

In another advanced work, the second system with simultaneous SWIPT is in a spectrum sharing context was presented. Mover especially, a secondary user (SU) transmitter transmits to several SU receivers (SU-Rxs) under the peak interference power constraint on the primary user receiver and the SU optimum transfer energy limitation. A SU-Rx with the best channel condition among a set of multiple SU-Rxs satisfying a threshold is selected for information transfer was considered in **[61; 62]**.

Therefore, in this part, we investigate the outage probability and throughput of the full-duplex relay system with a new application of energy collecting and information transfer. Based on the analytical expressions, system outage probability and throughput are studied and according to the practical situation, we can suggest which model can attain the best gain.

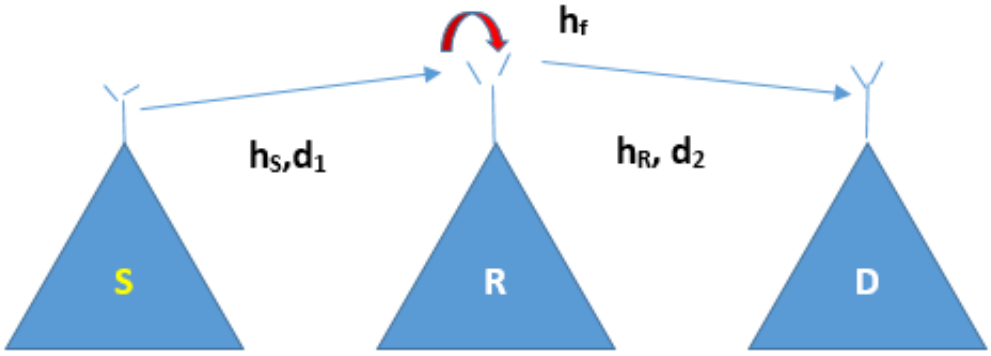

FIGURE 7.16: System model of the full-duplex relaying.

7.3.1 The System Model

As illustrated in Fig. (7.16), a DF relaying cooperative network is considered, where the information is transferred from the source node denoted by S to the destination node denoted by D, via a power-constrained relay node denoted by R. Every node has two antennas, one for the information transmission, the other for the data receiving. Assume that between the source and the destination node, there is not any direct link. A DF relay helps the connection between source and destination. At first, the DF relay receives energy from the source signals. Next, it uses the collected energy to forward the information to D. The distance $S \rightarrow R$ and $R \rightarrow D$ are denoted by d_1 and d_2.

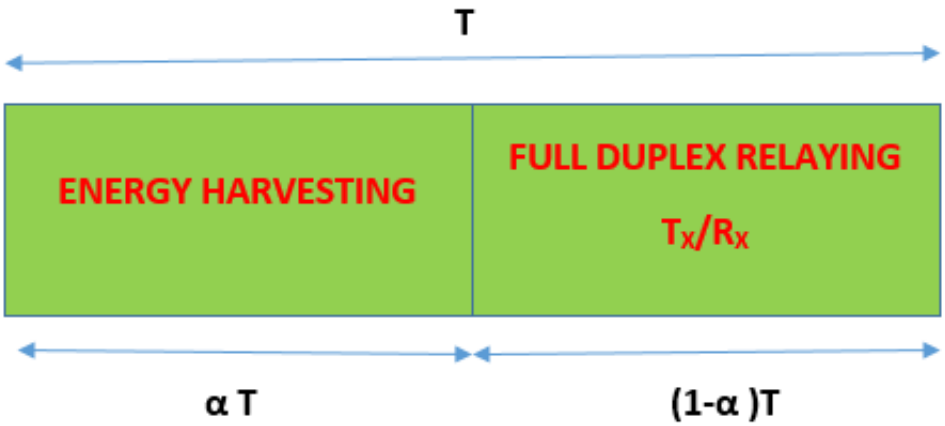

FIGURE 7.17: The parameters of TSR protocol.

The residual self-interference (RSI) channel at R is denoted by h_f, it exists because the noise canceled technique is not perfect.

The model utilized in this paper is the Time Switching- Relaying (TSR) protocol as shown in Fig. (7.17).
As we can see in Fig. (7.17), there are two phases of the information transfer process. Initially, energy is sent from S to R within a time slot of length $\alpha T, (0 < \alpha < 1)$. The next time slot, $(1-\alpha)\,T$, is given to transfer information, where α is a time-switching factor, while, the duration pf each communication frame is T.

In the energy harvesting phase, at R, we receive a signal

$$y_R = \sqrt{\frac{P_S}{d_1^m}} h_S x_S + n_R, \tag{7.37}$$

where P_S is the source transmit power, n_R is the additive white Gaussian noise at R with variance of σ_r^2 and zero-mean.

According to **[13]**, the received energy at R is written as

$$E_h = \eta \alpha T \frac{P_s |h_S|^2}{d_1^m}, \tag{7.38}$$

where m denotes the exponent path loss factor, η is the energy conversion efficiency, the channel coefficients are h_S, h_R respectively like in Fig. (7.16). Assuming that x_S is the signal transferred from S to R and x_R is re-transmitted signals from R to D for simplicity, we set $E\left[|x_i|^2\right] = 1$ and $E\left[x_i\right] = 0$, $j \in \{S, R\}$, respectively. Another expression of received signal at R is given as in **[83]**

$$y_R = \sqrt{\frac{P_S}{d_1^m}} x_S h_S + h_R x_R + n_R. \tag{7.39}$$

For DF mode, we have:

$$x_R(i) = \sqrt{\frac{P_R}{P_S}} x_S[i - \tau]. \tag{7.40}$$

Here, R harvested energy and thence uses it to assists the communication in the next phase, so P_R is given as

$$P_R = \frac{E_h}{(1-\alpha)\,T} = \mu P_S \frac{|h_S|^2}{d_1^m}, \tag{7.41}$$

where $\mu \cong \frac{\alpha\eta}{1-\alpha}$; and

$$y_D = \frac{h_R}{\sqrt{d_2^m}} \left(\sqrt{\frac{P_R}{P_S}} x_S(i-\tau) \right) + n_D, \tag{7.42}$$

where n_D is the Gaussian noise at D with variance of $\sigma_d^2 = \sigma_r^2 = \sigma^2$ and zero-mean.

Alternatively, the received SINR at D through R is given as

$$\gamma = \frac{E\left\{|signal|^2\right\}}{E\left\{|noise|^2\right\}}. \tag{7.43}$$

From there, a new formula is obtained after some simple calculations

$$\gamma_{DF} = \min\left(\frac{1}{\mu|h_f|^2}, \frac{\mu P_S |h_S|^2 |h_R|^2}{d_1^m d_2^m \sigma^2} \right), \tag{7.44}$$

where the channel gains $|h_S|^2$, $|h_R|^2$ and $|h_f|^2$ are independent and identically distributed (i.i.d.) exponent random variable.

7.3.2 Outage Probability and Throughput Analysis

In this section, we examine the outage probability and throughput of full-duplex relay network with SWIPT. Based on analytical results, the outage probabilities and throughput of two models are given. Finally, we can know which model is better than the other order to use them properly.

The Outage Probability Analysis

The outage probability in the delay-limited (DL) mode is given as

$$P_{DL} = \Pr\left(\gamma \le Z\right), \tag{7.45}$$

where R_1 is the transmission rate and $Z = 2^{R_1} - 1$.

Proposition:
The outage probability of the DL mode is given as

$$P_{DL} = 1 - \left(1 - e^{\frac{1}{\mu\lambda_r Z}}\right) \left(2\sqrt{\frac{\sigma^2 d_1^m d_2^m Z}{\mu\lambda_s\lambda_d P_S}} \right) K_1\left(2\sqrt{\frac{\sigma^2 d_1^m d_2^m Z}{\mu\lambda_s\lambda_d P_S}} \right), \tag{7.46}$$

where λ_s, λ_d, λ_r are the average value of the exponent random variables, h_S, h_R, h_f, respectively, and $K_1(x)$ is Bessel function defined by Eq. (8.423.1) in **[49]**.
Proof:

Base on the property of the statistics, the cumulative distribution function of x is calculated by

$$F_x(b) = \Pr(x \leq b) = 1 - 2\sqrt{b/\lambda_s\lambda_d}K_1\left(2\sqrt{b/\lambda_s\lambda_d}\right), \tag{7.47}$$

and x can be set up with the probability distribution function $f_y(c) = (1/\lambda_r)\, e^{(c/\lambda_r)}$.
We assign $x = |h_S|^2|h_R|^2$ and $y = |h_f|^2$, from Eq. (7.44), Eq. (7.45), we get:

$$P_{DL} = Pr\left(\min\left(\frac{1}{\mu y}, \frac{\mu P_S x}{d_1^m d_2^m \sigma^2}\right) \leq Z\right). \tag{7.48}$$

So,

$$P_{DL} = 1 - Pr\left(\frac{1}{\mu y} \geq Z\right)\Pr\left(\frac{\mu P_S x}{d_1^m d_2^m \sigma^2} \geq Z\right). \tag{7.49}$$

After some manual calculations, the Proposition is proved.

In the delay-tolerant (DT) context, the source transfers data at any fixed rate upper bounded by the ergodic capacity. As the code-word length is sufficiently big compared to the frame duration, the code-word could see all potential realizations of the channel. So, the ergodic capacity becomes a suitable metric.
Proposition 8:

Similar to the above section, we have the ergodic capacity as

$$C_{DT} = \int_0^\infty \frac{(1 - e^{\frac{-1}{\mu\lambda_r t}})\left(2\sqrt{\frac{d_1^m d_2^m \sigma^2 t}{\mu P_S \lambda_s \lambda_d}}\right) K_1\left(2\sqrt{\frac{d_1^m d_2^m \sigma^2 t}{\mu P_S \lambda_s \lambda_d}}\right)}{(1+t)ln2} dt. \tag{7.50}$$

Proof:
Using the cumulative distribution function $(c.d.f.)$ of the end-to-end SINR in Eq. (7.46), the desired result can be achieved after some simple manipulations.

The throughput analysis

In the Proposition, with the delay-limited transfer protocol, the transmitter is transmitted at a fixed transmission rate $R_1 bits/sec/Hz$ and $(1-\alpha)T$ is the effective communication time. So, the throughput of the DL system can be written as:

$$\tau_{DL} = (1 - P_{out})\, R_1\, (1 - \alpha). \tag{7.51}$$

Also, by another definition, the throughput of the DT system is also given as

$$\tau_{DT} = (1 - \alpha)\, C_{DT}. \tag{7.52}$$

Unfortunately, it is difficult to derive the optimal throughput mathematically, but we can achieve that value by the numerical method as mentioned in the next section.

7.3.3 Numerical Results

In this part, we employ the derived analytical results to figure out the maximal throughput. We set the target rate $R_1 = 3\,(bps/Hz)$ (except for Fig. (7.22)). The energy conversion efficiency is set to $\eta = 0.4$ (except for Fig. (7.19)), the $SNR = \frac{P_s}{N} = 1\ dB$, the path loss exponent is set to $m = 3$. We set the distance $d_1 = d_2 = 1$ (except for Fig. (7.18)), and $\lambda_s = \lambda_d = 1; \lambda_r = 0.1$, the noise factor is $\sigma^2 = 0.1$ (except for Fig. (7.20)), and the time switching factor α is 0.3 (except for Fig. (7.21)).
From Fig. (7.18), we easily see that throughput of two models changes when d_1 changes. As shown in the figure, when the relay is close to S or D, the throughput is better than that when the relay is far from S or D. The throughput gets the worst value at midway between S and D. The DT model takes advantage than the other because its transmission rate is independent.

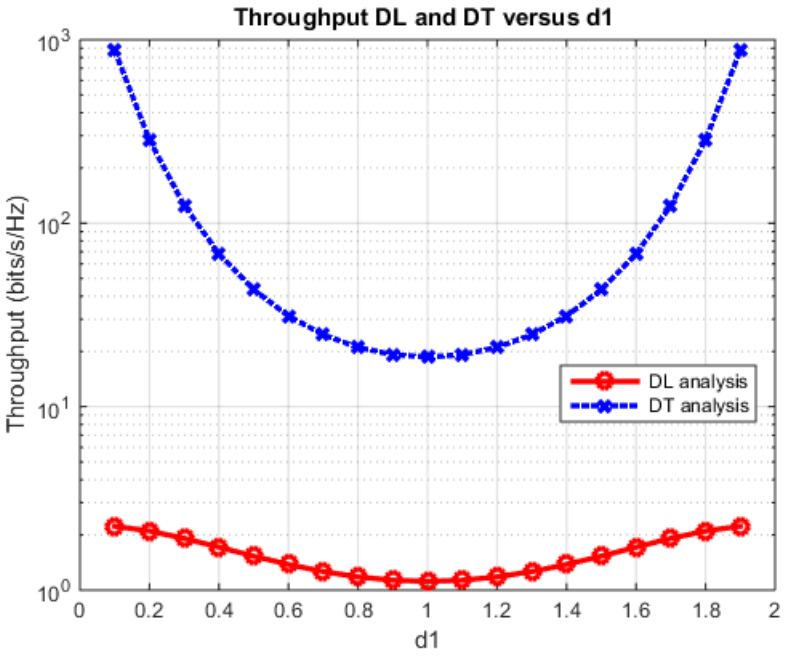

FIGURE 7.18: Throughput of DT and DL model versus distance.

Fig. (7.19) illustrates that the throughput of the DT models is remarkably better as η increases. Meanwhile, the throughput of the DL model increases slightly. Here, the throughput of the DT model is still better than that of the DL model. The reason is the same as previous part.
Fig. (7.20) proves the impact of the noise level on the throughput performance. When σ rises, the throughput decreases. This is because when σ increases, we have the worse throughput, which is shown clearly from Eq. (7.46), Eq. (7.50), Eq. (7.51), Eq. (7.52). It is also noting that throughput of DT model is better than that of DL model.

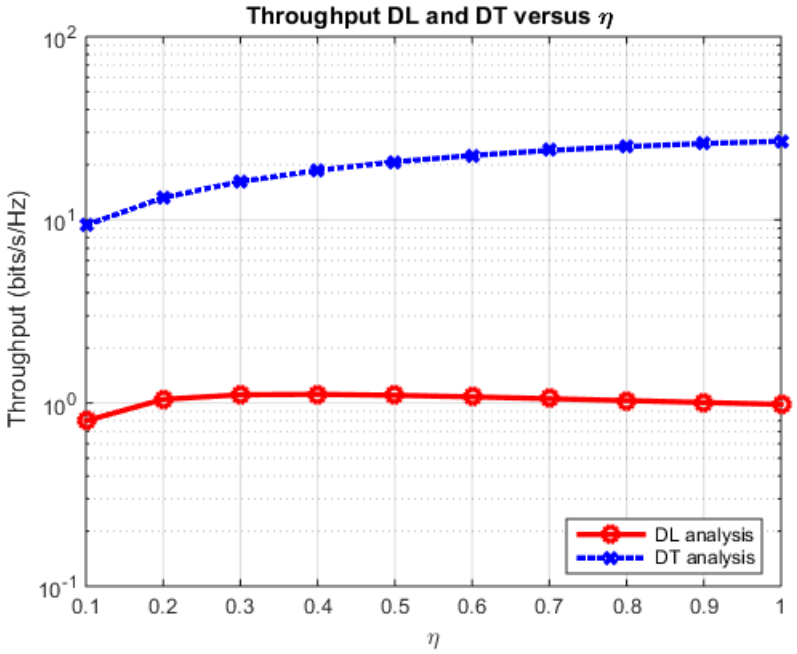

FIGURE 7.19: Throughput of DT and DL model versus η.

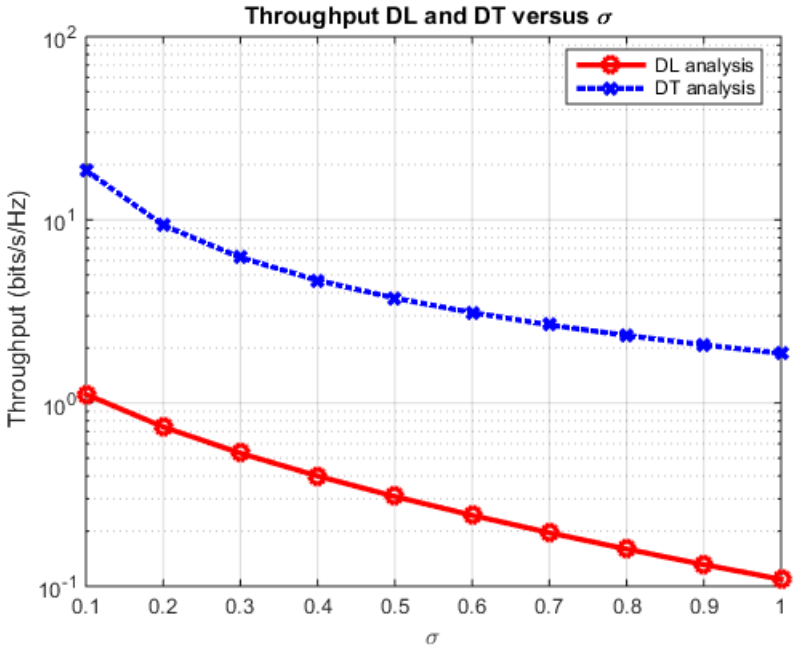

FIGURE 7.20: Throughput of DT and DL model versus σ.

Besides, Fig. (7.21) shows us the fact that the time switching factor contributes significantly on the throughput performance. When $\alpha \leq 0.4$ or $\alpha \geq 0.4$, the DT throughput decreases gradually; when $\alpha = 0.4$, DT model gets the best value. The same thing occurs with the DL model as $\alpha \geq 0.3$ or $\alpha \leq 0.3$. And this model attains the best value at $\alpha = 0.3$. With no exception, the throughput of the DT model is better than that of the DL one.

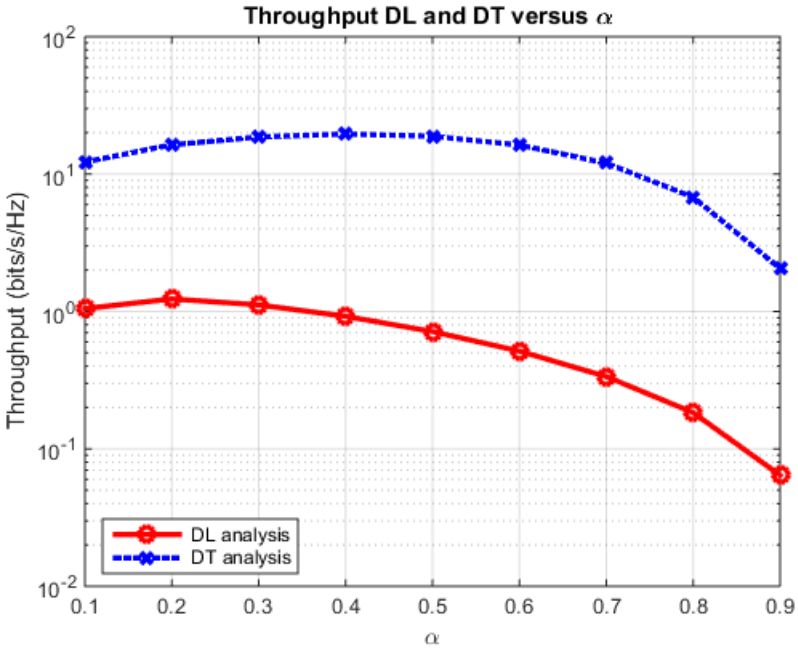

FIGURE 7.21: Throughput of DT and DL model versus α.

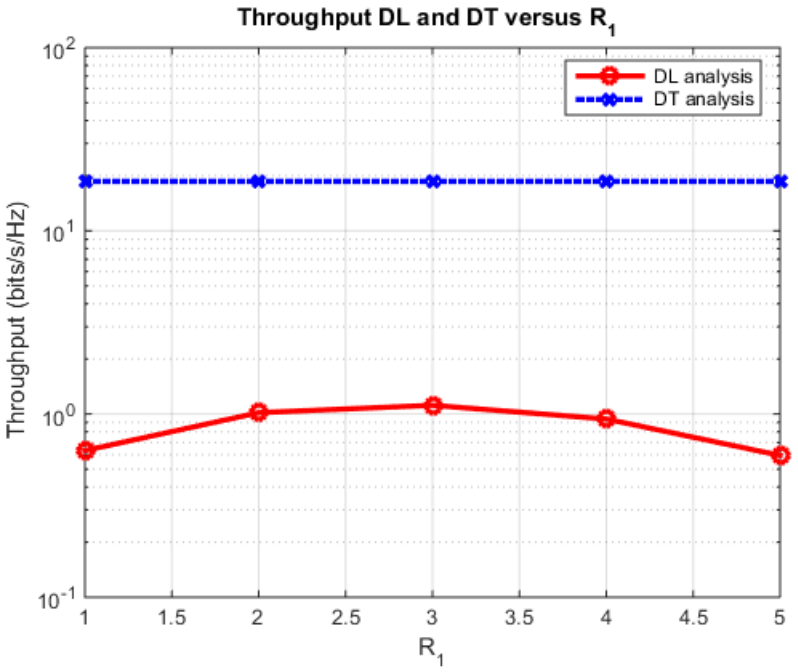

FIGURE 7.22: Throughput of DT and DL model versus R_1.

Moreover, Fig. (7.22) shows a plot versus the target rate R_1. For the DL model, its throughput gets the optimal value when $R_1 = 3$. When R_1 is smaller or bigger than this value, its throughput decreases. But for the DT model, the changes of R_1 do not impact on the throughput. This can also be explained easily because from Eq. (7.50), we can see that throughput expression do not contain R_1. The DT throughput is better than that of the DL throughput, too.

In this part, we have studied the DT and DL throughput of FD relaying in RF energy harvesting network. The analytical expressions were derived for the throughput of the system. From that, we can see the performance of the two models is depending on the time-switching factor, the noise coefficient, the relay position, the transmission rate as well as the energy conversion efficiency. Furthermore, comparing between two models, our results show that the DT model can promote the system throughput. So, it is an expecting measure for developing future RF energy harvesting cooperative systems.

7.4 A Performance Analysis of an AF Two-hop Model in the Energy Harvesting Relay Network

Lately, EH through RF signals has collected remarkable interest of the authors in **[26**; **73]**. A system where the secondary user can take channel access to transfer a packet or to collect RF power when the selected channel is free or withheld by the primary user was studied. An optimization algorithm to get the channel access strategy for the secondary user to maximize its throughput is presented by the authors in **[74]**.

Besides, wireless-energized cooperative communication system comprising of one hybrid access-point (AP), one source, and one relay is examined. Contrary to normal cooperative networks, the source and relay in the considered system have no power supply. They need to rely on the energy collected from the signals transmitted by the AP for their cooperative communication transmission in **[77]**.
On the other hand, a wireless EH and information transfer protocol in cognitive relaying systems, where an EH based secondary system shares the spectrum and collects power by exploiting the primary transmission was also studied. Especially, the secondary transmitter can collect power from the received primary signal and then conveys it along with the secondary signal as introduced in **[78]**.
In reality, the employment of radio information and energy transmission, an advanced concept of EH, to radio cooperative systems was mentioned. In particular, the focus is on a cooperation system in which a source contacts with a destination with the aid of relays and the relays are casually set up following to homogeneous Poisson point process as in **[89]**.
An EH cognitive radio (CR) network working in a slotted mode, where the secondary user (SU) does not have power supply and is energized by energy harvested from the surrounding environment is investigated. The SU can only do either power collecting, spectrum sensing or data transmission at a time due to hardware limitation such that a time slot is segmented into three non-overlapping parts as considered in **[62- 64**; **97]**.
In this part, we study an AF wireless two-hop relay networks in TSR protocol to perform the simultaneous wireless power and information transfer (SWIPT) mode. To maximize the throughput, we utilize the numerical method and study the performance. Hereby, it can be seen clearly that the DT transmission mode outperforms that of the DL one.

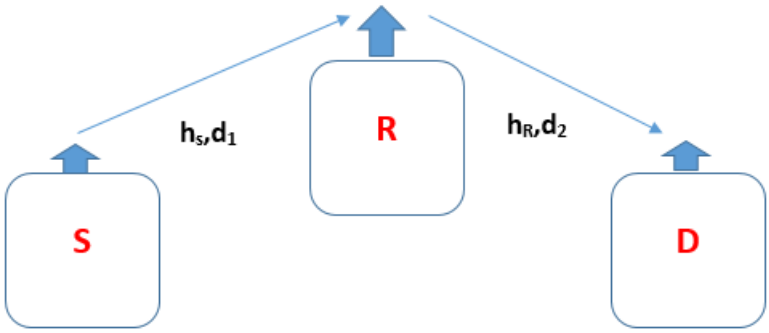

FIGURE 7.23: The AF two-hop system.

7.4.1 Network Model

Let consider a TSR system with two hops and three nodes, a source denoted by S, a relay by R, and the destination by D. Assume that there is no direct link connecting S and D because of the distance between S and D is very far. R operates in the TSR protocol, in which it employs the harvested energy to transmit information to D, as shown in Fig. (7.23), the distance between $S - R$ denoted by d_1, and the distance between $R - D$ denoted by d_2.

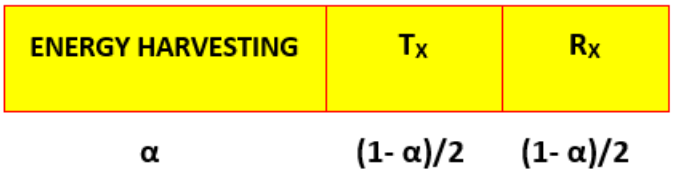

FIGURE 7.24: The parameters of TSR protocol.

As described in the TSR protocol proposed in Fig. (7.24), the communication process has two phases. Firstly, the energy is transmitted from S to R within a time slot of $\alpha T, (0 < \alpha < 1)$ and next, the remaining time slot of $(1 - \alpha) T$ is spent to convey information $(1 - \alpha) T/2$ from source to the relay, the other $(1 - \alpha) T/2$ for information transfer from R to S, where α is the time-switching factor and T is the total duration of one transmission block.
In the energy harvesting phase, the received signal at R is given as

$$y_R = \sqrt{\frac{P_S}{d_1^m}} h_S x_S + n_R, \tag{7.53}$$

where P_S is source power, n_R is the additive white Gaussian noise (AWGN) at R with zero mean and variance of σ_R^2.
So, the harvested energy at the relay is expressed by **[82]**

$$E_h = \eta \alpha T \frac{P_S |h_S|^2}{d_1^m}, \tag{7.54}$$

where m is the path loss exponent, η is the energy conversion efficiency, h_S, h_R are the channel gains of the S-R and the R-D link.
In the next phase, supposing that S propagates information x_S to R and R

transmits information x_R to D. Both signals have unit power and zero–mean, i.e., $E\left[|x_i|^2\right] = 1$ and $E\left[x_i\right] = 0$, with $i \in \{S, R\}$. The transmit power at R is provided as in **[83]**

$$P_R = \frac{E_h}{(1-\alpha)\,T/2} = 2kP_S\frac{|h_S|^2}{d_1^m}, \tag{7.55}$$

where $k = \frac{\alpha\eta}{1-\alpha}$. For AF mode, we get:

$$x_R = Hy_R, \tag{7.56}$$

where H is an amplification factor, which is given by

$$H = \sqrt{\frac{P_R}{\frac{P_S}{d_1^m}|h_S|^2 + \sigma^2}}. \tag{7.57}$$

So, the required signal at destination is found as

$$y_D = \frac{h_R}{\sqrt{d_2^m}}x_R + n_D, \tag{7.58}$$

where n_D is the AWGN at D with a zero-mean and variance of $\sigma_D^2 = \sigma_R^2 = \sigma^2$, for simplicity.
Alternatively, the instantaneous received SINR at D over R is computed as

$$\gamma = \frac{E\left\{|signal|^2\right\}}{E\left\{|noise|^2\right\} + E\left\{|RSI|^2\right\}}. \tag{7.59}$$

So, from Eq. (7.55), Eq. (7.56), Eq. (7.57), Eq. (7.58), and Eq. (7.59), and through some simple calculations, we get

$$\gamma = \frac{\frac{P_S|h_S|^2 P_R|h_R|^2}{d_1^m d_2^m \sigma^2}}{\frac{P_S|h_S|^2}{\sigma^2 d_1^m} + \frac{P_R|h_R|^2}{d_2^m\sigma^2} + 1}. \tag{7.60}$$

7.4.2 Outage Probability and Throughput Analysis

In this section, we investigate the throughput of the considered two-hop relay network with EH. Through analytical expressions, the throughput of DL and DT models are derived and the recommended model for the EH relay system is achieved, too.

The Outage probability analysis

The outage probability of the AF two-hop relay network in DL mode is calculated as

$$P_{out} = pr\left(\gamma \leq Z\right), \tag{7.61}$$

where R is the transmission rate and $Z = 2^R - 1$.
Proposition:

The outage probability of the EH enabled AF relay network is derived as

$$\begin{aligned} P_{out} &= pr\left\{\frac{\frac{P_S|h_S|^2 P_R|h_R|^2}{d_1^m d_2^m \sigma^2}}{\frac{P_R|h_R|^2}{\sigma^2 d_2^m}+\frac{P_S|h_S|^2}{d_1^m \sigma^2}+1} \le Z\right\} \\ &= 1-\frac{1}{\lambda_S}\int_{Z/P_S}^{\infty} \exp\left(-\frac{x}{\lambda_S}-\frac{Z(\frac{xP_S}{\sigma^2 d_1^m}+1)}{\lambda_D(\frac{2kP_S^2x^2}{d_1^m d_2^m \sigma^2}-\frac{2kZP_S x}{d_1^m d_2^m \sigma^2})}\right) dx. \end{aligned} \tag{7.62}$$

We set $x=|h_S|^2$ and $y=|h_R|^2$. Based on CDF and PDF of x are $f_y(b)=(1/\lambda_D)\,e^{(-b/\lambda_D)}$ and $F_{|h_S|^2}(c)=\Pr\left(|h_S|^2\le c\right)=1-e^{\frac{-c}{\lambda_S}}$.

Proof:

$$\begin{aligned} P_{out} &= pr\left\{\frac{\frac{P_S|h_S|^2 P_R|h_R|^2}{d_1^m d_2^m \sigma^2}}{\frac{P_R|h_R|^2}{\sigma^2 d_2^m}+\frac{P_S|h_S|^2}{d_1^m \sigma^2}+1} \le Z\right\} = pr\left\{|h_R|^2 \le H\right\} \\ &= 1-\int_0^{\infty} e^{-\frac{Z\left(\frac{xP_S}{\sigma^2 d_1^m}+1\right)}{\lambda_D\left(\frac{2kx^2P_S{}^2}{\sigma^2 d_2^m d_1^m}-\frac{2kZxP_S}{\sigma^2 d_2^m d_1^m}\right)}} f_{|h|^2}(x)dx, \end{aligned} \tag{7.63}$$

where $H=\left[\frac{z\left(\frac{xP_S}{\sigma^2 d_1^m}+1\right)}{\left(\frac{2kx^2P_S{}^2}{\sigma^2 d_2^m d_1^m}-\frac{2kZxP_S}{\sigma^2 d_2^m d_1^m}\right)}\right]$.

The Proposition is achieved easily after some simple manipulations, where λ_S, λ_D are means of the exponential random variable $|h_S|^2, |h_R|^2$ and the fading channel gains $|h_S|^2, |h_R|^2$ are the independent and identically distributed (i.i.d.) exponential random variables.

In DT mode, S propagates at any constant rate upper bounded by the ergodic capacity. Meanwhile, the code-word length is rather large compared to the transmission block, so the code-word could use all potential knowledge of the channel. Consequently, ergodic capacity becomes a suitable metric for system performance.

Proposition 9:

The ergodic capacity is expressed as

$$C=\frac{G_{4\ \ 2}^{1\ \ 4}\left(\frac{2kP_S\lambda_S\lambda_D}{\sigma^2 d_1^m d_2^m}\middle|\begin{matrix}0,0,1,1\\1,0\end{matrix}\right)}{\ln 2}-\frac{e^{\frac{d_2^m}{2k\lambda_D}}}{\lambda_S \ln 2}\int_0^{\infty} E_1\left(\frac{\sigma^2 d_1^m d_2^m+P_S x d_2^m}{2kP_S\lambda_D x}\right)e^{\frac{-x}{\lambda_S}}, \tag{7.64}$$

where $x=|h_S|^2|h_R|^2$, $G_{p\ \ q}^{m\ \ n}(x)$ is the Meijer G-function, Eq. (9.301) in **[50]**, $E_n(x)$ is the exponential integral function as Eq. (5.1.4) in **[51]**.

Proof:

The achievable rate of the network can be alternatively calculated by

$$C=E\left\{\log_2\left(1+\frac{2kP_S|h_S|^2|h_R|^2}{\sigma^2 d_1^m d_2^m}\right)\right\}-E\left\{\log_2\left(1+\frac{2kP_S|h_S|^2|h_R|^2}{\sigma^2 d_1^m d_2^m+P_S|h_S|^2 d_2^m}\right)\right\}. \tag{7.65}$$

Recall that PDF of x is express by

$$f(x)=\frac{2}{\lambda_S\lambda_D}K_0\left(2\sqrt{\frac{x}{\lambda_S\lambda_D}}\right), \tag{7.66}$$

where $K_n(x)$ is the n^{th} order modified Bessel function of the second kind of Eq. (8.432.1) in **[50]**.
The first term of Eq. (7.66) can be calculated as

$$C_1 = E\left\{\log_2\left(1+\frac{2kP_S|h_S|^2|h_R|^2}{\sigma^2 d_1^m d_2^m}\right)\right\} = \frac{G_{2\ 2}^{4\ 1}\left(\frac{2kP_S\lambda_S\lambda_D}{\sigma^2 d_1^m d_2^m}\middle|\begin{matrix}0,0,1,1\\1,0\end{matrix}\right)}{\ln 2}$$
$$= \frac{2}{\lambda_S\lambda_D}\int_0^\infty G_{2\ 2}^{2\ 1}\left(\frac{kP_S x}{\sigma^2 d_1^m d_2^m}\middle|\begin{matrix}1,1\\1,0\end{matrix}\right) K_0\left(2\sqrt{\frac{x}{\lambda_S\lambda_D}}\right)dx, \tag{7.67}$$

from the relationship of Eq. (8.4.6.5) in **[75]** and by employing the integral identity as in Eq. (7.821.3) in **[49]**.
The second term, conditioned on $|h_R|^2$, is computed as

$$C_2 = E\left\{\left\{\log_2\left(1+\frac{2kP_S|h_S|^2}{\sigma^2 d_1^m d_2^m + P_S|h_S|^2 d_2^m}|h_R|^2\right)\right\}\right\} = \frac{e^{\frac{\sigma^2 d_1^m d_2^m + P_S|h_S|^2 d_2^m}{2kP_S|h_S|^2}}}{\ln 2} H_2.$$
$$H_2 = E_1\left(\frac{\sigma^2 d_1^m d_2^m + P_S|h_S|^2 d_2^m}{2kP_S|h_S|^2}\right). \tag{7.68}$$

Then, by averaging Eq. (7.68) over $|h_S|^2$, we get the expected result.

The throughput analysis

In the above Proposition, the outage probability for the DL model is derived. In the delay-limited transmit protocol, the transmitter propagates information at a fixed transmission rate R bits/sec/Hz and $(1-\alpha)T$ is the effective information time. So, the DL throughput of the two-hop network is given as

$$\tau_{DL} = (1-P_{out})\,R\frac{(1-\alpha)}{2}. \tag{7.69}$$

Also, in Proposition 9, the throughput of the DT system is given as

$$\tau_{DT} = C\frac{(1-\alpha)}{2}. \tag{7.70}$$

Unluckily, it is hard to derive the maximal throughput mathematically, but we can get that value by the numerical approach as described in the next part.

7.4.3 Numerical Results

In this section, we employ the derived analytical results to study the outage probability as well as the throughput of two models. We set the source transmission rate $R = 3\ (bps/Hz)$ (except for Fig. (7.28)), $\alpha = 0.3$ (except for Fig. (7.27)). The energy conversion efficiency is set to be $\eta = 0.4$ (except for Fig. (7.26)), the path loss exponent factor is set to be $m = 3$. For simplicity, we set the distance $d_1 = d_2 = 1$ (except for Fig. (7.29)). Also, we set $\lambda_s = \lambda_d = 1; \lambda_r = 0.1$ and $P_S(dB) = 10$, $\sigma^2 = 0.1$ (except for Fig. (7.25)). These values are chosen because they provided the best asymptotic between curves.
Fig. (7.25) reveals that the noise coefficient has an impact on system performance. When σ^2 changes from 0 to 1, the throughput of two models also

changes. The bigger the σ^2 is, the smaller the throughput of two models, gets. This proves the impact of noise on system performance. We can see clearly that the throughput of the DT model is better than that of the DL one.

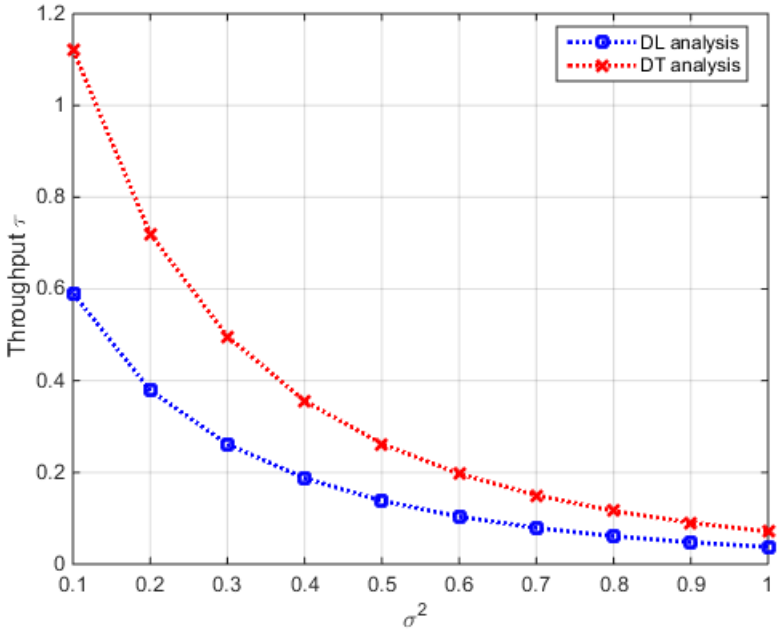

FIGURE 7.25: The throughput of DL and DT model versus σ^2.

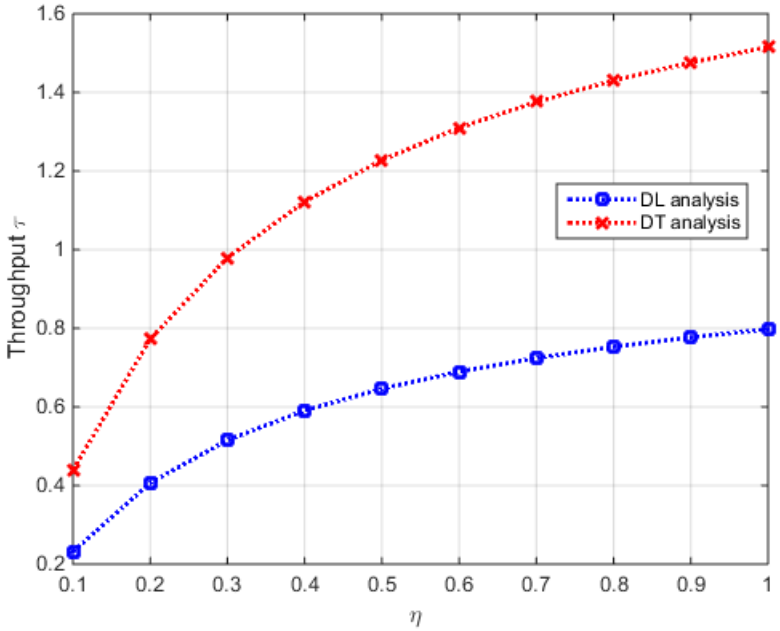

FIGURE 7.26: The throughput of DL and DT model versus η.

It can be shown in Fig. (7.26) that η also has effect on the throughput of both models. The bigger η is, The bigger the throughput of two models gets, the throughput of the DT model is better than that of the DL model. It is easy to know for big η, more energy is available at the relay to help relay send information to the destination easily.

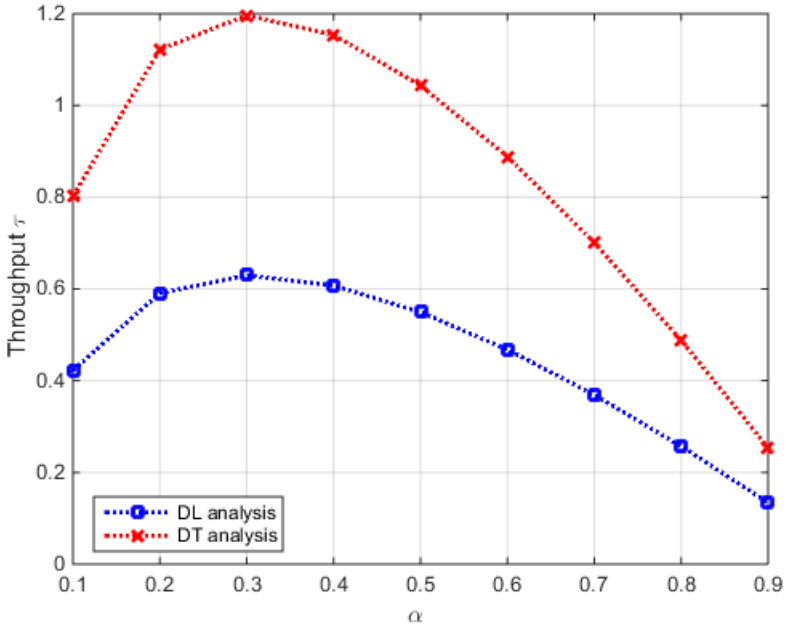

FIGURE 7.27: The throughput of DL and DT model versus α.

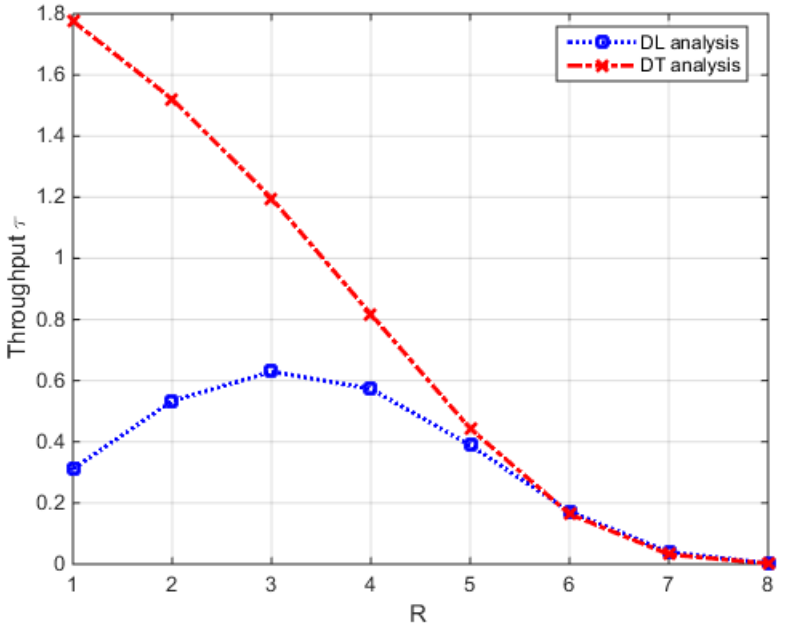

FIGURE 7.28: The throughput of DL and DT model versus R.

Fig. (7.27) also says that the time-switching factor has an impact on system operation. When α changes from 0 to 1, the throughput of two modes also alters. When $\alpha = 0.3$, the two modes get the best value. The DT throughput is always better than that of the DL mode.

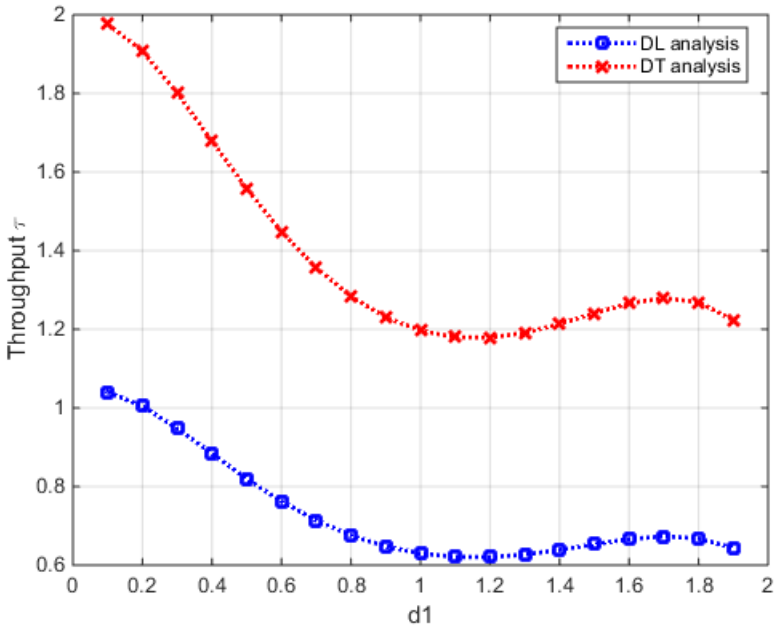

FIGURE 7.29: The throughput of DL and DT model versus d_1.

As observed in Fig. (7.28), the curves tell us that the target transmission rate affects system performance. When R changes, the throughput of the two models also changes. For bigger R, the throughput of the DT mode becomes smaller. Meanwhile, the throughput of the DL mode gets the best value when $R = 3$. When $R \geq 5$, the throughput of two models concurs together. We can see that the throughput of the DT modes is better than that of the DL one.
Fig. (7.29) illustrates the throughput of two models versus the relay position. In the assessment, we set $d_1 + d_2 = 2$, and d_1 varies from 0 to 2. As shown in Fig. (7.29), for both models, the relay should be close to the source to get the optimal throughput. Two suggested models have the worst throughput performance at midway. The bigger d_1 is, the smaller the throughput of two models, gets. Moreover, Fig. (7.29) shows that the DT mode gets the throughput performance better than that of the DL mode. On the other hand, because of noise, when R is close to the destination, the throughput values of two models have a little improvement and then decrease again. This is easy to understand because the noise near the relay affects the system operation but it is not strong enough to promote signal.
In this part, we have studied two-hop relay networks with the wireless energy harvesting and information transmission protocol, in which an energy-constrained relay node collects energy from the received RF signal and spends that harvested energy to forward the information to the destination. Here, the performance in two modes is compared. To find out the

appropriate mode, the analytical expressions of the throughput in TSR protocol are verified by the simulation.
As expected, through simulations, we easily see that the DT mode performance outperforms that of DL one in the two-hop relay system, and the DT relaying system can normally promote the throughput performance.

7.5 Summary

In this chapter, we studied the performance of the considered EH FD relaying network for three different transmission modes, namely instantaneous transmission, delay-limited transmission, and delay-tolerant transmission. The mathematical closed-form expressions for the throughput of the system at three transmission modes have been derived rigorously. The simulation results verified that the DF relaying strategy outperforms the AF one in most of the cases. Furthermore, the throughput value in delay-tolerant mode was greater than that of delay-limited one. Last but not least, the mathematical result matched well with the numerical one obtained by Monte Carlo simulation.

8 Conclusions and future work

In this dissertation, we have investigated the system performance of EH for full-duplex relaying network based on TSR and PSR protocols, together with AF and DF relaying strategies. All analytical outcomes are summarized here. Furthermore, the possible shortcomings of this research as well as potential development of my achieved results are also introduced.

8.1 Summary of results and insights

In Chapter 5, we investigate RF EH technology together with FDRNs to fulfill Aim 1. Regarding the time switching factor, we can expose that there exists an optimal value for each AF and DF mode, that provides the maximal throughput value. This value can also be found by the numerical algorithm **[TNK02]**. It has been shown that the DF strategy outperforms the AF one in most of the cases **[TNK02; TNK08; TNK23]**. It has been verified that the full-duplex communication can provide huge improvement on capacity so that it can satisfy the demand of 5G mobile networks **[TNK1; TNK10; TNK13]**.
Chapter 6 deals with the second aim of this dissertation, i.e., providing the performance analysis of various antenna configurations at the relay node in the considered systems, especially single-antenna configuration versus two-antenna configuration. In other words, I studied the system performance in two cases: (1) Only one antenna is used to collect energy from the source, while the other is used for information forwarding and (2) Both antennas are exploited to collect energy, while only one of them is used to transmitting the information signal. In both two cases, analytical expressions have been derived for outage probability and throughput of this network. Generally, two-antenna configuration outperforms single-antenna one. However, the gap between these two models disappears when the signal source is large enough **[TNK08- TNK09; TNK22]**. Furthermore, multiple-antenna configuration, i.e., MIMO, has also been implemented to enhance the overall system performance. In particular, three diversity techniques for MIMO have been investigated: Zero Forcing at Transmitter (TZF), Zero Forcing (RZF), and Maximal Ratio Combining (MRC) at the receiver **[TNK03-TNK06]**.
Finally, for Aim 3 of the dissertation, the extension of performance analysis of FDRNs for three transmission modes, namely: instantaneous, delay-limited, delay-tolerant transfer, has been provided. The results verified that DF strategy outperforms AF one in most of cases. The throughput values in delay-tolerant mode are greater than that of delay-limited one **[TNK1; TNK10; TNK11; TNK19- TNK20]**. From the mathematical analysis, the impact of different parameters on the performance of the considered system such as the position of the relay, the AWGN at the relay, the energy

conversion factor as well as TSR or PSR parameters, has been studied in detail. An interesting result is that a big scale of the potential gain given by FD relaying with energy harvesting capability can be implemented with only the knowledge of channel statistics and without the demand of instantaneous CSI. So, this is a hopeful solution for enforcing future RF energy harvesting cooperation networks.

The important contributions of my dissertation can be summarized as follows. First, the performance of energy harvesting protocols for wireless full-duplex relay networks in terms of outage probability and throughput has been fully evaluated. The closed-form expressions of outage probability and throughput have been derived for different energy harvesting protocols, different relaying strategy, different antenna configurations, and different transmission modes. Secondly, from the performance analysis, I have provided the optimal energy harvesting parameters, including time switching and power splitting factors, as well as recommended the best communication strategies for EH-based full-duplex relay networks depending on each specific channel conditions (Rayleigh, Nakagami-m, with hardware impairment, etc.). Finally, I propose the integration of energy harvesting with advanced techniques like NOMA or MIMO for full-duplex relay networks to improve the outage performance.

8.2 Future work

Development of an advanced system for EH full-duplex relaying network is the expected contribution to the scientific community. The following issues are considered as the extensions of my dissertation.
Regarding Aim 1, my investigation can be extended further by utilizing the Rician fading channel instead of Rayleigh fading one. We can also optimize the time-switching factor of TSR protocol in DF mode, and then compare this value with the optimal point in AF mode, which we had found in a past job. Another interesting work is to consider the hybrid TSR-PSR protocol to get higher efficiency.
Regarding Aim 2, we can extend my work with multiple-antenna configuration for EH full-duplex relaying networks in which AF and DF schemes will be studied in detail. And then, we compare the performance of hardware impairment and ideal impairment with three diversity technologies to improve system performance.
Finally, for Aim 3, to extend the work, the Rician fading channel can also be considered. On the other hand, information security is another requirement for communications, which is proved why physical security in EH FD relaying networks can be another research direction.

Bibliography

[1] C.-X. Wang, F. Haider, X. Gao, X.-H. You, Y. Yang, D. Yuan, H. Aggoune, H. Haas, S. Fletcher, and E. Hepsaydir, Cellular architecture and key technologies for 5G wireless communication networks, Communications Magazine, IEEE, vol. 52, no. 2, pp. 122–130, February 2014.

[2] M. Bellanger, M. Renfors, T. Ihalainen, and C. da Rocha, OFDM and FBMC transmission techniques: a compatible high performance proposal for broadband power line communications, in Power Line Communications and Its Applications (ISPLC), 2010 IEEE International Symposium on, March 2010, pp. 154–159.

[3] N. Michailow, M. Matthe, I. Gaspar, A. Caldevilla, L. Mendes, A. Festag, and G. Fettweis, Generalized frequency division multiplexing for 5th generation cellular networks, Communications, IEEE Transactions on, vol. 62, no. 9, pp. 3045–3061, Sept 2014.

[4] Y. Saito, Y. Kishiyama, A. Benjebbour, T. Nakamura, A. Li, and K. Higuchi, Non-orthogonal multiple access (noma) for cellular future radio access, in Vehicular Technology Conference (VTC Spring), 2013 IEEE 77th, June 2013, pp. 1–5.

[5] H. Nikopour and H. Baligh, Sparse code multiple access, in Personal Indoor and Mobile Radio Communications (PIMRC), 2013 IEEE 24th International Symposium on, Sept 2013, pp. 332–336.

[6] E. Larsson, O. Edfors, F. Tufvesson, and T. Marzetta, Massive MIMO for next generation wireless systems, Communications Magazine, IEEE, vol. 52, no. 2, pp. 186–195, February 2014.

[7] D. Aziz, et al. , METIS final project report, ICT-317669-METIS/D8.4, 2015.

[8] T. Rappaport, S. Sun, R. Mayzus, H. Zhao, Y. Azar, K. Wang, G. Wong, J. Schulz, M. Samimi, and F. Gutierrez, Millimeter wave mobile communications for 5g cellular: It will work Access, IEEE, vol. 1, pp. 335–349, 2013.

[9] M. Hadzialic, B. Dosenovic, M. Dzaferagic, and J. Musovic, Cloud-ran: Innovative radio access network architecture, in ELMAR, 2013 55th International Symposium, Sept 2013, pp. 115–120.

[10] X. Shen, Device-to-device communication in 5g cellular networks, Network, IEEE, vol. 29, no. 2, pp. 2–3, March 2015.

[11] S. Bi, C. K. Ho, and R. Zhang, Wireless Powered Communication: Opportunities and Challenges, IEEE Communication Mag. , vol. 53, no. 4, Apr. 2014, pp. 117–25.

[12] Tam Nguyen Kieu, Tran Hoang Quang Minh, Thuan Do Dinh and Miroslav Vozňák. An Instantaneous Transmission Mode Analysis in Energy Harvesting for Half-Duplex and Full-Duplex Relaying Network, International Journal of Grid and Distributed Computing, Vol. 9, No. 3 (2016), pp.11-20.

[13] Tam Nguyen Kieu, Khanh Nhan Nguyen Huu , Long Nguyen Ngoc, Hung Ha Duy, Thuan Do Dinh, Miroslav Voznak, Dominik Uhrin, An Operation Analysis in DF Full Duplex Relay Network, 2016 XI International Symposium on Telecommunications (BIHTEL) October 24-26, 2016, Sarajevo, Bosnia and Herzegovina.

[14] W. C. Brown, J. R. Mims, and N. I. Heenan, An experimental microwave-powered helicopter, IEEE Int. Convention Record, vol. 13, pp. 225–235, Mar. 1966.

[15] P. E. Glaser, Power from the sun: its future, Science, vol. 162, no.3856, pp. 857–861, Nov. 1968.

[16] Energous Corporation homepage.[Online]. Available: http://www.energous.com/.

[17] Ossia Inc. homepage. [Online]. Available: http://www.ossia.com/.

[18] M. Knox, Single antenna full-duplex communications using a common carrier, in 13th Annual Wireless and Microwave Technology Conference Apr. 2012.

[19] W. Lumpkins, Nikola Tesla's dream realized: Wireless power energy harvesting, IEEE Consumer Electronics Mag., vol. 3, no.1, pp.39–42, Jan. 2014.

[20] M. Pinuela, P. Mitcheson, and S. Lucyszyn, Ambient RF energy harvesting in urban and semi-urban environments, IEEE Trans. Microwave Theory and Techniques, vol. 61, no. 7, pp. 2715–2726, Jul. 2013.

[21] L. R. Varshney, Transporting information and energy simultaneously, in Proc. IEEE ISIT 2008, Toronto, Canada, July 2008, pp. 1612–1616.

[22] P. Grover and A. Sahai, Shannon meets Tesla: Wireless information and power transfer, in Proc. IEEE ISIT 2010, Austin, TX, June 2010, pp. 2363–2367.

[23] R. Zhang and C. Ho, MIMO broadcasting for simultaneous wireless information and power transfer, IEEE Trans. Wireless Communication, vol. 12, no. 5, pp. 1989–2001, May 2013.

[24] Z. Xiang and M. Tao, Robust beam-forming for wireless information and power transmission, IEEE Wireless Communication, Letters, vol. 1, no.4, pp. 372–375, 2012.

[25] L. Liu, R. Zhang, and K. C. Chua, Wireless information and power transfer: A dynamic power splitting approach, IEEE Trans. Communication, vol. 61, no. 9, pp. 3990–4001, Sep. 2013.

[26] X. Zhou, R. Zhang, and C. Ho, Wireless information and power transfer: Architecture design and rate-energy trade-off, IEEE Trans. Communication, vol. 61, no. 11, pp. 4754–4767, Nov. 2013.

[27] D. W. K. Ng, E. S. Lo, and R. Schober, Wireless information and power transfer: Energy efficiency optimization in OFDMA systems, IEEE Trans. Wireless Communication, vol. 12, no. 12, pp. 6352–6370, Dec. 2013.

[28] A. M. Fouladgar and O. Simeone, On the transfer of information and energy in multi-user systems, IEEE Communication. Letters, vol. 16, no. 11, pp. 1733–1736, Nov. 2012.

[29] K. Huang and V. K. N. Lau, Enabling wireless power transfer in cellular networks: architecture, modeling and deployment, IEEE Trans. Wireless Communication, vol. 13, no. 2, pp. 902–912, Feb. 2014.

[30] B. Medepally and N. B. Mehta, Voluntary energy harvesting relays and selection in cooperative wireless networks, IEEE Trans. Wireless Communication, vol. 9, no. 11, pp. 3543–3553, Nov. 2010.

[31] A. A. Nasir, X. Zhou, S. Durrani, and R. Kennedy, Relaying protocols for wireless energy harvesting and information processing, IEEE Trans. Wireless Communication, vol. 12, no. 7, pp. 3622–3636, Jul. 2013.

[32] A. A. Nasir, X. Zhou, S. Durrani, and R. A. Kennedy, Wireless energy harvesting and information relaying: Adaptive time-switching protocols and throughput analysis, IEEE Trans. Wireless Communication, Submitted. [Online] Available: http://arxiv.org/abs/1310.7648.

[33] A. A. Nasir, X. Zhou, S. Durrani, and R. A. Kennedy, Throughput and ergodic capacity of wireless energy harvesting based DF relaying network, in Process. IEEE ICC 2014, Sydney, Australia.

[34] Z. Ding, S. M. Perlaza, I. Esnaola, and H. V. Poor, Power allocation strategies in energy harvesting wireless cooperative networks, IEEE Trans. Wireless Communication, Accepted.

[35] Z. Ding and H. V. Poor, Cooperative energy harvesting networks with spatially random users, IEEE Signal Process. Letter, vol. 20, no. 12, pp. 1211–1214, Dec. 2013.

[36] Z. Ding, I.Krikidis, B. Sharif, and H. V. Poor, Wireless information and power transfer in cooperative networks with spatially random relays, IEEE Trans. Wireless Communication, Accepted.

[37] I. Krikidis, Simultaneous information and energy transfer in large scale networks with/without relaying, IEEE Trans. Communication, vol. 62, no. 3, pp. 900–912, Mar. 2014.

[38] T. Riihonen, S. Werner, and R. Wichman, Hybrid full-duplex/half-duplex relaying with transmit power adaptation, IEEE Trans. Wireless Communication, vol. 10, pp. 3074-3085, Sept. 2011.

[39] T. Riihonen, S. Werner, and R. Wichman, Mitigation of loop-back self-interference in full-duplex MIMO relays, IEEE Trans. Signal Processing, vol. 59, pp. 5983-5993, Dec. 2011.

[40] B. P. Day, A. R. Margetts, D. W. Bliss, and P. Schniter, Full-duplex MIMO relaying: Achievable rates under limited dynamic range, IEEE J. Select. Areas Communication, vol. 30, pp. 1541-1553, Sept. 2012.

[41] A. Sabharwal, P. Schniter, D. Guo, D. Bliss, S. Rangarajan, and R.Wichman, In-band full-duplex wireless: challenges and opportunities, IEEE J. Select. Areas Communication, Accepted. [Online] Available: http://arxiv.org/abs/1311.0456.

[42] I. Krikidis, H. A. Suraweera, P. J. Smith and C. Yuen, Full-duplex relay selection for amplify-and-forward cooperative networks, IEEE Trans. Wireless Communication, vol. 11, pp. 4381-4393, Dec. 2012.

[43] H. A. Suraweera, I. Krikidis, G. Zheng, C. Yuen and P. J. Smith, Low complexity end-to-end performance optimization in MIMO full-duplex relay systems, IEEE Trans. Wireless Communication, vol. 13, pp. 913-927, Feb. 2014.

[44] P. Popovski and H. Yomo, Bi-directional amplification of throughput in a wireless multi-hop network, in Proc. of Vehicular Technology Conference, vol. 2, Melbourne, Australia, May 7-10, 2006, pp. 588–593.

[45] R. H. Louie, Y. Li, and B. Vucetic, Practical physical layer network coding for two-way relay channels: performance analysis and comparison, IEEE Transactions on Wireless Communications, vol. 9, no. 2, pp.764–777, 2010.

[46] B. Rankov and A. Wittneben, Achievable rate regions for the two-way relay channel in Proc. of IEEE International Symposium on Information Theory, Seattle, WA, USA, 2006, pp. 1668–1672.

[47] C. Zhong, H. A. Suraweera, G. Zheng, I. Krikidis and Z. Zhang, Wireless Information and Power Transfer With Full-Duplex Relaying, in IEEE Transactions on Communications, vol. 62, no. 10, pp. 3447-3461, Oct. 2014.

[48] T. Kwon, S. Lim, S. Choi, and D. Hong, Optimal duplex mode for DF relay in terms of the outage probability, IEEE Trans. Veh. Technology, vol. 59, no. 7, pp. 3628–3634, Sep. 2010.

[49] H. A. David, Order Statistics. New York, NY, USA: Wiley, 1970.

[50] I. S. Gradshteyn and I. M. Ryzhik, Table of Integrals, Series, and Products, Orlando, FL: Academic Press, 5th ed., 1994.

[51] M. Abramowitz and I. A. Stegun, Handbook of mathematical functions, New York: Dover Publication Inc., 1974.

[52] T. Riihonen, S. Werner, R. Wichman, Comparison of Full-Duplex and Half-Duplex Modes with a Fixed Amplify-and-Forward Relay, IEEE 2009 IEEE Wireless Communications and Networking Conference Budapest, Hungary, 2009.

[53] Jingrui Yang, Xuefang Liu, Qinghai Yang, Power Allocation of Two-Way Full-Duplex AF Relay under Residual Self-Interference, IEEE 2014 14th International Symposium on Communications and Information Technologies (ISCIT) - Incheon, South Korea.

[54] Dinh-Thuan Do, Power Switching Protocol for Two-way Relaying Network under Hardware Impairments, Radio Engineering Journal, Vol. 24, No. 3, 2015.

[55] C. Zhong, H. A. Suraweera, G. Zheng, I. Krikidis, Relay Control for Full-Duplex Relaying with Wireless Information and Energy Transfer, IEEE Transactions on Communications, Vol. 62, No. 10, 2014.

[56] W. Zihao, C. Zhiyong, Y. Yao, X. Bin, and L. Hui, Wireless energy harvesting and information transfer in cognitive two-way relay networks, in Global Communications Conference (GLOBECOM), 2014 IEEE, 2014, pp. 3465-3470.

[57] X. Ke, F. Pingyi, and K. Ben Letaief, Time-switching based SWPIT for network-coded two-way relay transmission with data rate fairness, in Proc. of 2015 IEEE International Conference on Acoustics, Speech and Signal Processing (ICASSP), 2015, pp. 5535-5539.

[58] X. Ke, F. Pingyi, Z. Chuang, and K. Ben Letaief, Wireless Information and Energy Transfer for Two-Hop Non-Regenerative MIMO-OFDM Relay Networks, IEEE Journal on Selected Areas in Communications, vol. 33, pp. 1595-1611, 2015.

[59] I. Krikidis, S. Timotheou, S. Nikolaou, Z. Gan, D. W. K. Ng, and R. Schober, Simultaneous wireless information and power transfer in modern communication systems, IEEE Communications Magazine, vol. 52, pp. 104-110, 2014.

[60] Y. Liu and X. Wang, Information and Energy Cooperation in OFDM Relaying: Protocols and Optimization, IEEE Transactions on Vehicular Technology, vol. PP, pp. 1-1, 2015.

[61] S. A. Mousavifar, L. Yuanwei, C. Leung, M. Elkashlan, and T. Q. Duong, Wireless Energy Harvesting and Spectrum Sharing in Cognitive Radio, in Process. of Vehicular Technology Conference (VTC Fall), 2014, pp. 1-5.

[62] L. Sibomana, H. J. Zepernick, and T. Hung, Wireless information and power transfer in an underlay cognitive radio network, in Proc. of 2014 8th International Conference on Signal Processing and Communication Systems (ICSPCS), 2014, pp. 1-7.

[63] Y. Sixing, Z. Erqing, Q. Zhaowei, Y. Liang, and L. Shufang, Optimal Cooperation Strategy in Cognitive Radio Systems with Energy Harvesting, IEEE Transactions on Wireless Communications, vol. 13, pp. 4693-4707, 2014.

[64] Y. Sixing, Q. Zhaowei, and L. Shufang, Achievable Throughput Optimization in Energy Harvesting Cognitive Radio Systems, IEEE Journal on Selected Areas in Communications, vol. 33, pp. 407-422, 2015.

[65] A. El Shafie, Space 2013; Time Coding for an Energy Harvesting Cooperative Secondary Terminal, IEEE Communications Letters, vol. 18, pp. 1571-1574, 2014.

[66] A. H. Sakr and E. Hossain, Cognitive and Energy Harvesting-Based D2D Communication in Cellular Networks: Stochastic Geometry Modeling and Analysis, IEEE Transactions on Communications, vol. 63, pp. 1867-1880, 2015.

[67] A. A. Alkheir and M. Ibnkahla, Performance Analysis of Cognitive Radio Relay Networks Using Decode and Forward Selection Relaying over Rayleigh Fading Channels, in Global Telecommunications Conference (GLOBECOM 2011), 2011 IEEE, 2011, pp. 1-5.

[68] C. Tong, D. Zhiguo, and T. Guiyun, Wireless information and power transfer using energy harvesting relay with outdated CSI, in High Mobility Wireless Communications (HMWC), 2014 International Workshop on, 2014, pp. 1-6.

[69] H. Yang and B. Clerckx, Joint Wireless Information and Power Transfer for an Autonomous Multiple Antenna Relay System, Communications Letters, IEEE, vol. 19, pp. 1113-1116, 2015.

[70] L. Yuanwei, W. Lifeng, M. Elkashlan, T. Q. Duong, and A. Nallanathan, Two-way relaying networks with wireless power transfer: Policies design and throughput analysis, in Global Communications Conference (GLOBECOM), 2014 IEEE, 2014, pp. 4030-4035.

[71] I. Ahmed, A. Ikhlef, R. Schober, and R. K. Mallik, Joint Power Allocation and Relay Selection in Energy Harvesting AF Relay Systems, Wireless Communications Letters, IEEE, vol. 2, pp. 239-242, 2013.

[72] X. Hong, W. Kai-Kit, and A. Nallanathan, Secure wireless energy harvesting-enabled AF-relaying SWIPT networks, in Communications (ICC), 2015 IEEE International Conference on, 2015, pp. 2307-2312.

[73] S. H. Lee, R. Zhang, and K. B. Huang, Opportunistic wireless energy harvesting in cognitive radio networks, to appear in IEEE Trans. Wireless Communication, 2013.

[74] H. Dinh Thai, D. Niyato, W. Ping, and K. Dong In, Opportunistic Channel Access and RF Energy Harvesting in Cognitive Radio Networks, IEEE Journal on Selected Areas in Communications, vol. 32, pp. 2039-2052, 2014.

[75] A. P. Prudnikow, Y. A. Brychkov and O. I. Marchev, Integrals and Series, Volumne 3: More Special Functions, New York: Gordon and Breach Science Publishers, 1990.

[76] Y. Huan, L. Yunzhou, X. Xibin, and W. Jing, Energy harvesting relay-assisted cellular networks based on stochastic geometry approach, in Intelligent Green Building and Smart Grid (IGBSG), 2014 International Conference on, 2014, pp. 1-6.

[77] C. He, L. Yonghui, J. Luiz Rebelatto, B. F. Uchoa-Filho, and B. Vucetic, Harvest-Then-Cooperate: Wireless-Powered Cooperative Communications, Signal Processing, IEEE Transactions on, vol. 63, pp. 1700-1711, 2015.

[78] W. Zihao, C. Zhiyong, L. Ling, H. Zixia, X. Bin, and L. Hui, Outage analysis of cognitive relay networks with energy harvesting and information transfer, in Communications (ICC),IEEE International Conference on 2014, pp. 4348-4353.

[79] Yiyang N., Shi J., Ran T., Kai-Kit W., Hongbo Z.Shixiang S, Outage analysis for device-to-device communication assisted by two-way decode-and-forward relaying, Wireless Communications and Signal Processing (WCSP), International Conference on 2013, pp. 1-6.

[80] K. Tutuncuoglu, B. Varan, and A. Yener, Energy harvesting two-way half-duplex relay channel with decode-and-forward relaying: Optimum power policies, in Digital Signal Processing (DSP), 18th International Conference on 2013, pp. 1-6.

[81] L. Seunghyun, Z. Rui, and H. Kaibin, Opportunistic Wireless Energy Harvesting in Cognitive Radio Networks, IEEE Transactions on Wireless Communications, vol. 12, pp. 4788-4799, 2013.

[82] C. Huang, R. Zhang, and S. Cui, Throughput maximization for the Gaussian relay channel with energy harvesting constraints, IEEE J. Sel. Areas in Communication, vol. 31, no. 8, pp. 1469–1479, Aug. 2013.

[83] T. N. Kieu, D.-T. Do, X. N. Xuan, T. N. Nhat, and H. H. Duy, AETA 2015: Recent Advances in Electrical Engineering and Related Sciences. Cham: Springer International Publishing, 2016, ch. Wireless Information and Power Transfer for Full-Duplex Relaying Networks: Performance Analysis, pp. 53–62. [Online]. Available: http://dx.doi.org/10.1007/978-3-319-27247-4-5.

[84] N. Dang Khoa and H. Ochi, On the impact of transceiver impairments to cognitive DF relay networks, IEEE Asia Pacific Conference on in Circuits and Systems (APCCAS), 2014, pp. 125-128.

[85] Z. Jian, C. Ruohan, G. Hui, L. Haijing, and L. Tiejun, Secrecy communication of wireless information and power transfer system with green relay, in Communication Workshop (ICCW), IEEE International Conference on 2015, pp. 2040-2045.

[86] X. Jia, Z. Xing, W. Jiewu, Z. Zhenhai, and W. Wenbo, Performance analysis of cognitive relay networks with imperfect channel knowledge over Nakagami-m fading channels, in Wireless Communications and Networking Conference (WCNC), 2014 IEEE, 2014, pp. 839-844.

[87] X. Hong, C. Zheng, D. Zhiguo, and A. Nallanathan, Harvest-and-jam: Improving security for wireless energy harvesting cooperative networks, in Global Communications Conference (GLOBECOM), 2014 IEEE, 2014, pp. 3145-3150.

[88] P. Mugen, L. Yuan, T. Q. S. Quek, and W. Chonggang, Device-to-Device Underlaid Cellular Networks under Rician Fading Channels, IEEE Transactions on Wireless Communications, vol. 13, pp. 4247-4259, 2014.

[89] S. Zhengguo, D. L. Goeckel, K. K. Leung, and D. Zhiguo, A stochastic geometry approach to transmission capacity in wireless cooperative networks, in Personal, Indoor and Mobile Radio Communications, 2009 IEEE 20th International Symposium on 2009, pp. 622-626.

[90] J. Williams, ÒNarrow-band analyzer (Thesis or Dissertation style), Ó Ph.D. dissertation, Dept. Elect. Eng., Harvard Univ., Cambridge, MA, 1993.

[91] H. A. David and H. N. Nagaraja, Order Statistics in Parametric Inference. John Wiley and Sons, Inc., 2005, pp. 171–237. [Online]. Available: http://dx.doi.org/10.1002/0471722162.ch8.

[92] A. Minasian, R. S. Adve, and S. Shahbazpanahi, Energy harvesting for relay-assisted communications, in Acoustics, Speech and Signal Processing (ICASSP), International Conference on 2014 IEEE, 2014, pp. 4763-4767.

[93] L. Mohjazi, M. Dianati, G. K. Karagiannidis, S. Muhaidat, and M. Al-Qutayri, RF-powered cognitive radio networks: technical challenges and limitations, Communications Magazine, IEEE, vol. 53, pp. 94-100, 2015.

[94] S. Misra, N. E. Majd, and H. Hong, Approximation Algorithms for Constrained Relay Node Placement in Energy Harvesting Wireless Sensor Networks, Computers, IEEE Transactions on, vol. 63, pp. 2933-2947, 2014.

[95] O. Orhan and E. Erkip, Energy harvesting two-hop networks: Optimal policies for the multi-energy arrival case, in Sarnoff Symposium (SARNOFF), 2012 35th IEEE, 2012, pp. 1-6.

[96] H. Chuan, Z. Rui, and C. Shuguang, Delay-constrained Gaussian relay channel with energy harvesting nodes, IEEE International Conference on in Communications (ICC, 2012, pp. 2433-2438.

[97] M. Le, V. Ngo, H. Mai, X. N. Tran, M. Di Renzo, Spatially modulated orthogonal space-time block codes with non-vanishing determinants, IEEE Transactions on Communications 62 (1) (2014) 8599. doi:10.1109/TCOMM.2013.112913.130219.

[98] A. F. Coskun, O. Kucur, Performance analysis of maximal-ratio transmission/receive antenna selection in nakagami-m fading channels with channel estimation errors and feedback delay, IEEE 315 Transactions on Vehicular Technology 61 (3) (2012) 10991108.

[99] X. Rui, Analysis of MIMO MRT/SC systems, Wireless Personal Communications 62 (1) (2012) 117126.

[100] A. Y-lmaz, O. Kucur, Performance of transmit antenna selection and maximal-ratio combining in dual hop amplify-and-forward relay network over nakagami-m fading channels, Wireless Personal 320 Communications 67 (3) (2012) 485503.

[101] L. P. Tuyen, V. N. Q. Bao, Comparison of diversity combining techniques for MIMO systems, in: The 17th Asia Pacific Conference on Communications, IEEE, 2011, pp. 295300.

[102] A. H. Gazestani, S. A. Ghorashi, B. Mousavinasab, M. Shikh-Bahaei, A survey on implementation and applications of full duplex wireless communications, Physical Communication 34 (2019) 121 325 134.

[103] B. C. Nguyen, T. M. Hoang, P. T. Tran, T. N. Nguyen, Outage probability of noma system with wireless power transfer at source and full-duplex relay, AEU-International Journal of Electronics and Communications 116 (2020) 152957.

[104]] B. C. Nguyen, T. M. Hoang, X. N. Pham, P. T. Tran, Performance analysis of energy harvesting330 based full-duplex decode-and-forward vehicle-to-vehicle relay networks with non-orthogonal multiple access, Wireless Communications and Mobile Computing 2019.

[105] R. Magueta, D. Castanheira, A. Silva, R. Dinis, A. Gameiro, Hybrid multi-user equalizer for massive MIMO millimeter-wave dynamic sub-connected architecture, IEEE Access 7 (2019) 79017 79029

[106] D. Castanheira, G. Barb, A. Silva, A. Gameiro, A multi-user linear equalizer for up-link broadband millimeter wave massive MIMO, Digital Signal Processing 92 (2019) 6272.

[107] I. Ahmed, H. Khammari, A. Shahid, A. Musa, K. S. Kim, E. De Poorter, I. Moerman, A survey on hybrid beam-forming techniques in 5g: Architecture and system model perspectives, IEEE Communications Surveys and Tutorials 20 (4) (2018) 30603097.

[108] F. B. Hildebrand, Introduction to numerical analysis, Courier Corporation, 1987. International Conference on in Communications (ICC, 2012, pp. 2433-2438.

[109] E. Ahmed, A. M. Eltawil, All-digital self-interference cancellation technique for full-duplex systems, IEEE Transactions on Wireless Communications 14 (7) (2015) 35193532. doi: 10.1109/TWC.2015.2407876.

[110] A. Almradi, K. A. Hamdi, MIMO full-duplex relaying in the presence of co-channel interference, IEEE Transactions on Vehicular Technology 66 (6) (2016) 48744885.

[111] S. Narayanan, H. Ahmadi, M. F. Flanagan, On the performance of spatial modulation MIMO for full-duplex relay networks, IEEE Transactions on Wireless Communications 16 (6) (2017) 37273746.

[112] H. Holma, A. Toskala, LTE for UMTS, Evolution to LTE Advanced, John Wiley and Sons, 2011.

[113] L. V. Nguyen, B. C. Nguyen, X. N. Tran, L. T. Dung, Closed-form expression for the symbol error probability in full-duplex spatial modulation relay system and its application in optimal 355 power allocation, Sensors 19 (24) (2019) 5390.S. Dey, E. Sharma, R. Budhiraja, Scaling analysis of hardware-impaired two-way full-duplex

[114] S. Dey, E. Sharma, R. Budhiraja, Scaling analysis of hardware-impaired two-way full-duplex massive mimo relay, IEEE Communications Letters 23 (7) (2019) 12491253.

[115] O. Taghizadeh, A. C. Cirik, R. Mathar, Hardware impairments aware transceiver design for full-duplex amplify-and-forward MIMO relaying, IEEE Transactions on Wireless Communications 360 17 (3) (2017) 16441659.

[116] W. Xie, X. Xia, Y. Xu, K. Xu, Y. Wang, Massive MIMO full-duplex relaying with hardware impairments, Journal of Communications and Networks 19 (4) (2017) 351362

[117] K. Guo, K. An, B. Zhang, Y. Huang, D. Guo, G. Zheng, S. Chatzinotas, On the performance of the uplink satellite multi-terrestrial relay networks with hardware impairments and interference, 365 IEEE Systems Journal 13 (3) (2019) 22972308.

[118] X. Li, J. Li, Y. Liu, Z. Ding, A. Nallanathan, Residual transceiver hardware impairments on cooperative NOMA networks, IEEE Transactions on Wireless Communications.

[119] X. Li, M. Liu, C. Deng, P. T. Mathiopoulos, Z. Ding, Y. Liu, Full-duplex cooperative NOMA relaying systems with I/Q imbalance and imperfect SIC, IEEE Wireless Communications Letters 370 9 (1) (2019) 172020.

[120] X. Tian, Q. Li, X. Li, H. Peng, C. Zhang, K. M. Rabie, R. Kharel, I/Q imbalance and imperfect SIC on two-way relay NOMA systems, Electronics 9 (2) (2020) 249.

[121] X. Li, M. Huang, C. Zhang, D. Deng, K. M. Rabie, Y. Ding, J. Du, Security and reliability performance analysis of cooperative multi-relay systems with nonlinear energy harvesters and 375 hardware impairments, IEEE Access 7 (2019) 102644102661.

[122] E. Bjornson, J. Hoydis, M. Kountouris, M. Debbah, Massive MIMO systems with non-ideal hardware: Energy efficiency, estimation, and capacity limits, IEEE Transactions on Information Theory 60 (11) (2014) 71127139.

[123] A. Papazafeiropoulos, S. K. Sharma, T. Ratnarajah, S. Chatzinotas, Impact of residual addi380 tive transceiver hardware impairments on rayleigh-product MIMO channels with linear receivers: Exact and asymptotic analyses, IEEE Transactions on Communications 66 (1) (2017) 105118.

[124] X. Zhang, D. Guo, K. An, B. Zhang, Secure communications over cell-free massive mimo networks with hardware impairments, IEEE Systems Journal.

[125] B. C. Nguyen, X. N. Tran, et al., Transmit antenna selection for full-duplex spatial modulation 385 multiple-input multiple-output system, IEEE Systems Journal.

[126] G. C. Alexandropoulos, N. C. Sagias, K. Berberidis, On the multivariate weibull fading model with arbitrary correlation matrix, IEEE Antennas and Wireless Propagation Letters 6 (2007)9395.

[127] G. C. Alexandropoulos, N. C. Sagias, F. I. Lazarakis, K. Berberidis, New results for the mul390 tivariate nakagami-m fading model with arbitrary correlation matrix and applications, IEEE Transactions on Wireless Communications 8 (1) (2009) 245255

[128] K. P. Peppas, G. C. Alexandropoulos, P. T. Mathiopoulos, Performance analysis of dual-hop af relaying systems over mixed and fading channels, IEEE Transactions on Vehicular Technology 62 (7) (2013) 31493163.

[129] T. T. Duy, G. C. Alexandropoulos, V. T. Tung, V. N. Son, T. Q. Duong, Outage performance of cognitive cooperative networks with relay selection over double-rayleigh fading channels, IET Communications 10 (1) (2016) 5764.

[130] K. M. Rabie, B. Adebisi, M.-S. Alouini, Half-duplex and full-duplex AF and DF relaying with energy-harvesting in log-normal fading, IEEE Transactions on Green Communications and Net400 working 1 (4) (2017) 468480

[131] A. F. Coskun, O. Kucur, Performance analysis of hybrid transmit antenna selection maximal ratio transmission in nakagami-m fading channels, Wireless Communications and Mobile Computing 13 (13) (2013) 12341245

[132] B. C. Nguyen, X. N. Tran, Performance analysis of full-duplex amplify-and-forward relay system 405 with hardware impairments and imperfect self-interference cancellation, Wireless Communications and Mobile Computing 2019 (2019) 10. doi:10.1155/2019/4946298.

[133] S. Teodoro, A. Silva, R. Dinis, F. M. Barradas, P. M. Cabral, A. Gameiro, Theoretical analysis of nonlinear amplification elects in massive mimo systems, IEEE Access 7 (2019) 172277172289.

[134] E. Bjornson, M. Matthaiou, M. Debbah, A new look at dual-hop relaying: Performance limits 410 with hardware impairments, IEEE Transactions on Communications 61 (11) (2013) 45124525. .

[135] E. Everett, A. Sahai, A. Sabharwal, Passive self-interference suppression for full-duplex infrastructure nodes, IEEE Transactions on Wireless Communications 13 (2) (2014) 680694.

[136] D. Bharadia, E. McMilin, S. Katti, Full duplex radios, in: ACM SIGCOMM Computer Communication Review, Vol. 43, ACM, 2013, pp. 375386.

[137] G. C. Alexandropoulos, M. Duarte, Joint design of multi-tap analog cancellation and digital beam-forming for reduced complexity full

duplex MIMO systems, in: 2017 IEEE International Conference on Communications (ICC), IEEE, 2017, pp. 1.

[138] G. J. Gonzalez, F. H. Gregorio, J. E. Cousseau, T. Riihonen, R. Wichman, Full-duplex amplifyand- forward relays with optimized transmission power under imperfect transceiver electronics, EURASIP Journal on Wireless Communications and Networking 2017 (1) (2017) 76.

[139] B. C. Nguyen, T. M. Hoang, et al., Performance analysis of vehicle-to-vehicle communication with full-duplex amplify-and-forward relay over double-rayleigh fading channels, Vehicular Communications 19 (2019) 100166.

[140] B. C. Nguyen, X. N. Tran, D. T. Tran, et al., Full-duplex amplify-and-forward relay system with 425 direct link: Performance analysis and optimization, Physical Communication 37 (2019) 100888

[141] C. Li, Z. Chen, Y. Wang, Y. Yao, B. Xia, Outage analysis of the full-duplex decode-and-forward two-way relay system, IEEE Transactions on Vehicular Technology 66 (5) (2017) 40734086. doi:10.1109/TVT.2016.2610004

[142] A. Goldsmith, Wireless communications, Cambridge university press, 2005.

[143] A. Leon-Garcia, Probability, statistics, and random processes for electrical engineering, Pearson/Prentice Hall 3rd ed. Upper Saddle River, NJ, 2008.

[144] B. C. Nguyen, T. M. Hoang, P. T. Tran, Performance analysis of full-duplex decode-and-forward relay system with energy harvesting over nakagami-m fading channels, AEU-International Journal of Electronics and Communications 98 (2019) 114122.

[145] A. Jerrey, D. Zwillinger, Table of integrals, series, and products, Academic press, 2007

Candidate published results cited in this work and indexed in WoS or Scopus

[TNK01] **Tam Nguyen Kieu**, Tran Hoang Quang Minh, Thuan Do Dinh and Miroslav Vozňák, An Instantaneous Transmission Mode Analysis in Energy Harvesting for Half-Duplex and Full-Duplex Relaying Network (2016) International Journal of Grid and Distributed Computing, 9(3), pp.11-20. DOI:10.14257/ijgdc.2016.9.3.02.

[TNK02] **Tam Nguyen Kieu**, Thuan Do Dinh, and Miroslav Voznák, An Optimal Analysis in Wireless Powered Full-duplex Relaying Network (2017) Radioengineering 26(1):369-375. DOI:10.13164/re.2017.0369. IF 1.048 (2017)

[TNK03] Dinh-Thuan Do, Chi-Bao Le, Hong-Nhu Nguyen, **Tam Nguyen Kieu**, Si-Phu Le, Ngoc-Long Nguyen, Nhat-Tien Nguyen and Miroslav Voznak, Wireless Power Transfer enabled NOMA Relay Systems: Two SIC modes and Performance Evaluation (2019) Telkomnika, 17(6). DOI:10.12928 telkomnika.v17i6.

[TNK04] Ba Cao Nguyen, **Tam Nguyen Kieu**, Tran Manh Hoang, Tran Thanh Phuong, Miroslav Voznak, Analysis of MRT/MRC Diversity Techniques to Enhance the Detection Performance for MIMO Signals in Full-Duplex Wireless Relay Networks with Transceiver Hardware Impairment (2020) Physical Communication, Vol. 42, 101132. DOI:10.1016/j.physic communication.2020.101132. IF 1.594 (2019)

[TNK05]**Tam Nguyen. Kieu**, Duc-Dung Tran, Dac-Binh Ha, Miroslav Voznak, On Secure QoS-based NOMA Networks with Multiple Antennas and Eavesdroppers over Nakagami-m Fading 2019) IETE Journal of Research, 2019, pp. 1-13. DOI:10.1080/03772063.2019.1610088. IF 1.125 (2019)

[TNK06] **Tam Nguyen Kieu**, Duc-Dung Tran, Dac-Binh Ha, and Miroslav Voznak, Secrecy Performance Analysis of Cooperative MISO NOMA Networks Over Nakagami-m Fading (2019) IETE Journal of Research, 2019, pp. 1-12. DOI: 10.1080/03772063.2019.1643267. IF 1.125 (2019)

[TNK07] **Tam Nguyen Kieu**, Long Nguyen Ngoc, Hung Kieu Quoc, Hung Ha Duy, Thuan Do Dinh, Miroslav Voznak and Martin Mikulec, A Performance Analysis in Energy Harvesting Full-Duplex Relay, Proceedings of the 39th International Conference on Telecommunication and signal processing TSP, Vienna, Austria, July 2016. DOI: 10.1109/TSP.2016.7760850.

[TNK08] **Tam Nguyen Kieu**, Khanh Nhan Nguyen Huu, Nguyen Ngoc Long, Hung Ha Duy, Tuan Dao Huy, Thuan Do Dinh, Miroslav Voznak, A Performance Analysis in The One-Way Full-Duplex Relaying Network,

19th The International Conference on Network Based Information Systems (NBiS) Ostrava, SEP 7-9, 2016. DOI: 10.1109/NBiS.2016.62.

[TNK9] **Tam Nguyen Kieu**, Hung Ha Duy, Long Nguyen Ngoc, Tuan Dao Huy, Nhu Nguyen Hong and Miroslav Voznak, An Instantaneous Transmission Mode Analysis in The Half-Duplex and Full-Duplex Relaying Network, 2016 3rd National Foundation for Science and Technology Development Conference on Information and Computer Science (NICS), Da Nang, Viet Nam, SEP 14-16, 2016. DOI: 10.1109/NICS.2016.7725663.

[TNK10] **Tam Nguyen Kieu**, Khanh Nhan Nguyen Huu, Long Nguyen Ngoc, Hung Ha Duy, Thuan Do Dinh, Miroslav Voznak, Dominik Uhrin, An Operation Analysis in DF Full-Duplex Relay Network, 2016 XI International Symposium on Telecommunications (BIHTEL) October 24-26, 2016, Sarajevo, Bosnia and Herzegovina. DOI: 10.1109/BIHTEL.2016.7775726.

[TNK11] Phuoc Huynh Tan, **Tam Nguyen Kieu**, Thuan Do Dinh, Miroslav Voznak, Dominik Uhrin, A Performance Analysis about Impact of I/Q Imbalance in AF Two-Hop Relay System, 2016 XI International Symposium on Telecommunications (BIHTEL) October 24-26, 2016, Sarajevo, Bosnia and Herzegovina. DOI: 10.1109/BIHTEL.2016.7775720.

[TNK12] Khanh Nhan Nguyen Huu, **Tam Nguyen Kieu**, Hung Ha Duy, Long Nguyen Ngoc, Tuan Dao Huy, Thuan Do Dinh, Miroslav Voznak, A DF Performance Analysis in Half-duplex and Full-Duplex Relaying Network, 3rd AETA, Recent Advances in Electrical Engineering and Related Sciences. Cham: Springer International Publishing, 2016, Busan (Republic of Korea), December 7-8, 2016. DOI: 10.1007/978-3-319-50904-4-80.

[TNK13] Nguyen Dao, Khanh Nhan Nguyen Huu, **Tam Nguyen Kieu**, Nhu Nguyen Hong and Miroslav Voznak, A Performance Analysis of an AF Two Hops Model in the Energy Harvesting Relay Network, 3rd AETA, Recent Advances in Electrical Engineering and Related Sciences. Cham: Springer International Publishing, 2016, Busan (Republic of Korea), December 7-8, 2016. DOI: 10.1007/978-3-319-50904-4-77.

[TNK14] Nguyen Van Cuu, Nhu Nguyen Hong, Long Nguyen Ngoc, Nguyen Thi Phuong Loan, **Tam Nguyen Kieu**, Miroslav Voznak and Jaroslav Zdralek, An AF Performance Analysis in the energy harvesting Relaying Network, 2017 4rd National Foundation for Science and Technology Development Conference on Information and Computer Science (NICS), Ha Noi, Viet Nam, November 24-25,2017. DOI:10.1109/NAFOSTED.2017.8108033.

[TNK15] Long Nguyen Ngoc, Nhu Nguyen Hong, **Tam Nguyen Kieu**, Jaroslav Zdralek and Miroslav Voznak, A Performance Analysis in AF Full-Duplex Relay Selection Network, on ICAS2 (Ho Chi Minh City, Vietnam). AIP Conference Proceedings, June 24-25,2018. 040013 (2018).

DOI: 10.1063/1.5033413.

[TNK16] **Tam Nguyen Kieu**, Nhu Nguyen Hong, Long Nguyen Ngoc, Tu-Trinh Thi Nguyen, Jaroslav Zdralek and Miroslav Voznak, An Examination of outage Performance for Selected Relay and Fixed Relay in Cognitive Radio- Aided NOMA, Proceedings of the 5 th AETA, Recent Advances in Electrical engineering and Related Sciences. Cham: Springer International Publishing, 2018, Czech republic, September 12-14, 2018. DOI: 10.1007/978-3-030-14907-9-35.

[TNK17] Phu Tran Tin, Pham Minh Nam, Tran Trung Duy, Tran Thanh Phuong, **Tam Nguyen Kieu** and Miroslav Voznak IEEE, Senior member, Throughput Analysis of Power Beacon-Aid with Multi-hop Relaying Networks Employing Non-Orthogonal Multiple Access with Hardware Impairment, Czech republic, September 12-14, 2018. DOI: 10.1007/978-3-030-14907-9-36.

Other results achieved within the dissertation and cited in the thesis

[TNK18] **Tam Nguyen Kieu**, Miroslav.Voznak, Thuan Do Dinh, Hung Ha Duy, Long Nguyen Ngoc, Tuan Dao Huy. A Performance Analysis for AF Mode in the Full-duplex Relaying Network, 5-6 September, in 16th Knowledge Telecommunication Technologies and Optics 2016 KTTO at Ostrava, Republic of Czech.

[TNK19] Khanh Nhan Nguyen Huu, Long Nguyen Ngoc, **Tam Nguyen Kieu** and Miroslav Voznak, A Performance Analysis of the AF Propagation Two stages Model in PSR Network, Proceedings of the 1st International Conference on ICAS1 December, 2017. DOI: 10.1007/978-3-319-50904-4-80.

[TNK20] Long Nguyen Ngoc, Khanh Nhan Nguyen Huu, **Tam Nguyen Kieu** and Miroslav Voznak, A Performance Analysis of a Propagation Two Hops Model in the Cooperative Relaying Network, Proceedings of the 1st International Conference on ICAS1 (Ho Chi Minh City, Vietnam, 5-7 July 2016). DOI: 10.1007/978-3-319-50904-4-77).

[TNK21] **Tam Nguyen Kieu**, Nhu Nguyen Hong, Long Nguyen Ngoc, Thanh-Duc Le and Jaroslav Zdralek and Miroslav Voznak, A Performance Analysis of DF Model in the Energy Harvesting Half-duplex and Full-Duplex Relay Networks, Innovative Computing, Optimization and Its Applications, chapter First Online: 22 November 2017, pp 1-19, Part of the Studies in Computational Intelligence book series (SCI, volume 741). DOI: 10.1007/978-3-319-66984-7-1.

[TNK22] **Tam Nguyen Kieu**, Tuan Nguyen Hoang, Thu-Quyen T. Nguyen, Hung Ha Duy, D .-T Do, and M. Voznak, A Performance Analysis in Energy Harvesting Full-Duplex Relay, ICAMER 2016, May 5th, 2016. Applied Mathematics in Engineering and Reliability : Proceedings of the 1st International Conference on Applied Mathematics in Engineering and Reliability (Ho Chi Minh City, Vietnam, 4-6 May 2016).

List of candidate's research results and activities

Publication activities

I provide the following list indexed results in relevant scientific databases, in order to document my research activities within the entire period of my doctoral study:

- Records in Web of Science: 14 (5 articles in journals).
- Records in Scopus: 17 (4 articles in journals).
- 28 citations in Scopus and 20 citations in ISI/Web of Science.
- ORCID: 0000-0003-4641-0729
- Research ID: AAP-8826-2020.

Project memberships and participations

- Proj. reg. no. SP2020/65 - Networks and Communications Technologies for Smart Cities III., Student Grant Competition of VSB-TUO (2020).
- Proj. reg. no. SP2019/41 - Networks and Communications Technologies for Smart Cities II., Student Grant Competition of VSB-TUO (2019).
- Proj. reg. no. SP2018/59 - Networks and Communications Technologies for Smart Cities I., Student Grant Competition of VSB-TUO (2018).
- Proj. reg. no. SP2017/174 - Networks, Security, Modelling, Simulation, and Knowledge Retrieval and Communications Technologies for Smart Cities, Student Grant Competition of VSB-TUO (2017).
- Proj. reg. FOSTECH. 2016. BR 21 – Energy Harvesting Enabled Wireless Network: Protocol Design and Performance Analysis of Ton Duc Thang University, Viet Nam (2016).